Vol. 63 August, 1959 No. 8

THE JOURNAL OF PHYSICAL CHEMISTRY

(Registered in U. S. Patent Office)

CONTENTS

NOTES

THE JOURNAL OF PHYSICAL CHEMISTRY

(Registered in U. S. Patent Office)

Published monthly by the American Chemical Society at 20th and Northampton Sts., Easton, Pa.

Second-class mail privileges authorized at Easton, Pa. This publication is authorized to be mailed at the special rates of postage prescribed by Section 132.122.

The *Journal of Physical Chemistry* is devoted to the publication of selected symposia in the broad field of physical chemistry and to other contributed papers.

Manuscripts originating in the British Isles, Europe and Africa should be sent to F. C. Tompkins, The Faraday Society, 6 Gray's Inn Square, London W. C. 1, England.

Manuscripts originating elsewhere should be sent to W. Albert Noyes, Jr., Department of Chemistry, University of Rochester, Rochester 20, N. Y.

Correspondence regarding accepted copy, proofs and reprints should be directed to Assistant Editor, Allen D. Bliss, Department of Chemistry, Simmons College, 300 The Fenway, Boston 15, Mass.

Business Office: Alden H. Emery, Executive Secretary, American Chemical Society, 1155 Sixteenth St., N. W., Washington 6, D. C.

Advertising Office: Reinhold Publishing Corporation, 430 Park Avenue, New York 22, N. Y.

Articles must be submitted in duplicate, typed and double spaced. They should have at the beginning a brief Abstract, in no case exceeding 300 words. Original drawings should accompany the manuscript. Lettering at the sides of graphs (black on white or blue) may be pencilled in and will be typeset. Figures and tables should be held to a minimum consistent with adequate presentation of information. Photographs will not be printed on glossy paper except by special arrangement. All footnotes and references to the literature should be numbered consecutively and placed in the manuscript at the proper places. Initials of authors referred to in citations should be given. Nomenclature should conform to that used in *Chemical Abstracts*, mathematical characters marked for italic, Greek letters carefully made or annotated, and subscripts and superscripts clearly shown. Articles should be written as briefly as possible consistent with clarity and should avoid historical background unnecessary for specialists.

Notes describe fragmentary or incomplete studies but do not otherwise differ fundamentally from articles and are subjected to the same editorial appraisal as are articles. In their preparation particular attention should be paid to brevity and conciseness. Material included in Notes must be definitive and may not be republished subsequently.

Communications to the Editor are designed to afford prompt preliminary publication of observations or discoveries whose value to science is so great that immediate publication is imperative. The appearance of related work from other laboratories is in itself not considered sufficient justification for the publication of a Communication, which must in addition meet special requirements of timeliness and significance. Their total length may in no case exceed 500 words or their equivalent. They differ from Articles and Notes in that their subject matter may be republished.

Symposium papers should be sent in all cases to Secretaries of Divisions sponsoring the symposium, who will be responsible for their transmittal to the Editor. The Secretary of the Division by agreement with the Editor will specify a time after which symposium papers cannot be accepted. The Editor reserves the right to refuse to publish symposium articles, for valid scientific reasons. Each symposium paper may not exceed four printed pages (about sixteen double spaced typewritten pages) in length except by prior arrangement with the Editor.

Remittances and orders for subscriptions and for single copies, notices of changes of address and new professional connections, and claims for missing numbers should be sent to the American Chemical Society, 1155 Sixteenth St., N. W., Washington 6, D. C. Changes of address for the *Journal of Physical Chemistry* must be received on or before the 30th of the preceding month.

Claims for missing numbers will not be allowed (1) if received more than sixty days from date of issue (because of delivery hazards, no claims can be honored from subscribers in Central Europe, Asia, or Pacific Islands other than Hawaii), (2) if loss was due to failure of notice of change of address to be received before the date specified in the preceding paragraph, or (3) if the reason for the claim is "missing from files."

Subscription Rates (1959): members of American Chemical Society, $8.00 for 1 year; to non-members, $16.00 for 1 year. Postage free to countries in the Pan American Union; Canada, $0.40; all other countries, $1.20. Single copies, current volume, $1.35; foreign postage, $0.15; Canadian postage $0.05. Back volumes (Vol. 56–59) $15.00 per volume; (starting with Vol. 60) $18.00 per volume; foreign postage, per volume $1.20, Canadian, $0.15; Pan-American Union, $0.25. Single copies: back issues, $1.75; for current year, $1.35; postage, single copies: foreign, $0.15; Canadian, $0.05; Pan-American Union, $0.05.

THE JOURNAL OF
PHYSICAL CHEMISTRY

(Registered in U. S. Patent Office) (© Copyright, 1959, by the American Chemical Society)

VOLUME 63 AUGUST 19, 1959 NUMBER 8

A REACTION MECHANISM FOR THE HYDROGENATION OF CARBON MONOXIDE INCLUDING A REVERSIBLE CATALYST REACTION

BY JOHN E. POWERS

Chemical Engineering, The University of Oklahoma, Norman, Oklahoma

Received July 11, 1958

A reaction mechanism is proposed to account for observed effects of pressure, temperature and hydrogen to carbon monoxide ratio on the rate of hydrogenation of carbon monoxide in a differential reactor. The mechanism includes a reversible catalyst reaction and parallel, irreversible hydrogenation reactions. Equations based on this mechanism represent the data satisfactorily. Activation energies are calculated for both the catalyst reactions and hydrogenation reactions.

Introduction

The results of a study of the rate of hydrogenation of carbon monoxide over an iron base catalyst were reported recently by Frye, Pickering and Eckstrom.[1] (Further reference to this article will be made as F.P.E.) The data presented by these authors demonstrate that catalyst kinetics play an important part in some reactions. The authors conclude that proper interpretation of kinetic data under these circumstances is impossible unless such catalyst effects are properly taken into account.

The consistency of the trends displayed in the data presented by these authors suggests that a simple mechanism might explain the observed results. Such a mechanism would be useful in interpreting the data quantitatively and might contribute to the further understanding of the hydrocarbon synthesis reaction.

Summary of Experimental Observations

Any mechanism proposed for the hydrogenation of carbon monoxide over an iron base catalyst must account for the following experimental observations reported by Frye, Pickering and Eckstrom (F.P.E.).

(1) A step change in total pressure at constant gas phase composition causes an immediate change in rate of CO conversion followed by a continuing change in rate over an extended period of time. The immediate change is approximately first order with respect to pressure whereas the total change after steady state is attained is approximately second order. (See Figs. 3, 6 and 7 in article by F.P.E. and Figs. 1 and 2 of this article.)

(2) A step change in H_2/CO ratio at constant total pressure causes no sudden change in rate but a relatively slow change occurs over an extended period of time. The immediate change is zero order with respect to CO partial pressure whereas the total change is approximately first order in CO partial pressure. (See Fig. 4 of F.P.E. and Fig. 2 of this article.)

(3) A step change in temperature generally produces an immediate change in reaction rate followed by a relatively slow change *of the opposite sign.* (Figs. 1 and 2 of F.P.E. and Fig. 3 of this article.) The effect is apparently dependent on the particular catalyst employed.

(4) All three of the changes mentioned above are reversible, *i.e.*, the steady-state reaction rate for a particular catalyst is a function of temperature, pressure and gas composition only and is essentially independent of the immediate previous history of the catalyst.

Proposed Reaction Mechanism

The activity of the catalyst used in the hydrocarbon synthesis is strongly dependent on the method of catalyst preparation. This fact is accounted for by proposing that a number of "active sites," AS, exist on the catalyst and that this number depends only on the method of pretreatment. (This ignores the effects of catalyst poisons and long-time catalyst activity decline.) In order to account for the fact that a change in rate

(1) C. G. Frye, H. L. Pickering and H. C. Eckstrom, THIS JOURNAL, **62**, 1508 (1958).

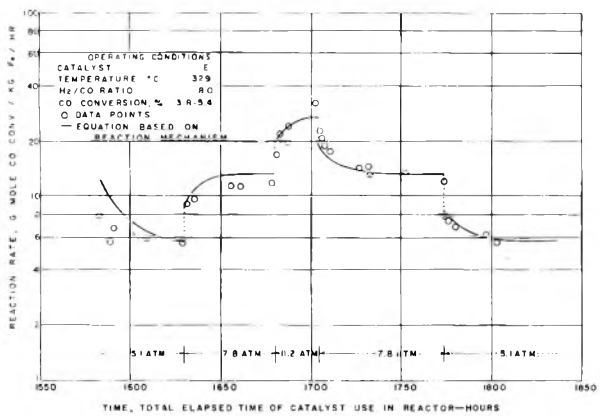

Fig. 1.—Effect of step changes in total pressure on rate of hydrogenation of carbon monoxide.

with time occurs following any change in CO partial pressure (either as total pressure or H_2/CO ratio), it is proposed that the "active sites" produced in catalyst pretreatment *do not* enter into reaction directly to form hydrocarbons. Instead an "effective site," ES, is visualized that is formed in the presence of CO.

$$AS + CO \underset{k_2}{\overset{k_1}{\rightleftharpoons}} ES \qquad (1)$$

Under steady-state conditions, equilibrium exists and the number of effective sites remains constant but a change in CO partial pressure will bring about a slow shift to a new equilibrium.

It is assumed that this shift is very slow compared with all other reactions and therefore the catalyst reaction can be studied independent of other reactions.

Consider equation 1

$$d(ES)/dt = k_1(AS)p_{CO} - k_2(ES) \qquad (2)$$

Under conditions such that temperature, CO partial pressure and (AS) are maintained constant, equation 2 is solved for the number of effective sites as a function of time.

$$(ES) = \frac{k_1}{k_2}(AS)p_{CO}\left[1 - \left(1 - \frac{k_2(ES)_0}{k_1(AS)p_{CO}}\right)\exp(-k_2t)\right] \qquad (3)$$

Another mechanism involving two parallel reactions is proposed to explain the immediate change in rate with a step change in total pressure and the lack of any detectable immediate change with a similar step change in H_2/CO ratio.

$$ES + CO \xrightarrow{k_3} ES{\cdot}CO^* \qquad (4)$$

$$ES + H_2 \xrightarrow{k_4} ES{\cdot}H_2^* \qquad (5)$$

The activated complexes, $ES{\cdot}CO^*$ and $ES{\cdot}H_2^*$ react immediately to form the activated intermediate $CO{\cdot}H_2^*$ and regenerate the effective sites.

$$ES{\cdot}CO^* + H_2 \xrightarrow{k_5} CO{\cdot}H_2^* + ES \qquad (6)$$

$$ES{\cdot}H_2^* + CO \xrightarrow{k_6} CO{\cdot}H_2^* + ES \qquad (7)$$

Even though equations 4 and 5 are considered to be rate determining for the production of the activated intermediate, $CO{\cdot}H_2^*$, the rates of these two reactions are still extremely rapid when compared to the change in catalyst characteristics as represented by equation 1. This assumption is consistent with the development of equation 2 and further permits one to ignore the small amount of CO used in the slow catalyst change in developing an expression for the rate of CO disappearance.

Consider only equations 4 and 7

$$-dCO/dt = k_3(ES)p_{CO} + k_6(ES{\cdot}H_2^*)p_{CO} \qquad (8)$$

Since the rate in equation 7 is assumed to be very rapid

$$k_4(ES)p_{H_2} = k_6(ES{\cdot}H_2^*)p_{CO} \qquad (9)$$

Substitution of equation 9 into equation 8 yields

$$-dCO/dt = k_3(ES)p_{CO} + k_4(ES)p_{H_2} \qquad (10)$$

If it is further assumed that the rates of the parallel reactions (equations 4 and 5) are essentially equal

$$-dCO/dt = k_3(ES)(p_{CO} + p_{H_2}) \qquad (11)$$

The value of (ES) as established in equation 3 is substituted into equation 11

$$-dCO/dt = (k_1k_3/k_2)(AS)p_{CO}(p_{CO} + p_{H_2})\left[1 - \left(1 - \frac{k_2(ES)_0}{k_1(AS)p_{CO}}\right)\exp(k_2t) - \right] \qquad (12)$$

Notation

A	activation energy (assumed independent of temp.)
(AS)	concentration of "active sites"
(ES)	concentration of "effective sites"
k	reaction rate coefficient
p	partial pressure
R	gas constant
r	rate of CO conversion per unit weight of catalyst
T	absolute temperature
t	time measured from a step change in operating conditions
τ	$\frac{(T^-)(T^+)}{(T^+ - T^-)}$

Subscripts

CO	indicates carbon monoxide (partial pressure)
H_2	indicates hydrogen (partial pressure)
0	evaluated at $t = 0$
0^+	evaluated immediately following a step change
0^-	evaluated immediately preceding a step change
SS	evaluated at steady-state conditions
SS^+	steady-state conditions after change
SS^-	steady-state conditions preceding change

Superscripts

+	indicates a value for $t > 0$
−	indicates a value for $t < 0$

Discussion

Qualitative Comparison of Equation Derived from Proposed Mechanism with Experimental Observations.—In comparing equation 12 with experimental observations it will be convenient to consider several restricted forms of the equation.

Steady-State.—The exponential term in equation 12 becomes negligible at large values of time.

$$r_{SS} = (-dCO/dt)_{SS} = (k_1k_3/k_2)(AS)p_{CO}(p_{CO} + p_{H_2}) \qquad (13)$$

Equation 13 predicts that the steady-state reaction rates will be second order with respect to a change of total pressure and first order with respect to a change in CO partial pressure at constant total pressure (the result of a change in H_2/CO

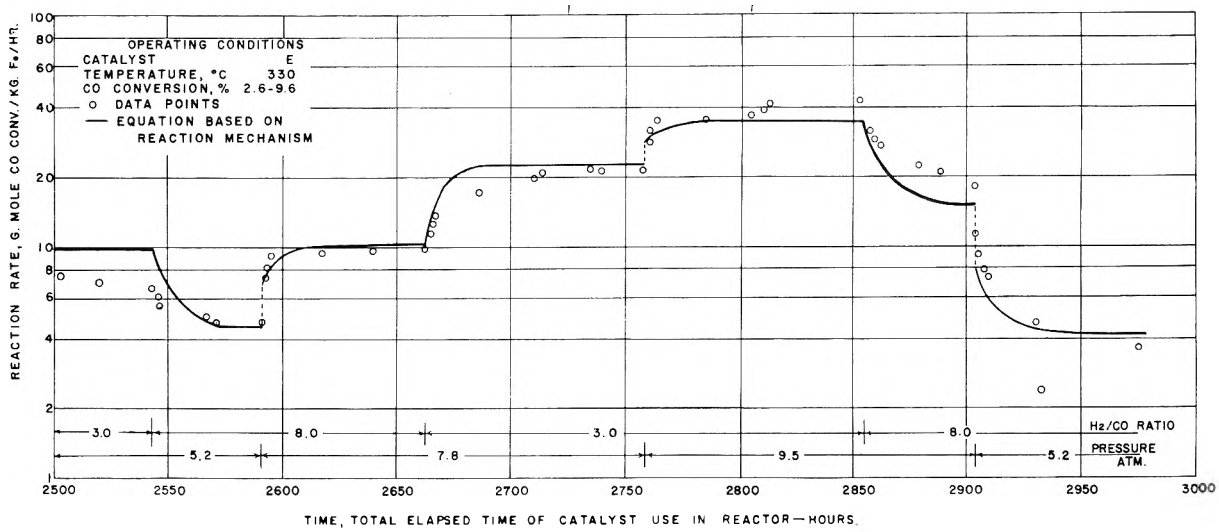

Fig. 2.—Effect of step changes in total pressure and hydrogen to carbon monoxide ratio on rate of hydrogenation of carbon monoxide.

ratio). Both of these conclusions are in agreement with the experimental observations.

Consideration of temperature effects is deferred to a later section.

Immediate Change.—The rate immediately following a change in conditions, r_0^+, is obtained from equation 12 by substituting $t = 0$.

$$r_0^+ = k_3^+ (p_{CO}^+ - p_{H_2}^+)(ES)_0 \qquad (14)$$

The rate immediately preceding the change in conditions, r_0^-, is obtained from equation 11

$$r_0^- = k_3^-(p_{CO}^- - p_{H_2}^-)(ES)_0 \qquad (15)$$

Comparison of equations 14 and 15 leads to the conclusion that the immediate change in rate is first order with respect to total pressure and independent of CO partial pressure. Both of these results agree with the experimental observations.

Transient Behavior.—Combination of equations 12, 13 and 14 yields

$$r(t) = r_0^+ + [r_{SS}^+ - r_0^+][1 - \exp(-k_2^+ t)] \qquad (16)$$

Thus the transient behavior following any change in conditions will decay exponentially. This is substantiated by the data presented by F.P.E. (see also Figs. 1, 2 and 3).

In obtaining many of the data on the transient behavior, step changes in conditions were made with the catalyst at steady-state conditions. For this special case (equation 3)

$$(ES)_0 = (ES)_{SS}^- = (k_1^-/k_2^-)(AS)p_{CO}^- \qquad (17)$$

and equation 12 becomes

$$r(t) = \frac{k_1^+ k_3^+}{k_2^+}(AS)p_{CO}^+ (p_{CO}^+ + p_{H_2}^+) \left[1 - \left(1 - \frac{k_1^- k_2^+ p_{CO}^-}{k_1^+ k_2^- p_{CO}^+}\right)\exp(-k_2^+ t)\right] \qquad (18)$$

Quantitative Comparison of Theoretical Equations and Experimental Data.—F.P.E. presented reaction rate data for four successive step changes in total pressure, all other conditions being maintained constant (their Table I). These data are shown graphically in Fig. 1. The solid line on Fig. 1 represents equation 18 with the values

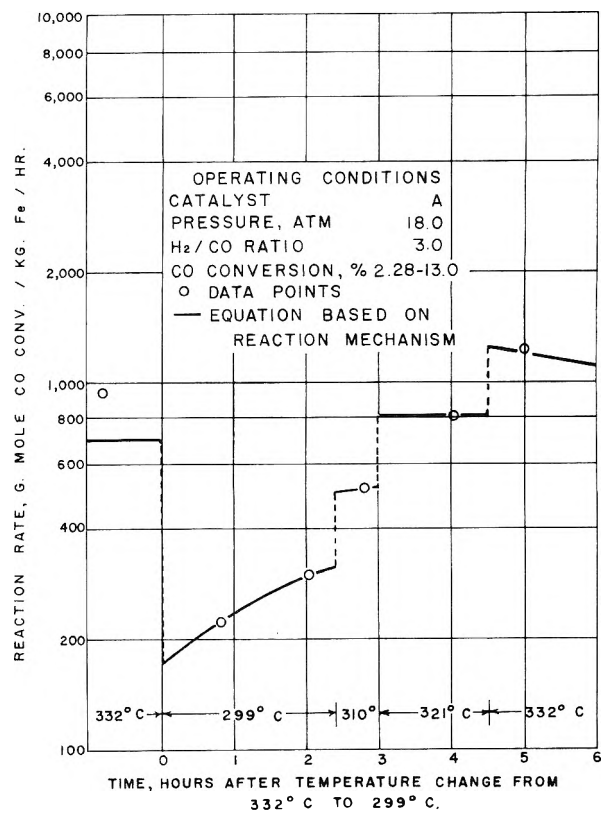

Fig. 3.—Effect of step changes in reactor temperature on the rate of hydrogenation of carbon monoxide.

$(k_1^+ k_3^+/k_2^+)(AS) = 1.94$ g.mole CO conv./kg. Fe hr. atm.^{2}

$k_2^+ = 1/8$ hr.$^{-1}$

The equation predicts all trends as discussed previously and is fairly accurate in predicting rate values for the entire time interval of over 200 hours.

Other data have been made available by the Pan American Petroleum Corporation to test the proposed mechanism. These data were obtained with the same catalyst and at the same temperature as the data presented in Fig. 1 and they cover three changes in total pressure and three changes in H_2/CO ratio (CO partial pressure), other con-

ditions being held essentially constant. These data are shown graphically in Fig. 2. The solid line on Fig. 2 represents equation 18 with the values

$(k_1{}^+k_3{}^+/k_2{}^+)(AS) = 1.42$ g.mole CO conv./kg. Fe hr. atm.^{2}

$k_2{}^+ = 1/8$ hr.$^{-1}$

The value of $k_2{}^+$ remains constant in the 700-hour period between the two experimental investigations, but apparently the concentration of active sites, (AS), has decreased about 25%. Again the trends are reproduced for all changes even though the absolute values are not in exact agreement.

Use of one pair of constants to fit the data (solid line on Fig. 2) is based on an assumption of isothermal conditions. Actually, the temperature varied between a minimum of 325° and a maximum of 333° during the 500 hour period.

The data presented by F.P.E. on their Fig. 3 were obtained with a different catalyst (Catalyst B) and at a different temperature (297°). The data on their Fig. 3 are well represented by equation 18 with

$(k_1{}^+k_3{}^+/k_2{}^+)(AS) = 8.01$ g. mole CO conv./kg. Fe hr. atm.^{2}

$k_2{}^+ = 1/6$ hr.$^{-1}$

Temperature Effects.—Typical data on the rate of CO conversion as a function of time following a step change in temperature have been presented by F.P.E. (their Figs. 1 and 2). These and other data are presented in Table I.

TABLE I

Identification	Pressure, atm.	H_2/CO	Temp., °C.	Time from step change, hr.	Reaction rate, (g. mole CO conv./kg. Fe hr.)	CO Conv., %
CRC-18-A	18.0	3.0				
Catalyst G			332	0$^-$	204	4.28
			299	0$^+$	....	...
				0.4	56.2	1.15
				2.2	103	2.11
			310	2.7	....	...
				3.2	177	3.65
			321	3.6	....	...
				4.0	223	4.59
			332	4.4	....	...
				4.7	258	5.35
CRA-20-C	18.0	2.9				
Catalyst A			332	0$^-$	950	9.95
			299	0$^+$	....	...
				0.8	223	2.28
				1.7	300	3.11
			310	2.4	....	...
				2.8	515	5.43
			321	3.0	....	...
				4.0	808	8.49
			332	4.5	....	...
				5.0	1230	13.1
CRA-26-C	18.0	2.9				
Catalyst B			229	0$^-$	750	3.04
			332	0$^+$	....	...
				0.5	2160	9.10
				1.0	2040	8.72
				5.7	1540	6.69

The Arrhenius equation is used to relate the reaction rate coefficients, k_1, k_2 and k_3, to temperature

$$k^+/k^- = \exp\left[\frac{A}{R}\left(\frac{1}{T^-} - \frac{1}{T^+}\right)\right] \quad (19)$$

Solving equation 19 for the activation energy A

$$A = R\tau \ln (k^+/k^-) \quad (20)$$

where

$$\tau = (T^-)(T^+)/(T^+ - T^-) \quad (21)$$

Estimation of A_3.—For a step change in temperature with other operating conditions held constant, equations 14 and 15 are combined to yield

$$r_0{}^+/r_0{}^- = k_3{}^+/k_3{}^- \quad (22)$$

Therefore

$$A_3 = R\tau \ln (k_3{}^+/k_3{}^-) = R\tau \ln (r_0{}^+/r_0{}^-) \quad (23)$$

F.P.E. based their estimates of A_3 on values of $r_0{}^+$ and $r_0{}^-$ obtained by graphical extrapolation of the reaction rate data. Their reported values range from 22 to 38 kcal./g. mole for a variety of catalysts. An average value of 29 kcal./g.mole with an average deviation of 3 kcal./g.mole is reported.

Many other experimental determinations of rate data were made in a manner described by F.P.E. and illustrated by the last three points on Fig. 3. Extrapolation of such data is meaningless. However if rate determinations are made at two different temperatures in one hour or less, these two rates can be used as $r_0{}^-$ and $r_0{}^+$ in equation 23 to estimate A_3. The values thus estimated should be low but the error in all cases should be much less than 25%.

Data obtained from 103 pairs of data resulting from step changes in temperature were used to estimate values of A_3 in the manner described above. These data were obtained at temperatures between 265 and 362°, pressures between 6.1 and 28.2 atm. and H_2/CO ratios from 2.9 to 8.7. CO conversion was less than 10% in all cases. Only data taken in time intervals of one hour or less were considered.

Typical data are presented in Table II. The average value of A_3 for all data is 29.2 kcal./g.mole with a standard deviation of 6.2 kcal./g.mole. This average supports the value of 29 kcal. reported by F.P.E. The large standard deviation indicates the magnitude of scatter in the data.

Estimation of $A_2 - A_1$.—For a step change in temperature with the catalyst at steady-state conditions combination of equations 13, 14 and 17 yields

$$r_0{}^+/r_{SS}{}^+ = k_1{}^-k_2{}^+/k_1{}^+k_2{}^- \quad (24)$$

Application of equation 20 produces

$$A_2 - A_1 = R\tau \ln (k_1{}^-k_2{}^+/k_1{}^+k_2{}^-) = R\tau \ln (r_0{}^+/r_{SS}{}^+) \quad (25)$$

Unfortunately none of the experimental measurements following a step change in temperature were continued until a new steady-state was attained. Therefore, data obtained during the transient period were used to estimate the new steady-state rate. Equation 16 is solved for $r_{SS}{}^+$

$$r_{SS}{}^+ = r_0{}^+ + (r(t) - r_0{}^+)/[1 - \exp(-k_2{}^+t)] \quad (26)$$

In order to apply equation 26 to determine $r_{SS}{}^+$ (and therefore $A_2 - A_1$ by equation 25) it is necessary to know the value of k_2 at the experimental temperature. Fortunately, the reaction

TABLE II

Identification	Pressure, atm.	H_2/CO	Temp., °C. 1	Temp., °C. 2	Reaction rate, g.mole CO conv./ kg. Fe hr. 1	Reaction rate, g.mole CO conv./ kg. Fe hr. 2	CO conv., % 1	CO conv., % 2	Energy kcal./ g.mole	Time interval, hr.
CRC-6-A-9	24.8	8.0	310.0	321.6	93.4	164.7	1.70	3.00	33.48	0.2
CRC-6-A-10	24.8	8.0	321.6	332.2	164.7	269.9	3.00	4.89	33.31	.2
CRC-8-A-2	24.8	8.1	334.4	312.2	92.6	29.0	1.22	0.38	36.90	.5
CRC-8-A-3	24.8	8.1	312.2	334.4	29.0	93.7	0.38	1.24	37.26	1.0
CRC-9-A-2	24.8	8.2	332.2	298.3	396.0	87.9	8.21	1.72	30.53	0.5
CRC-9-A-3	24.8	8.2	298.3	310.0	87.9	162.6	1.72	3.21	34.91	.3
CRC-9-A-4	24.8	8.2	310.0	321.1	162.6	266.6	3.21	5.42	30.64	.3
CRC-9-A-5	24.8	8.2	321.1	332.7	266.6	451.4	5.42	8.82	32.29	.3
CRC-9-B-3	24.8	8.2	298.8	309.4	44.8	86.5	0.65	1.21	41.23	.6
CRC-9-B-4	24.8	8.2	309.4	321.1	86.5	147.8	1.21	2.05	31.54	.3
CRC-9-B-5	24.8	8.2	321.1	332.7	147.8	228.6	2.05	3.17	26.73	.3
CRC-10-A-3	24.8	8.0	299.4	311.6	76.0	121.7	1.52	2.45	25.61	.6
CRC-10-A-4	24.8	8.0	311.6	321.6	121.7	210.4	2.45	4.21	37.84	.4
CRA-9-B-3	11.2	7.9	334.4	321.6	54.3	33.0	4.47	2.80	28.07	.3
CRA-9-B-4	11.2	7.9	321.6	332.7	33.0	50.1	2.80	4.28	26.98	.5
CRC-17-A-5	28.2	2.9	321.6	332.7	121.7	199.5	2.32	3.79	31.88	.8
CRA-9-B-5	11.2	7.9	332.7	345.0	50.1	72.3	4.28	6.04	22.29	.4
CRC-18-A-2	18.0	3.0	333.3	300.0	203.0	55.9	4.28	1.15	26.69	.8
CRA-9-B-7	11.2	7.9	345.0	333.3	61.5	49.1	5.13	4.10	14.38	.8
CRC-18-A-4	18.0	3.0	300.0	311.1	102.4	176.8	2.11	3.65	32.71	1.0
CRA-9-B-8	11.2	7.9	333.3	311.1	49.1	20.9	4.10	1.75	26.97	0.7
CRC-18-A-5	18.0	3.0	311.1	321.1	176.8	223.0	3.65	4.59	16.01	.8
CRA-9-B-9	11.2	7.9	311.1	333.3	20.9	50.1	1.75	4.18	27.64	.5

rate determinations presented by F.P.E. (their Fig. 3) were made with the same catalyst and at the same temperature as several of the determinations presented in Table I and Fig. 3 of this article. A value for k_2 of $^1/_6$ hr.$^{-1}$ was determined for this catalyst at 297° as reported previously. The calculation of $A_2 - A_1$, from these data is summarized below

Identification	Catalyst	r_{ss}^+ g. mole CO conv./ kg. Fe hr.	r_0^+ g. mole CO conv./ kg. Fe hr.	$A_2 - A_1$, kcal./ g. mole
CRA-20-C	A	612	171	+26.5

It will be noted that the value of $A_2 - A_1$ thus determined differs little from the value of A_3 previously reported (+29 kcal./g.mole). Combination of equations 23 and 25 and rearrangement yield

$$r_{ss}^+ = r_{ss}^- \exp[(A_3 - (A_2 - A_1))/R\tau] \quad (27)$$

Therefore, this analysis predicts that temperature change has a very slight effect on the steady-state rate of hydrogenation of carbon monoxide using this particular catalyst. The data that are available (Table I) support this conclusion.

It is possible to estimate a value of A_2 from the data obtained at different temperature levels presented in Fig. 3 and Table I. However, very little accuracy is obtained in such a calculation. This is illustrated by the black line on Fig. 3 which fits the data very well but uses a constant value of $^1/_6$ hr.$^{-1}$ for k_2 at all temperature levels. Other data used in determining the line on Fig. 3 are

$$A_2 - A_1 = +26.5 \text{ kcal./g.mole}$$
$$A_3 = +29 \text{ kcal./g.mole}$$

The vertical location of the curve was established by setting r_0^+ at $t = 0$ equal to 173 g.mole CO conv./kg. Fe hr.

Similar agreement was obtained in analyzing the other data presented in Table I. Values of $A_2 - A_1$ calculated from these data using the same value for k_2 agreed within ± 5 kcal./g.mole with the value reported above.

The last two rates reported for experimental group CRC-18A fell markedly below those predicted using the activation energies listed above. A statistical analysis was made using data obtained from the 103 similar measurements which were reported previously. It is concluded within 97% confidence limits that the last two rates in group CRC-18A are in error.

Results and Conclusions

(1) Equations based on the proposed reaction mechanism reproduce all experimentally observed effects of temperature, pressure and H_2/CO ratio and are adequate for correlation of the experimental results.

(2) Provisional values of activation energies for the reaction rate coefficients of both the catalyst reactions and the hydrogenation reaction as defined by equation 1 and 4 are

$$A_2 - A_1 = +26.5 \text{ kcal./g.mole}$$
$$A_3 = +29 \text{ kcal./g.mole}$$

Accurate individual values for A_1 and A_2 cannot be estimated from the data available.

Acknowledgments.—The author wishes to thank the Pan American Petroleum Corporation for permission to publish the data appearing in this article. The financial support of the Socony Mobil Corporation during final preparation of this article is appreciated. The University of Oklahoma donated the use of the IBM 650 computer for the statistical evaluation of activation energies. Professor F. C. Morris prepared the figures.

STUDIES ON THE ANODIC AND CATHODIC POLARIZATION OF AMALGAMS. PART II. MERCURY IN AMMONIUM HYDROXIDE SOLUTIONS

By A. M. Shams El Din, S. E. Khalafalla and Y. A. El-Tantawy

Contribution from the Chemistry Department, Faculty of Science, Cairo University, Egypt

Received July 14, 1958

Mercury oxidizes anodically in 0.1 *N* ammonium hydroxide solution to give a mercuric amino compound of the probable formula $HgO \cdot HgNH_2 \cdot OH$, the potential determining compound being, however, the mercury oxide constituent of the compound. The anodic oxidation is governed by diffusion laws as in the case of sodium hydroxide solutions (Part I). At later stages of polarization, ammonia is oxidized to nitrite and nitrate at a considerable overvoltage. The cathodic reduction of the amine is coulombic in nature. The difference in the log i–log τ curves for the anodic and cathodic experiments enabled the determination of the diffusion coefficient of the diffusing ion. The value obtained, 1.35×10^{-7} cm.^{2} sec.$^{-1}$, suggest that OH^- or ion $O^=$ is the diffusing species and not the mercuric ion.

The object of the present paper is to describe the anodic behavior of mercury in ammonium hydroxide solutions. No previous work on mercury from the present standpoint has been reported.

Experimental

The electrical circuit used and the electrolytic cell were essentially the same as described in Part (I).[1] One tenth *N* ammonium hydroxide solution was prepared from a B.D.H. brand stock solution by proper dilution. The experimental technique used for obtaining anodic, cathodic and decay time–potential curves is practically the same as described in part I.[1] The solution in the cell was deoxygenated by bubbling pure hydrogen through it. Before being introduced, the purified gas was made to pass through 3 bubblers containing the same solution as that in the electrolytic cell. Each experiment was carried out on a new electrode and a fresh solution. To reduce any probable oxide present on the surface of the metal, the electrode was subjected to precathodization for a period of 5 minutes at the current at which the experiment was to be performed. Measurements were carried out at room temperature of 25 ± 2°.

Measurements of Oxide Potentials of Mercury.—In order to clarify the nature of the anodic products obtained on the mercury electrode, the potentials set up by the different oxides and oxi-compounds of mercury were directly measured. We have prepared the grey and white mercuric amine compounds[2] by the addition of ammonia to mercurous and mercuric nitrate solutions, respectively. Mercurous nitrate (B.D.H.) was used in preparing the grey variety. Mercuric nitrate solution was obtained by oxidizing the mercurous solution by means of concentrated nitric acid. This solution gave on the addition of dilute ammonia the white precipitate of mercuric amine nitrate. The black precipitate obtained upon the addition of sodium hydroxide to mercurous nitrate solution and ascribed to be mercurous oxide[3] also was prepared. The precipitates were filtered through a sintered glass crucible, washed till ammonia or alkali free, and then dried at 110° to constant weight. For the measurement of their potentials when in contact with mercury, the electrode was completely covered with the oxide or oxi-compound under investigation and then immersed in the solution which was previously deaerated by hydrogen. Measurements were carried out in 0.1 *N* sodium hydroxide as well as 0.1 *N* ammonium hydroxide solutions.

Results and Discussion

In Fig. 1 are shown anode potential–time curves for mercury in 0.1 *N* ammonium hydroxide solution. The currents used varied between 25 and 100 μa./electrode. The curves in Fig. 1 show two steps before the potential of oxygen evolution was attained. Along step (a), the metal was found to lose its luster and acquire a dark silvery appearance that increased in intensity with increase in the polarization time. The potential of this step was not definite and depended on the polarizing current used. A plot of this potential against the polarizing current yielded a straight line denoting the presence of an iR drop in the measured potentials. Extrapolation of this straight line to zero polarizing current gave the value of +0.31 v.

The products of reaction of mercury salts with ammonia and alkali hydroxides are not known with certainty. According to Treadwell and Hall,[2] the addition of ammonium hydroxide solution to a solution of mercuric nitrate will lead to the formation of a white precipitate of mercuric aminonitrate of the formula

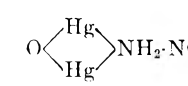

Mercurous nitrate solutions also give the same product together with finely divided mercury which imparts a black color to the precipitate. Sodium hydroxide solution, on the other hand, will react with mercurous salt solution to give a dark grey precipitate claimed by the same authors to be mercurous oxide Hg_2O. X-Ray examination of this precipitate, however, showed only mercury and mercuric oxide.[4] The static potentials obtained when these forms of oxides and oxisalts were placed in contact with metallic mercury are reported in Table I. The values obtained with the red and yellow mercuric oxides are also included for comparison.

Table I

Static Potentials of the Different Oxides of Mercury in 0.1 *N* Sodium and Ammonium Hydroxide Solutions

Oxide	Potential measd. against the normal hydrogen electrode—In 0.1 *N* NaOH	In 0.1 *N* NH_4OH	Remark
$Hg_2(NO_3)_2$ + NH_4OH	+0.220	+0.290	Dark grey
$Hg_2(NO_3)_2$ + NH_4OH	+ .220	+ .310	White
$Hg_2(NO_3)_2$ + NaOH	+ .220	+ .300	Dark grey
HgO	+ .190	+ .145	Red
HgO	+ .220	+ .150	Yellow
Calcd. Hg/HgO	+ .180	+ .270	From thermal data

(1) A. M. Shams El Din, S. E. Khalafalla and Y. A. El Tantawy, This Journal, **62**, 1307 (1958).

(2) F. D. Treadwell and W. T. Hall, "Analytical Chemistry," Vol. I, John Wiley and Sons, Inc., New York, N. Y., 1948, p. 106, 121.

(3) Reference 2, p. 106.

(4) W. M. Latimer, "The Oxidation States of the Elements and their Potentials in Aqueous Solutions," Prentice-Hall, Inc., New York, N. Y., 1953, p. 175.

This table represents some interesting results. Thus, in sodium hydroxide solution, all the different types of the oxide gave almost the same potential which is that of the Hg/HgO system at this *p*H value. From this result it could be concluded that the dark grey precipitate obtained by the addition of sodium hydroxide to a mercurous salt solution is not mercurous oxide, as was claimed by Treadwell and Hall,[3] but mercuric oxide and finely divided mercury.[4] Also, the fact that both the grey and the white forms of the amino compounds give the same potential, supports the conclusion that they do not differ radically from each other. That both compounds give the potential of the Hg/HgO system at this *p*H value strongly suggests that the oxide constituents of these compounds is the potential determining factor. This conclusion, therefore, supports an open formula of the type HgO·$HgNH_2OH$ rather than the cyclic formula.[2] The potential developed with the white and the grey forms of the amino-compound in 0.1 *N* ammonia solution is found to agree satisfactorily with that developed with the freshly precipitated mercuric oxide and the calculated value of the Hg/HgO system at this *p*H value. This again supports the conclusion that the oxide constituent of the amine is the potential determining compound. The red and the yellow forms of mercuric oxide, in the ammonia solution, gave potentials which were considerably lower than expected. The reason for this behavior is not yet fully understood but may be due to a slower rate of saturation of the metal solution interface with mercuric oxide, since aged oxides are known to be less soluble than fresh ones.[5]

State (b) in the anodic polarization curves has no definite potential but depends on the value of the polarizing current. The potential of this step does not coincide with any of the known oxidation potentials of mercury in aqueous ammonia solutions. This together with the fact that no corresponding step was obtained in either the cathodic or the anodic-decay curves, Fig. 3, which do not show a step corresponding to the process taking place at stage (b), supports the conclusion that the oxidation during this step occurs on the solution side rather than the metal side, and that the oxidation products do not adhere to the mercury surface. Ammonia solutions are known to oxidize on metallic anodes.[6] The oxidation products depend on the electrode material as well as on the presence in the electrolyte of an ammonium salt. In the present study ammonia was found to be oxidized anodically on the mercury electrode giving nitrite and nitrate radicals. This was proved as follows. Pure ammonia solution contained in a narrow cup having mercury as the anode was subjected to anodic oxidation for 3.5 hours using 1 ma./electrode. Spot tests for both nitrite and nitrate proved the existence of these ions in solution. The test for nitrite consisted of spraying a Whatman No. 1 filter paper strip carrying spots of the oxidized solution with a

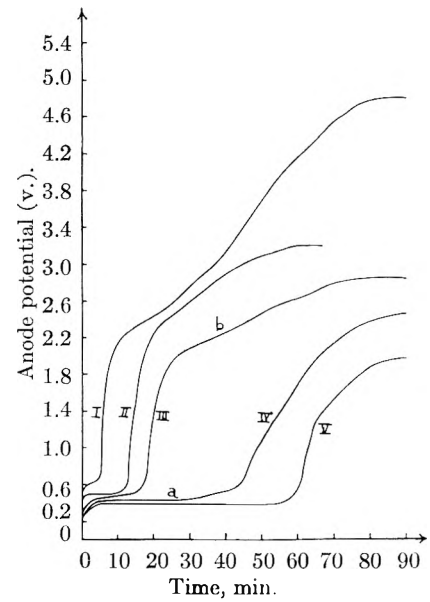

Fig. 1.—Anodic potential–time curves for mercury in 0.1 *N* ammonium hydroxide solution: I, 100 μa./electrode; II, 75; III, 50; IV, 35; V, 25.

solution of 0.5% brom thymol blue in ethyl alcohol.[7] A pale green color developed denoting the presence of nitrite. A blank experiment with ammonia not subjected to oxidation failed to give the color. The test for nitrate was done by spraying a strip of filter paper carrying spots of the oxidized solution with a dilute solution of ammoniacal silver nitrate. This was followed by drying in an air-oven whereby the whole strip turned brown except for where the spots of the ammonia solution were introduced. Again, a blank experiment did not show the test. These experiments indicate that the break in the potential–time curves corresponds to the oxidation of the ammonium ion to both nitrite and nitrate. Such an oxidation process is believed to be highly irreversible. This was ascertained by calculating the theoretical potentials necessary for these reactions to occur, and comparing them with the experimentally observed values. By taking the free energy of the ammonium ion as −19.00 kcal./mole, and those of OH^-, NO_2^-, NO_3^- and H_2O as, respectively, −37.595, −8.25, −26.43 and −56.69 kcal./mole[8]; the free energy change in the reactions

$$NH_4^+ + 8OH^- = NO_2^- + 6H_2O + 6e$$
$$NH_4^+ + 10OH^- = NO_3^- + 7H_2O + 8e$$

were calculated to be −28.63 and −28.31 kcal., hence, $E^0_{OH^-,\ NH_4^+,NO_2^-}$ and $E^0_{OH^-,NH_4^+,NO_3^-}$ would be +0.207 v. and +0.154, respectively. Taking the ionization constant of NH_4OH as $1.8 + 10^{-5}$,[9] the concentration of OH^- ion in solution was calculated to be 1.34×10^{-3} (*p*H 11.1). Assuming the concentration of NH_4^+ to be equal to that of NO_2^- and NO_3^- at the electrode surface, the above equations lead to

(5) Cited in I. M. Kolthoff and N. H. Furman, "Potentiometric Titrations," John Wiley and Sons, Inc., New York, N. Y., 1947, p. 223, 225; I. M. Issa, S. E. Khalafalla and E. A. Sadek, *Rec. trav. chim.*, **74**, 1506 (1955).

(6) S. Glasstone and A. Hickling, "Electrolytic Oxidation and Reduction," Chapman and Hall, London, 1935, p. 366.

(7) This test is developed by Dr. I. I. M. Elbeih of this Department, to whom the authors are thankful.

(8) Reference (4) p. 38, 90.

(9) L. P. Hammett, "Solutions of Electrolytes," McGraw-Hill Book Co., Inc., New York, N. Y., 1936, p. 65.

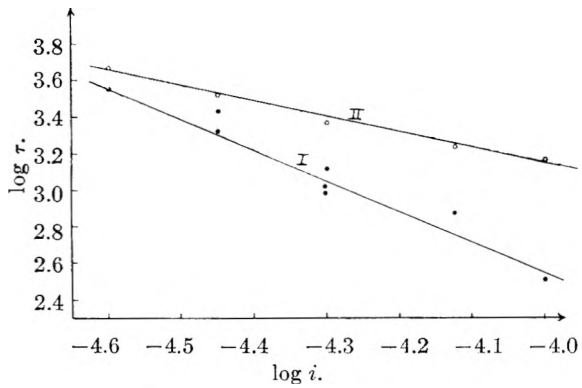

Fig. 2.—Variation of log τ with log i for the mercury electrode: I, anodic process; II, cathodic process.

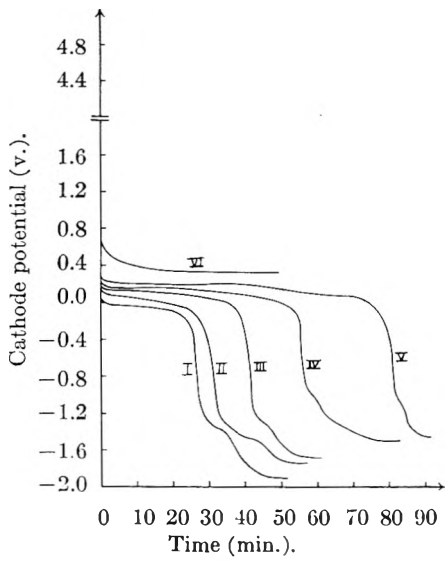

Fig. 3.—Cathodic curves for the reduction of the mercury amino complex: I, 100 μa./electrode; II, 75; III, 50; IV, 35; V, 25; VI, anodic-decay curve.

$$E_{NH_4^+,\ NO_2^-} = E^0 + \frac{0.06}{6}\log(1.34 \times 10^{-3})^{-8}$$

$$E_{NH_4^+,\ NO_3^-} = E^0 + \frac{0.06}{8}\log(1.34 \times 10^{-3})^{-10}$$

which gives the values of +0.44 and +0.37 v. for the above two reactions, respectively. These potentials are very far from those observed experimentally (~2 v.) for the break in the potential–time curves, supporting the conclusion of a considerable overvoltage for the oxidation process or possibly a different mechanism for the oxidation process.

It is of interest to remark here that Sand's equations for diffusion under conditions of constant flux[10] hold for the oxidation of mercury in ammonia solutions.[1] A plot of log τ *versus* log i is shown in curve (1) Fig. 2. The experimental points fall around a line whose slope is −1.7. This value is not far from that predicted from the equation

$$i\tau^{1/2} = \frac{nFCD^{1/2}\pi^{1/2}}{2} \qquad (1)$$

where τ is the passivation time, n is the number of electrons involved in the reaction, D is the diffusion coefficient of the diffusing species and the rest of the terms have their usual physico-chemical significance. The deviation from the expected value may be due in part to the complex reactions occurring at the surface of the electrode, and in part to slight irreproducibility in the yield of this step.

Figure 3 represents some cathodic curves for the reduction of the mercury amino complex. The potential at which reduction commenced was again found to depend on the polarizing current. A plot of this potential against the polarizing current gave a straight line, which when extrapolated to zero current, gave the potential of +0.31 v. This value is the same as that obtained from a similar curve for the anodic potentials and represents, therefore, the true oxidation–reduction potential of this system. The process of reduction proceeded with a decrease in the thickness of the film, and when practically all the oxide was reduced, the potential changed to more negative values. A pale transparent film persisted on the surface of the metal thus exhibiting a definite break in the potential–time curve until it finally ruptured. During this halt in potential, the surface of the electrode was found to be subjected to a very faint vibrational motion which is not as strong as the violent motion observed in sodium hydroxide solutions (Part I). The potential was also fairly constant, save for an oscillation of amplitude ~0.01–0.05 v. for a short duration. When this film finally broke up, the potential changed to hydrogen (and ammonium) deposition values.

A comparison between the times taken in the formation and reduction of the mercury amino compound at corresponding currents showed that the reduction process required longer times. This was thought to be due either to a difference in the rates of oxidation and reduction of the film, or to a further thickening of the film during advanced stages of anodic polarization. To determine which of the two factors was responsible for this behavior, the following experiment was conducted: anodic polarization of the mercury anode in 0.1 N ammonia solution was allowed to proceed with a current of 50 μa./electrode until the amino compound was formed. When the potential started to change to more positive values polarization was reversed to reduce the film. Under these conditions, the quantity of electricity necessary to reduce the oxide was found to be exactly that consumed in the oxidation process. This result proved that the difference between the times of formation and reduction of the amino compound was due to a secondary thickening of the film during advanced stages of polarization.

A log τ *vs.* log i plot for the reduction process is shown by curve (2) in Fig. 2. The slope of the line obtained is only one-half of that of the anodic curve (−0.84). The fact that this value could be roughly approximated to −1 strongly suggests that the process of reduction is mainly coulombic in nature. Thus, according to Faraday's law, the reduction per unit area will be given by $Q = i\tau = nFC\delta$, where C is the concentration of the reducible species and δ is the thickness of the amino compound film. The log τ *vs.* log i plot, therefore, should give a straight line with a slope of −1 and makes an intercept at log $i = 0$ of log $nFC\delta$. On the other hand the log τ *vs.*

(10) H. J. Sand, *Phil. Mag.*, **1**, 45 (1901).

log i plot for the oxidation process (which is diffusion controlled), would make an intercept at log $i = 0$ of 2 log $nFCD^{1/2}\pi^{1/2}/2$. Therefore,

$$[\log \tau_{\text{anodic}} - 2 \log \tau_{\text{cathodic}}]_{\log i=0}$$

will be equal to 2 log $D^{1/2}\pi^{1/2}/2\delta$, which enables the determination of the diffusion coefficient of the species diffusion through the amino complex, if δ is known. From experiments conducted at 75, 100, and 125 μa./electrode, an average value of 0.025 $\pm$ 0.001 cm. for δ was measured optically by means of a cathetometer. The intercept of the anodic curve was found to be -4.17 while that of the cathodic line was -0.20. Therefore, D was calculated to be 1.35×10^{-7} cm.^{2} sec.$^{-1}$.

Diffusion coefficients of metal atoms through their oxides at room temperature were calculated to range between 10^{-35} and 10^{-50} cm.^{2} sec.$^{-1}$.[11]

(11) M. T. Shim and W. J. Moore, *J. Chem. Phys.*, **26**, 802 (1957); E. A. Secco and W. J. Moore, *ibid.*, **26**, 942 (1957).

Although our value of 1.35×10^{-7} cm.^{2} sec.$^{-1}$ is not free from error due to the deviation of the slopes of the anodic and cathodic curves from their expected values, yet it is considerably larger than those for metal cations. This eliminates the possibility for the mercurous ion to be the diffusing species.

It is therefore suggested that the diffusing species during the anodic passivation of mercury is either oxygen or hydroxyl ions. A similar conclusion was reached at by Okamoto, Kabota and Nagayama[12] in their investigation on the corrosion of iron. These authors reported that oxygen is the diffusing species through the oxide. The above conclusion is further substantiated by the experimentally observed fact that the thickening of the oxide film proceeds from the inside rather than from the outside surface as indicated in part (I)[1] of this series.

(12) G. Okamoto, H. Kabota and M. Nagayama, *J. Electrochem. Soc. Japan*, **22**, 18 (1954).

THE ELECTRONEGATIVITY OF GROUPS

BY A. F. CLIFFORD

Contribution from the Richard Benbridge Wetherill Laboratory of Chemistry, Purdue University, Lafayette, Indiana

Received September 2, 1958

The electronegativity relationships presented in a previous paper have been consolidated and regularized to give the general relationship for all covalent substances $MX_n(s)$ yielding ions in water solution, $pK_{sp}/(1 + n) = 14.8 - 8.5\Delta x$, where n is 1 to 4, X is any uninegative group and Δx is the difference in electronegativity between M and X. Likewise, for dinegative groups in M_mX_n, the relationship is $pK_{sp}/(m + n) = 48.7 - 37.5\Delta x$. Each negative group except OH has been found to have a characteristic group electronegativity, usually close to the average of the electronegativities of its individual atoms, which is constant in compounds with metals of varying valence. The apparent electronegativity of OH decreases with increasing metal valence but is constant for constant valence. Group electronegativities for positive groups have also been determined and have been found to approximate the electronegativity of the metal in the group.

Although much work has been done on the relative electron-withdrawing power of organic groups and inorganic groups (such as $-NO_2$) frequently associated with organic compounds, very little attempt has been made to estimate the group-electronegativities of inorganic groups, although there are some data in the literature from which inferences can be drawn. Thus, when the halogen is found to constitute the negative end of the NCBr molecule, but the positive end of the ICN molecule, it must be assumed that the electronegativity of the covalent cyano group lies between that of bromine (2.8) and that of iodine (2.5). It is interesting to note that the average (2.75) of the electronegativities of carbon (2.5) and nitrogen (3.0) does in fact lie between these two values. Likewise[1] from the hydrolysis of NO_2Cl which yields HOCl and HNO_2, it may be inferred that the NO_2 group is more electronegative than Cl (average of NO_2 = 3.33). The hydrolysis of NOCl to HCl and HNO_2 cannot be taken as evidence that the NO group is less electronegative than Cl, since, if HOCl and HNO were formed, reaction between them would be expected to produce HCl and HNO_2. Since in a previous paper[2] it was shown that for insoluble binary substances of considerable covalent character, the solubility in water solution to give ions obeys the relationship

$$pK_{sp} = A - C\Delta x$$

where Δx is the difference in electronegativity between the elements in the binary compound and A and C are constants for any given series of substances, it was felt that for polyatomic inorganic groups forming insoluble "salts" of sufficiently covalent character a similar relationship might hold which would give a good indication of the electronegativities of the groups.

The justification given in ref. 2 assumed that for the relationship between pK_{sp} and Δx to be linear, Δx must be less than 0.5. Nevertheless, abundant evidence was offered that the linearity of the relationship held for metal hydroxides in which the Δx between the metal and oxygen was as much as 1.5. However, if it be realized that in actual fact the more electronegative species is the hydroxyl group with an electronegativity characteristic of the group and considerably less than that of oxygen itself, the discrepancy becomes much less.

The Insoluble Halides and Hydroxides.—From the discussion in ref. 2, it can be seen that for the dihydroxides and dihalides for which the data are the most abundant the functions for the relation-

(1) E. S. Gould, "Inorganic Reactions and Structure," Henry Holt and Co., Inc., New York, N. Y., 1955, p. 241.

(2) A. F. Clifford, *J. Am. Chem. Soc.*, **79**, 5404 (1957).

ships between pK_{sp} and Δx differ only in the intercepts, the slopes being almost identical. Consequently, by eliminating the data for $Pt(OH)_2$, $Be(OH)_2$ and $Sn(OH)_2$, it is possible to reconcile the data for both groups of compounds by means of equation 1

$$pK_{sp} = 46.4 - 24.4\Delta x \quad (1)$$

the electronegativity of the hydroxyl group being 2.75.

In the same way, if the data for the cuprous compounds (as well as AuCl and AuI) be rejected, the relationship for all compounds MX becomes

$$pK_{sp} = 29.0 - 18.1\Delta x \quad (2)$$

However, the pK_{sp}'s of the hydroxides (including the alkali hydroxides, which agree unexpectedly well) give the electronegativity of the hydroxyl group as 3.1 in this case. The data for the cuprous halides indicate the electronegativity of Cu(I) to be 1.65, which is more consistent with the value of 1.7 given for Cu(II) in ref. 2. This relationship predicts the pK_{sp}'s for AuCl and AuI to be 12.7 and 22.8, respectively.

The pK_{sp}'s of the trihalides considered in ref. 2 were all calculated from free energy data reported by Latimer.[3] However, since in no single case was the free energy of formation of the trivalent cation (Au^{+3}, Ir^{+3}, Rh^{+3}) known with any accuracy, the pK_{sp}'s used were highly doubtful.

Examination of the data available for the trihalides sufficiently covalent to obey the electronegativity relationship revealed that the auric halides are the most promising. The free energy of Au^{+3} given by Latimer (103.6 kcal. per mole) was calculated by him from the solubility of $Au(OH)_3$ in 0.43 *m* nitric acid as reported by Jirsa and Jelinek.[4] This calculation was made apparently on the assumption that there would be no hydrolysis of Au^{+3} in acid of this concentration. For an element as electronegative as gold, however, this seems a very dubious assumption, and the ion in solution was more probably $AuOH^{+2}$ or even a more highly hydrolyzed species. The pK_{sp} of $Au(OH)_3$ should therefore be larger than that (44.07) given by Latimer.

Examination of the relationship given in ref. 2 for the trihydroxides

$$pK_{sp} = 86.1 - 27.4\Delta x \quad (3)$$

reveals that the only trihydroxide falling far off the line is $Au(OH)_3$, and that because of too small a pK_{sp}. If $Au(OH)_3$ be now placed on the line with the other $M(OH)_3$'s, its pK_{sp} becomes 53.0. Now accepting the Bureau of Standard's value[5] for the free energy of formation of $Au(OH)_3$ (−69.3 kcal. per mole), the free energy of formation of Au^{+3}(aq) becomes 116.1 kcal. per mole. The pK_{sp}'s of the auric halides calculated from this value are given in Table I.

The pK_{sp}'s of $BiCl_3$ and $IrCl_3$ were calculated in the same manner by fitting $Bi(OH)_3$ and [$^1/_2$ Ir_2O_3 + $^3/_2$ H_2O] to eq. 3 to obtain the ΔF_f^0's for Bi^{+3} and Ir^{+3}. The free energy of formation of $TiCl_3$ was calculated from the heat of formation given by Woolf[6] and the $(\Delta F - \Delta H_{298})/T$ value of Brewer.[7]

TABLE I

FREE ENERGIES OF FORMATION AND CALCULATED pK_{sp} VALUES FOR THE AURIC HALIDES

AuX_3	ΔFf^0	pK_{sp}
$Au(OH)_3$	−69.3[a]	53.0
AuF_3	−69.6[b]	−9.4
$AuCl_3$	−11.6[c]	24.5
$AuBr_3$	− 5.9[c]	35.4
AuI_3	16.3[d]	46

[a] Reference 5. [b] A. A. Woolf[6] gives ΔH_f^0 = −83.3 kcal. per mole for AuF_3. The free energy was calculated from the free energy function given by Brewer.[7] Since the complex fluoride AuF_4^- has been shown[8] to be covalent, inclusion of AuF_3 as a "covalent" halide was deemed justified. [c] Reference 3. [d] By comparison with other noble metal halides Brewer's estimate[7] of −14 kcal. per mole for ΔH_{298} for AuI_3 seems too high. Consequently a value of −20 kcal. per mole was used with Brewer's free energy function to calculate ΔF_{298}^0 and the pK_{sp} for AuI_3 given in Table I.

From these values the electronegativity relationship for MX_3 is calculated to be

$$pK_{sp} = 52.9 - 35.5\Delta x \quad (4)$$

Fitting the pK_{sp}'s of the trivalent hydroxides to eq. 4 gives an electronegativity value of 2.15 ± 0.02 for the hydroxyl group in $M(OH)_3$.

Because of the paucity of good data on either the halides or the hydroxides of the tetravalent elements, the treatment of the substances MX_4 can be only highly approximate. (The relationship given in ref. 2 was assumed to be invalid in view of the electronegativities for Th(IV) and U(IV) given by Gordy and Thomas[9] which differed appreciably from those used in ref. 2.) The K_{sp}'s of $Sn(OH)_4$, $U(OH)_4$ and $Th(OH)_4$ were accepted as given by Latimer.[3] From the free energy for $Pd(OH)_4$ and the potential for the Pd^{+2}–Pd^{+4} couple given by Latimer the pK_{sp} of $Pd(OH)_4$ was calculated to be 70.2. The pK_{sp} for $Ge(OH)_4$ (*i.e.*, $GeO_2 + 2H_2O$) was calculated from the free energies given by Latimer and the experimental potential for the germanium couples reported by Everest[10] from which ΔF_f^0 for Ge^{+4} was calculated to be −12.0 kcal./mole. From these data, the curve for the tetrahydroxides was calculated to be

$$pK_{sp} = 133.1 - 43.8\Delta x \quad (5)$$

taking $x_{OH} = 3.5$.

In order now to establish the true x_{OH} for this series, and the true value of the pK_{sp} intercept, pK_{sp}'s for some tetrahalides were fitted to the curve. The chlorides, bromides and iodides of germanium family elements could not be used because they are liquid rather than crystalline. The only series of crystalline tetrahalides promising to be covalent enough to obey the electronegativity relationship and for which sufficient data were available were the platinic halides. However, free energies of formation were known neither for Pt^{+4} nor for

(3) W. M. Latimer, "Oxidation Potentials," 2nd Ed., Prentice-Hall, Inc., New York, N. Y., 1952.

(4) F. Jirsa and H. J. Jelinek, *Z. Elektrochem.*, **30**, 286, 535 (1924).

(5) F. D. Rossini, U. S. Bureau of Standards, Research Paper 686, 1934.

(6) A. A. Woolf, *J. Chem. Soc.*, 4694 (1954).

(7) "The Chemistry and Metallurgy of Miscellaneous Materials. Thermodynamics," edited by L. L. Quill, McGraw-Hill Book Co., Inc., New York, N. Y., 1950, Chap. 6, p. 99.

(8) W. Klemm, *Bull. soc. chim. France*, 1325 (1956).

(9) W. Gordy and W. J. O. Thomas, *J. Chem. Phys.*, **24**, 439 (1956).

(10) J. C. S. Everest, *J. Chem. Soc.*, 660 (1953).

$Pt(OH)_4$. From the potentials given by Latimer ΔF_f^0 for PtO_2 was calculated to be -17.5 kcal. From Gordy's electronegativity for platinum (2.1), the pK_{sp} for $Pt(OH)_4$ was calculated to be 71.8 from eq. 5 (for which $x_{OH} = 3.5$). If now the free energy of $Pt(OH)_4$ be taken as equal to the sum of the free energies ($PtO_2 + 2H_2O$), then ΔF_f^0 (Pt^{+4}) = 120.5 kcal. The pK_{sp}'s for $PtCl_4$, $PtBr_4$ and PtI_4 become then 28.1, 40.5 and 68.2, respectively. The electronegativity of the hydroxyl group for the series MX_4 becomes, therefore, 2.15 ± 0.1, the uncertainty arising from the halides. The relationship then becomes

$$pK_{sp} = 75.0 - 43.8\Delta x \qquad (6)$$

The apparent electronegativity of the hydroxyl group is thus seen to change as the valence of the metal with which it is associated changes, being 3.1 ± 0.25 in MOH, 2.75 ± 0.08 in $M(OH)_2$, 2.15 ± 0.09 in $M(OH)_3$ and 2.15 ± 0.1 in $M(OH)_4$ as nearly as it can be established, while the electronegativities of other polyatomic groups appear to remain constant (as is indicated below). A possible explanation for this phenomenon may lie in the fact that, of all the groups studied, the hydroxyl group is the only one which should be capable of extensive pi-bonding with the metal atoms. Since the pi-bonding should increase as the valence of the metal increases, the metal–to–oxygen bond will become less polar more rapidly with increase in valence than the bonds to groups not capable of such extensive multiple bonding. In this study, this will show up as an apparent decrease in the electronegativity of the hydroxyl group. A similar effect might be expected from increasing the electronegativity of the metal while keeping the valence constant. This would result in changing the slope of the pK_{sp} *versus* Δx curves for each valence type from that observed for other negative groups. It may therefore be that for the higher valences, it is a mistake to attempt to put the hydroxides on the same curve as the halides, since the hydroxide curves appear to tend toward somewhat lesser slopes than the halide curves. However, at present there are insufficient data to settle this question.

The Insoluble Chalcogenides.—The revision of the electronegativity value for Cu(I) requires a recalculation of the relationship for the monovalent chalcogenides. The data[3] for Ag_2S, Cu_2S, Tl_2S and Tl_2Se yield the relationship

$$pK_{sp} = 124.8 - 100.0\Delta x \qquad (7)$$

Additional information available for Al_2S_3 and Al_2Se_3,[11] for Bi_2S_3, Bi_2Se_3 and Bi_2Te_3[12] and for In_2S_3[13] also makes possible a re-evaluation of the relationship for the sesquichalcogenides, yielding the relationship

$$pK_{sp} = 235.1 - 171.7\Delta x \qquad (8)$$

The relationship developed for the monochalcogenides in ref. 2 was accepted without change.

$$pK_{sp} = 102.5 - 80.6\Delta x \qquad (9)$$

Comparison of the Relationships.—The constants in equations 2, 1, 4 and 6 and in equations 7, 9 and 8 can now be seen to have an even greater degree of regularity than was indicated in ref. 2. For each series the value of the constants in the individual equations divided by the power of the activities in the corresponding $K_{sp} = (M)^m(X)^n$ equations is essentially constant. Thus a general expression can be written for compounds involving uninegative groups, MX_n, as

$$pK_{sp}/(1 + n) = 14.8 - 8.5\Delta x \qquad (10)$$

and for compounds involving dinegative groups, M_mX_n, as

$$pK_{sp}/(m+n) = 48.7 - 37.5\Delta x \qquad (11)$$

The Electronegativities of Groups.—When the solubilities of the salts of polyatomic ions are examined in the light of the relationships developed above, the ionic groups are found to exhibit remarkably constant electronegativities. From the calculated electronegativities given in Table II, it can be seen that in general the electronegativity of a negative group approximates the average for the atoms in the group, whereas the electronegativity of a positive group approximates that of the metal atom in the group—at least where the group is a well defined one. (The groups BiO^+, SbO^+, TiO^{+2} and ZrO^{+2} undoubtedly do not exist as discrete units and

TABLE II

THE ELECTRONEGATIVITIES OF ELEMENTS AND GROUPS

Radical	Charge on free ion	Av. x	Calcd. x	Standard dev.	No. of data	Gordy's x
H	−1		2.7	0.04	4	2.1
He	0		5.2[a]			
Li	+1		1.4		1	1.0
Be	+2		1.5		1	1.5
B	+3					2.0
C	+4					2.5
CN	−1	2.75	2.6	0.17	5	
CNO	−1	3.0	2.9	.20	2	
N	+3					3.0
N_3	−1	3.0	2.95	.09	4	
NCN	−2	2.8	2.95		1	
NCO	−1	3.0	3.05		1	
$N(CN)_2$	−1	2.8	2.9		1	
$C(CN)_3$	−1	2.7	2.95		1	
NO_2	−1	3.35	3.2	.00	2	
N_2O_2	−2	3.25	2.75		1	
O	−2					3.5
OH^b	−1	2.8	3.1	.25	7	
OH^c	−1	2.8	2.75	.08	15	
OH^d	−1	2.8	2.15	.09	18	
OH^e	−1	2.8	2.15	.1	5	
CHO_2	−1	2.9	3.3	.02	4	
CH_3CO_2	−1		3.3	.08	2	
C_6H_5O	−1		3.1		1	
F	−1		4.0			3.95
Ne	0		4.4[a]			
Na	+1		1.1		1	0.9
Mg	+2		1.3		1	1.2
Al	+3		1.55		1	1.5
Si	+4					1.8
P	−3					2.1
PH_2O_2	−1	2.65	3.15	.15	2	
PHO_3	−2	2.95	2.8		1	
S	−2					2.5

(11) Y. Kaputinski and M. Golutwin, *Bull. Acad. Sci. USSR, Cl. Sci. chim.*, 192 (1951).

(12) G. Gattow and A. Schneider, *Angew. Chem.*, **67**, 306 (1955).

(13) A. J. Thompson, M. F. Stubbs and J. A. Schuffle, *J. Am. Chem. Soc.*, **76**, 341 (1954).

TABLE II (*Continued*)

Radical	Charge on free ion	Av. x	Calcd. x	Standard dev.	No. of data	Gordy's x
S_2	−2	2.5	2.4	.04	5	
SO_2	−2	3.25	2.85	.08	4	
S_2O_3	−2	3.1	2.75	.10	2	
S_3O_6	−2	3.2	3.05		1	
NCS	−1	2.7	2.9	.02	5	
Cl	−1					3.0
ClO_2	−1	3.3	3.0	.15	2	
ClO_3	−1	3.4	3.25	.10	2	
A	0		3.8[a]			
K	+1		0.85		1	0.80
Ca	+2		1.1		1	1.0
Sc	+3		1.35		1	1.3
Ti	+4					1.6
TiO	+2		2.05		1	
V	+3					1.4
V	+4					1.7
VO	+2		1.75		1	
V	+5					1.9
VO	+3		1.8		1	
VO_2	+1		2.3		1	
Cr	+2		(1.55[f])		1	1.4
Cr	+3		(1.45)		1	1.6
Cr	+6					2.2
Mn	+2		1.4	0.00	2	1.4
Mn	+3		1.65		1	1.5
Mn	+7					2.5
Fe	+2		1.45	.00	2	1.7
Fe	+3		1.7		1	1.8
Co	+2		1.5	.01	2	1.7
Co	+3		1.85	.01	2	
Ni	+2		1.5	.00	2	1.8
Cu	+1		1.65	.02	3	1.8
Cu	+2		1.7	.04	3	2.0
Zn	+2		1.5	.00	3	1.5
Ga	+3		1.65		1	1.5
Ge	+2		1.7		1	
Ge	+4		1.75		1	1.8
As	+3					2.0
AsO	+1		2.3		1	
$(CH_3)_2AsO_2$	−1		3.15		1	
Se	−2		2.4	.04	7	2.4
SeCN	−1	2.6	2.6		1	
SeO_3	−2	3.2	2.8	.14	10	
Br	−1					2.8
BrO_3	−1	3.4	3.15	.14	3	
Kr	0		3.3[a]			
Rb	+1		0.8		1	0.8
Sr	+2		1.0		1	1.0
Y	+3		1.15		1	1.2
Zr	+4					1.5
ZrO	+2		1.9		1	
Nb	+5					1.7
Mo	+4					1.6
Mo	+6					2.1
Tc	+5					1.9
Tc	+7					2.3
Ru	+3		2.0		1	2.0
Rh	+3		2.1		1	2.1
Pd	+2		2.1		1	2.0
Pd	+4		2.1		1	
Ag	+1					1.8
Ag	+2		2.15		1	
Cd	+2		1.5	0.02	3	1.5

TABLE II (*Continued*)

In	+3		1.6	0.08	2	1.5
Sn	+2		1.55		1	1.7
Sn	+4		1.75		1	1.8
$(CH_3)_3Sn$	+1		1.75		1	
$(C_2H_5)_3Sn$	+1		1.75		1	
Sb	+3		1.8		1	1.8
SbO	+1		2.45		1	
Sb	+5					2.1
Te	−2		2.25	.01	3	2.1
TeO_2H	+1		2.4		1	
I	−1		2.5			2.55
IO_3	−1	3.25	3.05	.17	12	
Xe	0		3.0[a]			
Cs	+1		0.7		1	0.75
Ba	+2		0.85		1	0.9
La	+3		1.2	.02	2	1.1
Ce	+3		1.2	.01	2	1.1
Ce	+4		1.35		1	
Hf	+4					1.4
Ta	+3					1.3
Ta	+5					1.7
W	+4					1.6
W	+6					2.0
Re	+5					1.8
Re	+7					2.2
Os						2.0
Ir	+3		2.1		1	2.1
Ir	+4		2.1		1	
Pt	+2		2.1		1	
Pt	+4					2.1
Au	+1		2.1		1	
Au	+2		2.2			
Au	+3					2.3
Hg_2	+2	1.9	1.8	.07	9	1.8
Hg	+2		1.9			1.8
CH_3Hg	+1		1.75	.16	4	
C_6H_5Hg	+1		1.85	.11	3	
Tl	+1		1.5	.09	5	1.5
Tl	+3		1.95		1	1.9
$(C_2H_5)_2Tl$	+1		1.35	.15	2	
$(C_6H_5)_2Tl$	+1		1.75		1	
Pb	+2		1.55	.06	4	1.6
Pb	+4		1.95		1	
Bi	+3					1.8
BiO	+1		2.0	.15	2	
Po						2.0
At						2.2
Rn	0		2.8[a]			
Fr	+1					0.7
Ra	+2					0.9
Ac	+3					1.1
Th	+2					1.0
Th	+4		1.35		1	1.4
Pa	+3					1.3
Pa	+5					1.7
U	+3		1.0		1	
U	+4		1.5		1	1.4
U	+6					1.9
UO_2	+2		1.8	.03	2	
Np						1.1
Pu						1.3
PuO_2	+1		1.65		1	
PuO_2	+2		1.7		1	

[a] Calculated from ionization potential and electron affinity. [b] With univalent metals. [c] With bivalent metals. [d] With tervalent metals. [e] With the quadrivalent metals.

[f] From the K_{sp} for $Cr(OH)_2$ given by D. N. Hume and H. W. Stone, *J. Am. Chem. Soc.*, **63**, 1197 (1941), which seems too small. A larger electronegativity for Cr(II) than for Cr(III) is unreasonable. Gordy's values for Cr(II) and Cr(III) are undoubtedly to be preferred.

deviate from this rule.) In the case of the negative groups, the electronegativity falls below the average when the least electronegative atom in the group is directly available for bonding (as in $N_2O_2^{-2}$, IO_3^-, $S_2O_3^{-2}$, etc.), but lies above the average when only oxygen is available, as in $PH_2O_2^-$, PHO_3^{-2}, CHO_2^-, $CH_3CO_2^-$ and $C_6H_6O^-$. This is in agreement with the expectation that the apparent electronegativity of the group will be dominated by the point at which the positive reference group or atom is attached and that the attachment will occur preferentially at the least electronegative atom (when available) for covalent bonding. Since attachment of positive groups to negative reference groups or atoms should occur uniquely at the metal atom for the discrete groups examined, the electronegativity of the group should be determined by that of the metal, again as observed.

The electronegativities of the elements in the valence states studied were recalculated from available experimental pK_{sp}'s and the appropriate equations, taking the average where several data were available. These are listed in Table II along with Gordy and Thomas' values[9] for comparison.

THERMOGRAVIMETRIC ANALYSIS: THE METHOD OF ISOBARIC DEHYDRATION

BY E. ROY BUCKLE*

Department of Chemistry, University of Aberdeen, Scotland

Received September 11, 1958

The influence of the recording technique upon the form of dehydration isobars shows that kinetic factors are important, especially in the interpretation of curves for composite specimens. A "quasi-static" technique is described which is capable of greater resolution than the usual dynamic recording methods. New data, obtained using this technique, are reported for hydrated calcium silicates and related compounds examined in powder form. Decomposition temperatures are given for each compound which are fairly characteristic, although sensitive to the presence of admixed phases. The effect of particle size upon the shape of isobars for powders is probably not noticeable with particles larger than about a micron.

Introduction

Dehydration methods have been used for many years in the study of the structure and the composition of solids. These techniques have generally been applicable to decompositions of all types where at least one of the products is volatile. The course of the reaction is followed by measuring the loss of weight (gravimetric methods), the volume of volatile product (eudiometric methods), or the pressure developed in a closed apparatus (tensimetric methods).

Eitel[1] has reviewed much of the early work, particularly in the field of silicate chemistry. Later developments[2-9] usually have concentrated on closer control of atmosphere or temperature, and on the use of automatic recording and programming.

The method recently used in this Laboratory by Howison[6] is an elaboration of the conventional spring balance technique. In this method the weight of the specimen is measured while it is in the furnace, in a continuous-flow atmosphere of controlled humidity.

In the present study the design of Howison's apparatus and the experimental procedure have been modified, and new data obtained for calcium silicates and related compounds.

Experimental

Dehydration isobar experiments with hydrated calcium silicates are of lengthy duration, and where mixtures are studied,[2,6] may take up to 6 weeks to complete. For this reason 6 dehydration columns have been constructed, and these are used simultaneously in many cases.

Dehydration Columns.—A diagram of the column assembly is given in Fig. 1. The specimen, usually a powder and weighing about 200 mg., is suspended in a platinum bucket at the end of a silica fiber. The fiber hangs in a vitreous silica furnace tube (28 mm. i.d.; 2 ft. long) from a spring of the same material. The spring has a sensitivity of about 25 cm./g., and is supported by a nylon thread in a glass section 2.5 ft. long, adequate tension being maintained in the thread by a stainless-steel weight. The height of the spring and its attachments can be adjusted in the column by winding the thread with a winch made from a solid glass stopcock. This has a circular groove cut opposite the connecting tube, and a constriction in the latter guides the nylon into the groove when the spring assembly is raised. The glass upper section is joined to the furnace tube by a rubber sleeve and a glass spherical joint, which allow easy alignment. The bucket is removed by separating the sections at the spherical joint.

The furnace housing is made from tubular Sindanyo and is screwed to a brass base plate. This carries three levelling screws located with pop-marks in a hardwood shelf. The winding consists of about 10 yd. of 29G Nichrome V wire wound on asbestos paper over the middle 8 in. of the furnace tube. The gap between tube and housing is tightly packed with asbestos wool, and the winding leads connect with brass terminals mounted on the Sindanyo. Current is obtained from a 200-230 volt, 50-cycle a.c. supply, and controlled by a Variac. An equilibrium temperature of about 800° is registered by the chromel–alumel thermocouple when the e.m.f. is 140 volts and the air flow rate about 100 ml. per min.

The over-all length of the column is 5 ft. which allows a

* Chemical Engineering Department, Imperial College, London S. W. 7, England.

(1) W. Eitel, "The Physical Chemistry of the Silicates," University of Chicago, Chicago, Illinois, 1954.

(2) H. F. W. Taylor, *J. Chem. Soc.*, 163 (1953); *Proc. 27th Congress, Industr. Chem.*, **3**, 63 (1954).

(3) E. P. Hyatt, I. B. Cutler and M. E. Wadsworth, *Amer. Ceramic Soc. Bull.*, **35**, 180 (1956).

(4) L. S. Dent, Ph.D. Thesis, Aberdeen, 1957.

(5) E. Calvet, H. Thibon and G. Pialat, *Bull. soc. chim. France*, 225 (1957).

(6) J. W. Howison, Ph.D. Thesis, Aberdeen, 1957.

(7) J. G. Hooley, *Can. J. Chem.*, **35**, 374 (1957).

(8) C. Groot and V. H. Troutner, *Anal. Chem.*, **29**, 835 (1957).

(9) P. D. Garn, *ibid.*, **29**, 839 (1957).

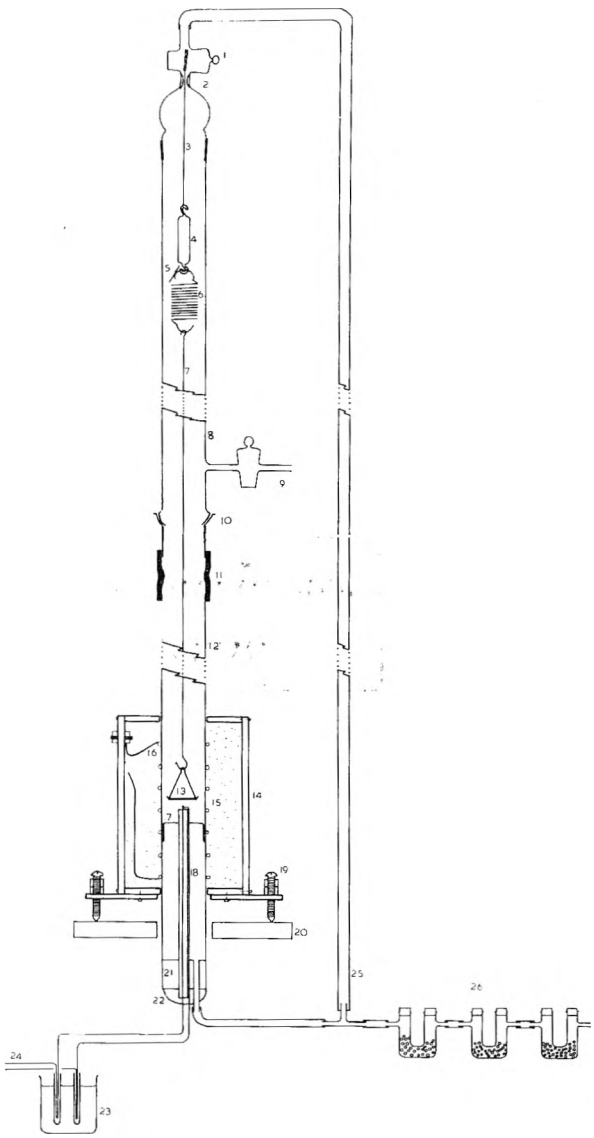

Fig. 1.—Dehydration column: 1, stopcock winch; 2, constriction; 3, nylon thread; 4, tension weight; 5, aluminized cover-slip; 6, silica spring; 7, silica thread; 8, glass column; 9, air inlet; 10, glass spherical joint; 11, rubber sleeve; 12, silica tube; 13, platinum bucket; 14, Sindanyo furnace housing; 15, asbestos wool packing; 16, nichrome element; 17, nickel wire axial guide; 18, chromel/alumel thermocouple; 19, levelling screw; 20, base board; 21, bung; 22, picein wax seal; 23, liquid paraffin cold junction; 24, copper leads to millivoltmeter; 25, convection current bypass; 26, KOH guard-tubes with glass beads.

clearance of 3 ft. between the furnace and the spring, minimizing errors due to heat transfer.

Gas Train.—Air is supplied from a compressor operated by a pressure-sensitive switching device. Pressure is built up in a cast iron reservoir, the air flow from which is controlled by a needle valve. Carbon dioxide and water vapor are removed by lime towers and sulfuric acid bubblers, and the line divides into 6 branches at a manifold. In each of these branches the humidity is adjusted with bubblers containing aqueous solutions. A convenient source of water vapor for general purposes is saturated aqueous calcium chloride, which gives $p(H_2O) = 6.5$ mm. at 23°.

Air flow from the humidifier to the column is adjusted by a screw clip, the air entering at the side-arm and flowing through the apparatus at about 100 ml. per min. It leaves *via* potash guard-tubes, pressure fluctuations due to thermal convection in the furnace being reduced by a by-pass to the top of the column.

The problem of CO_2 contamination when studying calcium silicates makes it vital to ensure adequate seals at all joints in the column. Aging of the rubber connection may cause trouble, especially when the furnace is run for long periods at high temperatures. A liberal coating of stiff grease, such as Apiezon M with magnesia as a filler, is a useful remedy.

Materials.—A number of hydrated calcium silicates and related compounds have been examined in powder form. Particle size varied with conditions of formation but never exceeded 0.2 mm. In some cases material was cryptocrystalline.

Procedure.—When studying calcium silicates the weight of the specimen at a given temperature is followed by cathetometer readings of the spring-length. Where practicable these measurements are made at four-hourly intervals. Whenever the loss of weight over this period falls within experimental error the temperature is increased by 5–10°. The total loss at each temperature is expressed as a percentage of the initial weight of sample taken, and plotted against the thermocouple temperature to give the isobar. The maximum operating temperature, as registered by the thermocouple, is usually about 850°: at higher values the silica furnace tube devitrefies rapidly since its temperature is even higher.

The main experimental error occurs at higher temperatures, and is due to oscillation of the specimen bucket which must be kept clear of the thermocouple to avoid sticking. Limits to the probable experimental error are estimated at ±0.1–0.7%, depending on the weight of the sample. By comparison, buoyancy corrections are negligible for calcium silicates since the true volume of the bucket and about 250 mg. of solid is only 0.1 ml.

Results

Calcium Carbonate.—Reagent grade material was used, and examination by X-rays showed that it consisted entirely of calcite. Pyrolysis was carried out in the usual atmosphere, freedom from CO_2 being ensured by including in the gas train an absorption tube containing self-indicating soda-asbestos. The decomposition temperature depended upon the time interval between successive weighings; as this was increased the decomposition temperature decreased. Typical curves are shown in Fig. 2. Although in each case the onset of reaction was quite sharp, the time required for complete decomposition increased as the decomposition temperature was lowered. At 600° two days was sufficient.

Calcium Hydroxide.—All samples were taken from stock reagents and were contaminated with calcite. The isobars show a two-stage loss (Fig. 3), the first stage being due to water from the hydroxide, and the second to CO_2 from the carbonate. Decomposition temperatures for calcium hydroxide were found to vary considerably, with a given technique, depending on the purity of the sample. For lime present in hydrated tricalcium silicate pastes they ranged from 360 to 410°.

Dicalcium Silicate α-Hydrate.—This was prepared by autoclaving β-dicalcium silicate in aqueous suspension at 160°. The isobar (Fig. 4) shows a rather indefinite decomposition temperature, but most of the water is lost above 400°. Small amounts of calcium hydroxide and tobermoritic material probably account for the loss at lower temperatures. The second step, at 600°, is typical, and is ascribed to retention of the last traces of water by adsorption on the unoriented β-dicalcium silicate formed in the reaction.[10] The total water-loss above 300° was 9.5%, in good agreement with the theoretical value of 9.47 corresponding to the composition $2CaO{\cdot}SiO_2{\cdot}H_2O$.

Dicalcium Silicate γ-Hydrate (Dicalcium Silicate Hydrate C).—Specimens were prepared by autoclaving β-dicalcium silicate suspensions. Figure 5 shows the isobar for a product made at 320°. The first step is attributed to calcite decomposition, and the second to water-loss from the γ-hydrate. There is a suggestion of a third step, poorly resolved, at about 675°. The small loss recorded at 500° was attained by 417°, and possibly represents calcium hydroxide and tobermoritic material. There is evidence[11] that the γ-hydrate is a complex mixture of poorly-crystallized calcium silicate

(10) L. Heller, Proc. 3rd Symp. Chem. Cements, Stockholm, 237 (1952).

(11) E. R. Buckle, Ph.D. Thesis, Aberdeen, 1958.

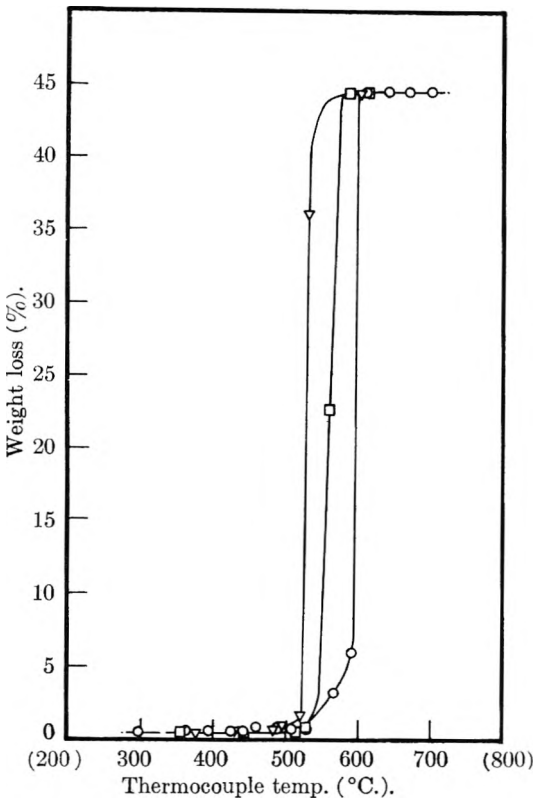

Fig. 2.—Pyrolysis curves for calcite.

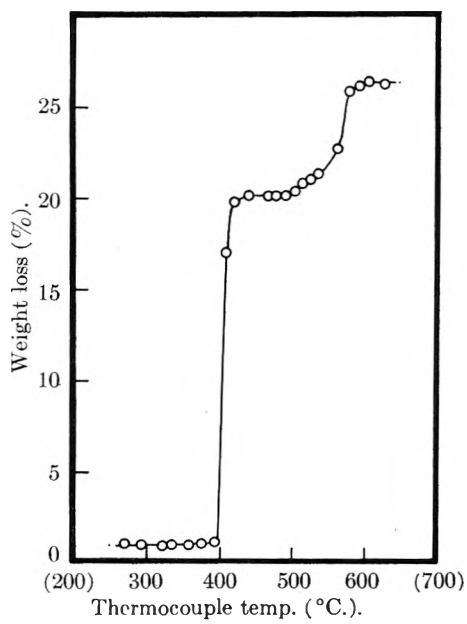

Fig. 3.—6.5 mm. isobar for calcium hydroxide containing calcite impurity.

hydrates, and an analysis of the isobar will not be possible until their nature is elucidated.

Dicalcium Silicate Hydrate D.—Flint, McMurdie and Wells[12] obtained this substance by autoclaving dicalcium silicate α-hydrate with water at 450°, assigning to it the composition $6CaO \cdot 3SiO_2 \cdot 2H_2O$, corresponding to a water content of 6.5%. In the present work the compound was made hydrothermally from β-dicalcium silicate at 350–370°. The isobar (Fig. 6) shows a sharp water-loss of 2.7% at about 630°, corresponding to the dehydration of the silicate.

(12) E. P. Flint, F. McMurdie and L. S. Wells, *Bur. Standard J. Research*, **21**, 617 (1938).

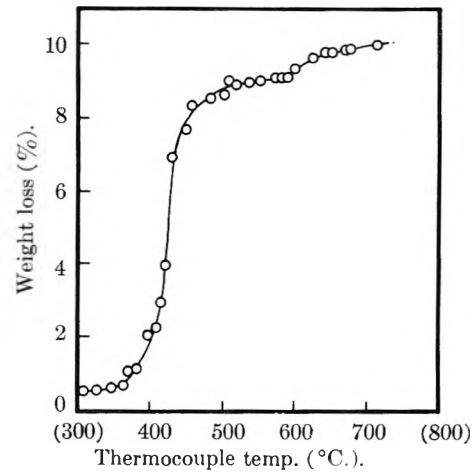

Fig. 4.—6.5 mm. isobar for dicalcium silicate α-hydrate.

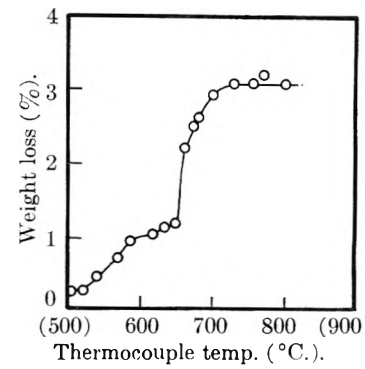

Fig. 5.—6.5 mm. isobar for dicalcium silicate γ-hydrate.

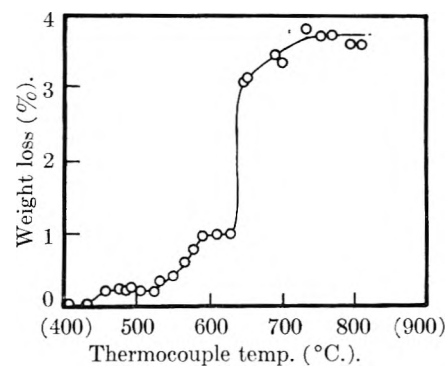

Fig. 6.—6.5 mm. isobar for dicalcium silicate hydrate D.

A small amount of water was lost at about 430° from traces of calcium hydroxide, and the calcite impurity decomposed at about 520°. These results suggest that the water content of dicalcium silicate hydrate D is much less than the value reported by Flint, *et al.*

Other Hydrated Calcium Silicates.—Dehydration isobars for tricalcium silicate hydrate, $6CaO \cdot 2SiO2 \cdot 3H_2O$, calciochondrodite, $5CaO \cdot 2SiO_2 \cdot H_2O$, and calcium silicate hydrate I preparations have already been reported.[13-15] Figure 7 shows dehydration curves for an impure specimen of tricalcium silicate hydrate. Curve A is an isobar recorded using the quasi-static procedure and apparatus described in the present account. Curve B was obtained using a thermobalance. In the latter case the temperature was raised continuously by 4° per min. and no control was exercised over the furnace atmosphere. Resolution is good at the

(13) E. R. Buckle, J. A. Gard and H. F. W. Taylor, *J. Chem. Soc.*, 1351 (1958).

(14) E. R. Buckle and H. F. W. Taylor, *Amer. Min.*, **43**, 818 (1958).

(15) H. F. W. Taylor and J. W. Howison, *Clay Minerals Bull.*, **3**, 98 (1956).

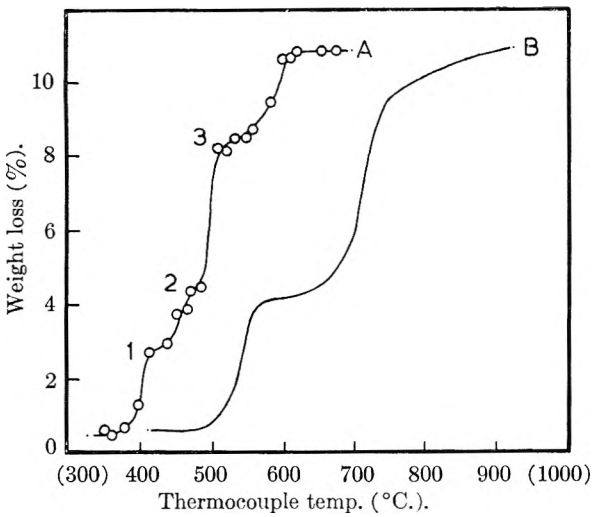

Fig. 7.—Dehydration curves for an impure specimen of tricalcium silicate hydrate: A, 6.5 mm. isobar recorded quasi-statically; B, thermobalance curve recorded at 4° per min.

points marked (1) and (3) on the isobar; at the point marked (2) it is less reliable, although this inflection is a characteristic of isobars for tricalcium silicate hydrate. In the thermobalance curve there appears to be improved resolution at (2) but no trace is found of the inflections at (1) and (3).

Discussion

Phase Rule Considerations.—Early workers in the field of dehydration studies were guided by phase rule theory, with the necessary assumptions of equilibrium and phase homogeneity. Such an approach was thought to be justified by the results obtained with well-crystallized salt hydrates and hydroxides, such as copper sulfate pentahydrate and calcium hydroxide. These compounds gave sharp discontinuities at points in the temperature-composition diagrams corresponding to the release of water vapor. Even so, as pointed out by Taylor,[2] the need for control of humidity in the gas phase was not generally recognized.

Such inconsistencies have remained in recent years despite the development of more precise theoretical knowledge. Ubbelohde[16] has stressed the inadequacy of the classical phase rule as applied to solid–solid transformations. Evidence of "smeared" or continuous transitions is provided by specific heat and specific volume data. This author has pointed out that certain energy terms, due to the presence of internal surfaces and strains characteristic of many solids, are not allowed for in the classical derivation of the phase rule. Inclusion of such terms has the effect of increasing the number of degrees of freedom available to the system.

Although the phase rule predicts sharp decomposition at specific temperatures and pressures, thermal dehydration curves for powders are frequently sigmoid in shape. Rounding of the curve in the early stages of dehydration has long been attributed to the influence of varying particle size upon the equilibrium vapor pressure of the solid. Bigelow and Trimble[17] investigated the vaporization of iodine and sulfur from crystals of various sizes. They found that the effect of crystal size upon vapor pressure predicted by an equation due to Thompson[18] could not be observed and concluded that the surface area effect upon which the theory was based was negligible for particles greater than about a micron. A similar conclusion was reached more recently by Calvet, *et al.*,[5] by comparing the dehydration curves for various hydrated aluminas. From other evidence,[11] however, it seems more likely that the observed rounding is due to a kinetic factor such as spontaneous nucleation.

Irreversibility and Hysteresis.—Weiser and Milligan[19] made the additional suggestion that the rounding of the terminal portion of a dehydration curve might be due to retardation of water-loss by strong adsorption on the dehydration product. With the present apparatus this type of rounding usually is found with decompositions occurring above about 600°. Although it is plausible to attribute small but discrete terminal losses, such as are found with dicalcium silicate α-hydrate (Fig. 4), to this cause, more frequently it is found that the final approach to complete reaction appears to be asymptotic with temperature. With the present, quasi-static procedure this indicates that the reaction is asymptotic with time, due to the slowness of the final stages. Murray and White[20] realized that dehydration would eventually be complete at all temperatures at which clay minerals released structural water, since such processes were known to be irreversible. Nevertheless this asymptotic approach to completion of reaction, occurring at all temperatures above the decomposition point for an irreversible process, appears to have escaped the attention of many investigators of mineral systems, who regard their final losses at each temperature as equilibrium values, in spite of the behavior when reversal of the process is attempted.

The occurrence of hysteresis in isobars for calcium silicate hydrate I minerals was observed by Taylor[2] and others,[21] and indicates irreversibility. Similar effects in the pyrolysis of carbonates are well known[22,23] and lead to so-called "false equilibria."

Rate of Reaction.—Since, for a slow, irreversible process, the extent of decomposition at a given temperature depends on the time of heating, the shape of the isobar is dependent on recording technique, as illustrated by Fig. 7. For a rapid decomposition this may not be so. Thus the curve obtained for pure calcium hydroxide rises so steeply that very few points are obtained corresponding to partial reaction.

The escape of water or other volatile product from a decomposing solid involves a large increase of entropy in the system. This factor outweighs the influence of the enthalpy change so that the

(16) A. R. Ubbelohde, *Quart. Rev.*, **11**, 246 (1957).

(17) S. L. Bigelow and H. M. Trimble, This Journal, **31**, 1798 (1927).

(18) W. Thompson (1888). See, *e.g.*, J. R. Partington, "An Advanced Treatise on Phys. Chem.," Vol. 2, Longmans, London, 1951, p. 265.

(19) H. B. Weiser and W. O. Milligan, *Chem. Revs.*, **25**, 1 (1939).

(20) P. Murray and J. White, *Trans. Brit. Ceram. Soc.*, **48**, 187 (1949); **54**, 137 (1955).

(21) H. Steinour, *Chem. Revs.*, **40**, 391 (1947).

(22) R. M. Caven and H. J. S. Sand, *J. Chem. Soc.*, 1359 (1911).

(23) W. E. Garner, "Chemistry of the Solid State," London, 1956, Chap. 7.

endothermic forward process is possible. The position of equilibrium for a reversible change will depend on the free energy decrease, but if reaction takes place in an open system the recombination process may be so slow that decomposition is virtually complete. Under these conditions isobars for reversible and irreversible decompositions are closely similar, and a single recording technique suffices for both. Preliminary observations on the dehydration kinetics of calcium hydroxide, which will be reported later, indicate that the activation energy is close to the calculated enthalpy change. Reversibility is also indicated by the dissociation pressure experiments of Halstead and Moore.[24]

The quasi-static recording technique described furnishes isobars which are in general steeper than those obtained using "dynamic" methods. For isobars of pure materials the shape of the curve is not important; the extent of the loss is usually all that is required. The recorded loss will not differ appreciably from the true water content provided that the final stages of dehydration are not too slow. In some cases difficulty is experienced in ascertaining the completion of reaction, since loss of water occurs progressively with increasing temperature, at rates which are persistently close to the lower limit of detectability ($k \sim 10^{-7}$, sec.$^{-1}$, with the present technique[11]). This difficulty can sometimes be avoided by altering the recording technique in the final stages of dehydration.

Resolution.—With mixtures the possible complications due to rate factors are both more numerous and more serious. Resolution of processes giving adjacent steps on the isobar may vary with the experimental procedure, as shown in Fig. 7 where the quasi-static run has resolved four steps, and the thermobalance only two.

The influence of recording speed on the resolution of successive steps is indicated in Fig. 8. The first diagram shows the flattening produced in the curve for a slow process by increasing the recording speed. In Fig. 8b a slow process (1) is followed by a rapid one (2), the conditions being conducive to good resolution, *i.e.*, slow recording. Curve 3 represents curve 1 recorded more speedily; the faster process (2) is only slightly changed by increasing the recording speed. The complete isobar (4) has now failed to resolve the two steps. Moreover, any attempt to deduce the height of the first step from the position of a point of inflection, or by

(24) P. E. Halstead and A. E. Moore, *J. Chem. Soc.*, 3873 (1957).

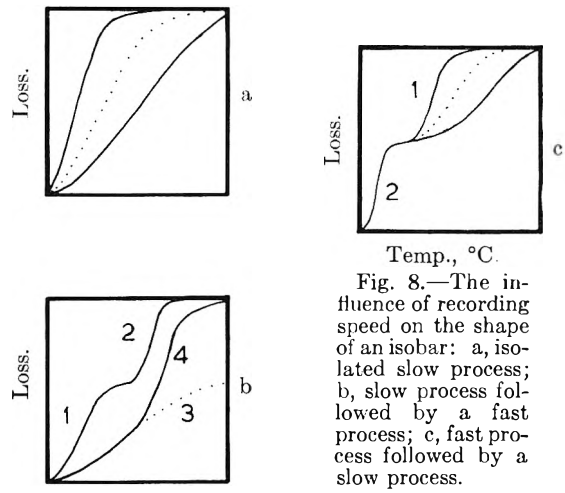

Fig. 8.—The influence of recording speed on the shape of an isobar: a, isolated slow process; b, slow process followed by a fast process; c, fast process followed by a slow process.

drawing tangents, is likely to give inaccurate results. In Fig. 8c the order of the two processes has been reversed, the first curve (2) now representing the faster reaction. The effect of increase of recording speed is to improve the resolution, although in this case any subsequent slow process might not be resolved (Fig. 8b).

It is possible on this basis to suggest an explanation of the curves in Fig. 7. If the relative rates of the various stages in curve A were, successively, slow, fast, slow and fast, then under conditions of more rapid recording the form of this curve would be expected to resemble that of curve B. This explanation is of interest in connection with the structure of tricalcium silicate hydrate, which was decomposed in the second and third steps of the isobar.[12]

Conclusions

The form of isobaric dehydration curves is largely determined by the recording technique. Decomposition temperatures for the compounds described are fairly characteristic for a given technique, but are sensitive to the presence of other phases.

An obvious advantage of the procedure described is the ease with which the recording program may be varied during a run. This is especially important where mixtures are being examined, since only the quasi-static technique is capable of resolving slow decompositions, and therefore of providing accurate analytical data.

Thanks are due to the Johns–Manville Corporation (Manville, New Jersey, U.S.A.) for financial help and for permission to publish this account.

THE RATES OF THE ELECTRON EXCHANGE REACTION BETWEEN U(IV) AND U(VI) IONS IN WATER, ETHANOL AND WATER–ETHANOL SOLVENTS

BY DANIEL M. MATHEWS, JACK D. HEFLEY AND EDWARD S. AMIS

Contribution from the Chemistry Department of the University of Arkansas, Fayetteville, Arkansas

Received October 9, 1958

The rate of the electron exchange reaction between U(IV) and U(VI) ions was studied at 25° in water, ethanol and water–ethanol solvents and at various concentrations of U(IV), U(VI) and hydrochloric acid. The order of the reaction with respect to each of these substances was found to depend strongly on the composition of the solvent. Mechanistic and kinetic expressions are suggested which can account for these orders in solvents up to 60 volume per cent. ethanol.

Introduction

Rona[1] has studied the electron exchange reaction between uranium(IV) and uranium(VI) chlorides in water solution. The reaction was studied as a function of the uranium, uranyl and hydrogen ion concentrations. The salt effect also was investigated. The neptunium(V)–neptunium(VI) reaction has been studied in water, water–glycol and water–sucrose solvents. The acidity was controlled using perchloric acid.[2]

Rona found that there was no salt effect in the uranium(IV)–uranium(VI) reaction. The neptunium(V)–neptunium(VI) reaction was found to be independent of the physical properties of the mixed solvents used. It was felt that it would be of interest to study uranium(IV)–uranium(VI) reaction in mixed solvents to ascertain whether this reaction is also independent of the physical properties of the solvent.

Experimental

Weights were calibrated against Bureau of Standards weights and the thermometer used was calibrated against a Bureau of Standards calibrated thermometer. The temperature was controlled to 25.00 ± 0.05°. Distilled water was boiled to remove oxygen and cooled under a nitrogen atmosphere. Absolute ethyl alcohol was made oxygen free by bubbling nitrogen through it for two hours. The alcohol was stored under nitrogen. Glassware was calibrated.

MacKay Chemical Company uranium tetrachloride was loaded into a sublimation chamber in a dry box containing an argon atmosphere. The chamber was connected to a vacuum pump and evacuated using a Welch Duo Seal vacuum pump. The chamber was heated with a Fisher burner so that slow sublimation of the uranium tetrachloride resulted. After sublimation the chamber was isolated, disconnected and returned to the dry box containing the argon atmosphere. It was opened in the dry box and the large lumps were removed with tweezers and their outside surfaces scraped off using a stainless steel spatula. This surface was removed because it appeared somewhat off-color from the bulk of the sublimed material. This was repeated two more times in order to obtain a high purity of product. The lumps were placed in a tared weighing bottle and the bottle closed in the argon atmosphere. The bottle was reweighed, the uranium tetrachloride dissolved in oxygen-free alcohol and poured into a volumetric flask which was flushed with nitrogen. The flask was filled to the mark with oxygen-free alcohol and the flask was closed with a ground-glass stopper lightly greased with silicone grease. This solution was analyzed for total uranium by taking 2-ml. aliquots, exposing them to air in a tared crucible until oxidized to the uranyl compound, evaporating to dryness and burning to U_3O_8. To ensure oxidation in some instances two drops of concentrated nitric acid were added to the alcoholic solution of uranium salt in the crucible before evaporating. The salt was found to have a chloride to uranium ratio of 3.94 and a purity of 99.42% UCl_4 as calculated from the amount of chloride present.

Uranyl chloride was prepared by dissolving reagent grade uranyl nitrate hexahydrate in concentrated hydrochloric acid. The hydrochloric acid solution was evaporated to the point where solid began to crystallize. A small amount of hydrochloric acid was added to the solution which was again evaporated until the solid began to crystallize. This procedure was repeated until the modified brucine test described below indicated that there was no nitrogen in the solution. The brucine test was made by dropping a hydrochloric acid solution of uranium into sulfuric acid contained on a spot test plate. After the foaming had stopped a small amount of brucine was added and if no red color developed the absence of nitrogen was proven. This procedure for the brucine test[3] was checked using more and more dilute solutions of silver nitrate. The sensitivity to the presence of nitrogen proved as good as the normal procedure using brucine. The nitrogen-free material in the evaporating dish was evaporated with stirring until it solidified into lumps. The lumps were allowed to cool slightly, transferred to a clean mortar and thionyl chloride sufficient to wet the surface added. The thionyl chloride prevented the material from becoming sticky due to the absorbed moisture. The material was crushed by an operator wearing rubber gloves, placed in a reflux flask, covered with thionyl chloride and refluxed until there was no further evolution of gas. Excess thionyl chloride was decanted, the flask connected to a fitting which led to an aspirator through a calcium chloride drying tube. The remaining thionyl chloride was removed by heating the flask to 90° in a water-bath under the partial vacuum created by the aspirator. The absence of thionyl chloride was indicated by the lack of odor of SO_2, HCl or thionyl chloride. This procedure resulted in the formation of uranyl chloride monohydrate. The material was hygroscopic and had to be protected from atmospheric moisture. Analysis of the material for uranium and for chloride showed it to be 99.99% pure and gave a chlorine to uranium ratio of 2.000.

The stock solution was made approximately to 0.25 *M* by placing a weighed amount of uranyl chloride monohydrate in a volumetric flask, dissolving in boiled, distilled water and diluting to the mark. The exact strength of the solution was determined by analysis of 2-ml. aliquots for uranium by placing them in tared crucibles, evaporating under an infrared lamp and burning to U_3O_8 in a crucible furnace maintained at 1100°.

The stock solution of acid was prepared by diluting concentrated hydrochloric acid with boiled, distilled water and analyzing with a sodium hydroxide solution.

The tracer solution furnished by the Oak Ridge National Laboratories was a citrate–nitrate complex of uranium-233 containing about 0.05 g. of uranium per 15 ml. of aqueous solution.

The concentration of stock cupferron solution depended on the concentration of the uranium(IV) in the kinetic run. Sufficient cupferron was weighed out and diluted to 100 ml. so that one ml. of stock solution contained five times as many moles of cupferron as one ml. of the kinetic run of highest uranium(IV) concentration contained moles of uranium(IV). For the precipitation of uranium(IV) in kinetic runs containing lower concentrations of uranium(IV), the stock solution of cupferron was diluted so that the ratio of cupferron to uranium(IV) remained five to one. These precautions were necessary because it was found that the ratio of cupferron to uranium(IV) to give optimum accuracy

(1) E. Rona, *J. Am. Chem. Soc.*, **72**, 4339 (1950).

(2) D. Cohen, J. C. Sullivan, E. S. Amis and J. C. Hindman, *ibid.*, **78**, 1543 (1956).

(3) Fritz Feigl, "Spot Tests," Vol. I, Edition IV, Elsevier Publishing Co., New York, N. Y., 1954, p. 300.

must be in the range of four to one to six to one. In our range of uranium(IV) concentrations it was found that if the cupferron to uranium(IV) ratio exceeded six to one uranium(VI) was precipitated in part by the cupferron.

A stock solution of approximately 6 *N* hydrochloric acid was prepared. This solution was used to stop the electron exchange reaction and to ensure the complete precipitation of uranium(IV).

In case of kinetic runs made in pure water the uranium(IV) stock solution was made using boiled distilled water. The 6 *N* hydrochloric acid solutions were made in a solvent composed of water and ethyl alcohol in the ratio of one to one. This ethyl alcohol caused the cupferron precipitated uranium(IV) to coagulate readily.

The reaction vessel consisted of a 50-ml. round-bottom flask to which was attached a side arm of 8 mm. tubing which served as a nitrogen inlet. At the top of the vessel another 8 mm. tube served as a nitrogen outlet. A tightly fitting piece of rubber tubing was fitted over the outlet tube and extended about 1.5 inches above the top of the tube. The total length was such that the tip of the 1-ml. pipet used in sampling reached nearly to the bottom of the reaction vessel when the bulb of the pipet was pressed against the top of the rubber tubing. In sampling, the bulb of the pipet was pressed firmly against the top of the rubber tubing thus closing the nitrogen outlet. The pressure of the nitrogen on the top of the solution in the flask caused the solution to rise in the pipet, thus producing a sample for withdrawal. The pipet was removed from the flask, wiped with a Kleenex and the solution allowed to drain to the mark in a beaker used for waste. The remainder of the solution in the pipes was drained into 6 *N* hydrochloric acid solutions, thus stopping the reaction.

The flowing nitrogen which was used as an inert atmosphere above the reaction solutions was tank nitrogen of 99.7% purity. Before being introduced into the reaction vessel it was saturated with solvent of the same composition by means of a gas washing bottle.

In order to start a reaction the appropriate amounts of water, ethanol, acid, uranium(VI) stock solution and tracer were added to the reaction vessel and placed in the constant-temperature-bath for a time sufficient to ensure temperature equilibrium. Then the proper amount of uranium(IV) stock solution in ethanol was added to start the reaction. In the case of water solvent the uranium(IV) was in water solution. The time of starting the reaction was taken as the time when about half of the uranium(IV) solution had drained from the pipet into the reaction vessel. The total volume of the reaction mixture was 20.2 ml. in all cases. One-ml. samples were taken at appropriate intervals and the time of the sample was recorded when about half of the sample had drained into the 6 *M* hydrochloric acid solution. The uranium(IV) was separated immediately by adding one ml. of a cupferron solution of the desired strength. In certain cases vigorous shaking was necessary to cause the precipitate to coagulate properly. As quickly as possible the mixture was centrifuged and the clear uranium(VI) solution remaining was decanted into a clean test tube and stored until it could be counted.

A 50 lambda portion of the uranium(VI) solution was spotted on a platinum disc, one inch in diameter, evaporated to dryness under a heat lamp, heated to redness over a Fisher burner and, after allowing it to cool, was counted in a Nuclear Chicago-type gas flow counter to a standard deviation of 1%. The procedure was done in triplicate on each sample and averaged to obtain each point on the rate plots.

The platinum discs were counted before spotting and this background count was subtracted from the count after spotting. The cleaning of these discs involved placing them in hot concentrated nitric acid from four to eight hr. when they were rinsed with distilled water and placed in hot chromic acid cleaning solution, where they were allowed to remain until needed for counting. Before using they were washed with soap and water and rinsed with distilled water.

Treatment of Data

The kinetics of isotopic exchange reactions has been discussed by Norris[4] and by Friedlander and Kennedy,[5] following the earlier treatments by MacKay[6] and Duffield and Calvin.[7] The result is obtained by considering a simple homogeneous exchange reaction occurring at equilibrium, expressed by the reaction

$$AX + BX^* = AX^* + BX$$

The rate of exchange of tracer will be first order from the initial to the final species regardless of the mechanism of the exchange. A solution of the rate equation leads to the equation

$$R = \frac{ab}{a+b} \times \frac{0.693}{t_{1/2}} \qquad (1)$$

where a and b are the concentrations of uranium(IV) and uranium(VI) in the system. R expressed in this manner represents the total number of exchanges, labeled and unlabeled, per unit time in the concentration units used.

In order to obtain R a plot of log counts per minute was made *versus* time on a semi-logarithmic plot and from this plot the count rate could be determined after the reaction mixture had reached equilibrium.

The value of the count rate at equilibrium was subtracted from the count rate at various times. The logarithms of these differences were plotted against time. This plot was extrapolated to zero time, and the half-life determined by reading the time at which the count rate was half that at zero time. Knowing the value of the half-life and the initial concentration of a and b, the value of R can be obtained. The zero time count rate on the semilogarithmic total count rate–time curve was obtained by taking the zero time count rate extrapolated from the semilogarithmic plot of the count rate *versus* time and corrected for the equilibrium and adding this extrapolated value to the equilibrium value of the count rate.

The ratio of the equilibrium count rate to the total count rate at zero time was taken and compared to the ratio of the concentration of uranium(VI) to the total uranium concentration. For complete exchange these two ratios must necessarily be equal.

It is also necessary to determine the total count rate before separation of the reacting species, since in many cases an exchange is induced by the separation procedure used. This total count rate before separation should be equal to the total extrapolated count rate of the uranium(VI) provided that there is no induced exchange upon separation. In case there is an induced exchange the total count rate before separation of the ionic species will be greater than the extrapolated value of that of uranium(VI) solution, assuming that the induction is from uranium(VI) to uranium(IV). The induced exchange may be corrected for if not complete.[8] In the present instance no induced exchange was found.

To find the order of a given substance in the reaction rate the usual procedure of plotting log R *versus* log concentration was used. The slope of this line is the order of the reaction with respect to the material that varied in concentration. This procedure

(4) T. H. Norris, THIS JOURNAL, **54**, 777 (1950).

(5) G. Friedlander and J. W. Kennedy, "Introduction to Radiochemistry," John Wiley and Sons Inc., New York, N. Y., 1950.

(6) H. S. C. MacKay, *Nature*, **142**, 997 (1938).

(7) R. B. Duffield and M. Calvin, *J. Am. Chem. Soc.*, **68**, 557 (1946).

(8) R. J. Prestwood and A. C. Wahl, *ibid.*, **70**, 880 (1948).

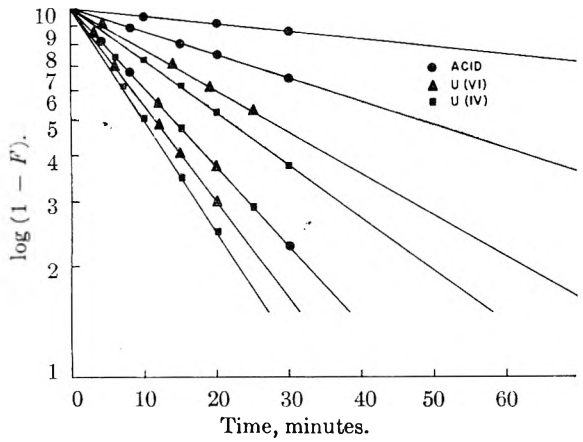

Fig. 1.—Logarithm (1 − *F*) *versus* time in minutes when the solvent was 30 volume % ethanol.

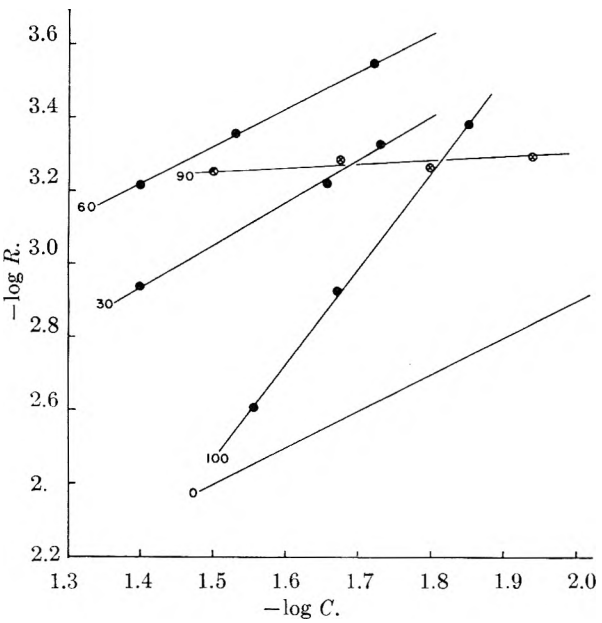

Fig. 2.—A plot of −log *R* against −log *C* of U(VI) at constant concentrations of U(IV) and acid and for various compositions of the solvent. The numbers on the various curves indicate the volume % of ethanol in the solvent.

was used to determine the order of acid, the uranium(VI) and uranium(IV) in the reaction mixture.

The data concerning the count rate has been converted to 1-fraction (1 − *F*) of complete exchange and are shown in Fig. 1 for 90 wt. % ethanol solvent. This figure shows the complete set of reactions for the given solvent composition. The other solvent compositions gave similar plots.

Figure 2 shows the plots of −log *R versus* −log *C* which were used to determine the order of the U(VI). Each line is representative of the order of that component at the noted solvent composition. The zero per cent. ethanol line was drawn in for comparative purposes from the data of Rona. The order of the reaction with respect to U(IV) and with respect to acid was determined in a similar manner and the data for these plots showed the same consistency as the data for U(VI) given in Fig. 2.

The orders of the reactions with respect to uranium(IV), uranium(VI) and acid concentrations are listed in Table I at the various solvent compositions. The data is shown graphically in Fig. 3.

TABLE I

Vol. % EtOH	U(IV) order	U(VI) order	H^+ order
0	2.0	1.0	−3.0
30	0.93	1.11	−1.74
60	0.87	1.08	−0.97
90	2.89	0.10	−1.06
100	0.0	2.70	−1.26

The orders at zero volume per cent. ethanol are those of Rona.[1] The orders in the other solvents were determined in this investigation. The orders from Table I and Fig. 3 are seen to depend in a remarkable way on the solvent composition.

The order with respect to hydrogen ion goes through a maximum with changing solvent composition, having a maximum value of about −1 at about 70 volume % ethanol.

Sullivan, Cohen and Hindman[9] found in the case of the Np(V)–Np(VI) exchange reaction that there is an exchange path involving hydrogen ion which becomes increasingly important at high acidities and with increasing percentages of D_2O in mixed D_2O–H_2O solvents. At 0° in H_2O and for $H^+ = 0.99$ *M* the rate of the exchange reaction is zero order with respect to hydrogen ion.[2] However, the reaction in the acid dependent path is first order with respect to hydrogen ion. Thus, the order of Np(V)–Np(VI) reaction varies with conditions such as acidity and solvent composition.

That the order of the reaction with respect to the various reactants varies with changing solvent composition indicates that the mechanism of the reaction depends in a complex way on the solvent composition.

Rona[1] gives a possible mechanism which explains the orders in water solvent. This mechanism includes equations involving water in the formation of reaction intermediates including the activated complex. The reactions in the different solvents must be quite different and involve the different solvent molecules in entirely different ways.

If it is assumed that the reacting species in water solutions are UOH^{+3} and UO_2OH^+, the orders in water, including the minus third order of hydrogen, can be explained. The orders in some of the mixed solvents can also be explained. The equilibrium constants K_1 and K_2 for the formation of the hydrolyzed species UOH^{+3} and UO_2OH^+, respectively, can be written

$$K_1 = \frac{[UOH^{+3}][H^+]}{[U^{+4}]} \qquad (2)$$

and

$$K_2 = \frac{[UO_2OH^+][H^+]}{[UO_2^{++}]} \qquad (3)$$

The equilibrium constant K_1 is reported to be 3.4×10^{-5},[10] and the equilibrium constant K_2 was found in this work to be 1.3×10^{-5} by measuring the *p*H of solution of known molarity of uranium(VI).

(9) J. C. Sullivan, D. Cohen and J. C. Hindman, *ibid.*, **79**, 3672 (1957); **77**, 4964 (1955).

(10) K. A. Kraus and F. Nelson, Oak Ridge National Laboratory Report ORNL-496, 1950.

The concentrations of the hydrolyzed species UOH^{+3} and UO_2OH^+ can be evaluated in terms of the hydrogen ion concentration and the equilibrium as

$$UOH^{+3} = \frac{K_1}{[H^+]}([U(IV) - UOH^{+3}]) = \frac{K_1[U(IV)]}{[H^+]\left(1 + \frac{K_1}{[H^+]}\right)} \quad (4)$$

Likewise

$$[UO_2OH^+] = \frac{K_2}{[H^+]}([U(VI)] - [UO_2OH^+]) = \frac{K_2[U(VI)]}{[H^+]\left(1 + \frac{K_2}{[H^+]}\right)} \quad (5)$$

Now if the rate of the reaction can be expressed by

$$\frac{dx}{dt} = k'[UOH^{+3}]^2[UO_2OH^+] = k'\frac{[U(IV)]^2[U(VI)]}{\left[\frac{[H^+]}{K_1} + 1\right]^2\left[\frac{[H^+]}{K_2} + 1\right]} \quad (6)$$

This would give a second-order dependence of the rate on U(IV) and a first-order dependence of the rate on U(VI) as was found by Rona studying aqueous solutions.

In the limiting case $[H^+]/K_1 > 1$ and $[H^+]/K_2 > 1$ the reaction would be minus third order with respect to $[H^+]$ as was observed by Rona in aqueous solvents. The assumption that $[H^+]/K_1 > 1$ is the same as that made by Rona when she discussed a minus fourth-order dependence of the rate of this reaction on hydrogen ion concentration. The assumption that $[H^+]/K_1 > 1$ at any of the acid concentrations used either by Rona or in this investigation seems hard to justify because of the magnitude of K_1. Because of the magnitude of K_2, the assumption $[H^+]/K_2 > 1$ seems more reasonable. If $[H^+]/K_1$ became less than one while $[H^+]/K_2$ remained greater than one the order of the reaction could become -1 with respect to $[H^+]$. This was approximately the case in solvents 60 volume % or richer in ethanol.

If the expression for the electron exchange reaction rate be written

$$\frac{dx}{dt} = k''[UOH^{+3}][UO_2OH^+] = k''\frac{[U(IV)][U(VI)]}{\left[\frac{[H^+]}{K_1} + 1\right]\left[\frac{[H^+]}{K_2} + 1\right]} \quad (7)$$

In this case the reaction would be first order with respect to both U(IV) and U(VI) and, in the case of the limiting conditions discussed above, minus second order with respect to hydrogen ion concentration. This was approximately the case for 30 volume % ethanol solvent. Under certain limiting conditions, the order of the reaction could become minus one with respect to $[H^+]$ as in 60 volume % ethanol.

Thus it would seem that the mechanism of the exchange reaction changes with solvent.

Up to and including 60% ethanol in the solvent, the intermediate ion species and the two rate expressions, equations 6 and 7, can be used to explain the order data on the assumption that the presence

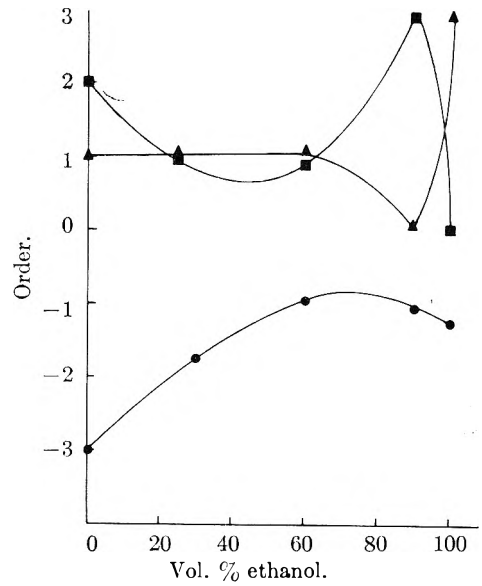

Fig. 3.—Order of the various reactants *versus* the volume % ethanol: ●, acid; ▲, U(VI); ■, U (IV).

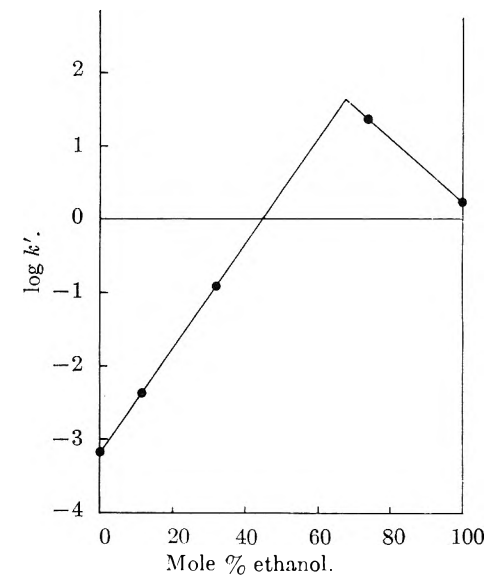

Fig. 4.—Logarithm of the specific velocity constant *versus* the mole per cent. ethanol in the solvent.

and the amount of alcohol determines the limiting conditions and the form of the rate expression but not the nature of the intermediate ions.

However, for solvents containing 90 to 100 volume % ethanol, drastic changes in ion intermediates, rate expression and limiting conditions would be necessary to explain the orders observed with respect to [U(IV)], [U(VI)] and $[H^+]$. At present the authors are aware of no simple explanation of these complex changes in the kinetics, but hope that investigations, now under way, of the ion species present in the various solutions may help in elucidating the observed orders.

In Table II, the specific velocity constants at various concentrations of reactants and various solvent compositions are listed. The velocity constants in water solvent were calculated from Rona's data. The velocity constants in the other solvents were calculated from the data taken in this investigation.

TABLE II[a]

HALF-LIVES, RATES AND SPECIFIC VELOCITY CONSTANTS AT 25.00° FOR THE U(IV)–U(VI) ELECTRON EXCHANGE REACTION

[U(IV)]	[U(VI)]	[H⁺]	$t_{1/2}$, min.	$R \times 10^6$, moles/l./min.	$k' \times 10^{-6}$
		0% ethanol			
0.030	0.0274	0.141		0.745	0.0846
.040	.0274	.141		1.335	.0855
.064	.0274	.141		3.380	.087
.025	.024	.141		0.287	.055
.025	.075	.141		0.954	.057
.025	.150	.141		1.800	.056
		30 volume % ethanol			
0.0190	0.0189	0.0326	14	46.9	0.652
.0190	.0189	.0651	47	14.0	.651
.0190	.0189	.1302	153	4.29	.398
.0095	.0147	.0326	21	19.0	.246
.0285	.0230	.0326	10	88.2	.515
.0190	.0294	.0326	11.5	61.4	.361
.0190	.0400	.0651	27.0	33.1	.278
		60 volume % ethanol			
0.0190	0.0294	0.0323	4.8	167	12.3
.0190	.0294	.0651	10.6	75.5	11.3
.0190	.0294	.1302	18.1	44.2	13.9
.0190	.0189	.1302	23.0	28.6	13.5
.0095	.0253	.1302	24.5	19.5	8.22
.0285	.0336	.1302	15.5	68.9	8.41
.0190	.0400	.1302	13.7	65.2	13.8
		90 volume % ethanol			
0.0168	0.0211	0.1865	9.0	72	2412
.0168	.0211	.2516	12.5	51.9	2314
.0168	.0211	.3145	15.8	41	2389
.0168	.0115	.2516	9.3	50.9	2412
.0168	.0158	.2516	10.3	54.8	2476
.0079	.0164	.2516	66	5.6	2261
.0237	.0280	.2516	6.2	144	2159
.0168	.0216	.2516	13.5	56.3	2405
		100 volume % ethanol			
0.0132	0.0141	0.0386	4.0	118	194
.0132	.0141	.0771	11.3	41.8	164
.0132	.0141	.1157	17.0	27.8	182
.0067	.0069	.00777	140	45.89	155
.0132	.0209	.0771	4.7	119	162
.0132	.0277	.0771	2.5	248	158
.0202	.0208	.0771	6.7	106	155

[a] In this paper the concentrations of hydrogen ion and of hydrochloric acid are assumed to be the same in the alcoholic solvents. Activities of hydrogen ion in such solvents have doubtful meaning. Perhaps we should have used the expression, "hydrochloric acid concentration" rather than, "hydrogen ion concentration" in the tables and in the discussion of order.

Since the orders with respect to concentrations of U(IV), U(VI) and hydrogen ion change so drastically with solvent composition, no attempt has been made to correlate the kinetic data for the U(IV)–U(VI) electron reaction with existing theories.[11–13] These theories assume a common mechanism for all solvents for a given reaction, but in the case of the U(IV)–U(VI) electron exchange reaction the mechanism undoubtedly changes with solvent. While it is not justifiable to average the specific velocity constants recorded in Table II for this reaction in a given solvent when the concentrations of highly charged ions and acid vary so widely, a rough idea of the drastic effect of the solvent on these constants can be observed by plotting the logarithms of the average of the constants in the different solvents *versus* the mole % of ethyl alcohol in these solvents. Such a plot is presented in Fig. 4. The figure shows a complex dependence of the rate constant upon the composition of the solvent with a maximum in the curve in the region of 60-70 weight % alcohol. This region of solvent composition has been found to exert marked influence with respect to other phenomena appertaining to ions in solution.[14]

The authors wish to thank the United States Atomic Energy Commission for a grant under Contract AT-(40-1)-2069, which made this research possible.

(11) R. J. Marcus, B. J. Zwolinski and H. Eyring, THIS JOURNAL, **58**, 432 (1954).

(12) R. A. Marcus, *J. Chem. Phys.*, **24**, 966 (1956); **26**, 867 (1957).

(13) Edward S. Amis, *Atti Accad. Nazl. Lincei, Rend., Classe sci. fis. mat. e nat.*, in press.

(14) E. S. Amis, THIS JOURNAL, **60**, 428 (1956).

RELATION OF WETTABILITY BY AQUEOUS SOLUTIONS TO THE SURFACE CONSTITUTION OF LOW-ENERGY SOLIDS[1]

BY M. K. BERNETT AND W. A. ZISMAN

U. S. Naval Research Laboratory, Washington 25, D. C.

Received October 18, 1958

Contact angles of a variety of pure anionic, cationic and non-ionic surface-active agents in aqueous solutions of various concentrations were measured on smooth, clean surfaces of two low-energy solids, polyethylene and Teflon. Wettability curves were obtained for each solid surface by plotting the cosine of the contact angle *versus* the surface tension of each solution. The critical surface tension of each solid thus obtained agrees well with previous values established from studies with various pure organic liquids. Aqueous solutions whose surface tensions are lower than 30 dynes/cm. were found to spread on polyethylene, whereas no solution had a surface tension low enough to spread on Teflon. The ability of aqueous solutions to spread on an organic low-energy solid surface was related to the value of γ_c of the solid and to the surface tension of the solution. Abrupt changes in slope were found in all wettability curves of micelle-forming compounds. The discontinuities for both surfaces occurred at approximately equal concentrations for a given wetting agent and were essentially determined by a change in the adsorption at the solution–air interface and not at the solid–solution interface. The concentrations at which the breaks in slope occurred were close to the reported critical micelle concentrations but were slightly lower. Compounds which were unable to form micelles did not produce discontinuities in slope of the wettability curves. The wetting properties of the aqueous solutions at high concentration of wetting agent were precisely those to be expected of organic liquids having the same surface composition and packing as the outermost (or hydrophobic) portion of the film of wetting agent at the air–solution interface. This means that the presence of the low-energy solid surface has little effect on the adsorption, orientation or packing of the wetting agent. These conclusions allow a rational explanation of all the observations reported on wetting agents. It is concluded that the minimum concentrations of the polar solute required to cause spreading on polyethylene and on Teflon are excellent indices of the effectiveness of the solute to function as a wetting agent. A reference standard for rating wetting effectiveness, which is less demanding than polyethylene, would be polystyrene or polyvinyl chloride.

Introduction

An aqueous solution will spread on a smooth solid if the Harkins initial spreading coefficient is positive, *i.e.*, if

$$\gamma_S^0 - (\gamma_{SL} + \gamma_{LV}) > 0$$

where γ_S^0 and γ_{SL} are the surface tensions of the solid *in vacuo* and against the liquid and γ_{LV} is the surface tension of the liquid against its vapor. The constitutive implications of this relation have not been found yet because the unit free energies γ_S^0 and γ_{SL} of the solid–air and solid–liquid interfaces are either not known sufficiently accurately or have not yet been related to constitution. Approximate relations to constitution are therefore desirable.

Present theories[2-4] about the wetting ability of surface-active agents in aqueous systems either state or imply that spreading results because the wetting agent becomes selectively adsorbed on the surface so as to orient the hydrophilic group of its molecule toward the aqueous solution. In the light of recent studies performed on adsorption at solid–air and solid–liquid interfaces[5-9] it seemed unlikely that the major mechanism of wetting could be based on the ability of the non-polar group of the wetting agent to adsorb by its hydrocarbon "tail" on the low-energy surfaces characteristic of many organic solids.

The working assumption was made that spreading on low-energy surfaces is caused to a first approximation by the lowering of the surface tension of water. Hence, changes in γ_{SL} must play a minor role in the presence of solutions of wetting agents. Therefore, one can assume that the ability of the aqueous solution to spread on such low-energy surfaces is determined by the value of the critical surface tension (γ_c) of the solid to be wetted and the amount of the wetting agent which must be dissolved in the water to depress the surface tension (γ_{LV}) of water below γ_c. The value of γ_c of a solid surface has been defined[5-11] earlier as that liquid surface tension above which all liquids show nonzero contact angles on the given surface. One advantage of this assumption about the relation of the surface tension of the aqueous solutions to the critical surface tensions of the solid organic surfaces is that the same approach also could be used to search for and rationalize the spreading behavior on low-energy surfaces of wetting agents effective in other solvents than water.

In order to verify these ideas, two low-energy solids, polyethylene ($\gamma_c \approx 31$ dynes/cm.) and Teflon ($\gamma_c \approx 18$ dynes/cm.) were chosen for study for several reasons. Pure water ($\gamma_{LV} = 71.9$ dynes/cm. at 25°) will not spread on either of these two surfaces. Fischer and Gans[12] have pointed out, however, that the conventional surface-active agents, which are derived from aliphatic or aromatic hydrocarbons, do not lower the surface tension of water at 25° below about 26–27 dynes/cm. It follows from the definition of the critical surface tension that whenever any wetting agent lowers the liquid surface tension below 31 dynes/cm., the solution will

(1) Presented at the Symposium on Energetics of Interfaces and Surfaces under the auspices of The Division of Colloid Chemistry, American Chemical Society, at the meeting in Chicago, Illinois, Sept. 9, 1958.

(2) F. M. Fowkes and W. D. Harkins, *J. Am. Chem. Soc.*, **62**, 3377 (1940).

(3) J. L. Moilliet and B. Collie, "Surface Activity," D. Van Nostrand Co., New York, N. Y., 1951, p. 6, 104.

(4) J. L. Moilliet, *J. Oil Colour Chemists' Assoc.*, **38**, 463 (1955).

(5) E. G. Shafrin and W. A. Zisman, *J. Colloid Sci.*, **7**, 166 (1952).

(6) W. A. Zisman, "Relation of Chemical Constitution to the Wetting and Spreading of Liquids on Solids," NRL Report 4932, May 1957; also in "A Decade of Basic and Applied Science in the Navy," U. S. Government Printing Office, Washington, D. C., p. 30, 1957.

(7) A. H. Ellison and W. A. Zisman, THIS JOURNAL, **58**, 260 (1954).

(8) H. W. Fox, E. F. Hare and W. A. Zisman, *ibid.*, **59**, 1097 (1955).

(9) H. W. Fox and W. A. Zisman, *J. Colloid Sci.*, **5**, 514 (1950).

(10) H. W. Fox and W. A. Zisman, *ibid.*, **7**, 109 (1952).

(11) H. W. Fox and W. A. Zisman, *ibid.*, **7**, 428 (1952).

(12) E. K. Fischer and D. M. Gans, *Ann. N. Y. Acad. Sci.*, **46**, 371 (1946).

spread on the surface of smooth clean polyethylene. However, no aqueous solutions containing conventional wetting agents should spread on Teflon, since a wetting agent capable of depressing the surface tension below 18 dynes/cm. would be needed. The choice of the wetting agents employed here was motivated not only by the desire to include all three classes, *i.e.*, anionic, cationic and non-ionic, but also to include as many diversified hydrocarbon structures as feasible in order to show properties or general trends common to all types of conventional surface-active agents.

Materials and Experimental Procedures

Nearly all of the surface-active agents used in this investigation were research samples of over 99% purity which had been especially purified for research on surface tension and consequently were used without further purification. The sulfosuccinates were obtained from Dr. J. K. Dixon of the American Cyanamid Company, the cetyltrimethylammonium bromide from the late Dr. W. Calcott of the du Pont Company, the sodium *p*-decyl benzenesulfonate from J. V. Shurman of the Colgate–Palmolive Company,[13] the sodium lauryl sulfate from Dr. A. C. Haven, Jr., of the du Pont Company, and the sodium dinonyl naphthalenesulfonate was prepared by S. Kaufman of this Laboratory. The only commercial compound used was Igepal CO-850, a nonylphenoxypolyoxyethylene-ethanol, obtained from Antara Chemicals.[14]

Solutions of the surface-active agents were prepared by diluting a weighed sample to appropriate solution concentrations with distilled water having a conductivity of 2.49×10^{-6} ohm^{-1}. The solutions were stored in acid-cleaned glass flasks and used for the experiments within a few days, since prolonged contact with glass may change the surface tension.[15]

Surface tensions usually were measured by the ring method with a du Noüy tensiometer, using the Harkins and Jordan correction tables.[16] As a freshly flamed platinum dish proved to be satisfactory, it was used because of the ease of cleaning. The surface tensions of solutions change with time until adsorption equilibrium is attained and markedly so when very dilute solutions are measured.[12,16,17-19] Equilibrium values with the most dilute solutions were not reached for several hours, but the lowering of the surface tension after the first hour was of such small value that it was an insignificant source of error for the purposes of this study. Reproducibility of the surface tensions was ±0.1 dyne/cm. for the most concentrated solution and ±0.5 dyne/cm. for the most dilute solution used.

Each solution was carefully observed before measurements to ascertain whether it completely wetted the platinum ring of the tensiometer. Only the lower concentrations of the cetyltrimethylammonium bromide solutions were found to make the ring hydrophobic; their surface tensions therefore were measured also by the pendant drop method.[20] which is independent of the contact angle. The values obtained by the two methods agreed within ±1%, which is within the margin of experimental error of the latter method.

The polyethylene used was a research sample of Super Dylan 6600, received from the Koppers Company in powder form (density of 0.956, melt index of 0.14 cm./10 min.) and free of antioxidants. As this material is a comparatively unbranched form of polyethylene (one terminal CH_3-group per 200 chain carbon atoms), the surface of the plastic consists essentially of methylene groups rather than a mixture of methylene and methyl groups. A 1/4-inch-thick disk was molded from the powder in a Carver press at 150° and 1000 lb. pressure. The disk was easier to remove from the mold when the powdered form was used instead of the pellets. Each disk was washed with concentrated Tide solution, rinsed with distilled water, pressed between dry acid-cleaned Pyrex plates at 1000 lb. pressure up to the softening point (150°), and cooled under pressure for at least 16 hours (the disk warped if removed too soon). Any electric static charges developed by this procedure were dissipated by placing the surface near an α-particle source for a minute or two. The resulting surface was smooth, exhibited specular reflection, and the contact angles of various pure liquids, such as water, methylene iodide, formamide and tricresyl phosphate, were in excellent agreement with previous data.[11]

Glossy Teflon surfaces were prepared as described previously,[9] except that it was found unnecessary to use acid cleaning. Washing with Tide solution has been found an effective cleaning method,[21] which made it possible to obtain reproducible contact angles. Contact angles with water ranged from 112 to 114°; previously reported values ranged from 108 to 110°.[9] This small discrepancy may be due to the different specimens of Teflon used for these studies. Contact angles of pure organic liquids (methylene iodide, tricresyl phosphate and *n*-hexadecane) are in excellent agreement with the reported values.[9]

Contact angles were measured on a number of sites on each of three separate specimens with the improved goniometer telescope described earlier[9] using the drop build-up method.[5] Since the surface tensions of many solutions were obtained after prolonged time intervals, the corresponding contact angles were also measured after the same intervals. To achieve this, the drop was exposed to an atmosphere saturated with water vapor to eliminate evaporation, which would ensure that any possible lowering of contact angle was solely a function of the surface tension. Even after 1-hour exposure, which is longer than the time required to attain surface tension equilibrium, the contact angle decreased at most only 2 to 3°. This change is not enough to alter significantly the curve of γ_{LV} *vs.* $\cos\theta$. Therefore, all contact angles reported here were obtained early after build-up of the drop. No significant differences were found between contact angles obtained on these hydrophobic solids in a water-saturated atmosphere and those obtained in the open air. With a few exceptions encountered using several concentrated solutions on polyethylene, measurements of the contact angle varied no more than ±2° from the mean; more often the maximum deviation was no more than ±1°. All data were observed at 25 ± 1° and 50 ± 2% R.H.

Experimental Results and Discussion

Figure 1 shows the knee-shaped surface tension *vs.* concentration curves so characteristic of aqueous surface-active agents. The steeper the curve, the more efficient the wetting agent. Curves for the dialkylsulfosuccinates agree very well with those reported by Dixon and co-workers,[22] and they constitute a valuable check on the methods used, since the time effect is very pronounced with dilute solutions and Dixon, *et al.*, did not specify at what time interval the surface tensions were measured. It is generally assumed that the bend of the curve coincides with, or at least bears a relationship to, the critical micelle concentration (c.m.c.) of the respective compound in the aqueous medium.[15,18,19,23,24] Since the breaks in the individual curves of Fig. 1 occur in the region of the c.m.c. values reported by various investigators, the above assumption can be made again for the agents discussed in this study. Dixon, *et al.*[22], observed that with decreasing chain length of the alkyl group the c.m.c. became marked

(13) F. W. Gray, J. F. Gerecht and I. J. Krems, *J. Org. Chem.*, **20**, 511 (1955).

(14) C. E. Stevens, *J. Am. Oil Chemist Soc.*, **34**, 181 (1957)

(15) G. C. Nutting, F. A. Long and W. D. Harkins, *J. Am. Chem. Soc.*, **62**, 1496 (1940).

(16) W. D. Harkins and H. F. Jordan, *ibid.*, **52**, 1751 (1930).

(17) I. W. Wark, THIS JOURNAL, **40**, 661 (1936).

(18) J. Powney and C. C. Addison, *Trans. Faraday Soc.*, **33**, 1243 (1937).

(19) N. K. Adam and H. L. Shute, *ibid.*, **34**, 758 (1938).

(20) J. M. Andreas. E. A. Hauser and W. B. Tucker, THIS JOURNAL, **42**, 1001 (1938).

(21) R. C. Bowers, W. C. Clinton and W. A. Zisman, *Modern Plastics*, **31**, (No. 6), 131 (1954).

(22) E. F. Williams, N. T. Woodberry and J. K. Dixon, *J. Colloid Sci.*, **12**, 452 (1957).

(23) J. W. Gershman, THIS JOURNAL, **61**, 581 (1957).

(24) F. M. Fowkes, presented at the 133d Spring Meeting of the American Chemical Society in San Francisco, Calif., April 1958.

by much less abrupt breaks in the surface tension curve, and Fig. 1 shows that same relationship for the sulfosuccinates.

The surface tension curve of sodium lauryl sulfate (Fig. 1) follows the previously observed values fairly closely[15,18,19,25,26] leveling off at about 37 dynes/cm. at 0.5% concentration. If one excludes di-*n*-butyl sulfosuccinate, the surface tension curves for this compound and di-*n*-octyl sulfosuccinate form the upper and lower bounds for all the other wetting agents studied. Observations were limited in some cases by poor solubility, but the compounds were so selected that in each case the leveling-off point was reached before the solubility limit prohibited further measurements.

The surface tension *vs.* cos θ curve obtained for each wetting agent on the smooth polyethylene surface is given in Figs. 2a and 2b. Analogous results using smooth Teflon surfaces are given in Figs. 3a and 3b. It can be seen that at the critical surface tension (cos θ = 1) there is only a narrow spread of the converging curves for each organic surface. From these intercepts one can estimate γ_c values for Teflon as between 16.5 and 19.5 dynes/cm. and for polyethylene as between 27.5 and 31.5 dynes/cm. These are in reasonable agreement with the values reported in earlier work on the wettability of these surfaces by various pure organic liquids.[9,10] Only solutions whose surface tensions were lower than 30 dynes/cm. (sodium di-*n*-octyl sulfosuccinate was the only one studied) were able to spread freely on polyethylene. No aqueous solution investigated had a surface tension low enough to spread freely on Teflon. This observation agrees with the assumption that the ability of aqueous solutions to spread on an organic, low-energy, solid surface is determined to a good first approximation by the value of γ_c of the solid and the surface tension of the solution.

Whereas the curves for the various wetting agents group in a narrow band intercepting the line cos θ = 1 at the value of γ_c, they do not converge to a point as would be anticipated, at the value of γ_{LV} = 71.9 dynes/cm. for pure water, but also exhibit a spread in θ of 2°. However, this spread is well within the experimental error of the contact angle measurements.

An unexpected and new phenomenon, however, is the abrupt change in slope in the middle zone of each of the γ_{LV} *vs.* cos θ curves of Figs. 2 and 3. The data in the first two columns of Table I (calculated from Figs. 1, 2 and 3) reveal that the discontinuities for polyethylene and Teflon occur at approximately equal concentrations for a given wetting agent. Hence, the discontinuities in slope *are determined by the constitution of the wetting agent and not by that of the solid.* When the surface tension corresponding to each discontinuity is referred to the surface tension *vs.* concentration curve of Fig. 1, it is found that it corresponds to the concentration in the region of greatest curvature. Therefore, there must be a close relation between the concentration at which discontinuity in the slope occurs in each wetting curve of Figs. 2 and 3 and the c.m.c. of the wetting agent in the same solution. For comparison purposes the last column of Table I gives the best literature values of the c.m.c. of each of these wetting agents at or near the temperature used here. It will be seen that there is a fair correlation between the concentration corresponding to the breakpoint in the wetting curve and the reported c.m.c.; also it appears that the c.m.c. is always slightly higher.

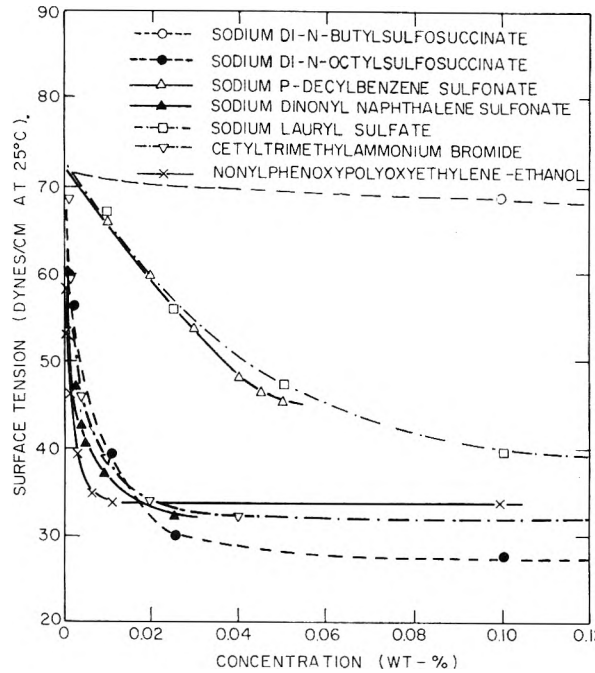

Fig. 1.—Surface tensions of wetting agents in aqueous solutions.

TABLE I

COMPARISON OF THE BREAKPOINT CONCENTRATIONS FOR THE VARIOUS WETTING AGENTS AND SURFACES

Compound	Concn. (moles/l.) Polyethylene	Teflon	C.m.c. (ref.)
Na-di-*n*-butyl sulfosuccinate	5.0×10^{-2}	4.2×10^{-2}	2×10^{-1} [22]
Na-di-*n*-octyl sulfosuccinate	6.8×10^{-4}	4.5×10^{-4}	6.8×10^{-4} [22]
Na-*p*-decyl benzenesulfonate	1.2×10^{-3}	1.2×10^{-3}	3×10^{-3} [23] at 50°
Na lauryl sulfate	3.0×10^{-3}	2.7×10^{-3}	8×10^{-3} [26]
Cetyltrimethylammonium bromide	4.3×10^{-4}	3.8×10^{-4}	1×10^{-3} [27] at 60°

The correctness of the preceding interpretation of the discontinuities in the curves of γ_{LV} *vs.* cos θ was supported by the following studies. Solutions of polar compounds believed not to form micelles were also investigated and their contact angles measured on the same low-energy solid surfaces. These compounds were ethanol (U.S.I., absolute 100% U.S.P.) butanol-1 (Eimer and Amend, Tested Purity Grade), 1,4-dioxane (EK white label, redistilled), propylene carbonate (Jefferson Chemicals, percolated through alumina gel and silica gel), diacetone alcohol (EK white label), dipropylene glycol (Carbon and Carbide Chemicals Corporation), butanone-2 (EK white label) and tetrahydrofuran (EK white label, redistilled). Surface tensions for these

(25) L. Shedlovsky. *Ann. N. Y. Acad. Sci.*, **46**, 427 (1956).

(26) G. Nilsson, THIS JOURNAL, **61**, 1135 (1957).

(27) H. B. Klevens, THIS JOURNAL, **52**, 130 (1948).

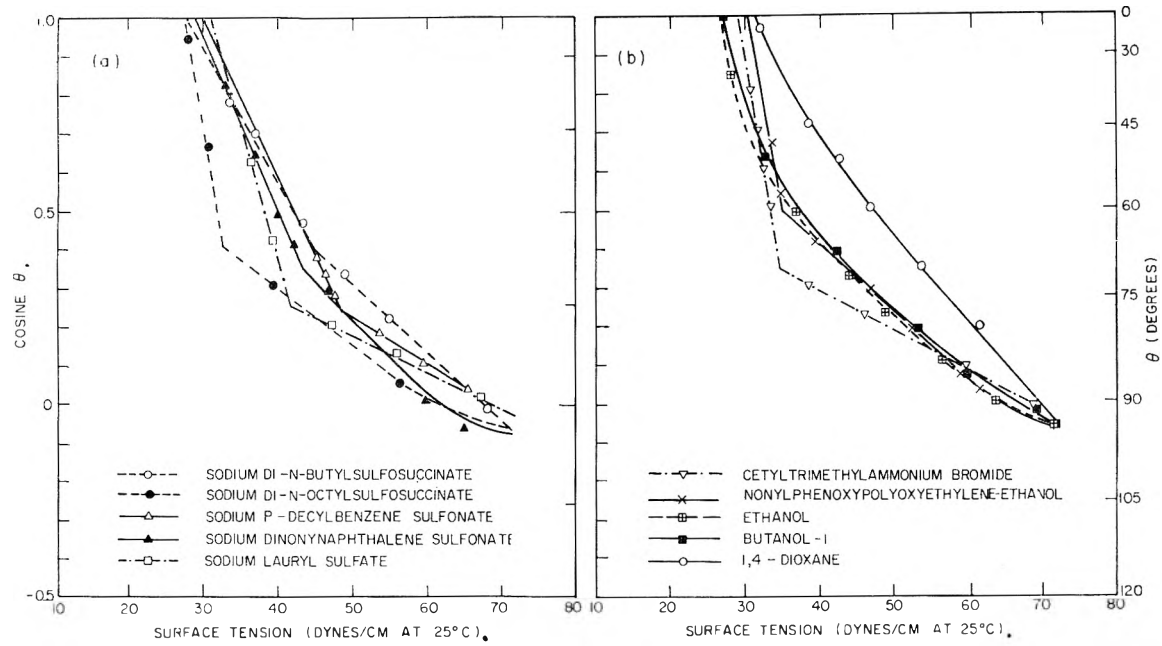

Fig. 2.—Wettability of polyethylene by aqueous solutions: (a) of anionic wetting agents; (b) of other compounds.

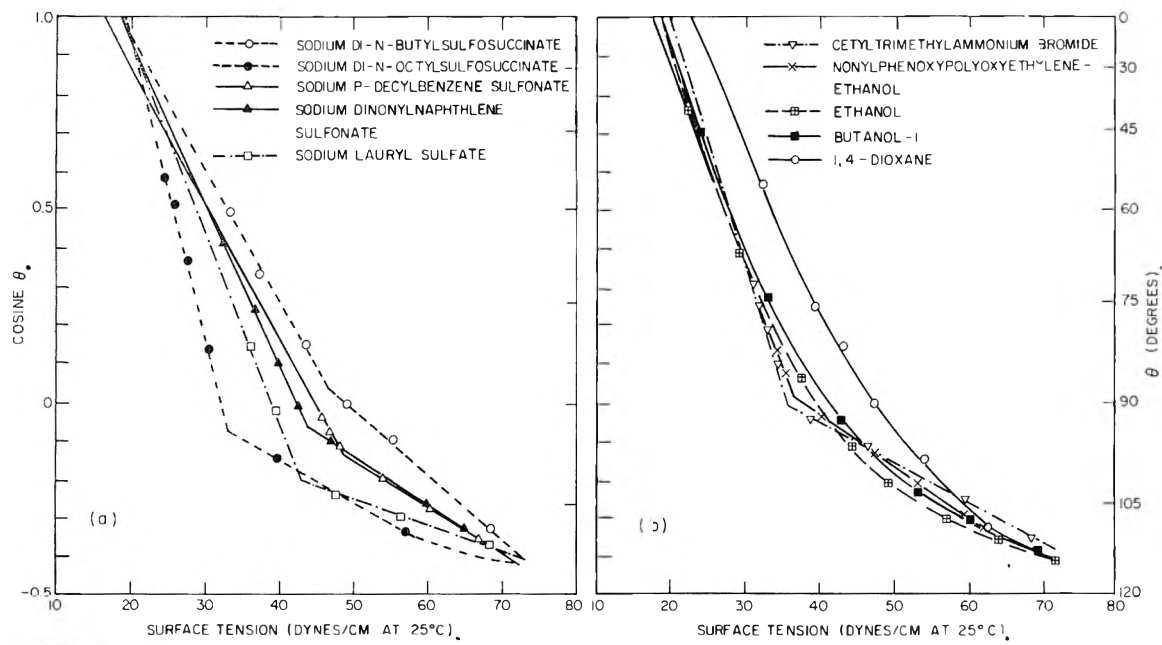

Fig. 3.—Wettability of Teflon by aqueous solutions: (a) of anionic wetting agents; (b) of other compounds.

compounds agreed well with literature values when available.[28] Table II gives the surface tensions at 25° of aqueous solutions in various concentrations of these compounds. None of these polar solutes form micelles in water and, as can be seen in Figs. 2b and 3b, no discontinuities in the slopes of the curves of $\cos\theta$ *vs.* γ_{LV} were observed for either solid surface. It is concluded therefore that no discontinuities in slope occur without the formation of micelles. Recent experiments by Allan[29] with ethanol–water solutions on thin commercial polyethylene films resulted in similar curves of γ_{LV} *vs.* $\cos\theta$.

(28) O. R. Quayle, *Chem. Revs.*, **53**, 439 (1953).

(29) A. J. G. Allan, presented at the 132d Meeting of the American Chemical Society in New York, N. Y., Sept. 8–13, 1957.

Each intercept at $\cos\theta = 1$ for Teflon falls within the expected range of γ_c values (Fig. 3b) with the exception of the intercept for the 1,4-dioxane curve which occurs at the higher value of 22.5 dynes/cm. Wetting curves on polyethylene are almost coincident for 1,4-dioxane and propylene carbonate, for diacetone alcohol and butanone-2, for dipropylene glycol and tetrahydrofuran, and are very similar for ethanol and butanol-1 (Fig. 2b). Table III shows the intercepts at $\cos\theta = 1$ of the compounds for Teflon and polyethylene. It already has been found in previous work[9,11] that the value of γ_c of any one solid surface varies somewhat among the various homologous series of liquids.

Recently Fowkes,[24] in studying interfacial tensions between aqueous salt solutions and solutions of

TABLE II

SURFACE TENSIONS FOR AQUEOUS SOLUTIONS OF NONMICELLE-FORMING COMPOUNDS AT 25°

Ethanol		Butanol-1		1,4-Dioxane		Propylene carbonate		Diacetone alcohol		Butanone-2		Dipropylene glycol		Tetrahydrofuran	
Concn.[a]	γ^b	Concn.[a]	γ^b	Concn.[a]	γ^b	Concn.[a]	γ^b	Concn.[a]	γ^b	Concn.[a]	γ^b	Concn.[a]	γ^b	Concn.[a]	γ^b
2	63.4	0.1	68.9	5	62.1	1.0	67.2	1	63.8	1	62.8	1	65.1	1	64.9
5	56.5	0.5	59.8	15	53.9	5.0	57.5	5	53.0	2	58.4	2	62.1	5	52.6
10	49.1	1.0	53.2	25	47.1	7.5	53.5	10	47.1	4	52.4	5	56.9	10	46.1
15	43.8	2.5	42.6	40	43.0	10.0	50.0	20	40.8	10	41.7	10	52.5	20	37.7
25	36.8	5.0	33.1	50	39.2	15.0	44.4	50	35.5	20	32.7	20	47.5	50	30.3
50	28.3	100.0	23.7	100	32.4	100.0	40.7	100	30.2	100	24.4	50	39.2	100	27.4
100	21.4											100	33.1		

[a] Volume per cent. [b] Dynes/cm.

TABLE III

CRITICAL SURFACE TENSIONS BY AQUEOUS SOLUTIONS OF NON-MICELLE-FORMING COMPOUNDS AT 25°

Solute	γ_{LV} (dynes/cm.) pure solute	γ_c (dynes/cm.) Polyethylene	γ_c (dynes/cm.) Teflon
Ethanol	21.4	27.5	18.5
Butanol-1	23.7	27.5	18.5
Butanone-2	24.4	27.5	...
Tetrahydrofuran	27.4	29.5	...
Diacetone alcohol	30.2	29.0	17.0
1,4-Dioxane	32.4	31.5	22.5
Dipropylene glycol	33.1	30.0	18.0
Propylene carbonate	40.5	29.5	19.5

dinonyl naphthalenesulfonates in various hydrocarbon media, obtained discontinuous curves of interfacial tensions *vs.* solute concentrations. The region of the break in each curve also indicated the c.m.c. value of the compound. Since discontinuities at the c.m.c. occur in curves of surface tension *vs.* concentration, interfacial tension *vs.* concentration and now in either cos θ *vs.* concentration or cos θ *vs.* surface tension, the generalization is proposed that micelle-forming compounds will produce discontinuities in the slopes of any surface-active property when plotted against either the concentration or the surface tension of the solution.

Because of their hydrophobic–hydrophilic structures, the most effective wetting agents each adsorb to form a thin film on the free surface of the aqueous solution. At sufficiently high solute concentrations, this film will make the aqueous liquid appear to be a hydrocarbon liquid whose surface is comprised of the oriented, packed hydrophobic groups characteristic of the organic structure of the wetting agent. The data obtained lead to the conclusion that bringing the low-energy surface of Teflon or polyethylene into contact with this film-coated water does not change the orientation or packing of the film adsorbed at the water–air interface. Fowkes and Harkins[2] reached essentially the same conclusion in their early study of the adsorption at the interface of aqueous solutions and paraffin wax. They found that the force–area curves for butyl alcohol, butyric acid and butylamine adsorbed at the paraffin–water interface were nearly the same as those for adsorption at the air–water interface.

From these considerations one can predict that γ_{SL} will decrease as adsorption of the wetting agents increases. At high solute concentrations, γ_{SL} will become small because the interface will be between an organic low-energy solid and a hydrocarbon-like liquid. In other words, the much greater adhesion of the polar groups to the water and the much lower adhesion of the hydrocarbon groups to the low-energy solid surface will have caused the interface determining spreading and wetting to become the hydrocarbon-like outer surface of the film of adsorbed wetting agent. Hence, γ_{SL} will decrease with increased solute concentration and will become nearly constant at high concentrations as the adsorbed film approaches closest packing. Thus, the value of γ_c will vary with the nature of the wetting agent only insofar as there are differences in the nature and packing of the hydrocarbon groups of the wetting agent in the adsorbed state at the water–air interface. One would expect γ_c to be least for *n*-alkane long-chain derivatives; it will be greater on each surface for branched hydrocarbon derivatives; and it will be largest for aromatic polar compounds. In going to solutes like 1,4-dioxane or propylene carbonate or the others in Table II, we are adsorbing a film at the water–air interface which has a higher free surface energy than one containing only hydrocarbon groups.

Any discontinuity in the slope of the force–area curve (or first-order phase change) in the film adsorbed at the water–air interface will be accompanied by a discontinuity in the slope of the cos θ *vs.* concentration or in the cos θ *vs.* γ_{LV} curve, since we have concluded that the contact angle was essentially that of a liquid having the same outermost hydrocarbon structure as the adsorbed solute. It is now evident why the breakpoints occur at a concentration which is dependent only on the nature of the wetting agent and not on the nature of the solid surface.

Evidently, the same approach and conclusion should hold for the wetting of polyvinyl chloride, polystyrene and other low-energy solid surfaces. In previous studies[5-8] we have shown that because of the highly localized nature of the forces of attraction at the exterior surface of adsorbed organic molecules, the wetting properties of such surfaces are identical with those of an organic solid of the same surface composition. Even a single close-packed adsorbed monolayer is sufficient to convert the wetting properties of a high-energy surface like gold, steel or fused silica into those of a low-energy surface. One can now predict that the same rule will hold for the wettability of any such film-coated surface by an aqueous solution.

However, the adsorbed monolayer may gradually dissolve in the aqueous phase, in which case one might say the aqueous solution has also operated either as a solvent or as a detergent. An-

other type of low-energy surface of interest would be any smooth solid coated or smeared with a polymolecular film of a hydrocarbon oil. Aqueous solutions of wetting agents should obey the same rules described here for polyethylene, but with γ_c depending on the composition of the hydrocarbon. Again, however, if the wetting agent is also a detergent additive (such as a micelle forming compound), the oil eventually would be removed from the solid surface, and the wetting properties could revert to those of the original uncoated solid surface.

The results reveal that in predicting the spreading properties on low-energy surfaces of aqueous solutions of wetting agents, one cannot neglect γ_{SL} at solute concentrations so low that the liquid surface phase is essentially water; but at concentrations high enough for the surface of the water to approximate close packing of adsorbed solute molecules, γ_{SL} becomes constant and small in value, and the wetting behavior becomes predictable by the critical surface tension approach.

It appears possible to rate the effectiveness of any hydrocarbon-type wetting agent by the minimum concentration necessary at 25° to cause the solution to spread on smooth polyethylene (γ_c = 30 dynes/cm.). Another interesting measure of wetting efficiency is the minimum concentration of the agent necessary to wet the smooth clean surface of Teflon (γ_c = 18 dynes/cm.); however, conventional wetting agents could not be so rated since they do not decrease γ_{LV} below 26–27 dynes/cm. A measure of intermediate value is the minimum concentration necessary to spread on the surface of a single crystal of hexatriacontane[10] (γ_c = 22 dynes/cm.). Polystyrene[30] (γ_c = 33 dynes/cm.) and polyvinyl chloride[7] (γ_c = 34 dynes/cm.) might also be considered useful low-energy surfaces for relatively rating the wetting agents incapable of lowering γ_{LV} below 30 dynes/cm. The value of such a scheme for relatively rating aqueous wetting agents is that it is quantitative, objective, requires small amounts of solution, has fundamental significance, and need not be confused by other properties such as detergency, capillarity and surface roughness.

(30) A. H. Ellison and W. A. Zisman, THIS JOURNAL, **58**, 503 (1954).

A THERMODYNAMIC STUDY OF SOME COÖRDINATION COMPLEXES OF METAL IONS WITH DIPROTIC NITROGEN COMPOUNDS CONTAINING ONE HETEROCYCLIC NITROGEN ATOM[1,2]

BY DAVID E. GOLDBERG AND W. CONARD FERNELIUS

Contribution from the Department of Chemistry, The Pennsylvania State University, University Park, Pa.

Received December 8, 1958

Formation constants were determined for 2-picolylamine, 2-picolylmethylamine and 2-(2-aminoethyl)-pyridine with copper, nickel, cobalt(II), zinc and cadmium ions over the temperature range 10–40°. Formation constants for iron(II) were determined at 30° with 2-picolylamine and 2-picolylmethylamine, but formation constants were unobtainable for silver with any of the amines listed. Stabilization due to dative π-bondng was shown by dividing the free energy of formation of a stepwise chelation reaction by the free energy of formation of an entirely protonated ligand. The denominator in such a ratio was used as a measure of the strength of the σ-bond in the chelation process, and thus a high ratio would indicate stabilization other than by σ-bonding. It was shown that the amines expected to show π-bond stabilization had higher ratios than did similar amines which could not form π-bonds.

Introduction

The literature contains many references to the formation constants for complexes of aliphatic mono- and poly-amines with a variety of metal ions.[3] Quite in contrast, the number of references to similar data on monoprotic heterocyclic nitrogen compounds is meager and limited to the ions Ag^+ and Hg^{++} for pyridine and its derivatives.[4,5] Among polyprotic heterocyclic nitrogen compounds the data are limited to bipyridyl, terpyridyl and *o*-phenanthroline.[3] Stability constants for the complexes of the monoprotic heterocyclic nitrogen compounds with metal ions are much lower than the stability constants of ammonia and the simple aliphatic amines. Data presently available indicate that the combinations of bipyridyl with most metal ions are weaker than those of such diamines as ethylenediamine.

There are presented here formation constant data on diprotic nitrogen compounds in which one of the nitrogen atoms is present in a heterocyclic nucleus and the other is present as an aliphatic amine. The only compound of this type previously investigated is histamine.[6-8] In harmony with previous work done in this Laboratory[9-11] for-

(1) This investigation was carried out under contract AT(30-1)-907 between The Pennsylvania State University and the U. S. Atomic Energy Commission.

(2) A portion of a thesis presented by David E. Goldberg in partial fulfillment of the requirements for the degree of Doctor of Philosophy, January, 1959.

(3) J. Bjerrum, G. Schwarzenbach and L. G. Sillen, "Stability Constants. I. Organic Ligands," Special Publication No. 6, The Chemical Society, Burlington House, London W. 1, 1957.

(4) G. A. Carlson, J. P. McReynolds and F. H. Verhoek, *J. Am. Chem. Soc.*, **67**, 1334 (1945).

(5) J. Bjerrum, *Chem. Revs.*, **46**, 381 (1950).

(6) B. L. Mickel and A. C. Andrews, *J. Am. Chem. Soc.*, **77**, 323, 5291 (1955).

(7) G. B. Hares, W. C. Fernelius and B. E. Douglas, *ibid.*, **78**, 1816 (1956).

(8) A. Albert, *Biochem. J.*, **60**, 690 (1952).

(9) G. McIntyre, Jr., B. P. Block and W. C. Fernelius, *J. Am. Chem. Soc.*, **81**, 529 (1959).

(10) J. Lotz, B. P. Block and W. C. Fernelius, THIS JOURNAL, **63**, 541 (1959).

(11) C. Bertsch, W. C. Fernelius and B. P. Block, *ibid.*, **62**, 444 (1958).

TABLE I

VALUES FOR THE THERMODYNAMIC QUANTITIES LOG K_n, $-\Delta F^0_n$, $-\Delta H^0_n$ AND ΔS^0_n INVOLVED IN THE REACTION AT 10, 20, 30 AND 40° OF SEVERAL BI-VALENT METAL IONS WITH SEVERAL AMINES

Ion	n	log K_n 10°	20°	30°	40°	$-\Delta F^0_n$ 10°	20°	30°	40°	$-\Delta H^0_n$ 10–40°	ΔS^0_n 10°
				2-Picolylamine							
H^+	1	9.09 ± 0.01	8.78 ± 0.01	8.51 ± 0.04	8.34 ± 0.005	11.8	11.8	11.8	12.0	10.3	5
	2			3.1	2.8						
Cu^{++}	1	9.90 ± .12	9.64 ± .05	9.45 ± .08	9.17 ± .07	12.8	12.9	13.1	13.1	9.61	11
	2	8.26 ± .02	7.98 ± .03	7.80 ± .04	7.58 ± .02	10.7	10.7	10.8	10.9	8.98	6
Ni^{++}	1	7.49 ± .04	7.23 ± .02	7.09 ± .025	6.86 ± .025	9.70	9.70	9.83	9.83	8.35	5
	2	6.56 ± .10	6.32 ± .025	6.08 ± .09	5.87 ± .12	8.50	8.48	8.43	8.41	9.25	−3
	3	5.31 ± .10	5.07 ± .04	4.95 ± .05	4.66 ± .025	6.88	6.80	6.86	6.67	8.43	−6
Co^{++}	1	5.75 ± .02	5.51 ± .03	5.41 ± .02	5.23 ± .03	7.45	7.39	7.50	7.49	6.77	2
	2	4.92 ± .04	4.70 ± .04	4.52 ± .03	4.39 ± .04	6.37	6.31	6.27	6.29	7.13	−3
	3	3.63 ± .05	3.45 ± .03	3.33 ± .04	3.17 ± .09	4.70	4.63	4.62	4.54	6.14	−5
Zn^{++}	1	5.53 ± .00	5.41 ± .02	5.17 ± .04	5.04 ± .02	7.16	7.25	7.17	7.22	6.81	1
	2	4.61 ± .04	4.44 ± .02	4.21 ± .07	4.09 ± .07	5.97	5.95	5.84	5.86	7.28	−1
	3	3.29 ± .05	3.12 ± .10	3.07 ± .08	2.83 ± .09	4.26	4.18	4.26	4.05	5.85	−6
Cd^{++}	1	4.91 ± .18	4.71 ± .04	4.59 ± .19	4.48 ± .09	6.36	6.32	6.36	6.42	5.88	2
	2	4.14 ± .06	3.88 ± .06	3.82 ± .03	3.66 ± .72	5.36	5.20	5.30	5.24	6.14	−3
	3	2.90 ± .03	2.50 ± .09		2.54 ± .56	3.76	3.35		3.64		
Fe^{++}	1			3.82 ± .01							
	2			3.34 ± .08							
				2-Picolylmethylamine							
H^+	1	9.30 ± 0.005	9.10 ± 0.01	8.82 ± 0.04	8.62 ± 0.01	12.04	12.20	12.23	12.35	9.43	9
	2			2.92 ± .20	2.91 ± .18						
Cu^{++}	1	9.53 ± .09	9.21 ± .06	9.27 ± .05	8.88 ± .04	12.34	12.35	12.85	12.72	7.67	17
	2	7.03 ± .02	6.81 ± .02	6.55 ± .04	6.31 ± .04	9.10	9.13	9.08	9.04	9.84	3
	3		2.49 ± .04	2.84 ± .09	2.25 ± .50						
Ni^{++}	1	7.15 ± .21	6.93 ± .02	6.66 ± .02	6.50 ± .06	9.26	9.29	9.23	9.31	9.04	1
	2	5.75 ± .04	5.48 ± .03	5.30 ± .02	5.12 ± .04	7.45	7.35	7.35	7.33	8.44	−4
	3	3.17 ± .19	2.88 ± .09	2.79 ± .12	2.90 ± .45	4.11	3.86	3.87	4.15	3.76	1
Co^{++}	1	5.35 ± .01	5.26 ± .03	5.10 ± .03	4.86 ± .01	6.93	7.05	7.07	6.96	6.59	1
	2	4.05 ± .01	3.84 ± .18	3.84 ± .03	2.59 ± .04	5.24	5.15	5.32	5.14	5.61	−1
	3	2.49 ± .11	2.53 ± .54	2.63 ± .11	2.23 ± .04	3.22	3.39	3.65	3.19	2.65	2
Zn^{++}	1	5.12 ± .03	4.95 ± .06	4.73 ± .03	4.76 ± .05	6.66	6.68	6.70	6.82	5.26	5
Cd^{++}	1	4.60 ± .03	4.60 ± .04	4.30 ± .10	4.30 ± .04	5.96	6.17	5.96	6.16	4.89	4
	2		3.53 ± .06	3.56 ± .21	3.28 ± .10						
	3		2.79 ± .07		2.48 ± .09						
Fe^{++}	1			3.53 ± .04							
	2			2.73 ± .08							
				2-(2-Aminoethyl)-pyridine							
H^+	1	10.03 ± 0.02	9.75 ± 0.01	9.52 ± 0.01	9.17 ± 0.01	12.99	13.07	13.20	13.13	11.4	6
	2	3.94 ± .05	3.78 ± .03	3.84 ± .02	3.61 ± .05	5.10	5.07	5.32	5.17	3.77	5
Cu^{++}	1	7.83 ± .02	7.48 ± .12	7.48 ± .01	7.13[a]	10.14	10.06	10.37	10.21	8.61	5
Ni^{++}	1	5.45 ± .12	5.25 ± .05	5.14 ± .02	4.90 ± .04	7.05	7.04	7.13	7.02	7.14	0
	2	3.59 ± .14	3.28 ± .02	3.20 ± .03	3.30 ± .09	4.65	4.40	4.44	4.73	4.06	2

[a] Value doubtful; K varies with $\bar{n}$.

mation constants were determined at a number of temperatures. Thus it is possible to calculate rough values for the heat of reaction (ΔH) and to evaluate the relative effect of the enthalpy and entropy on the equilibrium constants.

Experimental

Procedure.—Formation constants were determined by *p*H titrations as described initially by Bjerrum[12] and modified by McIntyre.[9] Low ionic strength solutions were employed and calculated to zero ionic strength. The calculations were made by the method of Block and McIntyre.[13]

Reagents.—Metal perchlorate solutions and perchloric acid solutions, except for iron(II) perchlorate, were prepared from G. F. Smith Chemical Co. reagent grade materials. The iron(II) perchlorate solution was prepared from standardized iron wire (Fisher Scientific Co.) by solution in perchloric acid. Standard analytical procedures were used to determine the concentrations of all the reagents.

The amine solutions were prepared using freshly boiled, distilled water. The normality of each was determined by titration with standardized perchloric acid.

Amines.—2-Picolylamine (Aldrich Chemical Co., Inc.) was distilled under vacuum and the fraction boiling at 96°

(12) J. Bjerrum, "Metal Ammine Formation in Aqueous Solution," P. Haase and Son, Copenhagen, 1941.

(13) B. P. Block and G. H. McIntyre, Jr., *J. Am. Chem. Soc.*, **75**, 5667 (1953).

(21 mm.) was collected; reported b.p. 91° (15 mm.)[14]; 92–93° (20 mm.).[15] The neutral equivalents of the solutions prepared were 108.6 and 107.9; calculated 108.14. The dihydrochloride of the amine was prepared; m.p. 183–186°. *Anal.*[16] Calcd. for $C_6H_{10}N_2Cl_2$: C, 39.64; H, 5.60. Found: C, 39.80; H, 5.57.

2-Picolylmethylamine (Aldrich Chemical Co., Inc.) was distilled twice at 79° (10 mm.). The neutral equivalents of the solutions prepared from two samples were 123.4 and 124.1; calculated 122.2.

2-(2-Aminoethyl)-pyridine (Sapon Laboratories) was distilled under vacuum, b.p. 92° (12 mm.), as reported by Löffler.[17] The dipicrate was prepared, m.p. 218° (reported[16] 215–216°). *Anal.* Calcd. for $C_{19}H_{16}N_8O_{14}$: C, 39.32; H, 2.78. Found: C, 39.36; H, 2.91. The neutral equivalent of the solution was found to be 125.0; calculated 122.2.

Discussion

The results of the determinations of dissociation constants and formation constants are listed in Table I.

Acid Dissociation Constants.—For 2-picolylamine at 30° pK_1 (for BH_2^{++}) is 3.1 and pK_2 (for BH^+) is 8.51. For ethylamine at 30° pK (for BH^+) is 10.6 and for ethylenediamine at 30° pK's are 6.79 and 9.81. The value of pK for the ridine at 30° is approximately 5.2. Thus, it may be expected that in 2-picolylamine the aliphatic nitrogen atom is more basic than the heterocyclic nitrogen atom.

2-Picolylmethylamine has a pK_2 value about 0.3 higher than the corresponding value of 2-picolylamine, although the difference in the pK_1 values is less. Analogously a higher base strength brought about by methyl substitution is shown with the systems ethylenediamine and its substitution products, N-methylethylenediamine, $pK_1 = 6.63$, $pK_2 = 9.90$; N,N'-dimethylethylenediamine, $pK_2 = 10.2$ (25°).

2-(2-Aminoethyl)-pyridine has a pK_2 (for BH^+) higher than the corresponding value for 2-picolylamine. This observation is in agreement with the values noted for the compounds ethylenediamine and 1,3-propanediamine. The pK_1 (for BH_2^{++}) value for 2-(2-aminoethyl)-pyridine was higher than that for 2-picolylamine. This effect is due to the increased separation between the protonated nitrogen atom and the basic atom in question.

Formation Constants.—Formation constants of 2-picolylamine and 2-picolylmethylamine were uniformly higher than those of 2-(2-aminoethyl)-pyridine. This effect is in agreement with the higher stability of five-membered *vs.* six-membered chelate rings with divalent metal ions. No data were obtainable with silver ion, due to the variation in values of log K with the value of $\bar{n}$. Schwarzenbach has noted a tendency of silver ion to form bimetallic complexes.[18] The formation constants of 2-picolylamine were uniformly higher than those of its methyl-substituted derivative. Moreover, this difference was greater in the coördination of the second and third molecules of ligand than it was in the coördination of the first. This is in agreement with the results obtained with ethylenediamine and its methyl-substituted derivative.[9]

(14) L. C. Craig and R. M. Hixon, *ibid.*, **53**, 4367 (1931).
(15) H. Veldstra and P. W. Wiardi, *Rec. trav. chim.*, **61**, 627 (1942).
(16) Microanalyses were performed by Galbraith Microanalytical Laboratories, Knoxville, Tennessee.
(17) K. Löffler, *Ber.*, **37**, 170 (1904).
(18) G. Schwarzenbach, *et al.*, *Helv. Chim. Acta*, **35**, 2337 (1952).

TABLE II

STABILIZATION DUE TO π-BONDING

1. Ethylenediamines and 2-picolylamines

	H	Cu	Ni	Zn
A. Formation constants				
Ethylenediamine[9]	9.81	10.36	7.27	5.55
	6.79	8.93	6.11	4.98
			4.20	
N-Methylethylenediamine[9]	9.90	10.06	6.97	5.29
	6.63	8.38	5.40	4.23
			2.68	
2-Picolylamine	8.51	9.45	7.09	5.17
	3.1	7.80	6.08	4.21
			4.95	3.07
2-Picolylmethylamine	8.82	9.27	6.66	4.83
	2.9	6.55	5.30	
		2.8	2.79	

Ionic strength → 0; T = 30°

B. Values for the ratio $\frac{\Delta F_i}{(\Delta F_H)_1 - (\Delta F_H)_2}$

	i	Cu	Ni	Zn
Ethylenediamine	1	0.62	0.44	0.33
	2	.54	.37	.30
	3		.25	
N-Methylethylenediamine	1	.61	.42	.32
	2	.51	.33	.26
	3		.16	
2-Picolylamine	1	.81	.61	.44
	2	.67	.52	.36
	3		.42	.26
2-Picolylmethylamine	1	.79	.56	.41
	2	.56	.45	
	3	.24	.24	

2. 2-(2-Aminoethyl)-pyridine and 1,3-propanediamine

	H	Cu	Ni
A. Formation constants			
2-(2-Aminoethyl)-pyridine	9.52	7.48	5.14
	3.84		3.20
1,3-Propanediamine[11]	10.32	9.45	6.18
	8.33		4.28

Ionic strength → 0; T = 30°

B. Values for the ratio $\frac{\Delta F_i}{(\Delta F_H)_1 + (\Delta F_H)_2}$

	i	Cu	Ni
2-(2-Aminoethyl)-pyridine	1	0.53	0.38
	2		.24
1,3-Propanediamine	1	.51	.33
	2		.23

C. Values for the ratio $\frac{\Delta H_i}{(\Delta H_H)_1 + (\Delta H_H)_2}$

	i	Cu	Ni
2-(2-Aminoethyl)-pyridine	1	0.57	0.47
	2		.27
1,3-Propanediamine	1	.51	.38
	2		.30

There was an apparent tendency for copper ion to exhibit a coördination number greater than four. Calculation of formation constants for the reaction of a third molecule of 2-picolylmethylamine per metal ion was possible.

Attainment of equilibrium was slow for the first few additions of the picolylamines to nickel ion

solutions, especially at 10 and 20°. This effect is not due to incipient precipitation, since the later additions proceed rapidly and with no sign of precipitation. The formation constants calculated from these measurements do not show any effect ascribable to precipitation. No reason is known why the equilibrium attainment is slow, but other workers have reported similar results with related systems.[19a,b]

Formation constants with copper and nickel, only, were obtainable for 2-(2-aminoethyl)-pyridine. Other metal ions yielded either precipitates, which preclude the possibility of calculation of formation constants, or values for the formation constants which were dependent on the value of $\bar{n}$. A third constant could not be obtained for the reaction of this ligand with nickel ion. Bertsch[11] was unable to obtain a third constant with 1,3-propanediamine.

Formation constants were obtained for 2-picolylamine and 2-picolylmethylamine with iron-(II). Only two constants were calculable for these systems.

Interpretation.—The heterocyclic, doubly-bonded nitrogen atom in these amines has the ability to form dative π-bonds with transition metal ions.[20] This behavior is given as the reason for the stability of the complexes of iron with *o*-phenanthroline and 2,2′-bipyridyl. This same effect is thought to be responsible for the unusually high stabilities of the metal carbonyls, the ferrocene-type complexes, and the metal derivatives of *o*-phenylenebis-(dimethylarsine).

Thus, it is expected that the bond strengths of the bonds formed by the ligands studied in this investigation should be higher than would be the case if there were no possibility of dative π bond formation.

A comparison of the bond strength of a σ-bonded ligand to that of a ligand bonded by both σ- and π-bonds is impossible without consideration of the changes in the other factors which affect bond stability—ring size, charge on the central ion and on the ligand, the donor atoms, the metal ion, steric properties of the ligand and base strength of the ligand. It is possible to keep the ring size, the charge type, the donor atoms and the metal ion the same in both reactions to be compared. Differences in steric properties are more difficult to eliminate from the two reactions, but efforts to duplicate steric properties as closely as possible probably would minimize the importance of this factor. However, change from one type ligand to another would affect the base strength greatly. Thus it is the difference in base strengths of the ligands which is the greatest deterrent to the direct comparison of the bond stabilities of the two systems to determine effect of π-bonding.

Several workers[21] have determined that the coordination stabilities of simple σ-bonding ligands are approximately proportional to the base strengths of the ligands. It seems reasonable to assume that the base strengths might be used as a measure of the σ-bonding portion of a coördinate bond. With this assumption it is possible to compare the coördination stability of a ligand–metal bond per unit base strength. The results of such calculations are shown in Table II. It seems that the coördination stability per unit base strength (including the base strength of all of the donor atoms) is higher for ligands which might be expected to form dative π-bonds than for those which are expected not to form dative π-bonds.

(These calculations should be made using ΔH rather than ΔF since it is the former which is directly related to bond strength. The data for 2-(2-aminoethyl)-pyridine are available to permit this, see Table II, 2C.)

Acknowledgment.—The authors are indebted to Dr. C. G. Haas, Jr., for the many helpful discussions.

(19) (a) J. Bjerrum, ref. 12, p. 213; (b) G. Schwarzenbach, private communication.

(20) J. Chatt, *Nature*, **165**, 637 (1950); J. Chatt and A. Williams, *J. Chem. Soc.*, 3061 (1951); S. Ahrland, J. Chatt and N. R. Davies, *Quart. Revs.*, **12**, 265 (1958).

(21) (a) M. Calvin and K. W. Wilson, *J. Am. Chem. Soc.*, **67**, 2003 (1945); (b) R. J. Bruehlman and F. H. Verhoek, *ibid.*, **70**, 1401 (1948); (c) L. G. Van Uitert, W. C. Fernelius and B. E. Douglas, *ibid.*, **75**, 2736 (1953); (d) L. G. Van Uitert and W. C. Fernelius, *ibid.*, **75**, 3862 (1953); (e) B. E. Bryant, W. C. Fernelius and B. E. Douglas, *ibid.*, **75**, 3784 (1953); (f) B. E. Bryant and W. C. Fernelius, *ibid.*, **76**, 1696, 3783, 4864 (1954); (g) F. A. Snavely, W. C. Fernelius and B. P. Block, *ibid.*, **79**, 1028 (1957); (h) F. A. Snavely, W. C. Fernelius and B. E. Douglas, *J. Soc. Dyers and Colourists*, **73**, 491 (1957).

THE TIME LAG IN DIFFUSION. IV

BY H. L. FRISCH

Bell Telephone Laboratories, Murray Hill, New Jersey

Received December 11, 1958

Certain aspects of "non-Fickian" diffusion are discussed and a classification of "non-Fickian" (as well as Fickian) diffusion is obtained according as the diffusion current is (or is not) derivable from a gradient of a scalar function, the potential of diffusion. In the former instance an expression for generalized time lag for permeation rate experiments with n-dimensional spherical symmetry is obtained. Finally we comment shortly on memory effects and frame of reference corrections.

1. Introduction

In a previous series of papers[1,2] we have been concerned with the calculation and properties of the time lag in one-dimensional Fickian diffusion under a concentration dependent diffusion coefficient. There exist also systems in which the diffusion of a component is anomalous in a number of regards, such as in the existence of an explicit time dependence of the diffusion coefficient, the existence of memory effects even in the steady-state flux of the

(1) H. L. Frisch, THIS JOURNAL, **61**, 93 (1957).

(2) H. L. Frisch, *ibid.*, **62**, 401 (1958).

diffusing species, etc. One often speaks in such instances of "non-Fickian" diffusion.[3] Recently Barrer and Ferguson[3] and Meares[4] have again observed an explicit time, as well as concentration, dependence of the differential diffusion coefficient $\mathfrak{D}$. Characteristically both of these groups of investigators found that the calculated $\mathfrak{D}$'s obtained from time lag (non-steady-state) data and steady-state permeation rate data differed considerably.

We will show by a suitable generalization of our previous calculations of the time lag L that the above observation is indeed a consequence of the explicit time dependence of $\mathfrak{D}$. The newly derived relations for L will indicate the extent of information obtainable concerning this time dependence from combinations of experimental steady-state and time lag measurements for certain functional classes of $\mathfrak{D}$, *e.g.*, for all the cases where $\mathfrak{D}$ is a suitable given function of c and t, $\mathfrak{D} = \mathfrak{D}(c, t)$, and not an arbitrary functional of c and t. The more general diffusion systems with which we shall be concerned will possess n-dimensional spherical symmetry and will correspond in the case $n = 1$ to one-dimensional diffusion through a flat membrane (of thickness l), $n = 2$ to two-dimensional radial diffusion through (infinite) concentric cylinders and $n = 3$ to three-dimensional radial diffusion between concentric spheres. Since most experimental arrangements possess spherical symmetry we restrict ourselves to the above even though our calculations can be carried out as well for certain other geometries.

2. The Potential of Diffusion.—Consider the diffusion of a component whose concentration is $c(r,t)$ in a volume element centered at r at time t. By Fick's first law the (uniform) diffusion current at r, $J(r,t)$ is given by

$$J(r,t) = -\mathfrak{D} \operatorname{grad} c(r,t) \tag{1}$$

where $\mathfrak{D}$ is the differential diffusion coefficient. By Fick's second law (conservation of mass) J satisfies the continuity equation

$$\frac{\partial c}{\partial t} + \operatorname{div} J = 0 \tag{2}$$

or

$$\frac{\partial c}{\partial t} - \operatorname{div} [\mathfrak{D} \operatorname{grad} c] = 0$$

We distinguish now between two classes of diffusion fields: (1) those for which J can be written as a gradient of a scalar potential function φ, say $\varphi = \varphi(c, r, t)$, *i.e.*

$$J = -\mathfrak{D} \operatorname{grad} c = -\operatorname{grad} \varphi \tag{3}$$

and (2) those for which J cannot be represented in this way. In the former instance we call φ the potential of diffusion (p.o.d.) while in the latter J can quite generally be represented as a sum of a gradient of a scalar function and a curl of a vector function where both functions can be derived in a straight forward way from the solution of a vectorial Poisson equation.[5] A necessary and sufficient condition that a p.o.d. exists (*i.e.*, eq. 3 applies) is that the

$$\operatorname{curl} J = 0 \tag{4}$$

Thus if $\mathfrak{D}$ is a function of c only, $\mathfrak{D} = \mathfrak{D}(c)$, the function φ may be taken to be[6]

$$\varphi = \int_0^{c(r,t)} \mathfrak{D}(u)\, du \tag{5}$$

Even if the diffusion is "non-Fickian," *i.e.*, $\mathfrak{D}$ is a function of both $c(r,t)$ and t, $\mathfrak{D} = \mathfrak{D}(c,t)$, a p.o.d. exists and φ may be taken to be

$$\varphi = \int_0^{c(r,t)} \mathfrak{D}(u,t)\, du \tag{6}$$

In either case eq. 2 becomes

$$\frac{\partial c}{\partial t} - \nabla^2 \varphi = 0 \tag{7}$$

and if a steady-state can be attained as $t \to \infty$, *i.e.*

$$c(r,t) \to c_s(r)$$
$$\varphi(c,r,t) \to \varphi_s(c_s,r) \tag{8}$$

we expect that (7) reduces to

$$\nabla^2 \varphi_s = 0 \tag{9}$$

The boundary conditions under which we seek solutions of these equations specify constant values of $c(r,t)$ on the bounding surfaces of our volumes available for diffusion (Dirichlet conditions). As physical consequences of (4) and (9) we have that: (a) the line integral between two points of J depends only on the end-points and not the path over which it is taken; and (b) the steady-state, if attained, is independent of the previous history of the system (no memory effects exist).

3. The Generalized Time Lag.—Consider the n-dimensional, spherically symmetrical diffusion boundary value problem which characterizes a diffusion transmission (permeation) experiment for which a p.o.d., $\varphi(c(r,t), r,t)$, exists (*cf.* eq. 7)

$$\frac{\partial c(r,t)}{\partial t} = \frac{1}{r^{n-1}} \frac{\partial}{\partial r} \left\{ r^{n-1} \frac{\partial \varphi(c,r,t)}{\partial r} \right\} \tag{10}$$
$$n = 1,2,\ldots$$

in $R_1 < r < R_2$, $t > 0$ where

$$c(R_1,t) = c_1 \text{ or } \varphi(c_1,R_1,t) = \varphi_1(t)$$
$$c(R_2,t) = c_2 \text{ or } \varphi(c_2R_2,t) = \varphi_2(t)$$
$$c(r,0) = c_0(r)$$

We assume φ is such that as $t \to \infty$ the solution of (10) satisfies eq. 8 where $\varphi_s(c_s, r)$ is the solution of the steady-state problem

$$\frac{1}{r^{n-1}} \frac{\partial}{\partial r} \left\{ r^{n-1} \frac{\partial \varphi_s}{\partial r} \right\} = 0 \tag{11}$$

with

$$\varphi_s(R_1) = \varphi_1^s = \lim_{t\to\infty} \varphi_1(t)$$
$$\varphi_s(R_2) = \varphi_2^s = \lim_{t\to\infty} \varphi_2(t)$$

The flux and total flow (to time t) through the n-dimensional sphere of radius R_2 are

$$\Phi(R_2,t) = -\omega_n \left[r^{n-1} \frac{\partial \varphi}{\partial r} \right]_{r=R_2}$$

and

$$Q(R_2,t) = \int_0^t \Phi(R_2,\tau)\, d\tau \tag{12}$$

(3) R. M. Barrer and R. R. Ferguson, *Trans. Faraday Soc.*, **54**, 989 (1958); see this paper for references to earlier considerations of "non-Fickian" diffusion. The reader should note our rather restricted use of the term "non-Fickian" diffusion.

(4) P. Meares, *J. Polymer Sci.*, **27**, 391, 405 (1958).

(5) See *e.g.*, C. E. Weatherburn, "Advanced Vector Analysis," G. Bell and Sons, Ltd., London, 1949, p. 44.

(6) F. Weiss, private communication.

respectively, with

$$\omega_n = 2(\sqrt{\pi})^n/\Gamma(n/2) \tag{13}$$

The corresponding steady-state flux and flow, $\Phi_s(R_2)$ and $Q_s(R_2, t)$, are obtained by replacing φ by φ_s in (12).

Equation 11 can be integrated immediately, so that we find

$$-\omega_n r^{n-1}\frac{\partial \varphi_s}{\partial r} = \Phi_s(R_2) = \frac{\omega_n(\varphi_1^s - \varphi_2^s)}{I_n(R_1,R_2)} \tag{14}$$

and

$$\varphi_s(c_s(r),r) = \varphi_2^s + (\varphi_1^s - \varphi_2^s)\frac{I_n(r,R_2)}{I_n(R_1,R_2)} \tag{15}$$

where

$$I_n(x,y) = \int_x^y \frac{dz}{z^{n-1}}$$

Inversion of (15) for $c_s(r)$ gives the steady-state concentration.

Again as $t \to \infty$, $Q(R_2, t)$ approaches the asymptotic flow

$$Q_s(R_2,t) = \Phi_s(R_2)(t - L) \tag{16}$$

which defines the time lag L. To calculate it we proceed in this way:

We multiply both sides of (10) by $\omega_n r^{n-1}$ and integrate over r from r to R_2 (*i.e.*, we apply the Gauss divergence theorem twice) to obtain

$$\omega_n \int_r^{R_2} \frac{\partial c(z;t)}{\partial t} z^{n-1}\,dz = -\Phi(R_2,t) - \omega_n r^{n-1}\frac{\partial \varphi(c,r,t)}{\partial r} \tag{17}$$

Dividing (17) by the surface area $\omega_n r^{n-1}$ and integrating over r from R_1 to R_2 we find using the boundary conditions of (10)

$$\int_{R_2}^{R_2}\frac{dr}{r^{n-1}}\int_r^{R_2}\frac{\partial c(z;t)}{\partial t} z^{n-1}\,dz = -\frac{\Phi(R_2,t)}{\omega_n} I_n(R_1,R_2) - [\varphi_2(t) - \varphi_1(t)] \tag{18}$$

Integrating (18) over t from 0 to t we find on rearranging that

$$Q(R_2,t) = -\frac{\omega_n}{I_n(R_1,R_2)}\int_{R_1}^{R_2}\frac{dr}{r^{n-1}}\int_r^{R_2}[c(z;t) - c_0(z)]z^{n-1}\,dz + \frac{\omega_n}{I_n(R_1,R_2)}\int_0^t [\varphi_1(\tau) - \varphi_2(\tau)]d\tau \tag{19}$$

Adding and subtracting $Q_s(R_2,t)$—given by virtue of (12) and (14) by

$$Q_s(R_2,t) = \Phi_s(R_2)t = \frac{\omega_n t}{I_n(R_1,R_2)}(\varphi_1^s - \varphi_2^s) \tag{20}$$

—to the right-hand side of eq. 19 we obtain

$$Q(R_2t) = \Phi(R_2)\left\{t - \frac{\int_{R_1}^{R_2}\frac{dr}{r^{n-1}}\int_r^{R_2}[c(z,t) - c_0(z)]z^{n-1}\,dz}{(\varphi_1^s - \varphi_2^s)} + \frac{\int_0^t [\varphi_1(\tau) - \varphi_2(\tau) - (\varphi_1^s - \varphi_2^s)]d\tau}{(\varphi_1^s - \varphi_2^s)}\right\} \tag{21}$$

Comparing (21) with (16) and using (8) we find finally the desired relation for L

$$L = \frac{\int_{R_1}^{R_2}\frac{dr}{r^{n-1}}\int_r^{R_2}[c_s(z) - c_0(z)]z^{n-1}\,dz}{(\varphi_1^s - \varphi_2^s)} - \frac{\int_0^\infty [\varphi_1(\tau) - \varphi_2(\tau) - (\varphi_1^s - \varphi_2^s)]d\tau}{(\varphi_1^s - \varphi_2^s)} \tag{22}$$

In particular, we note that if $\mathfrak{D} = \mathfrak{D}(c,t)$ then the p.o.d. φ is given by eq. 6 and

$$\varphi_1(t) - \varphi_2(t) = \int_{c_2}^{c_1}\mathfrak{D}(u,t)\,du$$

$$\varphi_1^s - \varphi_2^s = \lim_{t\to\infty}\int_{c_2}^{c_1}\mathfrak{D}(u,t)\,du \tag{23}$$

$$\lim_{t\to\infty}\int_{c_2}^{c_s(r)}\mathfrak{D}(u,t)\,du \Big/ \lim_{t\to\infty}\int_{c_2}^{c_1}\mathfrak{D}(u,t)\,du = I_n(r,R_2)/I_n(R_1,R_2)$$

by virtue of (15). From (22) and (23) we see immediately that the first term on the right-hand side of (22) is the time lag L_s which corresponds to the differential diffusion coefficient which is obtained from a steady-state permeation rate experiment. We note in passing that

$$\mathfrak{D}_s(c) = \lim_{\substack{t\to\infty \\ (c\ \text{fixed})}}\mathfrak{D}(c,t) \tag{24}$$

need not exist; all that is required for the attainment of a steady-state is that

$$\lim_{t\to\infty}\int_{c_2}^{c_1}\mathfrak{D}(u,t)\,du = (c_1 - c_2)\bar{D}_s(c_1,c_2) < \infty \tag{25}$$

i.e., that the limiting integral diffusion coefficient, $\bar{D}_s(c_1, c_2)$, exists.

When, $\mathfrak{D} = \mathfrak{D}(c)$, does not explicitly depend on time then the second term on the right-hand side of (22) vanishes identically, and

$$L = L_s = \frac{\int_{R_1}^{R_2}\frac{dr}{r^{n-2}}\int_r^{R_2}[c_s(z) - c_0(z)]z^{n-1}\,dz}{\int_{c_2}^{c_1}\mathfrak{D}(u)\,du} \tag{26}$$

Equation 26 reduces for $n = 1$, $R_2 - R_1 = l$, to our previously obtained result.[1] Furthermore for $n = 2$ and $\mathfrak{D} = \mathfrak{D}_0$; a constant we find from (23) and (26) directly that

$$L = \frac{(R_2^2 - R_1^2) + (R_1^2 + R_2^2)\ln R_1/R_2}{4\mathfrak{D}_0 \ln R_1/R_2} \tag{27}$$

This result agrees with that quoted by Barrer[7] and incidentally gives an independent means for obtaining certain sums involving Bessel functions (see *e.g.*, eq. 120 of ref. 7), which were first obtained by Jaeger[8] using Laplace transforms.

4. Non-Fickian Diffusion and Memory Effects.—In the case of "non-Fickian" diffusion whose current is derivable from a gradient of a p.o.d. eq. 15, 22 and 23 show that the time lag is known without having to solve (10) once the initial and boundary concentrations and the p.o.d. are given. In particular if $\mathfrak{D} = \mathfrak{D}(c, t)$ the last is known as soon as the functional form of $\mathfrak{D}$ is specified (*cf.* eq. 6). Conversely one can obtain a certain amount of information concerning the explicit time dependence of $\mathfrak{D}$ from a combination of steady-state data (permeation rates and sorption coefficients) and time lag measurements. The former give $\bar{D}_s(c_1, c_2)$ defined by eq. 25, as a function of the indicated boundary concentrations c_1. From such data L_s can be calculated.[1-3] To proceed further we need make only a very weak assumption: the explicit time dependence of $\mathfrak{D}$ arises from a relaxation behavior of

(7) R. M. Barrer, "Diffusion in and Through Solids," Cambridge at the University Press, 1951, p. 37.

(8) J. Jaeger, *Trans. Faraday Soc.*, **42**, 615 (1946).

the system. This relaxation need not have a single cause, but will in general depend on a spectrum of relaxation frequencies (reciprocal relaxation times). Thus the integral diffusion coefficient $\bar{D}(c_1,c_2;\ t)$ can be written

$$\bar{D}(c_1,c_2;t) = \bar{D}_s(c_1,c_2) - \int_0^\infty \psi(c_1,c_2;\omega)e^{-\omega t}\,d\omega \quad (28)$$

where ψ is the (integral) diffusion relaxation function. Introducing (28) into (22) we find that

$$\Delta L = L - L_s = + \frac{\int_0^\infty d\tau \int_0^\infty d\omega\psi(c_1,c_2;\omega)e^{-\omega t}}{\bar{D}_s(c_1,c_2)} = \frac{\int_0^\infty \psi(c_1,c_2;\omega)d\omega/\omega}{\bar{D}_s(c_1,c_2)} \quad (29)$$

As (29) shows ΔL tells us little about the form of ψ but does give us a measure of the mean relaxation time of the various processes affecting transient diffusion. Such information is particularly useful if the magnitude of ΔL or its variation with the temperature, concentration c_1, etc., allows us to identify (or rule out) a given set of relaxation processes.

It is now possible for the steady-state of a system to depend on the initial concentration of the diffusing species. Such, for example, is the behavior of a system possessing the diffusion coefficient

$$\mathfrak{D} = \mathfrak{D}\left\{\int_0^t f(r,\tau)c(r,\tau)d\tau,c(r,t),t\right\} \quad (32)$$

which is a functional of c and t and $f(r,t)$ is an arbitrary function of r and t. From (32) it is clear that the steady-state integral (or differential) diffusion coefficient will in general depend on the initial concentration as well as the history of the system previous to the attainment of its steady-state. It would be of some interest to determine whether the steady-state flux in instances of "non-Fickian" diffusion (say in polymer vapor systems) does indeed depend on the initial concentration of vapor in the membrane. Until further experimental data are available we shall not classify the various steady-state memory effects.

We have so far not discussed frame of reference corrections. In the simplest case where we need only correct for swelling of the membrane the corrections in the time lag, etc., can be carried out as indicated by Barrer and Ferguson.[3] More generally for diffusion into a deformable medium the diffusion equations written in this paper apply strictly only in a Lagrangian frame of reference. To transcribe the results for a fixed Eulerian reference frame a general procedure recently used in a different connection by Simmons and Dorn[9] should be applied.

(9) J. Simmons and J. E. Dorn, *J. Appl. Phys.*, **29**, 1308 (1958).

STUDIES ON THE ANODIC AND CATHODIC POLARIZATION OF AMALGAMS. PART III. PASSIVATION OF ZINC AMALGAM IN ALKALINE SOLUTIONS

BY S. E. KHALAFALLA, A. M. SHAMS EL-DIN AND Y. A. EL-TANTAWY

Contribution from the Chemistry Department, Faculty of Science, University of Cairo, Egypt (U.A.R.)

Received December 16, 1958

Anodic polarization of zinc amalgam at constant applied current is investigated in 0.1 *M* sodium hydroxide solution and found to exhibit one step corresponding to the formation of zinc oxide. The potential of this step changes with the mole fraction of zinc in the amalgam. The mercuric oxide step disappears even with the smallest concentrations of zinc. The quantity of electricity needed to passivate the amalgam increases with increase of the zinc content and depends on the value of the polarizing current. The process of passivation is found to be essentially diffusion controlled and the diffusing species is proved to be the hydroxyl ion through the hydroxide phase.

The study of the anodic behavior of amalgams has been the subject of a moderate number of articles[1-10] both from the theoretical and the analytical points of view. In these researches the amalgams were studied in acid or neutral solutions in which the amalgamated metals dissolve as simple ions. The study of the anodic characteristics of amalgams in solutions in which passivity can be established readily has attracted practically no attention. The object of this series is to fill this gap in view of understanding the mechanism by which metals can passivate. The zinc amalgam is first chosen in view of the ease by which it is prepared in a pure state and also because there are enough thermodynamical data for this metal to enable the interpretation of the results obtained.

Experimental

The electrical circuit used in obtaining the anodic potential–time curves under conditions of constant current was described in Part I.[11] The electrolytic cell has essentially the same features described before except that the anode cup was 1.806 cm.^{2} in area and was provided with a sealed-in platinum contact. The cathode compartment was situated over the anode and fitted with a sintered glass disc to prevent contamination with the anolyte. Pure hydrogen was used in deaerating the solution and was introduced

(1) J. Heyrovsky and N. Kalousek, *Coll. Czech. Chem. Commun.*, **11**, 464 (1939).
(2) J. J. Lingane, *J. Am. Chem. Soc.*, **61**, 779 (1939).
(3) M. V. Stackelberg and H. V. Freyhold, *Z. Elektrochem.*, **46**, 120 (1940).
(4) J. Heyrovsky and J. Forjet, *Z. physik. Chem.*, **193**, 77 (1943).
(5) G. Reboul and F. Bon, *Compt. rend.*, **224**, 1263 (1947).
(6) N. H. Furman and W. C. Cooper, *J. Am. Chem. Soc.*, **72**, 5667 (1950).
(7) A. Hickling and J. Maxwell, *Trans. Faraday Soc.*, **51**, 385 (1955).
(8) A. Hickling, J. Maxwell and J. V. Shennan, *Anal. Chem. Acta*, **14**, 287 (1956).
(9) K. W. Gardiner and L. B. Rogers, *Anal. Chem.*, **25**, 1393 (1953).
(10) J. W. Ross, R. D. DeMars and I. Shain, *ibid.*, **28**, 1768 (1956).
(11) A. M. Shams El-Din, S. E. Khalafalla and Y. A. El-Tantawy, THIS JOURNAL, **62**, 1307 (1958).

through a medium porosity sintered glass disc. The zinc amalgam was prepared electrolytically from a bath which was 2 *M* in zinc sulfate and 1 *N* in sulfuric acid. Thus when preparing any of the amalgam anodes studied, 1 ml. of redistilled mercury was introduced into the cup by means of a graduated medical syringe. The proper amount of the zinc sulfate solution was introduced into the cup and electrolysis was conducted under a fixed current of 250 ma./electrode. Electrolysis was continued with occasional stirring until all the zinc content of the solution was deposited. This was known by a sudden brisk evolution of hydrogen from the electrode surface; electrolysis was, however, allowed to proceed for a further 15 minute time with vigorous stirring. To ascertain the complete depletion of zinc from its solution, a spot test for zinc[12] utilizing 8-hydroxyquinaldine in methylated spirit was used. The amalgam was then washed thoroughly with conductivity water for several times and the wash water was drained off by a special pipet and then by small strips of filter paper. Each experiment was carried on a new electrode and a fresh solution.

When performing an anodic experiment, the amalgam electrode, prepared as described above, was introduced in the electrolytic cell containing the deaerated sodium hydroxide solution. In order to reduce any probable oxide on the surface of the electrode, it was subjected to a precathodization period of 30 minutes at a current of 1 ma./electrode. The polarizing current next was reduced to the value at which the anodic polarization was to be conducted and then reversed to start the experiment. The potential of the amalgam anode now was followed as function of time. All measurements were carried out in an air thermostat adjusted at 25 ± 0.1°.

Results and Discussion

The variation of the amalgam anodic potential with time is shown in Fig. 1 for various compositions of zinc amalgam ranging from 0.1 to 5% and at different currents ranging from 200–500 μa. From these results, it is seen readily that when forcing the amalgam electrode from the potential of hydrogen (and sodium) deposition to the oxygen evolution potential, only two steps are noticed. The first step observed at the foot of the curve is ascribed by analogy to pure mercury[11] to the discharge of the sodium that was previously reduced during the precathodization period. The quantities of electricity consumed in the discharge process were very reproducible and depended on the concentration of zinc in the amalgam. For zinc amalgam electrodes of compositions 0.1, 1.0, 2.3 and 5%, the quantities of electricity consumed in the discharge of sodium from the amalgam were 1408, 1024, 863, 708 mcoulomb, respectively. Comparison of these quantities of electricity with those consumed in its formation (1800 mcoulomb) reveals that the efficiency of reduction of sodium from 0.1 *N* sodium hydroxide solution is considerably less than 100%, being 78, 57, 48 and 39% for the 0.1, 1, 2.3 and 5% zinc amalgams, respectively. Thus the higher the zinc content of the amalgam, the lower is the efficiency of formation of sodium amalgam. The reason for this may be understood from a consideration of the hydrogen overpotential on both zinc and mercury. It is easier for hydrogen to evolve on zinc than on mercury cathodes. When dealing with a zinc amalgam cathode, the current will distribute itself between the deposition of zinc and mercury. When the zinc content of the amalgam is increased, the ratio of evolved hydrogen to electrodeposited sodium will increase with the result of a decrease in the efficiency of the sodium

(12) I. I. M. El-Beih and M. A. Abou El Naga, *Anal. Chem. Acta*, **17**, 397 (1957).

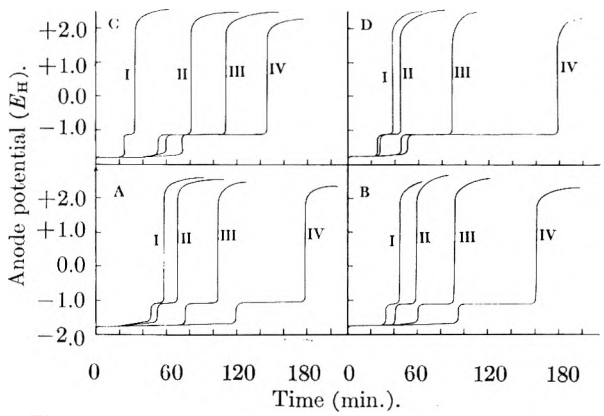

Fig. 1.—Anodic polarization of zinc amalgam in 0.1 *N* sodium hydroxide solution: (A) 0.1% zinc amalgam, I 200, II 300, III 400 and IV 500 μa./electrode; (B) 1% zinc amalgam, I 200, II 300, III 400 and IV 500 μa./electrode; (C) 2.3% zinc amalgam, I 200, II 250, III 300 and IV 500 μa./electrode; (D) 5% zinc amalgam, I 200, II 300, III 400 and IV 500 μa./electrode.

deposition. In the calculation of the efficiency of electro-reduction of sodium ions from solution, it was assumed that the discharge process is purely electrochemical in nature and that the chemical dissolution does not participate to any major extent in the discharge process.

The second step in the anodic potential–time curves of Fig. 1 is of some interest. The potential of this step was found to be constant for one and the same amalgam at different current densities but differed in the different amalgams studied. Table I gives a comparison between the potential of this step and the equilibrium potential of the system $Zn/Zn(OH)_2$ at the corresponding *p*H value after being corrected for the activity of zinc in the amalgam.

TABLE I

% of Zn in the amalgam	Starting potential of 2nd step (v.)	Equilibrium potential of $Zn/Zn(OH)_2$ system (v.)
0.1	1.10	1.113
1.0	1.14	1.142
2.3	1.15	1.152
5.0	1.15	1.161

The correction for the activity of zinc in the amalgam was made by applying the Nernst equation and assuming that the activity of zinc is equal to its mole fraction in the amalgam. The very close agreement between the values of potentials obtained from polarization curves and those calculated from thermodynamical data,[13] leaves no doubt that this step in the polarization curves correspond to the formation of zinc hydroxide on the surface of the electrode.

The quantities of electricity consumed in the second step were found to depend on both the zinc concentration in the amalgam and on the polarizing current imposed. Figure 2 represents the mode of dependence of the quantity of electricity required for passivation on the concentration of the amalgam. For the same polarizing current, the

(13) W. N. Latimer, "The Oxidation States of the Elements and their Potentials in Aqueous Solutions," Prentice-Hall Inc., New York, N. Y., 1953, p. 169.

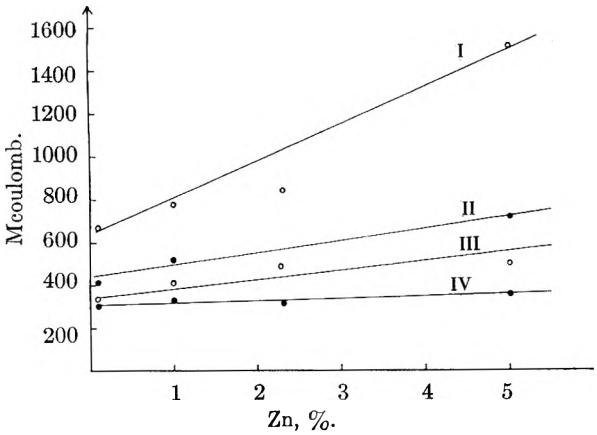

Fig. 2.—Quantity of electricity for passivation as a function of the % of zinc in the amalgam for various polarizing currents: I, 200; II, 300; III, 400; IV, 500 μa./electrode.

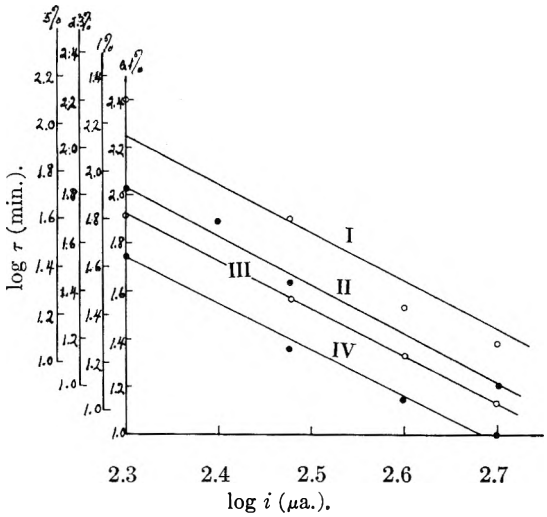

Fig. 3.—Log τ *vs.* log i plot for the passivation of zinc amalgam in 0.1 N sodium hydroxide: % of zinc: I, 5; II, 2.3; III, 1; IV, 0.1.

quantity of electricity needed for passivating the electrode increases with increase of the zinc content of the amalgam and also that with low currents, larger quantities of electricity are required to passivate the electrode than with higher currents.

After the completion of the zinc hydroxide step, the potential of the electrode changed directly to oxygen evolution value. The step corresponding to the oxidation of mercury of the amalgam was completely deleted; a zinc concentration as low as 0.01% (mole fraction 3.06×10^{-4}) failed to show any sign for the mercuric hydroxide step. Thus it appears that the presence of zinc impurities changes the electrochemical behavior of the amalgam from that of pure mercury to that of pure zinc electrode.

The relation between the polarizing current i and the time taken by the amalgam to acquire passivity τ is more quantitatively elucidated from a consideration of the log i–log τ curves in Fig. 3. For amalgams varying in composition between 1 and 5% in zinc, the log i–log τ plots are parallel straight lines with an average slope of -2. This suggests that the relation between the polarizing

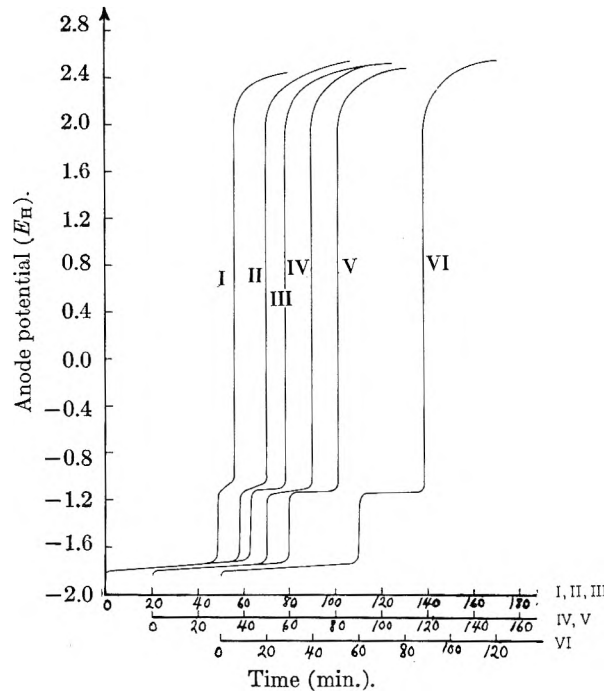

Fig. 4.—Anodic polarization of 1% zinc amalgam in: I, 0.04; II, 0.05; III, 0.06; IV, 0.08; V, 0.09; VI, 0.1 N sodium hydroxide solutions at the current density of 300 μa./electrode.

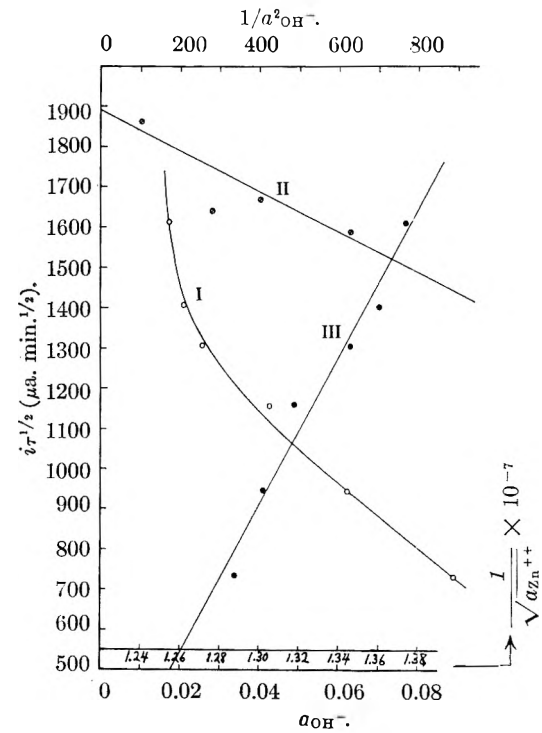

Fig. 5.—Variation of the quantity $i\tau^{1/2}$ with: I, the reciprocal of the square of hydroxyl ion activity; II, the reciprocal of the square root of zinc ion activity; III, hydroxyl ion activity.

current and the passivation time is of the form $i\tau^{1/2}$ = constant. In the first part of this series we have drawn attention to the similarity between the above observation and the results obtained from the equations of electrolysis at constant

current[14] where the supply of reducible material is controlled by diffusion to the electrode surface; the transition time in these equations is replaced by the passivation time. This proves conclusively that the process of passivation of the zinc amalgam in sodium hydroxide solutions is diffusion controlled. It becomes necessary to determine the diffusing species which brings about passivation. There are three possibilities for a diffusion process to occur in the solution phase: (1) diffusion of the OH ions from the bulk of the solution to the solution–hydroxide interface; (2) diffusion of zinc ions through the hydroxide phase to the zinc hydroxide–solution interface; and (3) diffusion of hydroxyl ions through the hydroxide layer to the hydroxide–amalgam interface.

The diffusion of hydroxyl ions from the bulk of the solution to the solution–hydroxide interface is ruled out since the solution is relatively concentrated in these ions and they can reach the interface mostly by migration rather than by diffusion.

If the zinc ions were the diffusing species through the oxide film according to the second possibility then Sand's equation for electrolysis under conditions of constant flux, could be written as

$$i\tau^{1/2} = \frac{nFD^{1/2}\pi^{1/2}}{2}(a_b - a_f)$$

where $(a_b - a_f)$ represents the activity (concentration) gradient causing diffusion, a_b being the initial activity where diffusion starts, a_f the boundary activity where diffusion terminates and D is the diffusion coefficient of the diffusing species. To test this possibility we used the same amalgam concentration (1%) in solutions of different normalities in sodium hydroxide. The anode potential–time curves obtained are shown in Fig. 4 in different concentrations of sodium hydroxide using the same current density of 300 μamp. throughout. It is evident that a_b is here a constant representing the activity of zinc ions in the surface of the amalgam and a_f represents the zinc ion activity in the hydroxide–solution interface and could be replaced by $S/a^2_{OH^-}$ where S is the solubility (activity) product of $Zn(OH)_2$ and a_{OH^-} is the activity of OH ions. The plot of $i\tau^{1/2}$ against $1/a^2_{OH^-}$ did not give a straight line as shown in curve I, Fig. 5. This eliminates the possibility of the zinc ions to be the diffusing species through the oxide.

If the hydroxyl ions were the diffusing species through the hydroxide layer, then a_b in Sands equation will represent the bulk activity of OH^- and a_f could be set equal to $(S/a_{Zn^{++}})^{1/2}$. The plot of the product $i\tau^{1/2}$ for the different amalgams against the reciprocal of the square root of the zinc ion activity gave the straight line II shown in Fig. 5. The slope of this line is expected to be $-{}^1/_2(nFD^{1/2}\pi^{1/2}S^{1/2} \times 10^{-3})$ and should make an intercept with the ordinate of ${}^1/_2(nFD^{1/2}\pi^{1/2} \times 0.0766 \times 10^{-3})$, where the factor 10^{-3} is used to convert activities into moles per cm.^{3} and 0.766 is taken as the activity coefficient of OH^- in 0.1 M sodium hydroxide solutions. The slope divided by the intercept should give the value of $S^{1/2}/0.0766$ enabling the determination of the solubility (activity) product of zinc hydroxide. From the parameters of this line, the activity product is calculated to be 1.5×10^{-17} which compares with satisfaction to the value 4.5×10^{-17} previously reported.[15] The uncertainties in the data used for the plot of this line may be due to the fact that the zinc ion activities were calculated from the measured potentials where every 0.03 volt represents a tenfold change in the zinc ion activity. If instead of using different amalgam concentrations, we used the same amalgam with different concentrations of sodium hydroxide, then Sand's equation will assume the form

$$i\tau^{1/2} = \frac{nFD^{1/2}\pi^{1/2}a_{OH^-}}{2} - \frac{nFD^{1/2}\pi^{1/2}}{2}\frac{S^{1/2}}{a_{Zn^{++}}{}^{1/2}}$$

The change in the product $i\tau^{1/2}$ with a_{OH^-} is linear as shown in line III Fig. 5, and proves the pretext that OH^- is the diffusing species through the oxide layer. The ratio of the intercept to the slope of this line gives us $-S^{1/2}/a_{Zn^{++}}{}^{1/2}$. Data for this line lead to the value 1.01×10^{-17} for the activity product of zinc hydroxide. The possibility of the hydroxyl ions to be the diffusing species through the oxide film was qualitatively presented in Part I[11] of this series. Thus for the passivation of pure mercury in sodium hydroxide solution, it was observed experimentally that the passivating oxide film grows from the inside rather than from the outside. In part (II),[16] which dealt with pure mercury in ammonium hydroxide solution the above argument was further substantiated by calculating the diffusion coefficient of the species undergoing diffusion and comparing it with the available data for the diffusion coefficients of metal atoms or ions through their oxides, where it was found to deviate considerably. The above arguments show that the hydroxyl ion is the diffusing species during the process of passivation and not the metallic atoms or ions as was believed before.

(14) P. Delahay, "New Instrumental Methods in Electrochemistry," Interscience Publishers, Inc., New York, N. Y., 1954, p. 184.

(15) Reference 13, p. 168.

(16) THIS JOURNAL, **63**, 1224 (1959).

THE SORPTION OF HYDROCARBON VAPORS BY SILICA GEL[1]

BY DOUGLAS W. MCKEE[2]

Department of Chemistry, Queen Mary College, University of London, England

Received December 15, 1958

The sorption isotherms of a series of liquid and gaseous hydrocarbons on a standard silica gel have been determined, mainly at 25°. Measurements also have been made with nitromethane, nitroethane and carbon tetrachloride for comparison purposes. All the liquid adsorbates investigated gave curves with well-pronounced, reproducible hysteresis loops, the size of which did not seem to vary significantly with change in the thickness of the adsorbed film (D). The point of hysteresis inception was found to shift to lower relative pressures as D increased and this point generally corresponded with a pore radius between 2 and 3D. The volumes of the liquids adsorbed at saturation obeyed Gurvitsch's rule and indicated the filling of a constant pore volume. The results suggested that a unimolecular layer of adsorbed molecules was initially formed on the surface and this process was followed by capillary condensation in the smallest gel pores, in agreement with the mechanism of the "open-pore theory."

Introduction

In recent years several investigations have been described on the sorption of an homologous series of compounds on a porous absorbent, and the results have been discussed in terms of the various theories of capillary condensation. Thus, Foster,[3] from studies of the isotherms of a series of aliphatic alcohols on silica and ferric oxide gels, failed to find any significant decrease in the size of the hysteresis loop as the thickness of the adsorbed layer increased. More recent work, however, by Brown and Foster,[4] has shown some evidence for this effect in the case of amines adsorbed on silica gels. These results lend support to the "open-pore theory" of capillary condensation[5] as a more satisfactory explanation of sorption hysteresis than the alternative "ink-bottle theory" of Katz.[6] The present work, in extending the above studies to an homologous series of hydrocarbons, offers support for the qualitative predictions of the "open-pore theory" but fails to detect any progressive change in size of the loop. The values of the relative pressure at the point where hysteresis begins suggests that a unimolecular layer of adsorbed molecules is necessary to initiate the process of capillary condensation.

Experimental

The silica gel used in this work was a commercial granular gel of 8/18 mesh, obtained from Silica Gel Limited, London, W. C. 2, and containing some 4.62% water before activation in an air oven at 130° for three hours. The adsorbates were high-purity Research Grade materials from Phillips Petroleum Company, and Eastman Kodak and these were further purified by intensive drying and distillation.

The sorption isotherms of the volatile liquid hydrocarbons were determined by a gravimetric technique similar to that used by Brown and Foster,[4,7] the amount of each vapor adsorbed at a given pressure being found directly from the increase in weight of the gel, the latter being evacuated at 10^{-6} mm. for 12 hours before the commencement of each run. Pressure measurements in the range 0.02 to 200 mm. were made with three different types of mercury manometer of varying sensitivity. A polyethylene glycol–cellulose acetate vacuum grease suggested by Polley[8] was found to resist the attack of the adsorbates and was quite satisfactory in use.

Adsorption data for propane and n-butane were determined in a volumetric adsorption apparatus based on that of Harkins and Jura[9] using high purity gas samples obtained from the National Physical Laboratory. The isotherms were determined in the neighborhood of the boiling points of the gases, the temperature being kept constant to ±0.1° by an aluminum-block cryostat.

A nitrogen isotherm at −183° also was determined in order to obtain the surface area of the gel by the B.E.T. method.

Results and Discussion

All the liquid absorbates gave isotherms of the same general shape which could be described as Type IV in the Brunauer classification,[10] in which the constant "c," giving the initial slope of the isotherm when plotted as moles adsorbed against pressure, had only a small value. Typical isotherms for normal paraffins are shown in Fig. 1 and for cyclic paraffins in Fig. 2. For convenience all the curves are plotted as relative pressure p/p_0 *vs.* relative coverage x/x_s where x_s is the saturation capacity. The isotherms rise from the origin to a value of some 250–300 mg./g. adsorbed at a relative pressure of 0.13–0.3 p/p_0. The gel then appeared to be saturated as virtually no adsorption took place between this low pressure and the saturation value, the curve being almost horizontal. In every case, a permanent hysteresis loop was obtained which was found to be entirely reproducible on subsequent cycles. The loop was usually small and extended over quite a narrow range of pressure.

Saturation Values.—As shown in Table I, the

TABLE I

SATURATION CAPACITIES FOR VARIOUS ADSORBATES

	q_s (mg./g.)	q_s (mmoles/g.)	V_s (cc.)
n-Hexane	282	3.28	0.431
2,3-Dimethylbutane	282	3.28	.429
2-Methylpentane	280	3.28	.431
n-Heptane	291	2.91	.431
2,2,3-Trimethylbutane	288	2.88	.420
n-Octane	303	2.66	.434
2,2,4-Trimethylpentane	300	2.63	.439
2,3,4-Trimethylpentane	303	2.66	.425
Cyclohexane	326	3.88	.421
Methylcyclohexane	325	3.32	.425
Ethylcyclohexane	335	2.99	.426
Benzene	384	4.92	.440
Nitromethane	508	8.33	.449
Nitroethane	453	6.03	.434
Carbon tetrachloride	668	4.30	.421

(1) Based on a thesis presented by the author for the degree of Ph.D in the University of London, 1954.

(2) Linde Company, Tonawanda, New York.

(3) A. G. Foster, *Proc. Roy. Soc.* (*London*), **150A**, 77 (1935).

(4) M. J. Brown and A. G. Foster, THIS JOURNAL, **56**, 733 (1952).

(5) A. G. Foster, *Trans. Faraday Soc.*, **28**, 645 (1932).

(6) S. M. Katz, THIS JOURNAL, **53**, 1166 (1949).

(7) M. J. Brown and A. G. Foster, *J. Chem. Soc.*, 1139 (1952).

(8) M. H. Polley, *Anal. Chem.*, **23**, 545 (1951).

(9) W. D. Harkins and G. Jura, *J. Am. Chem. Soc.*, **66**, 1366 (1944).

(10) S. Brunauer, "The Adsorption of Gases and Vapors," Princeton, N. J., 1943.

saturation volumes V_s, are constant round the mean value of 0.43 cc./g., the maximum deviation being 4%. A plot of q_s, the total mass adsorbed against d, the density of the adsorbate, gave a straight line passing through the origin. There is thus no evidence of "persorption" or sorption in tapering pores. According to Gurvitsch's rule,[11] this indicates the filling of a constant pore volume with the adsorbed liquid.

The amount of vapor adsorbed at a given relative pressure increases with molecular weight. In general ring systems are more strongly adsorbed than normal paraffins of equivalent molecular weight, while branched isomers are less strongly adsorbed than their straight chain homologs. These results can be explained in a general manner from a consideration of the adsorption forces involved. As the most important forces in this case, the adsorption of non-polar molecules on a polar surface are likely to be due to induction and dispersion effects, it is to be expected that the magnitude of these forces should increase with the size and polarizability of the adsorbed molecule and hence the adsorbability should also run roughly parallel to these properties. The correlation is, however, only a loose one and no quantitative relation can be derived.

Monolayer Capacities and Specific Surface of the Gel.—The estimation of the specific surface area S of a porous adsorbent is based on the determination of the monolayer capacity from the sorption isotherm. These two quantities are related by the expression

$$S = x_m \times \frac{N}{M} \times A_m$$

where A_m is the area occupied by the adsorbate molecule in the monolayer. The choice of a value for A_m is a matter of some difficulty but it is usual to assume that the adsorbed layer has the properties of a liquid film and A_m is calculated from the bulk density of the liquid adsorbate. This procedure, which ignores orientation effects in the monolayer, gives consistent results for gases such as nitrogen at low temperatures. The usual method of locating the point at which the monolayer is complete by application of the B.E.T. equation for unrestricted layer adsorption[10] often has led to inconsistent results when applied to systems of Type IV in which capillary condensation plays a large part. The monolayer capacities and specific surfaces for nitrogen, propane and *n*-butane which also gave reproducible Type IV isotherms, are given in Table II, columns

TABLE II

SPECIFIC SURFACE AREAS OF GEL

	Temp., °C.	V_m, cc.	"c"	A_m, Å.²	S, m.²/g.
Nitrogen	−183	130	80.2	16.2	566
Propane	− 42	73.6	6.6	27.4	542
n-Butane	0	57.9	5.4	32.1	500
n-Butane	− 15	66.1	7.1	32.1	569

3 and 6, the values of A_m given in column 5 being calculated on the assumption of hexagonal close packing in the monolayer. Taking the surface area of the gel as determined from the nitrogen isotherm as the true value, the calculated values for the hydrocarbons are seen not to differ from this figure by more than 12%, which is good agreement, considering the uncertainties of the method. It appears, therefore, that the gel used did not contain pores

(11) L. Gurvitsch, *J. Russ. Phys.-Chem. Soc.*, **47**, 805 (1915).

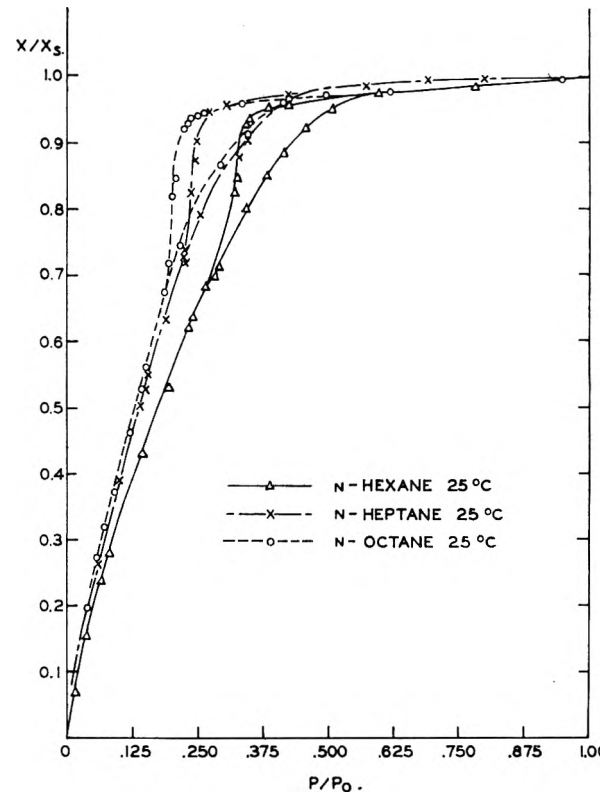

Fig. 1.—Adsorption isotherms of normal paraffins on silica gel at 25°.

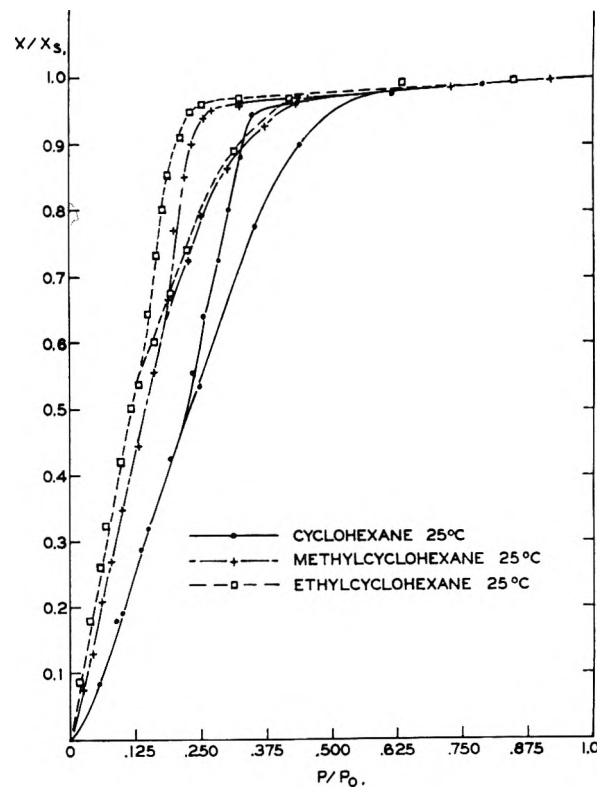

Fig. 2.—Adsorption isotherms of cyclic paraffins on silica gel at 25°.

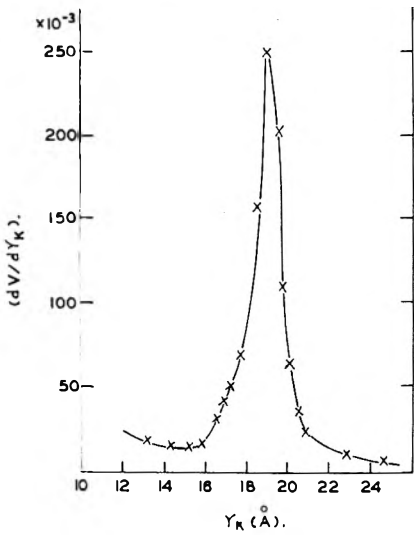

Fig. 3.—Pore radius distribution curve for silica gel (*n*-hexane, 25°).

small enough to exclude the hydrocarbon molecules while admitting those of nitrogen.

The determination of the monolayer capacities in the case of the higher hydrocarbons presented a further difficulty. The lower members, *e.g.*, hexane and heptane, generally gave fairly good B.E.T. plots over a small range of pressure, the constant "*c*" having values between 6 and 12. With increasing size of the adsorbate molecule, however, hysteresis and capillary condensation began to occur at progressively lower relative pressures and the region of applicability of the B.E.T. equation became smaller. With cyclohexane and its homologs, the isotherms dropped linearly from the base of the hysteresis loop to the origin with no indication of a change in slope at the monolayer. In these cases it was found impossible to assign an accurate value to the monolayer capacity although a value corresponding to the point of hysteresis inception gave rough agreement with the other systems investigated. In several cases where a good B.E.T. plot was not obtained, it was found possible to obtain a consistent value by using the method suggested by Gregg[12] in which the film compressibility β is given by the relation

$$\frac{\beta}{S} = \frac{1}{RT} \times \frac{1}{x^2} \times \frac{dx}{d(\log_e p)}$$

A plot of β/S against log p falls to a minimum at the monolayer. In Table III, columns 2 and 3 give values of the monolayer capacities as obtained by the compressibility and B.E.T. methods, respectively; these values are seen to be in close agreement. Column 5 gives the value of A_m calculated from the monolayer capacity; this may be compared with the value obtained assuming hexagonal close packing, column 6. In every case the monolayer is completed in the neighborhood of the beginning of hysteresis.

The Mechanism of Capillary Condensation.—The pore structure of the gel was determined using a method suggested by Foster[5] which involves finding the slope of the curve of volume adsorbed V against the corresponding pore radius calculated from the Kelvin equation. The results for *n*-hexane are shown in Fig. 3 and indicate a very narrow distribution of pore radii. The mean Kelvin radii for the other systems studied are listed in Table IV, column 2.

(12) S. J. Gregg, "The Surface Chemistry of Solids," Chapman and Hall, 1951.

TABLE III

MONOLAYER CAPACITIES AND ADSORBATE CROSS SECTIONAL AREAS

	V_m, cc.	V_m', cc.	"c"	A_m, Å.²	A_L (hex.), Å.²
Benzene	0.24	0.27	12.2	31.0	30.6
n-Hexane	.22	.29	7.5	42.5	39.5
2,3-Dimethylbutane	.31	.31	6.4	39.6	39.4
2-Methylpentane	.26	.30	7.6	42.0	39.7
n-Heptane	.28	.32	6.6	43.2	42.6
2,2,3-Trimethylbutane	.29	.31	9.6	44.1	42.4
n-Octane	.29	..	..	53.5	45.6
2,2,4-Trimethylpentane	.32	.35	10.6	44.4	46.1
2,3,4-Trimethylpentane	.28	..	..	53.5	44.9

TABLE IV

	r_k, Å.	$(p/p_0)_1$	r_1, Å.	$(p/p_0)_2$	$2r_1$, Å.	D_{hex}, Å.	r_1/D
					Calc. =		
n-Hexane	17.3	0.262	14.5	0.535	7.3	6.3	2.3
2-Methylpentane	18.1	.286	14.8	.560	7.4	6.3	2.4
2,3-Dimethylbutane	17.2	.318	15.5	.560	7.8	6.3	2.5
n-Heptane	16.6	.210	15.3	.450	7.7	6.5	2.4
2,2,3-Trimethylbutane	16.2	.210	14.1	.480	7.0	6.5	2.2
n-Octane	17.1	.175	16.1	.437	8.1	6.8	2.4
2,2,4-Trimethylpentane	17.3	.214	16.1	.437	8.1	6.8	2.4
2,3,4-Trimethylpentane	16.7	.165	15.4	.470	7.7	6.7	2.3
Cyclohexane	18.5	.214	14.1	.530	7.1	5.9	2.4
Methylcyclohexane	16.2	.170	13.8	.457	6.9	6.2	2.3
Ethylcyclohexane	17.3	.125	14.5	.380	7.3	6.5	2.2
Carbon tetrachloride	17.0	.210	12.3	.560	6.2	5.7	2.2
Benzene	15.5	.220	13.4	.580	6.7	5.5	2.4
Mean	17.0						

The Kelvin radii are fairly constant and do not vary by more than 9% from the mean value of 17.0 Å. The consistent values of the mean radius justify the use of the Kelvin equation in capillaries of such small dimensions.

A further check on the value of the mean radius is provided by the area under the distribution curve. The surface area of the gel S is given by the relation

$$S = \int_0^\infty \left(\frac{dS}{dr}\right) dr = \int_0^\infty \frac{2}{r}\left(\frac{dV}{dr}\right) dr = 2 \times 2.303 \int_0^\infty \left(\frac{dV}{dr}\right) d(\log r)$$

The value of S, obtained by graphical integration, was 605 m.²/g., in reasonable agreement with the value obtained from nitrogen adsorption.

The original version of the "open-pore" theory of capillary condensation as developed by Foster, explained hysteresis as due to a delay in the formation of a meniscus. During adsorption, layer formation continued until each pore became blocked at its narrowest point so as to form a meniscus. Further adsorption then took place on the spherical meniscus in accordance with the Kelvin equation. It follows from this explanation that the larger the size of the adsorbate molecule, the more readily will the pores become blocked at their narrowest points. The

theory thus predicts a decrease in the size of the loop with increasing temperature and molecular size. Also it is to be expected that the point of hysteresis inception would move to lower relative pressures as the thickness of the adsorbed layer increases. A later form of the "open-pore" theory, as developed by Cohan,[13] suggests that capillary condensation on adsorption would be assisted by a free-energy decrease due to the cylindrical film of liquid on the capillary walls. On adsorption, the pressure over a cylindrical film of radius r, is given by

$$P_a = P_0 e^{-\gamma V/rRT} = P_0 e^{-\gamma V/(r_c - D)RT}$$

where r_c is the true radius of the pore and D is the thickness of the adsorbed film. On desorption, the pressure will be determined by the Kelvin equation

$$P_d = P_0 e^{-2\gamma V/r_c RT}$$

This leads to a relation between the radius corresponding to the pressure at the point of hysteresis inception and the thickness of the adsorbed film D. Thus when

$$P_a = P_d = P_0 e^{-\gamma V/(r_c - D)RT} \text{ and } r_c = 2D$$

the thickness of the film is given by

$$D = \frac{-\gamma M}{d\, RT \log_e P_1/P_0}$$

where P_1 is the pressure at the beginning of hysteresis and is equal to

$$P_1 = P_0 e^{-\gamma V/DRT}$$

The present work indicates that one adsorbed layer is sufficient to initiate capillary condensation in the smallest capillaries. No progressive change in size of the loop was observed on ascending the series, but the range in size of the adsorbate molecules may have been too small to produce an observable effect. Table IV summarizes capillary condensation data for the various adsorbates. By comparing the pressure at the beginning of hysteresis (column 3) with the thickness of the adsorbed layer (column 7) it is seen that, for homologous series such as the normal paraffins and cycloparaffins, hysteresis begins progressively earlier on increasing the size of the adsorbate molecule. This is in accordance with the predictions of the "open-pore" theory but not with the "ink-bottle" theory. Column 5 gives the upper limit of hysteresis and the difference between columns 3 and 5 gives an indication of the size of the loop. Column 6 gives the value of the thickness of the adsorbed layer calculated from Cohan's relation. This shows only a rough qualitative agreement with the value based on the assumption of hexagonal close packing, column 7. Column 8 gives the ratio of r_L to D_{hex}, which is seen to lie between 2 and 3—a result which agrees with the observations of Emmett and Cines[14] for gases on porous glass and with those of Brown and Foster[4] for amines on silica gel.

Acknowledgments.—The author is indebted to Dr. D. C. Jones for his direction of this work and to the Governors of Queen Mary College for financial assistance. Thanks are due also to the Ministry of Education for the award of a maintenance grant.

(13) L. H. Cohan, *J. Am. Chem. Soc.*, **60**, 433 (1938); **66**, 98 (1944).

(14) P. H. Emmett and M. Cines, THIS JOURNAL, **51**, 1248 (1947).

THE THERMODYNAMICS OF DILUTE SOLUTIONS OF $AgNO_3$ AND KCl IN MOLTEN KNO_3, FROM ELECTROMOTIVE FORCE MEASUREMENTS. I. EXPERIMENTAL

BY MILTON BLANDER, F. F. BLANKENSHIP AND R. F. NEWTON

Oak Ridge National Laboratory,[1] *P. O. Box Y, Oak Ridge, Tennessee*

Received December 22, 1958

Measurements of the activities of $AgNO_3$ were made in a fused salt concentration cell at 370 and 436° in dilute solutions of Ag^+ and Cl^- ions. The activities of $AgNO_3$ obeyed the Nernst law at the low concentrations of $AgNO_3$ measured when no Cl^- ions were present. The dissolution of KCl in a $AgNO_3$–KNO_3 mixture lowered the activity of $AgNO_3$. The lowering was larger the larger the amount of KCl added and for a given concentration of KCl was also larger the smaller the initial concentration of $AgNO_3$. This shows that the Nernst law is not obeyed for $AgNO_3$ in the presence of Cl^- ion.

Introduction

No general theory of molten salt solutions has as yet been presented. As a consequence, much of the recent work on thermodynamics of molten salt solutions has been reported in terms of complex ion formation; such interpretations have obvious deficiencies and may yield a misleading picture of ionic interactions in the melt. If the molten system is of sufficient simplicity it is possible to derive a theory which takes account of non-random mixing in the melt. These studies afford a basis for testing the quasi-lattice model of molten reciprocal salt systems presented in the subsequent paper.[2]

Laity[3] from e.m.f. measurements on $AgNO_3$–$NaNO_3$ mixtures showed that the deviations from ideality of $AgNO_3$ in $NaNO_3$ are small. Freezing point lowering measurements indicate that the KNO_3–KCl system behaves ideally.[4] Flengas and Rideal[5] demonstrated the applicability of the Nernst equation to silver–silver nitrate electrodes

(1) Operated for the United States Atomic Energy Commission by the Union Carbide Corporation.

(2) M. Blander, THIS JOURNAL, **63**, 1262 (1959).

(3) R. W. Laity, *J. Am. Chem. Soc.*, **79**, 1849 (1957).

(4) E. Kordes, W. Bergman and W. Vogel, *Z. Elektrochem.*, **55**, 600 (1951).

(5) S. N. Flengas and E. K. Rideal, *Proc. Roy. Soc.* (*London*), **233A**, 443 (1956).

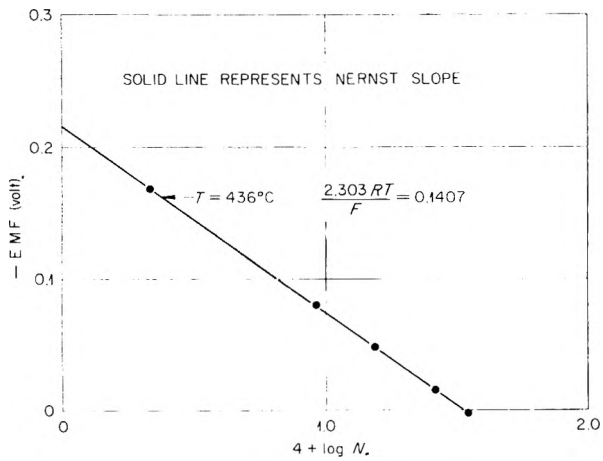

Fig. 1.—Check of Nernst slope for cell

$$\mathrm{Ag}\left|\begin{matrix}\mathrm{AgNO_3}(N')\\ \mathrm{KNO_3}\end{matrix}\right|\left|\begin{matrix}\mathrm{AgNO_3}(N)\\ \mathrm{KNO_3}\end{matrix}\right|\mathrm{Ag}$$

$$E = \frac{2.303\,RT}{F}\log\frac{N}{N'}$$

in molten $NaNO_3$–KNO_3 melts and used such half cells as reference electrodes for electrometric titrations of Ag^+ by halide, cyanide and chromate ions in molten $NaNO_3$–KNO_3. In the present study pure KNO_3 was used as the solvent. Electromotive measurements of $AgNO_3$ with KCl were performed at various concentrations of Ag^+ and Cl^- at two temperatures for the case where no precipitate had formed.

Experimental

Materials.—Reagent grade KNO_3 from Baker and Adamson was used as the solvent. This material was melted in the vessel to be used and was sparged for several hours at temperatures slightly above its melting point with helium from cylinders obtained from the Bureau of Mines and shown by analysis[6] to contain less than 1.5 p.p.m. of O_2. The $AgNO_3$ was obtained by selecting clear crystals from a C.P. preparation from Mallinckrodt Chemical Company. The KCl was of Reagent grade obtained from Baker and Adamson and was used after heating for several days at 200° in a current of dry helium.

Apparatus and Methods.—The electrometric measurements were made in the concentration cell

$$\mathrm{Ag^0}\left|\begin{matrix}\mathrm{AgNO_3}\ (N'_{\mathrm{Ag^+}})\\ \mathrm{KNO_3}\end{matrix}\right|\left|\begin{matrix}\mathrm{AgNO_3}\ (N_{\mathrm{Ag^+}})\\ \mathrm{KCl}\ (N_{\mathrm{Cl^-}})\\ \mathrm{KNO_3}\end{matrix}\right|\mathrm{Ag^0}$$

where N indicates concentration in ion fraction

$$N_{\mathrm{Ag^+}} = \frac{n_{\mathrm{Ag^+}}}{n_{\mathrm{Ag^+}} + n_{\mathrm{K^+}}} \text{ and}$$

$$N_{\mathrm{Cl^-}} = \frac{n_{\mathrm{Cl^-}}}{n_{\mathrm{Cl^-}} + n_{\mathrm{NO_3^-}}}$$

and n is the number of gram ions of the species indicated by the subscript. The cell consisted of a one-liter tall form beaker of Pyrex and contained 500 to 600 grams of the $AgNO_3$, KCl, KNO_3 solution corresponding to the right-hand electrode. This solution was stirred by a motor driven propeller of Pyrex. A straight length of 0.015-inch diameter wire of pure silver dipping into the melt served as a satisfactory and reproducible electrode. The reference (left hand) electrode which was immersed in the solution was prepared from a 16-inch length of 11/16-inch Pyrex tubing fitted with a standard-taper stopper; an asbestos fiber was sealed through the bottom of the reference half cell to serve as the conducting bridge. These half cells were assembled as needed by melting a weighed amount of KNO_3 in the tube, sparging with helium and then adding a weighed amount of $AgNO_3$. The electrode consisted of a spiral of 0.015-inch diameter wire of pure silver. When this wire was flattened over the region which passed the stopper an adequate seal could be made with stop-cock grease. Experiments with air in contact with the reference melts showed that precautions to maintain an inert atmosphere in the reference cell were unnecessary. Periodic checking of freshly prepared and aged reference half cells indicated that these half-cells were stable within 0.5 millivolt for several days.

The cell assembly was heated in a resistance furnace of about 5-inch inside diameter. The large thermal lag of the furnace made manual control by setting a Variac more satisfactory than automatic controllers for the temperature range used in this study. Temperatures were measured by a thermocouple of platinum and platinum–10% rhodium calibrated to ±1° against a similar thermocouple certified by the National Bureau of Standards. This thermocouple was contained in a Pyrex well immersed in the molten electrolyte; its output was read with a Leeds and Northrup portable precision temperature potentiometer connected through an ice-bath to the thermocouple. Measurements of e.m.f. of the cell were made with a Rubicon type "B" potentiometer.

The experimental procedure for the e.m.f. measurements was extremely simple. The Pyrex beaker containing a weighed quantity of KNO_3 was brought to the desired temperature in the furnace. After the molten KNO_3 had been sparged with helium the reference half-cell was introduced and positioned so that the liquid levels were equal. E.m.f. measurements were made after thermal equilibrium was achieved and at intervals thereafter as desired. The composition of melt in the test half-cell was adjusted by addition of weighed amounts of KCl or $AgNO_3$.

Results

Since the solutions used in this study always contained less than 0.01 ion fraction of Ag^+ and Cl^- and generally contained less than 0.006 ion fraction of either ion, the liquid junction potential due to transference of these ions should be small.[3]

For a cell of the type

$$\mathrm{Ag^0}\left|\begin{matrix}\mathrm{AgNO_3}\ (N'_{\mathrm{Ag^+}})\\ \mathrm{KNO_3}\end{matrix}\right|\left|\begin{matrix}\mathrm{AgNO_3}\ (N_{\mathrm{Ag^+}})\\ \mathrm{KNO_3}\end{matrix}\right|\mathrm{Ag^0} \qquad \text{(A)}$$

in which the solute concentration is so low that essentially all the bridge current is carried by solvent ions the e.m.f. is given by

$$E = \frac{2.303RT}{F}\log\frac{a_{\mathrm{AgNO_3}}}{a'_{\mathrm{AgNO_3}}} \qquad (1)$$

where a represents activity and the prime refers (as it does in all subsequent discussion) to the left hand (reference) half-cell. If the activity coefficients defined by

$$\gamma_{\mathrm{AgNO_3}} = \frac{a_{\mathrm{AgNO_3}}}{N_{\mathrm{Ag^+}}N_{\mathrm{NO_3^-}}} \qquad (2)$$

are constant as should normally be the case in very dilute solutions, equation 1 becomes the Nernst equation for a concentration cell

$$E = \frac{2.303RT}{F}\log\frac{N_{\mathrm{Ag^+}}}{N'_{\mathrm{Ag^+}}} \qquad (3)$$

where N represents ion fraction as defined above.

Cells of type (A), in which N_{AgNO_3} was varied by addition of $AgNO_3$ to the solvent, were shown to be quite stable and reproducible. E.m.f. values changed less than 0.5 mv. on standing overnight at temperatures below 440°. The concentration of $AgNO_3$ which would yield a cell potential of zero with a given reference half cell changed less than 1% over a period of four days at temperature. Figure 1 shows points representing typical data obtained from such cells at 436° with the line

(6) L. J. Brady, *Anal. Chem.*, **20**, 512 (1948).

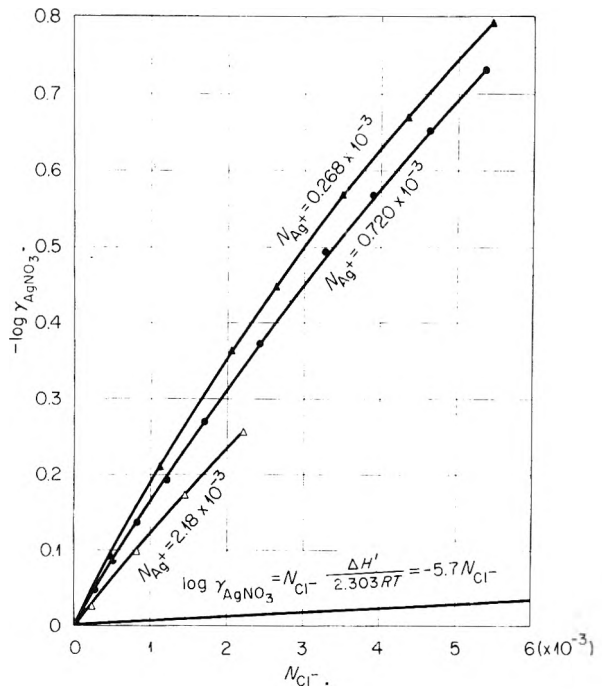

Fig. 2.—Comparison of measured values of γ_{AgNO_3} as a function of N_{Cl^-} in KNO_3–KCl–$AgNO_3$ mixtures to the theoretical values based on the assumption of random mixing of the ions; T = 370°.

representing values calculated from equation 3. Similar experiments at several temperatures from 344 to 423° demonstrated the agreement with the Nernst limiting law to better than 0.5 mv. This justifies neglect of the junction potential and indicates that the activity coefficient of $AgNO_3$ is constant within experimental error at mole fractions between 2×10^{-4} and 5×10^{-3}. Adoption of the standard state such that the activity coefficient is unity at infinite dilution leads to the conclusion that γ_{AgNO_3} is unity over the concentration range studied.

The e.m.f.'s have been measured for cells of the type

$$Ag^0 \left| \begin{matrix} AgNO_3\ (N'_{Ag^+}) \\ KNO_3 \end{matrix} \right\| \left| \begin{matrix} AgNO_3\ (N_{Ag^+}) \\ KCl\ (N_{Cl^-}) \\ KNO_3 \end{matrix} \right| Ag^0 \qquad (B)$$

as N_{Cl^-} was increased from zero by incremental additions of KCl. So long as no solid AgCl is precipitated any change (ΔE) from the initial e.m.f. of the chloride-free cell is a consequence of the change in γ_{AgNO_3} by the presence of Cl^-. Accordingly

$$\Delta E = \frac{2.303RT}{F} \log \gamma_{AgNO_3} \qquad (4)$$

where γ_{AgNO_3} is defined by equation 2. Values of e.m.f. reproducible to 0.5 mv. measured at two temperatures for cells of type (B) are given in Table I. Figures 2 and 3 show log γ_{AgNO_3} from these data at various initial values of N_{Ag^+} plotted against N_{Cl^-}. Large negative deviations from ideality of $AgNO_3$ in the presence of Cl^- were observed, being larger the larger N_{Cl^-} and the smaller the initial value of N_{Ag^+}. The interpretation of these data is given in the subsequent paper.

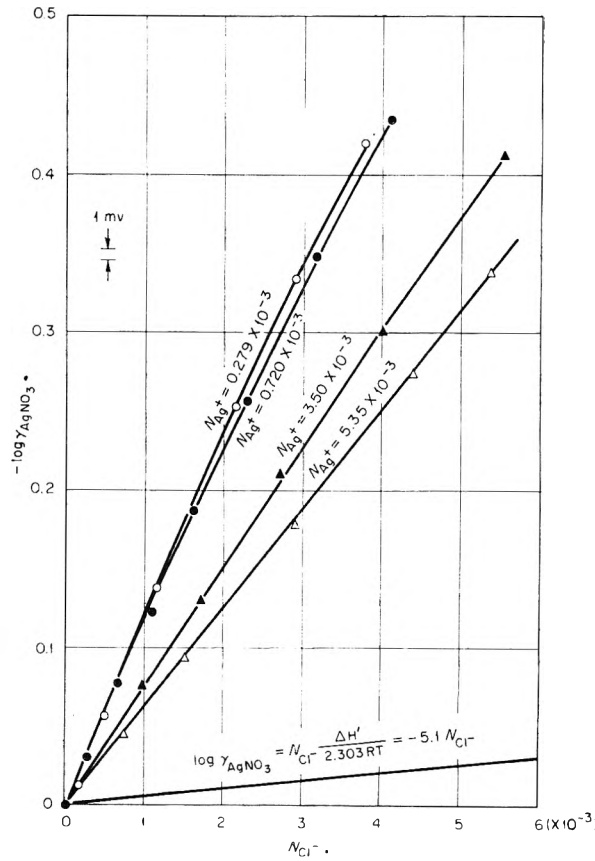

Fig. 3.—Comparison of measured values of log γ of $AgNO_3$ as a function of N_{Cl^-} in $AgNO_3$–KNO_3–KCl mixtures to theoretical values based on the assumption of random mixing of the ions; T = 436°.

TABLE I

E.M.F. CHANGE OF HALF-CELLS CONTAINING SOLUTIONS OF $AgNO_3$ IN KNO_3 UPON ADDITION OF KCl

Temperature = 370°

$N_{Ag^+} = 0.268 \times 10^{-3}$		$N_{Ag^+} = 0.720 \times 10^{-3}$		$N_{Ag^+} = 2.18 \times 10^{-3}$	
$N_{KCl} \times 10^3$	$-\Delta$e.m.f.	$N_{KCl} \times 10^3$	$-\Delta$e.m.f.	$N_{KCl} \times 10^3$	$-\Delta$e.m.f.
0.472	0.0117	0.261	0.0059	0.233	0.0034
1.11	.0270	.503	.0110	.813	.0124
2.05	.0464	.813	.0176	1.452	.0219
2.64	.0571	1.21	.0249	2.211	.0327
3.51	.0722	1.71	.0343	2.987	.0495
4.36	.0852	2.41	.0476	3.587	.0618
5.47	.1007	3.29	.0628		
		3.92	.0724		
		4.65	.0831		
		5.38	.0932		

Temperature = 436°

$N_{Ag^+} = 0.279 \times 10^{-3}$		$N_{Ag^+} = 0.720 \times 10^{-3}$		$N_{Ag^+} = 3.50 \times 10^{-3}$		$N_{Ag^+} = 5.35 \times 10^{-3}$	
$N_{KCl} \times 10^3$	$-\Delta$e.m.f.	$N_{KCl} \times 10^3$	$-\Delta$e.m.f.	$N_{KCl} \times 10^3$	$-\Delta$e.m.f.	$N_{KCl} \times 10^3$	Δe.m.f
0.192	0.0021	0.238	0.0042	0.954	0.0105	0.727	0.0062
.507	.0082	.618	.0108	1.696	.0182	1.504	.0130
1.168	.0194	1.110	.0187	2.732	.0294	2.842	.0249
2.14	.0357	1.62	.0264	3.972	.0421	4.381	.0386
2.90	.0472	2.25	.0361	5.524	.0581	5.348	.0477
3.79	.0591	3.16	.0491				
4.79	.0709	4.10	.0611				
6.11	.0870						
7.94	.1057						
9.70	.1218						

Acknowledgments.—The authors wish to express their appreciation to W. R. Grimes of this Laboratory for considerable help in writing this paper.

THE THERMODYNAMICS OF DILUTE SOLUTIONS OF $AgNO_3$ AND KCl IN MOLTEN KNO_3 FROM ELECTROMOTIVE FORCE MEASUREMENTS. II. A QUASI-LATTICE MODEL

BY MILTON BLANDER

Oak Ridge National Laboratory,[1] P. O. Box Y, Oak Ridge, Tennessee

Received December 22, 1958

A new theory based on a quasi-lattice model of the molten reciprocal salt system A^+, B^+, C^- and D^- dilute in A^+ ions in which the A^+ and C^- ions have an extra-coulombic interaction yields the result for the activity coefficient of the component AD: $\gamma_{AD} = \left[(1-X)^z\left(1+\frac{X}{\beta(1-X)}\right)^{z-1}\right]N_{D^-}$, where Z is the quasi-lattice coördination number, $\beta = e^{-\Delta E/RT}$, ΔE is the energy of formation of a mole of the ion pairs A^+–C^- and X, which can be calculated from the theory, is the fraction of positions adjacent to an A^+ ion occupied by C^- ions. $(1-X)^z$ is the fraction of A^+ ions that have no C^- ions adjacent to them. In the "complex" ion terminology these are "free" or "uncomplexed" A^+ ions and $(1-X)^z$ alone, in that terminology, should be equal to γ_{AD}. The other terms are significant for low values of β and high values of N_{C^-}. A comparison of the theory and measurements of the Ag^+, K^+, Cl^-, NO_3^- system at 370 and 436° indicates that the theory is valid at low values of X (<0.15) and of N_{Ag^+} ($\leqq 0.720 \times 10^{-3}$). A value of $\Delta E = -5.66$ kcal./mole and -5.64 kcal./mole for the energy of formation of the ion pair Ag^+–Cl^- is derived from the comparison for $Z = 6$ at 370 and 436°, respectively. While the value of ΔE is slightly sensitive to the arbitrary choice of Z the value of $Z\beta$ is relatively insensitive to Z. At higher concentrations of Ag^+ ions and higher values of X, the error due to the approximations made in the derivation of the theory becomes significant.

Introduction

For the interpretation of the behavior of molten salt reciprocal systems a quasi-lattice model should prove useful. A lattice model can probably be justified more easily for a molten salt mixture than for other types of mixtures. Because of the long range nature of the ionic interactions longer range order is to be expected in molten salt mixtures than in other types of solutions. Since the calculations are restricted to the calculation of free energy differences between the solution and the pure components of the solution most of the errors stemming from the approximation of a liquid by an ordered lattice will be cancelled. At any rate, since no detailed solution theory for molten salt mixtures exists, it seems desirable to investigate this simple model.

The quasi-lattice model for the system A^+, B^+, C^- and D^- is an assembly of charges *in vacuo* and consists of two interlocking sub-lattices, one a lattice of cations A^+ and B^+, the other of anions C^- and D^-. The nearest neighbors of the cations are anions and of the anions are cations. All the ions have the same coördination number Z. For simplicity we further restrict the model so that the radii of the ions of the same charge are the same. This restriction eliminates any difference in the long range coulombic interactions between either A^+ or B^+ ions, or C^- or D^- ions and their respective environments, and limits the model to short range extra-coulombic effects. The form of the equations derived from this model will probably apply approximately to systems with even different size ions of the same charge.

For a lattice dilute in A^+ ions we define the energy of formation of the ion pair A^+–C^- as indicated in Fig. 1, which is a two-dimensional representation of the lattice. The energy change for interchange of the circled C^- and D^- ions is $\Delta\epsilon = \Delta E/\mathfrak{N}$ where $\mathfrak{N}$ is Avogadro's number. Since the C^- and D^- ions are the same size the energy difference must be due to some extra-coulombic interaction. If the pair interaction energy of A^+–D^- is ϵ_1, of B^+–C^-, ϵ_2, of A^+–C^-, ϵ_3 and of B^+-D^-, ϵ_4 then

$$\Delta\epsilon = (\epsilon_4 + \epsilon_3) - (\epsilon_2 + \epsilon_1) = \frac{\Delta E}{\mathfrak{N}} \qquad (1)$$

The Random Mixing Approximation.—An approximation to the thermodynamics of this system can be made by assuming a random mixing of all the ions involved on their respective anion or cation lattices. This is analogous to the "zeroth" approximation of the quasi-chemical theory.[2] The partial molar entropy of mixing of the salt AD is then

$$\bar{S}_{AD} - \bar{S}^*_{AD} = -R \ln N_{A^+}N_{D^-} \qquad (2)$$

The asterisk refers to a standard state chosen so that the activity coefficients are unity at infinite dilution of all solutes in the solvent BD. If Z is the coördination number of A^+ ions, n_{A^+} the number of moles of A^+ ions in solution and if X is defined as the fraction of positions adjacent to an A^+ ion occupied by C^- ions then the number of moles of C^- ions adjacent to A^+ ions is $Zn_{A^+}X$ and the total heat of dilution ΔH_D is

$$\Delta H_D = Zn_{A^+}X\Delta E \qquad (3)$$

If the anions are randomly mixed on the anion lattice then $X = N_{C^-}$. Substituting this in equation 3 and differentiating the resultant expression with respect to n_{AD} we obtain the partial molar heat of dilution of AD.[3]

$$\bar{H}_{AD} - \bar{H}^*_{AD} = N_{B^+}N_{C^-}(Z\Delta E) \qquad (4)$$

Defining an activity coefficient as $\gamma_{AD} = a_{AD}/N_{A^+}N_{D^-}$ we obtain from (2) and (4)

$$\log \gamma_{AD} = N_{B^+}N_{C^-}\frac{Z\Delta E}{2.303RT} \qquad (5)$$

This equation for the random mixing approxi-

(1) Operated for the United States Atomic Energy Commission by the Union Carbide Corporation.

(2) (a) Sir R. Fowler and E. A. Guggenheim, "Statistical Thermodynamics," Cambridge, 1949; (b) E. A. Guggenheim, "Mixtures," Oxford, 1952.

(3) If we choose as our components AD, BC and BD then $n_{AD} = n_{A^+}$, $n_{BC} = n_{C^-}$ and $n_{BD} + n_{BC} = n_{B^+}$. Substituting these in (3) and differentiating by n_{AD} leads to (4).

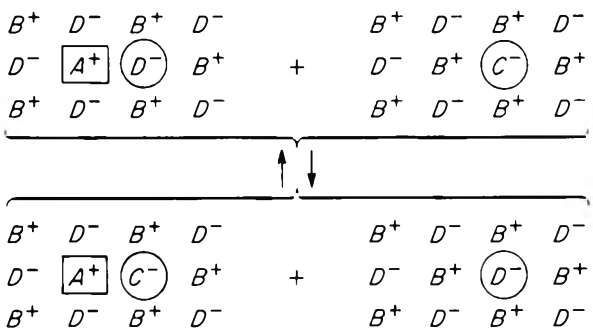

Fig. 1.—Two dimensional quasi-lattice representation of the formation of an A^+–C^- ion pair.

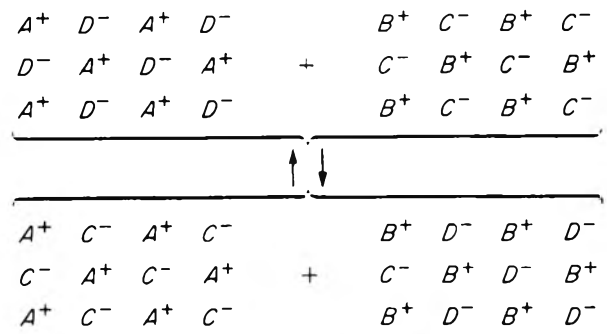

Fig. 2.—Two dimensional quasi-lattice representation of the metathetical reaction $AD(1) + BC(1) \rightleftarrows AC(1) + BD(1)$.

mation is of the same form as the theory of Flood, Forland and Grjotheim.[4]

A crude estimate for $Z\Delta E$[4] can be made which is probably not off by more than a factor of two. As will be seen, even a crude estimate will serve to test the random mixing approximation. Figure 2 is a two-dimensional quasi-lattice representation of the metathetical reaction

$$AD(1) + BC(1) \rightleftarrows AC(1) + BD(1) \qquad (A)$$

the heat change for which is $\Delta H'$ per mole. Since all the ions of the same charge have the same size we need only account for nearest neighbor interactions. The number of nearest neighbor pairs of the ions of each of these salts is $Z\mathfrak{N}$ per mole of salt. If each pair interaction were independent then the heat change[5] $\Delta H'$ for the metathetical reaction should be $Z\Delta E$ where ΔE is defined by equation 1. In a real system there is probably a "saturation" effect such that $\Delta H'/Z$ would be a low estimate for ΔE.

The correspondence of the system KNO_3–$AgNO_3$–KCl to the model system can be made by choosing Ag^+ as A^+, Cl^- as C^-, K^+ as B^+, and NO_3^- as D^-. Even though the sizes and shapes of Cl^- and NO_3^- are not alike this probably leads to only a small effect on the form of the functions derived from the lattice model for dilute solutions.

A calculation of $\Delta H'$ for reaction (A) yielded a value of -16.8 kcal./mole, using the data of Table I and neglecting the difference of the heat capacities of the reactants and products. Substituting this value in (5) leads to

$$\log \gamma_{AgNO_3} \cong -\frac{16.8 N_{Cl}}{2.303RT} \qquad (6)$$

where $N_{K^+} \sim 1$; and $Z\Delta E = \Delta H'$.

Values of $-\log \gamma_{AgNO_3}$ for this approximation are plotted in Figs. 3 and 4 of the preceding paper for comparison with the measured values of $-\log \gamma_{AgNO_3}$. They prove to be much smaller than the measured values of $-\log \gamma_{AgNO_3}$ and have a negligible dependence on N_{Ag^+} as compared to the strong dependence of the measured values of $\log \gamma_{AgNO_3}$ on N_{Ag^+}. The most probable reason for this difference is the non-random distribution of Cl^- ions about Ag^+ ions. If the ion pair Ag^+-Cl^- has a negative relative energy of interaction $\Delta\epsilon$ then there should be a preferential distribution of Cl^- ions about Ag^+ ions. This could cause the deviations from ideality to be greater than that calculated from the random mixing approximation and could cause the concentration dependence of the deviations from ideality.

Table I

Thermodynamic Data for Calculation of $\Delta H'$[a]

	Heat of formation of solid ΔH_{298}, kcal./mole	Heat of fusion ΔH_{fus}, kcal./mole	Heat of transition ΔH_{tr}, kcal./mole
$AgNO_3$	− 29.43	2.76	0.66
AgCl	− 30.36	3.16	..
KNO_3	−117.76	2.8	1.3
KCl	−104.175	6.1	..

[a] "Selected Values of Chemical Thermodynamic Properties," USNBS Circular 500, F. D. Rossini, *et al.*, 1952.

Calculation for Non-random Mixing.—A distribution function can be calculated from the model for dilute solutions of A^+ ions in BD. The positions available to C^- ions on the anion lattice are of two types, type a which are those adjacent to one A^+ and (Z-1) B^+ ions, and type b which are those adjacent to Z B^+ ions. The total number of the former type is $Zn_{A^+}\mathfrak{N} = L_A$ and of the latter is the remainder of anion positions $\mathfrak{N}(n_{A^+} + n_{B^+}) - L_A = L_B$ where $\mathfrak{N}$ is Avogadro's number.[6] This is true when the solution is dilute enough in A^+ to neglect positions adjacent to two A^+ ions. The C^- ions in any of the L_A positions are more stable by the energy $\Delta\epsilon$. A statistical calculation[7] gives us the quantity X which is the fraction of positions adjacent to A^+ ions occupied by C^- ions in the most probable distribution.[8]

$$X = (1 - X)\left(\frac{N_{C^-} - ZXN_{A^+}}{1 - ZN_{A^+}(1 - X) - N_{C^-}}\right)\beta \qquad (7)$$

where $\beta = e^{-\Delta E/RT}$. The total heat of dilution can be calculated from (3) and (7). The total entropy of mixing is calculated from

$$\Delta S = +k \ln \Omega \qquad (8)$$

(4) H. Flood, T. Forland and K. Grjotheim, *Z. anorg. allgem. Chem.*, **276**, 289 (1954).

(5) The difference between ΔH and ΔE is negligible in liquids.

(6) Electroneutrality requires $(n_{A^+} + n_{B^+}) = (n_{C^-} + n_{D^-})$.

(7) Appendix A.

(8) The similarity of the procedure used in this ternary system and the quasi chemical treatment[2] for binary systems should be noted although the models are significantly different. This distribution function is exact at all values of the concentration of the entities (C^- and D^- ions) being distributed since all pairs of neighbors can be counted independently, for dilute A^+.

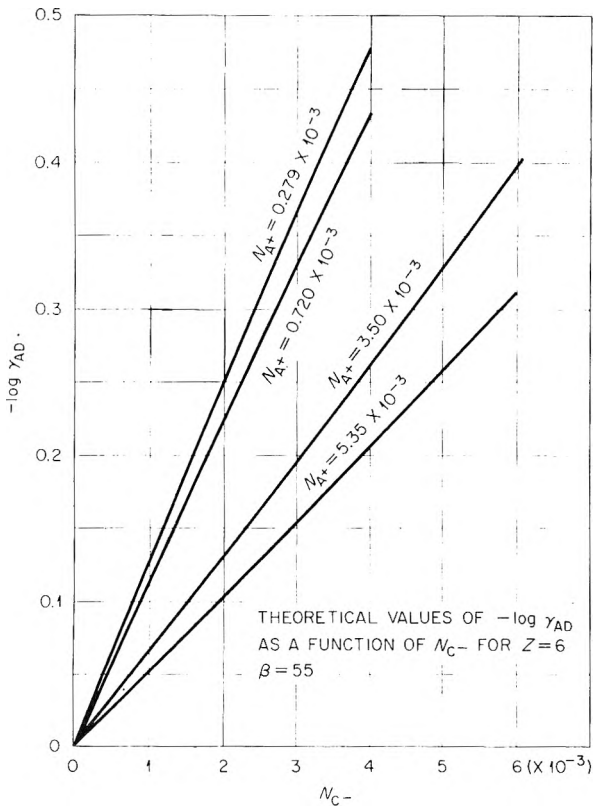

Fig. 3.—Theoretical values of $-\log \gamma_{AD}$ as a function of N_{C^-} for $Z = 6$, $\beta = 55$.

where Ω is the number of possible states in the most probable distribution and is given by

$$\Omega = \frac{[(n_{A^+} + n_{B^+})\mathfrak{N}]!}{(n_{A^+}\mathfrak{N})!(n_{B^+}\mathfrak{N})!} \times \frac{L_A!}{(L_A - M_A)!\, M_A!} \times \frac{L_B!}{(L_B - M_B)!\, M_B!} \quad (9)$$

The first term on the right of equation 9 is the number of possible configurations of the cations and the last two terms are the number of possible configurations of the anions in the most probable distribution, and $L_A = Zn_{A^+}\mathfrak{N}$, $M_A = ZXn_{A^+}\mathfrak{N}$, $L_B = (n_{A^+} + n_{B^+} - Zn_{A^+})\mathfrak{N}$ and $M_B = n_C\mathfrak{N} - M_A$ where M_A and M_B are the number of C^- ions in the regions a and b, respectively, in the most probable distribution. Calculating the total free energy of dilution from (3), (7) and (8) and differentiating by n_{AD} to obtain $\bar{F}_{AD} - \bar{F}^*_{AD}$ we get[9]

$$\bar{F}_{AD} - \bar{F}^*_{AD} = + RT \ln N_{A^+} (1 - X)^Z \left[1 + \frac{X}{\beta(1 - X)}\right]^{Z-1} \quad (10)$$

whence

$$\gamma_{AD} = \frac{(1 - X)^Z \left(1 + \frac{X}{\beta(1 - X)}\right)^{Z-1}}{N_{D^-}} \quad (11)$$

Equation 11 leads to an interesting conclusion. If the most probable distribution is also the average distribution, then $(1 - X)$ is the probability that a given position adjacent to an A^+ ion is not occupied by a C^- ion. $(1 - X)^Z$ is the probability that none of the Z positions adjacent to a given A^+ ion are occupied by C^- ions and is equal to the fraction of A^+ ions that are "free" or "uncomplexed." In the "complex" ion terminology, this term alone should be the activity coefficient of AD. The other terms

$$\frac{\left(1 + \frac{X}{\beta(1 - X)}\right)^{Z-1}}{N_{D^-}}$$

are an activity coefficient for the "free" A^+ ions. For large values of β and dilute solutions of C^- the difference is small. For weak interactions (small values of β) or solutions concentrated in C^- ions the difference is significant. This conclusion is contrary to the implied assumptions[10,11] used in describing the thermodynamics of reciprocal fused salt systems and is true even if long range interactions are insignificant.

The conditions implied in the model should restrict the validity of equation 11. We have assumed that the energy change for exchanging a D^- for a C^- ion in the region adjacent to an A^+ ion, is independent of the number of C^- ions already adjacent to A^+. If this were not true and if there were a "saturation" effect on the A^+-C^- interaction then the equation would not be valid at relatively high values of X, with the deviation from the theory depending on the magnitude of the "saturation" effect. The assumption has also been made that the concentration of A^+ ions is low enough to neglect configurations in which two A^+ ions are adjacent to one C^- ion. It is hoped to extend the theory so as to remove these restrictions in the future.

Keeping these restrictions in mind, we can test the validity of equation 11 by a comparison of the experimental results with the theory. Figure 3 is a plot of $-\log \gamma_{AD}$ *vs.* N_{C^-} as computed from theory for $\beta = 55$ and $Z = 6$ and corresponds to the experimental results at 436°. ΔE is -5.6_4 kcal./mole. The calculated values of $Z\beta$ were fairly insensitive to Z and $-\log \gamma_{AD}$ shows a striking qualitative similarity to the experimental results shown in the preceding paper. The correspondence of the theoretical values of $-\log \gamma$ and the measured values at 436° is within experimental error, for the low values of N_{Ag^+} ($=0.279 \times 10^{-3}$ and 0.720×10^{-3}) and X (<0.15). The theoretical values of $-\log \gamma$ at $N_{Ag^+} = 3.50 \times 10^{-3}$ and 5.35×10^{-3} are, respectively, about 10 and 20% too low. This probably is due to the neglect of A^+-C^--A^+ interactions in the theory. The experimental data taken at 370° at low values of N_{Ag^+} ($\leq 0.720 \times 10^{-3}$) and X (<0.15) when compared to the theoretical calculations yield a value of $\beta = 84$ when $Z = 6$. ΔE is -5.6_6 kcal./mole which is in surprisingly good agreement with the value of ΔE found at higher temperatures. Further investigations of the temperature dependence of $-\log \gamma$ in this system will be reported in a future publication.

Conclusions

The correspondence of the simple lattice theory to experiment, for the conditions implied in the derivation of the theory, is good and lends con-

(9) Appendix B.

(10) E. R. Van Artsdalen, THIS JOURNAL, **60**, 172 (1956).

(11) F. R. Duke, *ibid.*, **62**, 417 (1958).

fidence to a lattice model of fused salt solutions. The theory makes clear the need for caution in the "chemical" interpretation of thermodynamic behavior in fused salt solution in terms of "complex" ions *even if only nearest neighbor interactions are significant.* More experimental work at different temperatures, and using other anions in the concentration cell, and modifications of the lattice model will be submitted for future publication.

Acknowledgments.—The author wishes to express his thanks to Drs. R. F. Newton and F. F. Blankenship of this Laboratory and to Professor G. Scatchard for many valuable discussions, to W. R. Grimes for encouragement in this work and especially to Professor J. Braunstein of the University of Maine for helping to derive the final equations in closed form.

Appendix A

Calculation of the Most Probable Distribution.—The number of positions of the two types available to C^- ions are L_A and L_B in the regions a and b. The relative energy of each of the C^- ions in region a is ΔE and in region b is zero. The distribution of $\mathfrak{N}n_{C^-}$ C^- ions in these two regions is such that M_A' fall in region a and M_B' in region b and can be done in Ω' ways given by

$$\Omega' = \frac{L_A!}{(L_A - M_A')!\,M_A'!} \cdot \frac{L_B!}{(L_B - M_B')!\,M_B'!}$$

The most probable distribution can be calculated[12] by maximizing Ω' under the restriction of constant total energy and constant total number of C^- ions. The calculation yields

$$-\ln\left(\frac{M_A}{L_A - M_A}\right) + r + s\Delta\epsilon = 0 \qquad \text{(i)}$$

$$-\ln\left(\frac{M_B}{L_B - M_B}\right) + r = 0 \qquad \text{(ii)}$$

where r and s are the Lagrange multipliers and M_A and M_B are the number of C^- ions in regions a and b in the most probable distribution. Combining (i) and (ii) we get

$$\frac{M_A}{L_A - M_A} = \frac{M_B}{L_B - M_B}\,e^{-\Delta\epsilon/kT} = \frac{M_B}{L_B - M_B}\,\beta \qquad \text{(iii)}$$

where $\beta = e^{-\Delta E/kT}$. If X is the fraction of positions adjacent to all the A^+ ions that are occupied by C^- ions in the most probable distribution then $M_A = ZXn_{A^+}\mathfrak{N}$ and $M_B = (n_{C^-} - ZXn_{A^+})\mathfrak{N}$. Substituting this in (iii) we get equation iv

$$\frac{ZXn_{A^+}}{Zn_{A^+} - ZXn_{A^+}} = \left(\frac{n_{C^-} - ZXn_{A^+}}{n_{A^+} + n_{B^+} - Zn_{A^+}(1 - X) - n_{C^-}}\right)\beta = \left(\frac{N_{C^-} - ZXN_{A^+}}{1 - ZN_{A^+}(1 - X) - N_{C^-}}\right)\beta \qquad \text{(iv)}$$

Appendix B

Calculation of the Activity Coefficient of Component AD.—From equations 8 and 9 we get, recalling that $\mathfrak{N}k = R$ and that $\ln(G!) \cong G\ln(G/e)$

$$\frac{\Delta S}{R} = \frac{\ln\Omega}{\mathfrak{N}} = (n_{A^+} + n_{B^+})\ln(n_{A^+} + n_{B^+}) - n_{A^+}\ln n_{A^+} - n_{B^+}\ln n_{B^+} + \frac{L_A}{\mathfrak{N}}\ln L_A - \frac{(L_A - M_A)}{\mathfrak{N}}\ln(L_A - M_A) - \frac{M_A}{\mathfrak{N}}\ln M_A + \frac{L_B}{\mathfrak{N}}\ln L_B - \frac{(L_B - M_B)}{\mathfrak{N}}\ln(L_B - M_B) - \frac{M_B}{\mathfrak{N}}\ln M_B = \frac{\Delta S^+}{R} + \frac{\Delta S^-}{R} \qquad \text{(v)}$$

where ΔS^+ represents the first three terms on the right and ΔS^- the last six terms. Substituting for L_A, M_A, L_B and M_B and combining terms

$$\frac{\Delta S^-}{R} = -Zn_{A^+}\ln(1 - X) + ZXn_{A^+}\ln(1 - X) - ZXn_{A^+}\ln X\,(n_{A^+} + n_{B^+} - Zn_{A^+})\,[\ln(n_{A^+} + n_{B^+} - Zn_{A^+}) - \ln(n_{A^+} + n_{B^+} - Zn_{A^+} + ZXn_{A^+} - n_{C^-})] + (n_{C^-} - ZXn_{A^+})\,[\ln(n_{A^+} + n_{B^+} - Zn_{A^+} + ZXn_{A^+} - n_{C^-}) - \ln(n_{C^-} - ZXn_{A^+})] \qquad \text{(vi)}$$

Differentiating by n_{A^+}[3] and combining terms

$$-\frac{1}{R}\frac{\partial\Delta S^-}{\partial n_{A^+}} = Z\ln(1 - X) + (Z - 1)\ln\left(\frac{1 - ZN_{A^+}}{1 - ZN_{A^+} + ZXN_{A^+} - N_{C^-}}\right) + ZX\ln\beta + Zn_{A^+}\frac{\partial X}{\partial n_{A^+}}\ln\beta \qquad \text{(vii)}$$

$$-\frac{1}{R}\frac{\partial S^+}{\partial n_{A^+}} = \ln N_{A^+} \qquad \text{(viii)}$$

Differentiating equation 3

$$\frac{1}{RT}\frac{\partial\Delta H_D}{\partial n_{A^+}} = ZX\frac{\Delta E}{RT} + Zn_A\frac{\partial X}{\partial n_{A^+}}\frac{\Delta E}{RT} = \frac{\bar{H}_{AD} - \bar{H}^*_{AD}}{RT} \qquad \text{(ix)}$$

Adding (vii), (viii) and (ix) recalling that $\ln\beta = -\Delta E/RT$ and substituting from (7) we get

$$\frac{\bar{F}_{AD} - \bar{F}^*_{AD}}{RT} = Z\ln(1 - X) + (Z - 1)\ln\left[1 + \frac{X}{\beta(1 - X)}\right] + \ln N_{A^+} = RT\ln\gamma_{AD}N_{A^+}N_{D^-} \qquad \text{(x)}$$

(12) J. Mayer and M. Mayer, "Statistical Mechanics," John Wiley and Sons, New York, N. Y., 1940, p. 113.

PHASE EQUILIBRIA IN THE FUSED SALT SYSTEMS LiF–ThF_4 AND NaF–ThF_4

BY R. E. THOMA, H. INSLEY, B. S. LANDAU, H. A. FRIEDMAN AND W. R. GRIMES

Oak Ridge National Laboratory,[1] Reactor Chemistry Division, Oak Ridge, Tennessee

Received December 22, 1958

Detailed phase equilibrium diagrams are presented for the binary systems LiF–ThF_4 and NaF–ThF_4. Data for the determination of phase boundaries and solid state transitions were obtained from thermal analysis of heating and cooling curves and by quenching after equilibration. Phases were identified with the use of the X-ray diffractometer and the petrographic microscope. Four compounds, $3LiF{\cdot}ThF_4$, $7LiF{\cdot}6ThF_4$, $LiF{\cdot}2ThF_4$ and $LiF{\cdot}4ThF_4$, have been identified in the system LiF–ThF_4. These melt incongruently with the exception of $3LiF{\cdot}ThF_4$. Five compounds, $4NaF{\cdot}ThF_4$, $2NaF{\cdot}ThF_4$, $3NaF{\cdot}2ThF_4$, $NaF{\cdot}ThF_4$ and $NaF{\cdot}2ThF_4$ have been identified in the system NaF–ThF_4. These melt incongruently with the exception of $2NaF{\cdot}ThF_4$ and $3NaF{\cdot}2ThF_4$ which melt congruently. A metastable solid phase having the composition $7NaF{\cdot}6ThF_4$ has been identified. The compounds $4NaF{\cdot}ThF_4$ and $3NaF{\cdot}2ThF_4$ do not exist as equilibrium phases at low temperatures. The compound $4NaF{\cdot}ThF_4$ decomposes on cooling into NaF and $2NaF{\cdot}ThF_4$ at 565°; the compound $3NaF{\cdot}2ThF_4$ decomposes on cooling into $2NaF{\cdot}ThF_4$ and $NaF{\cdot}ThF_4$ at 693°. Optical measurements and X-ray diffraction data have been obtained for each of the solid phases observed in the systems LiF–ThF_4 and NaF–ThF_4.

Introduction

Molten fluoride mixtures containing uranium tetrafluoride have been shown to be useful as circulating fuels for high temperature nuclear reactors.[2a,b] Conversion of thorium to U^{233} can be accomplished in such a reactor if ThF_4 is included in the fuel or if a molten blanket containing ThF_4 surrounds the reactor. Solutions of UF_4 and ThF_4 in Li^7F–BeF_2 or in NaF–BeF_2 solvent mixtures have been proposed as fuels for such converters.[3]

Reliable phase diagrams of the related binary and ternary systems are essential to an understanding of phase behavior in the quaternary systems LiF–BeF_2–ThF_4–UF_4 and NaF–BeF_2–ThF_4–UF_4. Phase diagrams of the systems LiF–UF_4 and NaF–UF_4,[4] LiF–BeF_2[5,6] and NaF–BeF_2[7,8] have been published. Phase relationships have been investigated and diagrams have been constructed for the systems BeF_2–UF_4,[9] NaF–BeF_2–UF_4[10] and LiF–BeF_2–UF_4.[11] Phase diagrams of the systems LiF–ThF_4 and NaF–ThF_4 which represent interpretations of data from thermal analysis have been described.[12,13] However, no detailed examination of these binary systems appears to have been made. As a consequence, the LiF–ThF_4 and NaF–ThF_4 systems have been examined in this Laboratory by application of the several experimental methods previously applied in other examinations.

The equilibrium phase diagrams of these binary systems are considerably less complex than those observed in some alkali fluoride–quadrivalent systems, *e.g.*, NaF–UF_4[4] and NaF–ZrF_4.[14] However, the ease of formation of phases which can be shown to be metastable complicates considerably the interpretation of phase study data obtained on the NaF–ThF_4 system. Complete elucidation of the diagrams is, accordingly, greatly expedited by consideration of data from a variety of experimental methods. The diagrams presented in this paper are based on data from thermal analysis and from equilibration followed by quenching, along with examination of cooled melts from these procedures with the use of the petrographic microscope and by X-ray diffraction techniques.

Experimental

Materials.—The mixtures used for the phase equilibrium studies were prepared from reagent grade lithium fluoride, sodium fluoride and thorium tetrafluoride. Sodium fluoride was obtained from General Chemical Division of Allied Chemical and Dye Corporation, lithium fluoride from Foote Mineral Company and from Maywood Chemical Works, and thorium tetrafluoride from Iowa State College. A spectrographic analysis indicated that this thorium tetrafluoride was essentially free of rare earths.

Commercial preparations of LiF and NaF commonly contain small amounts of water, and thorium fluoride is easily hydrolyzed at elevated temperatures. Although hydrolysis does not readily produce the dioxide as does hydrolysis of UF_4, small amounts of hydrolysis products may be formed at high temperatures and impair the value of experimental results either by altering the nominal composition of a mixture or by causing a non-equilibrium phase to be stabilized against decomposition. It is necessary, therefore, if the sample under examination is to be free from extraneous phases due to the presence of oxides or oxyfluorides, to remove all water and to protect the heated sample from contact with air.

In some experiments, component mixtures were treated with anhydrous HF at temperatures above the melting point of the salt to ensure the absence of oxide or oxyfluoride in the samples under study. In many cases, $NH_4F{\cdot}HF$ was added to the salt mixture; this hydrofluorinating agent helped to remedy the effects of hydrolysis and was removed completely by sublimination at about 500°.

Apparatus and Methods.—The techniques used for meas-

(1) Operated for the United States Atomic Energy Commission by the Union Carbide Corporation.

(2) (a) A. M. Weinberg and R. C. Briant, *Nuclear Sci. and Eng.*, **2**, 797 (1957); (b) E. S. Bettis, J. L. Meem, R. E. Affel, W. B. Cottrell and G. D. Whitman, *ibid.*, 2, 804 (1957).

(3) W. R. Grimes, "Molten Salt Reactor Program Quarterly Progress Report for Period Ending Oct. 31, 1957," ORNL-2431, p. 32.

(4) C. J. Barton, H. A. Friedman, W. R. Grimes, H. Insley, R. E. Moore and R. E. Thoma, *J. Am. Ceram. Soc.*, **41**, No. 2, 63 (1958).

(5) A. V. Novoselova, Yu. P. Simanov and E. I. Yarembash, *Zhur. Fiz. Khim.*, **26**, 1244 (1952).

(6) D. M. Roy, R. Roy and E. F. Osborn, *J. Am. Ceram. Soc.*, **37**, 300 (1954).

(7) A. V. Novoselova, M. E. Levina, Yu. P. Simanov and A. G. Zhasmin, *J. Gen. Chem.* (*U.S.S.R.*), **14**[6], 385 (1944), English Summary.

(8) D. M. Roy, R. Roy and E. F. Osborn. *J. Am. Ceram. Soc.*, **36**, 185 (1953).

(9) J. F. Eichelberger, E. F. Joy, E. Orban, T. B. Rhinehammer and P. A. Tucker, Mound Laboratory, System BeF_2–UF_4, unpublished work.

(10) J. F. Eichelberger, C. R. Hudgens, L. V. Jones, G. Pish, T. B. Rhinehammer, P. A. Tucker and L. J. Wittenberg, Mound Laboratory, System NaF–BeF_2–UF_4, unpublished work.

(11) J. F. Eichelberger, D. E. Etter, C. R. Hudgens, L. V. Jones, T. B. Rhinehammer, P. A. Tucker and L. J. Wittenberg, Mound Laboratory, System LiF–BeF_2–UF_4, unpublished work.

(12) J. O. Blomeke, "An Investigation of ThF_4-Fused Salt Solutions for Homogeneous Breeder Reactors," ORNL-1030, June 19, 1951.

(13) V. S. Emelyanov and A. I. Evstyukin, *J. Nuclear Energy*, [II] **5**, 108 (1957).

(14) C. J. Barton, W. R. Grimes, H. Insley, R. E. Moore and R. E. Thoma, THIS JOURNAL, **62**, 665 (1958).

urement of the temperatures which define the phase diagrams as well as the methods for identifying phases have been discussed previously.[4,14] A variation of the design of the thermal quenching furnace was made to permit a higher maximum temperature of operation than was previously feasible.[15] This apparatus was employed only in those experiments which required long annealing periods at temperatures of 850° or higher.

Results and Discussion

The System LiF–ThF_4.—A phase diagram of the system LiF–ThF_4 derived entirely from thermal analysis has been reported from this Laboratory by J. O. Blomeke.[12] This diagram was the result of a study designed to outline the liquidus curve of the system; no observations of the solid phases occurring within the system were made. The present equilibrium diagram (Fig. 1) represents a synthesis of more recent thermal data and thermal gradient quenching data. The invariant equilibria for the system LiF–ThF_4 are listed in Table I. Thermal analysis data, not inclusive of the Blomeke data, are shown in Table II. Results of thermal gradient quenching experiments are given in Table III.

TABLE I

INVARIANT EQUILIBRIA IN THE SYSTEM LiF–ThF_4

Mole % ThF_4 in liquid	Invariant temp. (°C.)	Type of equilibrium	Phase reaction at invariant temp.
23	568	Eutectic	$L \rightleftarrows LiF + 3LiF\cdot ThF_4$[a]
25	573	Congruent m.p.	$L \rightleftarrows 3LiF\cdot ThF_4$
29	565	Eutectic	$L \rightleftarrows 3LiF\cdot ThF_4 + 7LiF\cdot 6ThF_4$
30.5	597	Peritectic	$LiF\cdot 2ThF_4 + L \rightleftarrows 7LiF\cdot 6ThF_4$
42	762	Peritectic	$LiF\cdot 4ThF_4 + L \rightleftarrows LiF\cdot 2ThF_4$
58	897	Peritectic	$ThF_4 + L \rightleftarrows LiF\cdot 4ThF_4$

[a] The symbol "L" refers to liquid.

Formulas for the three incongruently melting LiF–ThF_4 compounds were established by the fact that almost pure single-phase material[16] was found in quenched samples of mixtures containing 46.2, 66.7 and 80 mole % ThF_4 which were heated below the solidus temperature for sufficient time to achieve equilibrium. The length of time required depended on the composition of the sample. Fifty to one hundred hours was generally a sufficiently long annealing time for equilibrium to be established at temperatures just below the incongruent melting point. The formula of the compound $3LiF\cdot ThF_4$ was established by the fact that almost pure single-phase material was found both in slowly-cooled and quenched samples of mixtures containing 25 mole % ThF_4. The melting temperature of this compound was determined by the thermal gradient quenching technique, inasmuch as the compound displayed a tendency toward supercooling.

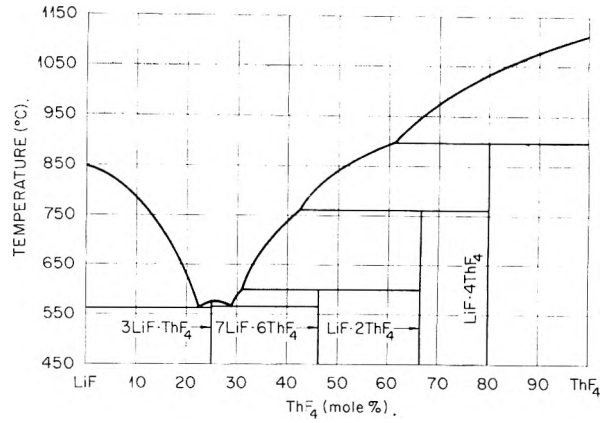

Fig. 1.—The system LiF–ThF_4.

TABLE II

THERMAL ANALYSIS DATA FOR LiF–ThF_4 MIXTURES

Mole % ThF_4 in liquid	Temp. (°C.)	Interpretation of thermal effect
5	823	Liquidus
	562	Eutectic
10	778	Liquidus
	568	Eutectic
15	712	Liquidus
	561	Eutectic
20	630	Liquidus
	568	Eutectic
25	563	Congruent melting of $3LiF\cdot ThF_4$ (supercooled)
30	600	Liquidus
	555[a]	Eutectic
33.3	658	Liquidus
	562	Eutectic
46.2	810	Liquidus
	750	Incongruent melting of $LiF\cdot 2ThF_4$
	560[a]	Eutectic
50	845	Liquidus
	750	Incongruent melting of $LiF\cdot 2ThF_4$
	558[a]	Eutectic
62	895	Liquidus or incongruent melting of $LiF\cdot 4ThF_4$
	740[a]	Incongruent melting of $LiF\cdot 2ThF_4$
66.7	967	Liquidus
	874	Incongruent melting of $LiF\cdot 4ThF_4$
	730[a]	Incongruent melting of $LiF\cdot 2ThF_4$
80	1040	Liquidus
	885	Incongruent melting of $LiF\cdot 4ThF_4$
90	1062	Liquidus

[a] Low because of supercooling.

No reports in the literature are known concerning measurement of any properties of the compounds in the system LiF–ThF_4. Optical properties and X-ray diffraction data of these compounds are listed in Tables IV and V, respectively. Supplementary X-ray diffraction phase analysis data to that in-

(15) H. A. Friedman, *J. Am. Ceram. Soc.*, in press.

(16) The expression "almost pure single-phase material" is used in view of the fact that very rarely does a solid phase at nominal compound composition appear to be absolutely free of traces of a second phase, because it is fortuitous that components can be weighed so precisely that an *exact* design composition will be produced. Occasional checks on the compositions of mixtures show that these normally fall within ±0.5 mole % of design composition. It is usual, therefore, that traces of impurity can be detected using the petrographic microscope which do not appear in X-ray diffraction patterns. Absolutely pure single phase material observed routinely at nominal compound compositions usually indicates solid solution rather than experimental precision in sample preparation. Thus, the phrase "almost pure single-phase material" here also denotes the absence of detectable solid solutions in the binary system.

TABLE III

DATA OBTAINED BY QUENCHING LiF–ThF_4 MIXTURES[a]

Compn. mole % ThF_4	Phase change temp. (°C.)	Phases found just above phase change	Phases found just below phase change	Interpretation of phase change
20	629 ± 3[b]	L[c]	LiF + L	Liquidus
20	568 ± 4	LiF + L	LiF + $3LiF \cdot ThF_4$	Eutectic
22	574 ± 4	L	LiF + $3LiF \cdot ThF_4$	Eutectic temp. and compn.
25	572 ± 3	L	$3LiF \cdot ThF_4$	Congruent m.p. of $3LiF \cdot ThF_4$
28	575 ± 5	L	$3LiF \cdot ThF_4$ + L	Liquidus
28	565 ± 5	$3LiF \cdot ThF_4$ + L	$3LiF \cdot ThF_4$ + $7LiF \cdot 6ThF_4$	Eutectic
28	568 ± 3	L	$3LiF \cdot ThF_4$ + $7LiF \cdot 6ThF_4$	Eutectic temp. and compn.
29	568 ± 3	L	$3LiF \cdot ThF_4$ + $7LiF \cdot 6ThF_4$	Eutectic temp. and compn.
33.3	648 ± 5	L	$LiF \cdot 2ThF_4$ + L	Liquidus
33.3	610 ± 6	L + $LiF \cdot 2ThF_4$	$7LiF \cdot 6ThF_4$ + L	Incongruent melting temp. of $7LiF \cdot 6ThF_4$
33.3	572 ± 5	$7LiF \cdot 6ThF_4$ + L	$7LiF \cdot 6ThF_4$ + $3LiF \cdot ThF_4$	Eutectic temp.
46.2	595 ± 5	$LiF \cdot 2ThF_4$ + L	$7LiF \cdot 6ThF_4$	Incongruent melting temp. of $7LiF \cdot 6ThF_4$
50	832 ± 7	L	$LiF \cdot 4ThF_4$ + L	Liquidus
50	768 ± 6	$LiF \cdot 4ThF_4$ + L	$LiF \cdot 2ThF_4$ + L	Incongruent melting of $LiF \cdot 2ThF_4$
50	606 ± 5	$LiF \cdot 2ThF_4$ + L	$7LiF \cdot 6ThF_4$ + $LiF \cdot 2ThF_4$	Incongruent melting of $7LiF \cdot 6ThF_4$
55	870 ± 9	L	$LiF \cdot 4ThF_4$ + L	Liquidus
55	769 ± 9	$LiF \cdot 4ThF_4$ + L	$LiF \cdot 2ThF_4$ + L	Incongruent melting of $LiF \cdot 2ThF_4$
60	754 ± 4	$LiF \cdot 4ThF_4$ + L	$LiF \cdot 2ThF_4$ + L	Incongruent melting of $LiF \cdot 2ThF_4$
62	751 ± 4	$LiF \cdot 4ThF_4$ + L	$LiF \cdot 2ThF_4$ + L	Incongruent melting of $LiF \cdot 2ThF_4$
66.7	967 ± 5	L	ThF_4 + L	Liquidus
66.7	896 ± 9	ThF_4 + L	$LiF \cdot 4ThF_4$ + L	Incongruent melting of $LiF \cdot 4ThF_4$
66.7	762 ± 9	$LiF \cdot 4ThF_4$ + L	$LiF \cdot 2ThF_4$ + L	Incongruent melting of $LiF \cdot 2ThF_4$
80	897 ± 7	ThF_4 + L	$LiF \cdot 4ThF_4$	Incongruent melting of $LiF \cdot 4ThF_4$

[a] Most of the phases were identified by optical microscopy. The phases underlined were also identified by X-ray diffraction. [b] The uncertainty in temperatures shown in column 2 indicates the temperature differences between the quenched samples from which the values were obtained. [c] The symbol "L" refers to liquid (observed as glass or quench growth).

cluded in Table III have been reported elsewhere.[17–19] Crystal parameters of LiF–ThF_4 compounds are reported separately.[20]

The liquidus curves and solidus lines from 0–22.5 mole % ThF_4 and from 70–100 mole % ThF_4 were determined principally by thermal analysis, with some corroboration by results from thermal gradient quenching experiments. In the composition region 22.5–70 mole % ThF_4 thermal analysis and thermal gradient quenching experiments served to augment and complement one another in the determination of the liquidus curve. Supercooling effects associated with the incongruent melting reactions $LiF \cdot 4ThF_4$ and $LiF \cdot 2ThF_4$ were so prevalent that only thermal gradient quenching experiments permitted determination of these temperatures within the ±5° precision considered to be requisite for these measurements. Heating and cooling curves of LiF–ThF_4 melts in the composition region 31–66.7 mole % ThF_4 showed no effects associated with the formation of $7LiF \cdot 6ThF_4$. Apparently the thermal effect associated with the formation of this compound by reaction of liquid with $LiF \cdot 2ThF_4$ is so small as to escape detection by the thermal analysis apparatus used in these experiments.

The phase equilibrium diagram of the system LiF–ThF_4 displays several noteworthy relationships with the system LiF–UF_4.[4] The liquidus profiles of the two systems are similar and the melting relationships of $LiF \cdot 4UF_4$ and $LiF \cdot 4ThF_4$ are analogous in that they melt incongruently to the tetrafluoride and liquid. The analogous compound pairs, $3LiF \cdot UF_4$–$3LiF \cdot ThF_4$, $7LiF \cdot 6UF_4$–$7LiF \cdot 6ThF_4$, and $LiF \cdot 4UF_4$–$LiF \cdot 4ThF_4$ are isostructural but remarkably different in melting–freezing character. The compound $3LiF \cdot ThF_4$ melts congruently whereas the compound $3LiF \cdot UF_4$ has no region of stability in the system LiF–UF_4, and is metastable with respect to $4LiF \cdot UF_4$ and LiF. The compounds $7LiF \cdot 6UF_4$ and $7LiF \cdot 6ThF_4$ display almost identical incongruent melting temperatures, but exhibit different melting relations, $7LiF \cdot 6UF_4$ melting to the 1:4 compound and liquid, and $7LiF \cdot 6ThF_4$ melting to the 1:2 compound and liquid. The incongruent melting temperatures of the compound $LiF \cdot 4UF_4$ and $LiF \cdot 4ThF_4$ differ by 130°.

Additional data, not listed in this paper, have served to corroborate the inferences regarding the precision of determination of LiF–ThF_4 phase relationships in the 20–80 mole % ThF_4 composition region. These data are part of an investigation of

(17) R. E. Thoma, "Results of X-Ray Diffraction Phase Analyses of Fused Salt Mixtures," Oak Ridge National Laboratory Central Files Memorandum No. CF-58-2-59, Feb. 18, 1958.

(18) R. E. Thoma, "X-Ray Diffraction Results," Oak Ridge National Laboratory Central Files Memorandum No. CF-58-2-42, Feb. 5, 1957.

(19) R. E. Thoma, "Results of Examinations of Fused Salt Mixtures by Optical and X-Ray Diffraction Methods," Oak Ridge National Laboratory Central Files Memorandum No. CF-58-11-40, Nov. 14, 1958.

(20) L. A. Harris, G. D. White and R. E. Thoma, (Oak Ridge National Laboratory), THIS JOURNAL, in press.

TABLE IV

OPTICAL PROPERTIES OF $LiF-ThF_4$ AND $NaF-ThF_4$ COMPOUNDS

Compound	Optical character	$2V$	Sign	$N\alpha$ or $N\omega$	$N\gamma$ or $N\epsilon$
		$LiF-ThF_4$ compounds			
$3LiF \cdot ThF_4$	Biaxial[a]	10°	−	1.480	1.488
$7LiF \cdot 6ThF_4$	Uniaxial		+	1.502	1.508
$LiF \cdot 2ThF_4$	Uniaxial		−	1.554	1.548
$LiF \cdot 4ThF_4$	Biaxial[a]	10°	−	1.528	1.538
		$NaF-ThF_4$ compounds			
α-$4NaF \cdot ThF_4$	Isotropic			1.400	
β-$4NaF \cdot ThF_4$	Biaxial	Small	−	1.397	1.402
$2NaF \cdot ThF_4$	Uniaxial		+	1.464	1.496
$3NaF \cdot 2ThF_4$	Isotropic			1.474	
$NaF \cdot ThF_4$	Biaxial	Small	−	≈1.503	
$NaF \cdot 2ThF_4$	Isotropic			1.550	
$2NaF \cdot ThF_4$[b]		Not known			
$7NaF \cdot 6ThF_4$[b]	Uniaxial		−	1.476	1.468
$NaF \cdot ThF_4$[b]	Biaxial	40°	−	1.506	1.540

[a] This routinely observed biaxiality appears to be a function of strain, inasmuch as the crystal type is tetragonal as determined by X-ray diffraction measurements.[20] [b] Metastable.

phase equilibria in the system $LiF-ThF_4-UF_4$ which will be reported later from this Laboratory. Extrapolations from $LiF-ThF_4-UF_4$ primary phase liquidus measurements and from boundary curve determinations have permitted a higher precision of estimation of $LiF-ThF_4$ temperature-composition values than was possible from the data represented by Tables II and III.

Compounds having the unusual 7:6 mole ratio have been observed in several other systems of alkali fluorides with heavy metal quadrivalent fluorides, *e.g.*, $LiF-UF_4$,[4] $NaF-UF_4$,[4] $KF-UF_4$,[21] $RbF-UF_4$[21] and $NaF-ZrF_4$.[14] In all cases in which the alkali fluoride is other than LiF the crystal type of the 7:6 compound is found to be of the hexagonal (rhombohedral) crystal system[22]; the two LiF compounds $7LiF \cdot 6UF_4$ and $7LiF \cdot 6ThF_4$ are tetragonal.[22]

The System $NaF-ThF_4$.—A phase diagram of the system $NaF-ThF_4$ has been reported by Emelyanov and Evstyukhin.[13] These authors indicate that the diagram is based on thermal, X-ray,[23] and other analyses. The phase equilibrium diagram reported here (Fig. 2) differs substantially from that reported by the investigators referred to above largely because of the capability of the thermal gradient quenching technique to permit the observance of the actual phase relationships occurring within the system. The phase equilibrium diagram of the system $NaF-ThF_4$ represents a synthesis from thermal analysis and thermal gradient quenching data. Identification of the phases present in samples was made by optical measurements using the petrographic microscope and by the use of X-ray defraction techniques. Formulas of the compounds $4NaF \cdot ThF_4$, $NaF \cdot ThF_4$ and $NaF \cdot 2ThF_4$ were established by the fact that almost pure single-phase material was found in quenched samples of mixtures containing 20, 50 and 66.7 mole % ThF_4 which were heated just below the incongruent melting temperature for sufficient time to achieve equilibrium. As in the case of the $LiF-ThF_4$ mixtures, 50–100 hours was generally a sufficiently long annealing time for equilibrium to be established at temperatures just below incongruent melting temperatures. The formula of the compound $2NaF \cdot ThF_4$ was established by the fact that almost pure single-phase material was found both in the slowly cooled melts and in samples quenched just below the liquidus temperature at 33.3 mole % ThF_4. Formula of the compound $3NaF \cdot 2ThF_4$ was established by the fact that almost pure single-phase material was found in samples quenched just below the liquidus temperature at 40 mole % ThF_4.

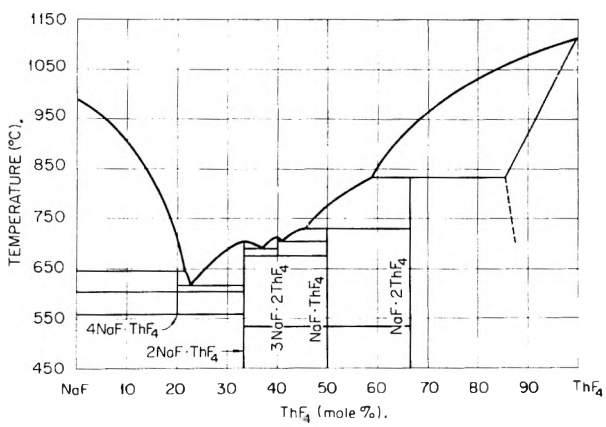

Fig. 2.—The system $NaF-ThF_4$.

The invariant equilibria for the system $NaF-ThF_4$ are listed in Table VI. Thermal analysis data for $NaF-ThF_4$ mixtures are listed in Table VII. Results of thermal gradient quenching experiments are given in Table VIII. Optical properties and X-ray diffraction patterns of $NaF-ThF_4$ compounds are listed in Tables IV and V, respectively. X-Ray diffraction phase analysis data which sup-

(21) R. E. Thoma, H. Insley, B. S. Landau, H. A. Friedman and W. R. Grimes, *J. Am. Ceram. Soc.*, **41**, [12], 538 (1958).

(22) L. A. Harris, "The Crystal Structure of 7:6 Type Compounds of Alkali Fluorides with Uranium Tetrafluoride," Oak Ridge National Laboratory Central Files Memorandum No. CF-58-3-15, March 6, 1958.

(23) W. H. Zachariasen, *J. Am. Chem. Soc.*, **70**, 2147 (1948).

Table V

X-Ray Diffraction Patterns for the Solid Phases Occurring in the Systems $LiF-ThF_4$ and $NaF-ThF_4$

$3LiF \cdot ThF_4$		$7LiF \cdot 6ThF_4$		$LiF \cdot 2ThF_4$		$LiF \cdot 4ThF_4$		α-$4NaF \cdot ThF_4$		β_2-$2NaF \cdot ThF_4$	
d (Å.)	I/I_1	d (Å.)	I/I_1	d (Å.)	I/I_1	d (Å.)	I/I_1	d (Å.)	I/I_1	d (Å.)	I/I_1
6.42	100	6.07	15	7.97	5	8.34	3	5.43	100	6.22	10
4.46	100	5.91	20	6.37	10	7.76	3	4.70	60	5.72	45
4.37	100	5.36	90	3.96	100	6.51	5	3.03	100	5.38	10
3.62	85	5.25	15	3.57	65	5.80	25	2.90	60	5.17	100
3.09	55	4.95	30	3.25	5	4.62	5	2.104	30	4.53	10
2.866	70	4.85	20	3.21	5	4.33	70	2.085	80	4.11	20
2.788	30	4.75	100	2.97	20	3.88	100	1.794	50	3.83	5
2.542	25	4.01	85	2.822	25	3.60	60	1.475	30	3.69	5
2.327	10	3.92	15	2.675	7	3.25	10	β-$4NaF \cdot ThF_4$		3.65	5
2.189	20	3.74	15	2.528	10	2.92	25	d (Å.)	I/I_1	3.40	10
2.104	65	3.55	65	2.388	5	2.822	25	7.37	10	3.31	15
2.071	25	3.44	10	2.123	85	2.603	10	6.37	70	3.07	35
2.036	40	3.39	70	2.053	30	2.398	10	5.18	100	2.99	70
1.959	30	3.29	60	2.001	65	2.137	25	4.03	90	2.863	20
1.933	60	3.03	100	1.787	7	2.053	35	3.66	10	2.590	55
1.877	25	2.814	25	1.701	10	2.040	10	3.40	5	2.442	5
1.771	25	2.747	25	1.689	5	2.018	10	3.31	5	2.374	10
1.743	30	2.578	20	1.603	5	2.005	30	3.19	6	2.352	20
1.701	35	2.430	10	1.519	5	1.937	20	3.00	100	2.197	40
1.661	10	2.392	10	$NaF \cdot 2ThF_4$[a]		1.820	20	2.715	25	2.056	5
1.618	10	2.302	20	d (Å.)	I/I_1	1.778	3	2.604	25	1.987	5
1.547	35	2.137	20	6.19	25	1.725	5	2.324	20	1.955	15
1.520	35	2.018	5	4.72	10	1.719	5	2.222	10	1.928	15
α-$NaF \cdot ThF_4$		2.001	15	4.36	100	1.666	5	2.181	40	1.909	10
d (Å.)	I/I_1	1.892	55	4.17	3	1.605	5	2.120	100	1.793	10
8.67	15	1.859	15	3.95	5	1.595	5	2.014	15	1.742	55
6.56	25	1.804	15	3.86	3	1.563	5	1.965	15	1.724	20
5.26	60	1.680	15	3.65	5	$7NaF \cdot 6ThF_4$		1.875	15	1.705	5
5.07	25	1.653	20	3.56	100	d (Å.)	I/I_1	1.836	15	1.609	5
4.72	60	1.600	20	3.42	5	7.87	25	1.782	5	1.572	5
4.39	15	δ-$2NaF \cdot ThF_4$		3.38	3	5.40	10	1.768	5		
3.66	50	d (Å.)	I/I_1	3.33	10	4.62	25	1.734	75	β-$NaF \cdot ThF_4$	
3.55	30	7.35	100	3.21	10	4.39	100	1.593	5	d (Å.)	I/I_1
3.32	100	5.32	45	3.09	50	4.32	25	1.568	20	6.11	100
3.22	85	4.31	65	2.759	45	3.74	20	$3NaF \cdot 2ThF_4$		5.05	70
2.97	20	3.07	50	2.683	3	3.48	15	d (Å.)	I/I_1	4.23	65
2.93	15	3.03	100	2.644	4	3.38	60	3.25	100	3.78	20
2.644	15	2.839	10	2.525	20	3.30	55	2.822	25	3.34	100
2.338	90	2.663	10	2.333	25	3.26	65	1.977	55	3.24	65
2.292	15	2.508	10	2.375	5	3.07	15	1.704	35	2.885	80
2.191	30	2.455	30	2.186	3	2.91	30	1.413	10	2.315	30
2.137	10	2.355	10	2.058	100	2.826	30			2.259	20
2.099	15	2.226	15	1.985	3	2.622	10			2.206	20
2.081	30	2.158	55	1.888	3	2.482	5			2.113	35
2.071	55	2.014	5	1.863	50	2.211	30			1.993	40
2.018	20	1.942	10	1.824	5	2.196	10				
1.993	30	1.920	20	1.781	30	2.146	10				
1.961	15	1.842	25	1.713	30	2.076	35				
1.926	10	1.797	20	1.655	3	2.040	20				
1.832	40	1.768	30	1.593	20	1.957	15				
1.775	15	1.742	20	1.499	60	1.756	15				
1.759	15	1.583	15			1.704	10				
1.662	10					1.637	5				
1.605	10					1.542	10				

[a] This diffraction pattern was derived routinely from samples of $NaF \cdot 2ThF_4$; it cannot, however, be analyzed as that of a body centered cubic crystal. (See Table IV and reference 23).

plement those included in Table VIII have been reported elsewhere.[17-19]

Crystal structure determinations of the Na–Th–F compounds $4NaF \cdot ThF_4$, $2NaF \cdot ThF_4$ and $NaF \cdot 2ThF_4$ have been made by Zachariasen.[23] A calculation of the X-ray lines characteristic of a cubic cell for $4NaF \cdot ThF_4$, having an a_0 of 12.707 Å., as given by Zachariasen, shows those lines to be only the most intense lines of the phase labeled β-$4NaF \cdot ThF_4$ in this report. If the determination of $4NaF \cdot ThF_4$ were made from lines appearing in samples of a slowly-cooled melt, it is probable that only the

TABLE VI

INVARIANT EQUILIBRIA IN THE SYSTEM NaF–ThF_4

Mole % ThF_4 in liquid	Invariant temp. (°C.)	Type of equilibrium	Phase reaction at invariant temp.
21.5	645	Peritectic	$NaF + L \rightleftarrows \alpha\text{-}4NaF\cdot ThF_4$[a]
22.5	618	Eutectic	$L \rightleftarrows \alpha\text{-}4NaF\cdot ThF_4 + 2NaF\cdot ThF_4$
...	604	Inversion	$\alpha\text{-}4NaF\cdot ThF_4 \rightleftarrows \beta\text{-}4NaF\cdot ThF_4$
...	558	Decomposition	$\beta\text{-}4NaF\cdot ThF_4 \rightleftarrows NaF + 2NaF\cdot ThF_4$
33.3	705	Congruent m.p.	$L \rightleftarrows 2NaF\cdot ThF_4$
37	690	Eutectic	$L \rightleftarrows 2NaF\cdot ThF_4 + 3NaF\cdot 2ThF_4$
40	712	Congruent m.p.	$L \rightleftarrows 3NaF\cdot 2ThF_4$
41	705	Eutectic	$L \rightleftarrows 3NaF\cdot 2ThF_4 + \alpha\text{-}NaF\cdot ThF_4$
...	683	Decomposition	$3NaF\cdot 2ThF_4 \rightleftarrows 2NaF\cdot ThF_4 + \alpha\text{-}NaF\cdot ThF_4$
45.5	730	Peritectic	$NaF\cdot 2ThF_4 + L \rightleftarrows \alpha\text{-}NaF\cdot ThF_4$
58	831	Peritectic	$ThF_4 + L \rightleftarrows NaF\cdot 2ThF_4$

[a] The symbol "L" refers to liquid.

most intense lines of β-$4NaF\cdot ThF_4$ could be found, inasmuch as $4NaF\cdot ThF_4$ has no equilibrium existence below 565°. Thus, $4NaF\cdot ThF_4$ should be found in melts cooled to room temperature as the minor phase. A high temperature form of $4NaF\cdot ThF_4$ has been observed in the present study and has an equilibrium existence between the incongruent melting temperature of 640° and the inversion temperature of 605°. When observed using the petrographic microscope, it is isotropic and has a

TABLE VII

THERMAL ANALYSIS DATA FOR NaF–ThF_4 MIXTURES

Mole % ThF_4 in liquid	Temp. (°C.)	Interpretation of thermal effect
11	887	Liquidus
	640	Incongruent melting of α-$4NaF\cdot ThF_4$
	594	Inversion of α-$4NaF\cdot ThF_4$ to β-$4NaF\cdot ThF_4$
	485	Unidentified[a]
15	827	Liquidus
	649	Incongruent melting of α-$4NaF\cdot ThF_4$
	600	Inversion of α-$4NaF\cdot ThF_4$ to β-$4NaF\cdot ThF_4$
	502[a]	Unidentified
18	753	Liquidus
	653	Incongruent melting of α-$4NaF\cdot ThF_4$
	605	Inversion of α-$4NaF\cdot ThF_4$ to β-$4NaF\cdot ThF_4$
20	705	Liquidus
	625	Eutectic
	605	Inversion of α-$4NaF\cdot ThF_4$ to β-$4NaF\cdot ThF_4$
21	645	Liquidus
	603	Inversion of α-$4NaF\cdot ThF_4$ to β-$4NaF\cdot ThF_4$
	507	Unidentified[a]
22	627	Liquidus
	605	Inversion of α-$4NaF\cdot ThF_4$ to β-$4NaF\cdot ThF_4$
	490	Unidentified[a]
23.5	618	Eutectic
	530	Unidentified[a]
	490	Unidentified[a]
24	617	Eutectic
26	642	Liquidus
	620	Eutectic
33.3	693	Congruent melting (supercooled)
37	687	Eutectic
	673	Decomposition of $3NaF\cdot 2ThF_4$
	650	Unidentified
	630	Unidentified
39	690	Eutectic
	672	Decomposition of $3NaF\cdot 2ThF_4$
	658	Unidentified
	610	Unidentified
40	710	Congruent melting of $3NaF\cdot 2ThF_4$
	675	Decomposition of $3NaF\cdot 2ThF_4$
	650	Unidentified
41	705	Eutectic
	635	Unidentified
43	720	Liquidus
	640	Unidentified
44.5	712	Eutectic
	650	Unidentified
	635	Unidentified
	500	Unidentified
46.2	722	Liquidus
	710	Eutectic
	685	Unidentified
	610	Unidentified
48	745	Liquidus
	727	Incongruent melting of $NaF\cdot ThF_4$
	680	Decomposition of $3NaF\cdot 2ThF_4$
	412	Unidentified
50	765	Liquidus
	735	Incongruent melting of $NaF\cdot ThF_4$
	725	Unidentified
	705	Eutectic
	714	Unidentified
	410	Unidentified
53	787	Liquidus
	720	Incongruent melting of $NaF\cdot ThF_4$
	700	Eutectic
	655	Unidentified
54	787	Liquidus
	732	Incongruent melting of $NaF\cdot ThF_4$
	417	Unidentified
60	855	Liquidus
	795	Incongruent melting of $NaF\cdot 2ThF_4$
	720	Incongruent melting of $NaF\cdot ThF_4$
66.7	932	Liquidus
	807	Incongruent melting of $NaF\cdot 2ThF_4$
	710	Unidentified
75	1005	Liquidus
	800	Incongruent melting of $NaF\cdot 2ThF_4$
	720	Incongruent melting of $NaF\cdot ThF_4$

[a] The 400–500° breaks near 20 mole % ThF_4 probably are due to delayed decomposition of β-$4NaF\cdot ThF_4$. Mixtures which show 400–500° thermal effects do not show a thermal effect at ~558°, the equilibrium decomposition temperature for β-$4NaF\cdot ThF_4$.

refractive index of 1.400. The X-ray diffraction pattern of this phase labeled by the authors as α-4NaF·ThF_4 appears to be tetragonal rather than cubic, and displays none of the X-ray lines common to those of a cubic cell having a 12.707 Å. edge.

Zachariasen has reported two forms of 2NaF·ThF_4, β_2-2NaF·ThF_4 and δ-2NaF·ThF_4.[23] The present study shows that of these only β_2-2NaF·ThF_4 has equilibrium existence in the system NaF–ThF_4. It is remarkable that these two crystal

TABLE VIII

DATA OBTAINED BY QUENCHING NaF–ThF_4 MIXTURES[a]

Compn. mole % ThF_4	Phase change temp. (°C.)	Phases found just above phase change	Phases found just below phase change	Interpretation of phase change
15	603 ± 4[b]	NaF + α-4NaF·ThF_4	NaF + β-4NaF·ThF_4	Inversion
15	607 ± 2	NaF + α-4NaF·ThF_4	NaF + β-4NaF·ThF_4	Inversion
15	564 ± 3	NaF + β-4NaF·ThF_4	NaF + β_2-2NaF·ThF_4	Dec. of β-4NaF·ThF_4
18	742 ± 6	L[c]	NaF + L	Liquidus
20	600 ± 4	α-4NaF·ThF_4	β-4NaF·ThF_4	Inversion
20	564 ± 3	NaF + β-4NaF·ThF_4	NaF + β_2-2NaF·ThF_4	Dec. of β-4NaF·ThF_4
20	552 ± 4	β-4NaF·ThF_4	β-4NaF·ThF_4 + NaF + β_2-2NaF·ThF_4	Dec. of β-4NaF·ThF_4
23	618 ± 4	L	β_2-2NaF·ThF_4 + L	Liquidus
23	610 ± 4	β_2-2NaF·ThF_4 + L	β_2-2NaF·ThF_4 + β-4NaF·ThF_4	Eutectic
23	553 ± 3	β_2-2NaF·ThF_4 + β-4NaF·ThF_4	NaF + β_2-2NaF·ThF_4	Dec. of β-4NaF·ThF_4
24	618 ± 5	L	β-4NaF·ThF_4 + β_2-2NaF·ThF_4	Eutectic temp. and compn.
24	559 ± 5	β-4NaF·ThF_4 + β_2-2NaF·ThF_4	NaF + β_2-2NaF·ThF_4	Dec. of β-4NaF·ThF_4
26	648 ± 4	L	β_2-2NaF·ThF_4 + L	Liquidus
26	618 ± 4	β_2-2NaF·ThF_4 + L	β_2-2NaF·ThF_4 + β-4NaF·ThF_4	Eutectic
26	553 ± 3	β_2-2NaF·ThF_4 + β-4NaF·ThF_4	NaF + β_2-2NaF·ThF_4	Dec. of β-4NaF·ThF_4
28	670 ± 4	L	β_2-2NaF·ThF_4 + L	Liquidus
28	610 ± 4	β_2-2NaF·ThF_4 + L	β-4NaF·ThF_4 + β_2-2NaF·ThF_4	Eutectic
28	556 ± 3	β-4NaF·ThF_4 + β_2-2NaF·ThF_4	NaF + β_2-2NaF·ThF_4	Dec. of 4NaF·ThF_4
31	695 ± 3	L	β_2-2NaF·ThF_4 + L	Liquidus
31	618 ± 4	β_2-2NaF·ThF_4 + L	β-4NaF·ThF_4 + β_2-2NaF·ThF_4	Eutectic
31	553 ± 3	β-4NaF·ThF_4 + β_2-2NaF·ThF_4	NaF + β_2-2NaF·ThF_4	Dec. of 4NaF·ThF_4
33.3	700 ± 6	L	β_2-2NaF·ThF_4	Congruent m.p. of β_2-2NaF·ThF_4
37	693 ± 3	L	3NaF·$2ThF_4$ + β_2-2NaF·ThF_4	Eutectic temp. and compn.
37	687 ± 3	3NaF·$2ThF_4$ + β_2-2NaF·ThF_4	β_2-2NaF·ThF_4 + α-NaF·ThF_4	Dec. of 3NaF·$2ThF_4$
37	684 ± 3	3NaF·$2ThF_4$ + β_2-2NaF·ThF_4	β_2-2NaF·ThF_4 + α-NaF·ThF_4	Dec. of 3NaF·$2ThF_4$
39	704 ± 3	L	3NaF·$2ThF_4$ + L	Liquidus
39	693 ± 3	3NaF·$2ThF_4$ + L	3NaF·$2ThF_4$ + β_2-2NaF·ThF_4	Eutectic
39	687 ± 3	3NaF·$2ThF_4$ + β_2-2NaF·ThF_4	β_2-2NaF·ThF_4 + α-NaF·ThF_4	Dec. of 3NaF·$2ThF_4$
39	688 ± 4	3NaF·$2ThF_4$ + L	3NaF·$2ThF_4$ + β_2-2NaF·ThF_4	Eutectic
41	707 ± 4	L	3NaF·$2ThF_4$ + L	Liquidus
41	701 ± 4	3NaF·$2ThF_4$ + L	3NaF·$2ThF_4$ + α-NaF·ThF_4	Eutectic
41	698 ± 3	α-NaF·ThF_4 + L	α-NaF·ThF_4 + 3NaF·$2ThF_4$	Eutectic
41	677 ± 3	α-NaF·ThF_4 + 3NaF·$2ThF_4$	β_2-2NaF·$2ThF_4$ + α-NaF·ThF_4	Dec. of 3NaF·$2ThF_4$
43	724 ± 2	L	α-NaF·ThF_4 + L	Liquidus
44.5	730 ± 4	L	α-NaF·ThF_4 + L	Liquidus
44.5	667 ± 4	α-NaF·ThF_4 + L	β_2-2NaF·ThF_4 + α-NaF·ThF_4	Non-equilibrium reaction
46.2	728 ± 3	L	α-NaF·ThF_4 + L	Liquidus
46.2	711 ± 3	α-NaF·ThF_4 + L	3NaF·$2ThF_4$ + α-NaF·ThF_4	Eutectic
46.2	673 ± 4	3NaF·$2ThF_4$ + α-NaF·ThF_4	α-NaF·ThF_4 + β_2-2NaF·ThF_4	Dec. of 3NaF·$2ThF_4$

50	773 ± 3	L	$NaF \cdot 2ThF_4$ + L	Liquidus
50	731 ± 3	$NaF \cdot 2ThF_4$ + L	α-$NaF \cdot ThF_4$ + $NaF \cdot 2ThF_4$	Incongruent melting of α-$NaF \cdot ThF_4$
53	799 ± 2	L	$NaF \cdot 2ThF_4$ + L	Liquidus
53	729 ± 4	$NaF \cdot 2ThF_4$ + L	α-$NaF \cdot ThF_4$ + $NaF \cdot 2ThF_4$	Incongruent melting of α-$NaF \cdot ThF_4$
60	852 ± 3	L	ThF_4 + L	Liquidus
60	832 ± 3	ThF_4 + L	$NaF \cdot 2ThF_4$ + L	Incongruent melting of $NaF \cdot 2ThF_4$
60	732 ± 5	$NaF \cdot 2ThF_4$ + L	α-$NaF \cdot ThF_4$ + $NaF \cdot 2ThF_4$	Incongruent melting of α-$NaF \cdot ThF_4$
66.7	820 ± 10	ThF_4 + L	$NaF \cdot 2ThF_4$	Incongruent m.p. of $NaF \cdot 2ThF_4$
75	811 ± 12	ThF_4 + L	ThF_4 + $NaF \cdot 2ThF_4$	Incongruent melting of $NaF \cdot 2ThF_4$
80	829 ± 3	ThF_4 + L	$NaF \cdot 2ThF_4$ + ThF_4	Incongruent melting of $NaF \cdot 2ThF_4$
85	824 ± 7	ThF_4 + L	$NaF \cdot 2ThF_4$ + ThF_4	Incongruent melting of $NaF \cdot 2ThF_4$
90	852 ± 5	ThF_4 + L	ThF_4	Solidus

[a] Most of the phases were identified by optical microscopy. The phases underlined were also identified by X-ray diffraction. [b] The uncertainty in temperatures shown in column 2 indicates the temperature differences between the quenched samples from which the values were obtained. [c] The symbol "L" refers to liquid (observed as glass or quench growth).

forms of $2NaF \cdot ThF_4$ are isostructural with polymorphs of $2NaF \cdot UF_4$ which have reverse stability relationships from these, *i.e.*, β_2-$2NaF \cdot UF_4$, the isostructural analog of β_2-$2NaF \cdot ThF_4$, has no stable existence in the system NaF–UF_4. In similar relationship, the only equilibrium form of $2NaF \cdot UF_4$ (labeled β_3-$2NaF \cdot UF_4$[24] by Agron, *et al.*[25]) is a structural analog of δ-$2NaF \cdot ThF_4$, which has no equilibrium existence in the system NaF–ThF_4.

Zachariasen has indicated that he made no investigation of the solid phases occurring between 33 and 67 mole % ThF_4.[23] The present phase equilibrium study shows that within this composition range the three compounds, $3NaF \cdot 2ThF_4$, $7NaF \cdot 6ThF_4$ and $NaF \cdot ThF_4$ occur. Two forms of $NaF \cdot ThF_4$ exist, α-$NaF \cdot ThF_4$ and β-$NaF \cdot ThF_4$. The compound $7NaF \cdot 6ThF_4$ does not appear as a NaF-ThF_4 equilibrium phase within the temperature limits of this study.

The incongruent melting temperature of $4NaF \cdot ThF_4$ was obtained only from thermal analysis data. No quenched samples were observed near 20 mole % ThF_4 in which liquid had been quenched to glass. The phase α-$4NaF \cdot ThF_4$ is optically isotropic and thus distinguished with difficulty from "quench growths." Thus, no optical measurement of the incongruent melting temperature of $4NaF \cdot ThF_4$ could be made.

The metastable phases δ-$2NaF \cdot ThF_4$ and $7NaF \cdot 6ThF_4$ become stabilized against inversion to the equilibrium phases in the system if moisture or air has contacted the sample at high temperature. Traces of hydrolysis products introduced in this manner stabilize an equilibrium involving the two solid phases $3NaF \cdot 2ThF_4$, $7NaF \cdot 6ThF_4$ and a liquid. Under the conditions described above quenched samples which have been cooled from higher than liquidus temperatures in the composition range between 40 and 46.2 mole % ThF_4 show that $3NaF \cdot 2ThF_4$ occurs as a solid solution containing more than 40 mole % ThF_4, and that liquid may be present in samples annealed at temperatures as low as 670°. In addition, the compound $7NaF \cdot 6ThF_4$, metastable with respect to $3NaF \cdot 2ThF_4$ and $NaF \cdot ThF_4$ may be formed under these conditions. The solid solution of $3NaF \cdot 2ThF_4$, the occurrence of $7NaF \cdot 6ThF_4$, and the metastable solidus (~670°) suggest that the metastable equilibrium involved with $3NaF \cdot 2ThF_4$ solid solution, $7NaF \cdot 6ThF_4$, and liquid is closely related to the unusual equilibrium solid solution of $3NaF \cdot 2ZrF_4$ and $7NaF \cdot 6ZrF_4$.[14]

Reproducible results were not obtained from either thermal analysis or thermal gradient quenching experiments which were definitive of the α-$NaF \cdot ThF_4 \rightleftharpoons \beta$-$NaF \cdot ThF_4$ transition temperature. Determinations of the $NaF \cdot ThF_4$ primary phase liquidus surface in the system NaF–BeF_2–THF_4 have shown reproducible results of this transition at 533 ± 7°.

Thermal analysis data show that thermal effects are frequent well below the equilibrium decomposition temperature of $3NaF \cdot 2ThF_4$. Derivation of an equilibrium phase diagram exclusively from the interpretation of the thermal effects related to both the metastable and stable equilibria occurring in the 40–50 mole % ThF_4 composition range appears to be impossible. Attempts at interpreting such effects very probably account for some of the diversity between the diagram reported here and that reported by Emelyanov and Evstyukhin.[13]

In the composition range 50–75 mole % ThF_4 so much undercooling occurs in thermal analysis that the liquidus as well as the incongruent melting temperatures of $NaF \cdot ThF_4$ and $NaF \cdot 2ThF_4$ were derived principally from results of thermal gradient quenching. In compositions higher than 75 mole % ThF_4 the thermal effects produced by cooling through the liquidus temperature are so minor and vary so widely in temperature that selection of liquidus values from these data becomes very difficult. Moreover, because of rapid crystallization of ThF_4 during quenching the microscopic distinction between "quench growths" and equilibrium crystallization below the liquidus becomes so uncertain that the gradient quenching method also is subject to considerable error. The melting point of pure ThF_4 was determined by thermal analysis and was found to be 1110 ± 5°. This value is within experimental limits of error of previously reported melting points of pure ThF_4.[26,27] The liquidus val-

(24) P. A. Agron, B. S. Borie, Jr., and R. M. Steele, unpublished work, Oak Ridge National Laboratory.

(25) Zachariasen discovered the phase δ-$2NaF \cdot UF_4$ in experiments conducted after publication of the structures of other Na–U–F compounds (reference 23) (personal communication).

(26) J. Asker, E. R. Segnit and A. W. Wylie, *J. Chem. Soc.*, 4470 (1952).

(27) A. J. Darnell and F. J. Keneshea, Jr., THIS JOURNAL, **62**, 1143 (1958).

ues between 75 and 100 mole % ThF_4 shown in the NaF–ThF_4 diagram thus are derived largely by interpolation between the liquidus values below compositions of 75 mole % ThF_4 and the melting point for ThF_4 of 1111°.

Solid solution between $NaF{\cdot}2ThF_4$ and ThF_4 was observed by an increasingly small interval between the solidus and liquidus in the composition range 85 to 100 mole % ThF_4, and by the presence of single phase monoclinic ThF_4 solid solution below the solidus in this composition range. The results of several thermal gradient quenching experiments in the 80 to 95 mole % ThF_4 composition region showed poor reproducibility of liquidus temperatures (these are reported in reference 18). These experiments demonstrate that the miscibility limit of the ThF_4 solid solution lies between 85 and 87.5 mole % ThF_4 at the solidus. At this limit the refractive indices of ThF_4 have been increased from $N_\beta = 1.518 \pm 0.002$ and $N_\gamma = 1.534 \pm 0.002$ to $N_\beta = 1.532 \pm 0.002$, and $N_\gamma = 1.542 \pm 0.002$. Although no comparable solid solution has been observed in the alkali fluoride–uranium tetrafluoride systems LiF–UF_4,[4] NaF–UF_4,[4] KF–UF_4[21] or RbF–UF_4,[21] or in LiF–ThF_4, a similar ThF_4 solid solution has been reported as occurring in the system KF–ThF_4.[26]

Summary

Detailed phase diagrams have been presented for the systems LiF–ThF_4 and NaF–ThF_4. These are regarded as complete with respect to the stable phase boundaries from the liquidus to about 300° and accurate to within 5° with respect to temperatures. The system LiF–ThF_4 contains four compounds; one melts congruently; none undergo inversion or decomposition on cooling within the temperature limits of this study. The system NaF–ThF_4 contains six compounds; two melt congruently, and two have lower temperature limits of stability. Polymorphic forms of two compounds are not equilibrium phases in this system. The complexity of phase relations undoubtedly is related to the lack of predominantly preferred configurations in a lattice involving cations with such a large disparity in charge. In other words, an unusually large number of different lattice arrangements seem to be about equally stable, depending on the composition and temperature range. This effect along with the occurrence of the compounds of the unusual 7:6 mole ratio is probably associated with the absence of stable discrete complex ions, such as ThF_5^-, as structural units.

Acknowledgments.—It is a pleasure to acknowledge the assistance of C. F. Weaver, R. A. Strehlow and T. N. McVay, who were responsible for much of the phase identification by optical microscopy, and to V. D. Frechette, who also ably assisted in some of the optical measurements. We are also grateful to L. A. Harris and C. D. White for their efforts and advice concerning many aspects of the crystal structure determinations. In addition, the authors are especially grateful to R. F. Newton, F. F. Blankenship and J. E. Ricci for helpful advice and suggestions concerning many phases of the investigation, and to the United States Atomic Energy Commission for its support of the work.

SALT EFFECTS IN THE RACEMIZATION OF A BIPHENYL HAVING A CATIONIC BARRIER GROUP[1]

BY W. H. GRAHAM[2a] AND J. E. LEFFLER[2b]

Contribution from the Department of Chemistry, Florida State University, Tallahassee, Florida

Received January 2, 1959

The racemization of *d-o*-(2-dimethylaminophenyl)-phenyltrimethylammonium ion is accelerated by added salts. The largest acceleration is a factor of 2.46. The activation enthalpy is in most cases decreased by salts, sometimes by almost 3 kcal./mole. The activation entropy is also decreased, as much as 6 cal./mole degree. The salts fall into two categories: small ions having an isokinetic effect on the activation parameters and producing only a small acceleration, and large ions having a non-isokinetic effect on the activation parameters and producing a larger acceleration. The results are discussed in terms of ion solvation, ion association and the formation of micelles.

The changes which the rates of racemization of the ionic biphenyl (I) undergo in aqueous alcohol as the proportion of alcohol is altered have been interpreted in terms of desolvation accompanying the conversion of the relatively static ground state to the hindered and vibrationally excited transition state.[3]

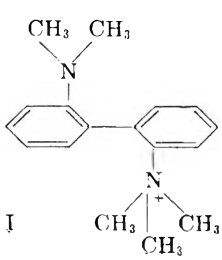

I

The present paper reports the results of an investigation of the effect of added salts on the rates and activation parameters for the racemization of *d-o*-(2-dimethylaminophenyl)-phenyltrimethylammonium *d*-camphor-sulfonate in several solvents. No long range effect due to a change in the macroscopic electrostatic character of the medium is to be expected since the ground and transition states are very much alike from the point of view of remotely situated molecules. However, effects can be expected if there is ion pair or ion aggregate associa-

(1) Presented in part at the Symposium, "Solvent Effects and Reaction Mechanisms," Queen Mary College, London, July, 1957.

(2) (a) Based on the doctoral dissertation of W. H. G.; (b) to whom requests for reprints should be addressed.

(3) J. E. Leffler and W. H. Graham, THIS JOURNAL, **63**, 687 (1959).

TABLE I

THE EFFECT OF SMALL IONS IN WATER

Salt	Concn. (M)[c]	$k \times 10^5$, sec.$^{-1}$[a] $k_{79.4°}$	$k_{100.0°}$	ΔH^*,[b] kcal./mole	ΔS^*,[b] cal./mole deg.
None	...	0.567	4.93	26.71 ± 0.06	−7.11 ± 0.15
NaCl	1.16	.602	4.97	26.08 ± .10	−8.77 ± .27
NaBr	1.85	.616	5.10	26.11 ± .16	−8.63 ± .44
KCl	0.19	.601	5.04	26.29 ± .09	−8.19 ± .24
	1.18	.610	5.09	26.18 ± .13	−8.45 ± .37
LiCl	0.35	.588	5.05	26.57 ± .11	−7.43 ± .29
	0.82	.604	5.04	26.19 ± .15	−8.45 ± .42
	1.18	.605	4.99	26.02 ± .13	−8.94 ± .35
NH_4Cl	1.16	.615	5.10	26.10 ± .11	−8.67 ± .31
$NaOOCCH_3$	1.28	.600	5.08	26.39 ± .10	−7.91 ± .26
$CaCl_2$	1.28	.633	5.05	25.64 ± .05	−9.94 ± .15
$BaCl_2$	0.54	.639	5.10	25.65 ± .07	−9.88 ± .20
$Na_2C_2O_4$	.21	.603	4.90	25.89 ± .15	−9.32 ± .42
Na_2SO_4	.61	.614	4.99	25.86 ± .19	−9.35 ± .53
Alanine	.95	.603	5.10	26.37 ± .10	−7.94 ± .27

[a] Average rate constants, expected error less than 1%. [b] For the significance of the probable errors see ref. 3. The expected error in ΔH^* is 0.10 kcal./mole. [c] The concentration of the biphenyl *d*-camphorsulfonate is 0.02 M in all of these experiments.

tion involving the biphenyl, or if added salts change the structure of the solvent. The solvent structure is important because removal of solvent molecules from the solvation shell of the biphenyl involves return of solvent molecules to the bulk solvent.

We were impelled to undertake this investigation by two earlier observations which suggested that the salt effects actually exist. The first of these is the report by Rieger and Westheimer[4] of a small ionic strength effect in the racemization of the sodium salt of a diphenic acid; the second is our own observation that the first-order rate constant for the racemization of *d*-*o*-(2-dimethylaminophenyl)-phenyltrimethylammonium ion is concentration dependent.[3]

Discussion of Results

The Effect of Small Ions in Water.—Inorganic salts and organic salts in which the ions are small accelerate the racemization of *d*-*o*-(2-dimethylaminophenyl)-phenyltrimethylammonium ion only to a very small extent. The activation enthalpies and entropies appear to be decreased somewhat by such salts and to obey an isokinetic relationship.[5] The rate constants and activation parameters are shown in Table I and the isokinetic relationship in Fig. 1.

Since these effects are all accelerative, they must be due either to association of the ions with the transition state, which is unlikely for small ions in water, or to a solvent–structure effect. At the high temperatures used in these experiments it is unlikely that water retains any ice-like character; hence the ions can be expected to have exclusively an orienting and order-producing effect on the water rather than a disordering effect. As we have proposed earlier[3] it is likely that the promotion of the biphenyl to the transition state is accompanied by release of molecules from solvation shell to the solution in general. Added ions, by binding water which would otherwise be relatively free in the solution, can therefore offset that part of the activation enthalpy and entropy which is due to the necessity of removing water molecules from the solvation shell of the biphenyl.

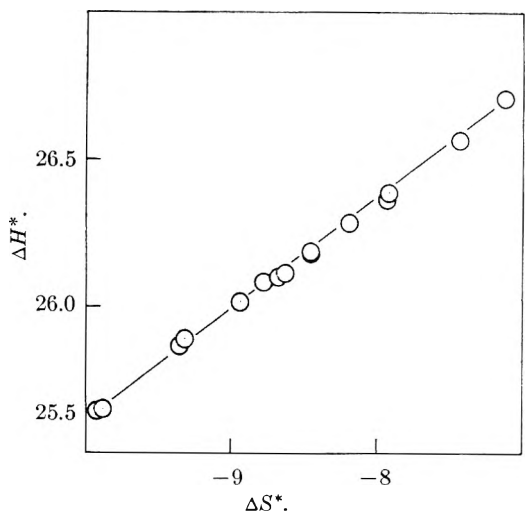

Fig. 1.—The isokinetic relationship of the effects of small ions.

Calcium and barium ions have a larger effect than the univalent ions. The zwitterion alanine has an effect not noticeably different from that of ammonium chloride.

The Effect of Large Organic Ions in Water.—The rate constants and activation parameters for the racemization in aqueous solutions containing large ions are given in Table II. Large ions differ from small ones in their effect in three ways. Firstly, they accelerate the reaction more than small ions do. Secondly, the activation parameters, with the partial exception of those for one salt, fall below the isokinetic line formed by the activation parameters in the presence of small ions. Finally, the acceleration is proportional or nearly proportional to the concentration of the added large ion. The distribution of the activation parameters for

(4) M. Rieger and F. H. Westheimer, *J. Am. Chem. Soc.*, **72**, 19 (1950).

(5) (a) Although the fit to a linear relationship between the enthalpy and entropy is excellent, it may nevertheless not be significant in the present case in view of the small magnitude of the changes in enthalpy and entropy; (b) J. E. Leffler, *J. Org. Chem.*, **20**, 1202 (1955).

TABLE II

THE EFFECT OF LARGE IONS IN WATER

Salt	Concn. (M)[c]	$k \times 10^5$, sec.$^{-1}$[a] $k_{79.4°}$	$k_{100.0°}$	ΔH^*,[b] kcal./mole	ΔS^*,[b] cal./mole deg.
None	...	0.567	4.93	26.71 ± 0.06	−7.11 ± 0.15
TMAC[d]	.19	.591	5.04	26.48 ± .08	−7.67 ± .21
	.33	.610	5.09	26.20 ± .05	−8.42 ± .14
	.57	.619	5.20	26.29 ± .06	−8.11 ± .16
	.95	.667	5.66	26.42 ± .08	−7.60 ± .22
	1.50	.704	5.82	26.08 ± .07	−8.45 ± .19
$(C_6H_5)_4PCl$	.06	.676	5.54	25.97 ± .08	−8.85 ± .21
Sodium benzoate	1.22	.774	6.29	25.88 ± .10	−8.85 ± .27
Sodium	.05	.614	5.29	26.63 ± .08	−7.17 ± .21
tosylate	.20	.696	5.69	25.92 ± .05	−8.92 ± .13
	.50	.820	6.47	25.49 ± .11	−9.83 ± .30
	.98	1.02	7.86	25.25 ± .09	−10.09 ± .24
	1.79	1.40	10.04	24.44 ± .11	−11.75 ± .30
PDADMAB[e]	0.126	0.582	5.02	26.63 ± .10	−7.28 ± .28
LTMAC[f]	.17	0.740	5.77	25.37 ± .05	−10.39 ± .14
$NaLSO_4$[g]	.17	1.32	10.01	25.13 ± .15	−9.94 ± .40
NaPSS[h]	.17	1.36	9.37	23.75 ± .16	−13.78 ± .44
Substrate	.11	0.714	5.95	26.19 ± .09	−8.11 ± .25

[a] Average rate constants, expected error less than 1%. [b] For the significance of the probable errors, see ref. 3. The expected error in ΔH^* is 0.10 kcal./mole. [c] Except where otherwise noted the concentration of the substrate, *d*-*o*-(2-dimethylaminophenyl)-phenyltrimethylammonium *d*-camphorsulfonate, is 0.02 *N*. [d] Tetramethylammonium chloride. [e] Polydiallyldimethylammonium bromide, concentration based on monomer. [f] Lauryltrimethylammonium chloride. [g] Sodium lauryl sulfate. [h] Sodium polystyrenesulfonate, concentration based on the monomer.

the large ions, in relation to the isokinetic line of the small ones is shown in Fig. 2. Figure 3 shows the linear effect on the rate as the concentration of sodium *p*-toluenesulfonate is changed at 80°.

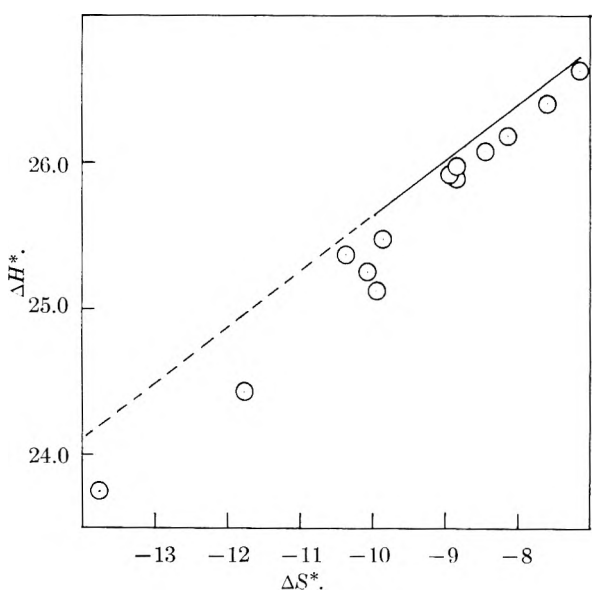

Fig. 2.—Salt effects of large ions. The solid line is that of Fig. 1. The points for low concentrations of tetramethylammonium chloride, and the point for polydimethyldiallylammonium bromide, which fall on the solid line, are not shown.

The accelerative effect might be due to binding of solvent molecules by the large ions, but this seems unlikely. The acceleration is *greater* rather than *less* for the larger ions. Furthermore, the acceleration does not show the saturation effect noted in the case of the small ions but continues to increase with increasing concentration of the added salt.

We therefore prefer to assume that large ions form ion pairs (and in some cases higher aggregates, such as micelles), some of the biphenyl molecules being partners in the ion pairs or components of the higher aggregates. Ion-pair formation between large ions

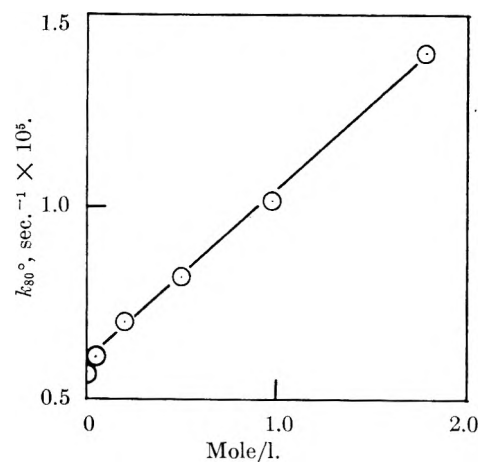

Fig. 3.—The effect of added sodium *p*-toluenesulfonate.

can be expected to be quite extensive even in water. For example, the ion-pair formation constant for tetrapropylammonium lauryl sulfate is estimated to be about 21 L/M on the basis of conductivity experiments.[6] Acceleration by ion-pair formation is understandable if the association between large organic ions is less intimate and less stereospecific than the association of the trimethylammonium group of the biphenyl with a small molecule such as water. The extrusion of water molecules from the solvation sphere in the transition state should increase the interaction of the two ions. Hence the ion pair should suffer less destabilization because of the desolvation than does an isolated ion of the biphenyl.

(6) P. Mukerjee and K. J. Mysels, THIS JOURNAL, **62**, 1400 (1958).

TABLE III

SALT EFFECTS IN AQUEOUS-ORGANIC MIXTURES

Solvent	Added salt	Concn.,[c] mole/l.	k, sec.$^{-1}$ × 10^5[a] $k_{79.4^0}$	$k_{100.0^0}$	ΔH^{*},[b] kcal./mole	ΔS^{*},[b] cal./mole deg.
63.5 wt. % ethanol	None	...	1.22	9.28	25.07 ± 0.06	−10.24 ± 0.18
	KCl	0.37	1.30	9.70	24.81 ± .06	−10.86 ± .16
	Sodium tosylate	.09	1.26	9.51	24.95 ± .08	−10.52 ± .23
	Sodium tosylate	.18	1.30	9.85	25.07 ± .06	−10.13 ± .18
	Sodium tosylate	.60	1.38	10.11	24.62 ± .06	−11.27 ± .15
48.7 wt. % ethanol	None	...	1.16	8.92	24.91 ± .07	−10.80 ± .20
	Sodium tosylate	.18	1.22	9.15	24.92 ± .06	−10.66 ± .16
	Sodium tosylate	.68	1.33	9.70	24.56 ± .12	−11.53 ± .32
50 wt. % dioxane	None	...	1.37	9.57	23.92 ± .09	−13.26 ± .24
	NaCl	1.17	1.54	11.01	24.23 ± .04	−12.14 ± .11
	Sodium tosylate	1.02	1.58	11.33	24.30 ± .09	−11.91 ± .26
	TMAC[d]	1.06	1.51	11.17	24.66 ± .12	−10.97 ± .34

[a] Average rate constants. [b] For the significance of the probable errors, see ref. 3. [c] The concentration of the biphenyl *d*-camphorsulfonate is 0.02 *M*. [d] Tetramethylammonium chloride.

Although the effect of large anions is greater than that of large cations, the latter can still exert an effect which is large compared to that of small ions. For example, tetraphenylphosphonium chloride accelerates the reaction at 80° by 19% when present in a concentration of only 0.06 *N*. On the other hand, lauryltrimethylammonium chloride, at 0.17 *N*, accelerates the reaction by 31%, considerably less than the 131% acceleration produced by sodium lauryl sulfate at the same concentration. The polymer sodium polystyrenesulfonate, at 0.17 *N* based on monomer, accelerates the reaction by 138%. It is likely that the association of large ions, especially those capable of forming micelles, is only partly dependent on the charge.[6]

The enthalpy–entropy relationship for varying concentrations of tetramethylammonium chloride is like an inverted letter N. One leg of the N, corresponding to low concentrations of the salt, coincides with the isokinetic line for the effects of small ions. Tetramethylammonium chloride apparently acts like the small ions at low concentration but acts like the large (associating) ions at high concentrations. At high concentrations the acceleration is greater and the activation parameters depart from the isokinetic line. Another salt which behaves like a non-associating ion is polydiallydimethylammonium bromide. Solubility limited the concentration of this polymer to about 0.12 *N*, based on monomer; the acceleration was about 2% at 80°. In respect to the size of the hydrocarbon chains attached to each quaternary ammonium center this polymer resembles tetramethylammonium chloride more than it does lauryltrimethylammonium chloride, and its behavior is thus consistent with its structure.

Salt Effects in Aqueous Organic Mixtures.—The racemization in a series of ethanol–water mixtures gives activation parameters which have a V-shaped relationship.[3] As the concentration of alcohol is increased the activation enthalpy and entropy first drop and then, after passing through a broad minimum in the range 44–76% ethanol, rise again to the value characteristic of pure alcohol. Preferential solvation of a salt added to an alcohol–water mixture of minimum activation enthalpy and entropy should cause the point representing the enthalpy and entropy to retreat either along the water-rich branch or the alcohol-rich branch of the curve, depending on the relative affinity of the salt for the two solvent components. As can be seen from Table III, the addition of salts to 48.7% alcohol or to 63.5% alcohol fulfilled neither of these expectations. Instead of rising along either branch, the points for the salt solution are found along a line slightly below that of the ethanol-rich part of the solvent curve. In the more concentrated salt solutions, for which the differences in enthalpy and entropy are more likely to be real, the enthalpies and entropies of activation are lower than those for the pure ethanol–water mixtures. We presume from this that the mechanism of the salt effect in aqueous alcohol is non-selective and similar to that in pure water.

The effect of salts in aqueous dioxane (Table III) is rather different. The full line in Fig. 4 represents

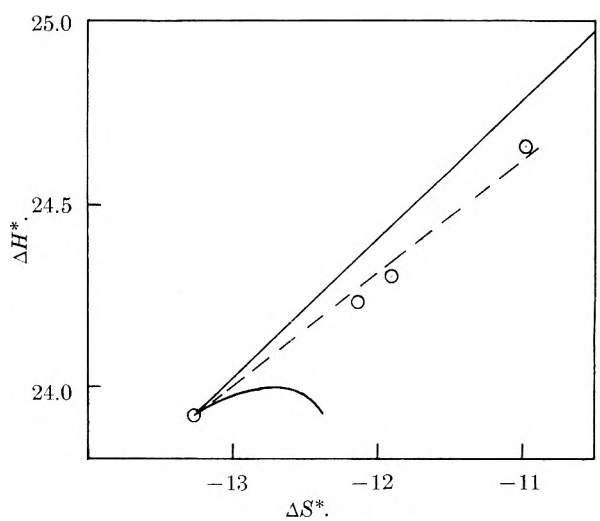

Fig. 4.—The solid line[3] is for the system dioxane–water. The circles show the effect of adding salts to 50 wt. % dioxane. From bottom to top: no salt, 1.17 *N* NaCl, 1.02 *N* sodium tosylate, 1.06 *N* tetramethylammonium chloride.

(7) It has been shown recently that the reactions of triarylmethane derivatives with water and hydroxide ion are markedly affected by the presence of micelles. Large cations decelerate the reaction of anionic triarylmethanes, while large anions have no effect. Large anions decelerate the reactions of cationic triarylmethanes, while large cations accelerate. On the basis of these results it may be inferred that large organic ions interact with micelles probably by incorporation into the micelles, even when the large ions of the substrate and the large ions of the micelle are of the same charge type. Private communication from E. F. J. Duynstee and E. Grunwald.

TABLE IV

SALT EFFECTS IN ACETIC ACID

Salt	Concn., mole/l.	k, sec.$^{-1}$ × 10^{5}[a] $k_{79.4°}$	$k_{100.0°}$	ΔH^{*},[b] kcal./mole	ΔS^{*},[b] cal./mole deg.
Substrate only	0.02	1.08	8.56	25.47 ± 0.01	− 9.34 ± 0.02
Substrate only	.04	1.05	7.91	24.90 ± .04	−11.03 ± .11
Sodium tosylate (0.04 *M* substrate)	.18	0.769	6.51	26.41 ± .14	− 7.36 ± .39

[a] Average rate constants. [b] For the significance of the probable errors, see ref. 3.

the effect of increasing the dioxane content of the dioxane–water mixtures. The point at which the curve doubles back upon itself represents 50.9 wt. % of dioxane, and this is approximately the solvent which we have used in our salt effect experiments. The branch of the curve representing solvents rich in the organic component is not a straight line in the case of the dioxane–water system. It is therefore quite different from any of the alcohol–water systems; the difference may be due to the fact that the points in the latter part of the curve are for solutions very near the solubility limit of the biphenyl. We mention this because salts added to 50% dioxane *raise* rather than *lower* the activation enthalpy and entropy.

Although the corresponding points do not fall on the dioxane-rich leg of the curve, they fall on a line resembling the alcohol-rich legs of the curves for the various alcohol–water systems. It may be that these salts exert their effect partly by preferential hydration in 50% dioxane–water, accelerating the reaction by increasing the effective dioxane concentration of the medium.

Salt Effects in Acetic Acid.—Sodium tosylate added to glacial acetic acid decelerates the racemization. Since the deceleration is accompanied by a marked increase in activation enthalpy and a marked decrease in specific rotation, we assume that the effect is due to increased protonation of the biphenyl, just as in the case of added water.[3] The data are presented in Table IV.

Diastereoisomeric Ion Aggregates.—The slight drift in the first-order rate constant for the racemization which is observed in certain hydroxylic solvents has been interpreted as due to aggregation of the biphenyl ions in solution and to change in the diastereoisomeric composition of the aggregates as the reaction proceeds.[3] Association of the biphenyl with *d*-camphorsulfonate ion, on the other hand, does not appear to be sufficiently intimate to show a stereospecific effect. We had already reached this conclusion on the basis that conversion of the ground state to the geometrically different transition state does not interfere with the association with large anions. We now find that the racemization rates are nearly the same for *d*-*o*-(2-dimethylaminophenyl) - phenyltrimethylammonium benzenesulfonate and *d*-camphorsulfonate, both in water and in alcohol (Table V). Furthermore, the position of the equilibrium for the *d*-camphor sulfonate is the same in chloroform, in which association of the cation with the anion is expected, as it is in dilute aqueous solution where the ions are free. We therefore conclude that the diastereoisomeric *o*-(2-dimethylaminophenyl)-phenyltrimethylammonium *d*-camphorsulfonate ion pairs racemize at equal rates.[8] An attempt to extend this experiment to include *d*-tartrate failed because the biphenyl methylates this ion in chloroform.

Experimental

For the preparation of the biphenyl, the rate measurements and the treatment of the data, see the previous paper of this series.[3] The added salts were of analytical reagent grade or had been recrystallized several times from various solvents and dried thoroughly. Tetraphenylphosphonium chloride, assaying 99.8%, was supplied by Mr. E. Duynstee. Polydiallyldimethylammonium bromide was furnished by Dr. G. B. Butler, University of Florida, Gainesville. The polymer was purified by grinding to a powder, covering with acetone for several hours, and heating to constant weight *in vacuo* at 85°. The average molecular weight is reported to be about 12,000. Sodium polystyrenesulfonate was furnished by the Monsanto Co.

The Diastereoisomeric Ion-pair Experiments.—A chloroform solution of *d*-*o*-(2-dimethylaminophenyl)-phenyltrimethylammonium *d*-camphorsulfonate was heated to equilibrium, the chloroform removed by evaporation, and the salt dissolved in water. The rotation of the aqueous salt solution was unchanged after heating to ensure equilibrium. The composition of the equilibrium mixture is therefore the same in both solvents. A similar experiment using the *d*-tartrate in chloroform and ethanol resulted in demethylation of the *o*-(2-dimethylaminophenyl)-phenyltrimethylammonium ion.

TABLE V

SUBSTRATE ANION EFFECT

Anion[c]	Solvent	k × 10^{-5}, sec.$^{-1}$[a] $k_{79.4°}$	$k_{100.0°}$	ΔH^{*},[b] kcal./mole	ΔS^{*},[b] cal./mole deg.
d-Camphorsulfonate	H_2O	0.567	4.93	26.71 ± 0.06	−7.11 ± 0.15
d-Camphorsulfonate	EtOH	1.18	9.50	25.70 ± .08	−8.51 ± .22
Benzenesulfonate	H_2O	0.565	4.92	26.74 ± .05	−7.03 ± .13
Benzenesulfonate	EtOH	1.20	9.41	25.44 ± .02	−9.20 ± .23

[a] Average rate constants. [b] For the significance of the probable errors, see ref. 3. [c] Concn. 0.02 *N*.

Acknowledgments.—This investigation was supported in part by the Office of Ordnance Research, U. S. Army. W.H.G. held a National Science Foundation Predoctoral Fellowship, 1957–1958.

(8) Some racemic rotamers have been converted into a predominance of one of the active forms by interaction with ions of opposite charge in chloroform. See the excellent review by E. E. Turner and M. M. Harris, *Quart. Rev.*, **1**, 299 (1947).

THE CRYSTAL AND MOLECULAR STRUCTURE OF TRIAMMINOCHROMIUM TETROXIDE[1]

BY E. H. MCLAREN[2] AND LINDSAY HELMHOLZ

Contribution from the Department of Chemistry, Washington University, St. Louis, Mo.

Received January 19, 1959

A determination of the structure of crystalline triamminochromium tetroxide has shown it to be composed of discrete monomeric molecules which may crystallize in more than one form. A monoclinic form was investigated and found to belong in space group C_{2h}^5–$P2_1/c$. The molecular unit is described in terms of a *deformed pentagonal bipyramid* complex with two superoxide ions and three ammino groups surrounding a central chromium atom, which is in the plus two oxidation state. Average intramolecular bond lengths found were 1.31 Å. for the oxygen to oxygen bond in the superoxide ion, 1.91 Å. for the chromium to oxygen bond and 2.01 Å. for the chromium to nitrogen bond. Conditions highly favorable for the formation of hydrogen bonds within the crystal are responsible for its stability.

Introduction

Compounds obtained by the action of peroxides on chromates are but little understood. Triamminochromium tetroxide, $(NH_3)_3CrO_4$, is one of the more stable of these compounds, as well as one of the more interesting because of the unusual apparent coördination of chromium.

Since this compound was discovered in 1897,[3] a number of workers have attempted to elucidate its molecular structure. Weide[4] assigned the crystalline material to the rhombic pyramidal system on the basis of optical examination. That nitrogen is present as ammino groups was indicated not only by the elementary analyses[3,5] but also by the fact that these groups could be replaced by other neutral molecules such as potassium cyanide.[4,6,7] A cryoscopic molecular weight determination indicated a monomer,[6] and the specific magnetic susceptibility was found to be 2.93 Bohr magnetons,[8] equivalent to two unpaired electrons per formula weight. Recent measurements have found an overall reducing capacity of three equivalents per formula weight for the substance.[9]

Several possible structures have been proposed for the molecule on the basis of this evidence (see, for example, references 8, 9 and 10). None of them seemed conclusive, however, and thus this X-ray investigation was undertaken.

Experimental

Preparation and Properties of Triamminochromium Tetroxide.—Crystals of $(NH_3)_3CrO_4$ were prepared by precipitation at 5° from aqueous 10% ammonia solution which had been saturated with ammonium chromate. Cooled 10% hydrogen peroxide solution was added slowly until the first appearance of bubbles, after which the solution was allowed to sit overnight at 5°. If no crystals had appeared then, the peroxide addition was repeated. A period of days to several weeks was necessary to grow crystals of about a millimeter in length. Growth of crystals amenable to X-ray examination proved difficult, as specimens were in general either too small or intergrown multiple twins.

The physical and chemical properties of these crystals have been described by previous investigators.[3-9,11] They are dark needle-like prisms of metallic luster, exhibiting rhombic pyramidal morphology. Examined under the polarizing microscope, the crystals were found to be highly birefringent and dichroic, appearing pale yellow in transmitted light polarized parallel to the needle axis and reddish brown in that polarized perpendicularly. The refractive indices range from 1.60 along the needle axis to greater than 1.71 in a direction perpendicular to this axis. The crystals are very brittle and exhibit excellent cleavage parallel to the long axis. Their density is 1.96 g. cm.$^{-3}$. If kept cool and dry, they are stable for many weeks, but decompose slowly at high room temperature or in the presence of moisture. At higher temperatures or on contact with concentrated sulfuric acid they decompose rapidly, after the fashion of ammonium dichromate. They appear very slightly soluble in water, with partial decomposition, but in no other neutral solvent. The compound decomposes to chromic complexes in aqueous acid and to chromate ion in alkaline solutions, with the evolution of oxygen in either case.

Selection of the Specimen.—Most (greater than 99%) of the crystals could be rejected by optical examination as being multiply twinned, often in a laminar manner parallel to the needle axis. Those which optically appeared to be single crystals were tested for twinning with Laue photographs. Only three specimens suitable for X-ray investigation were discovered among hundreds examined by this procedure.

X-Ray Methods.—Both Laue and oscillation photographs of the crystals were taken. Weissenberg equipment was utilized to obtain equatorial and layer photographs by use of the equi-inclination technique, with each of the crystallographic axes as an oscillation axis.

Crystal Constants and Symmetry.—The first two crystals exhibited orthorhombic Laue symmetry with axial lengths of 22.77, 7.63 and 9.75 Å., giving a unit cell containing twelve formula weights of $(NH_3)_3CrO_4$ (11.97 calculated). Systematic absences of $h0l$ with $h \neq 2n$ and $0kl$ with $k \neq 2n$ were observed. Taking into account the observed polar nature of the crystal, assignment was made to space group C^9_{2v}–$Pna2_1$.

A third crystal differed in that it was found to have a two fold axis as the only Laue symmetry element. The axial lengths and monoclinic angle were measured on Weissenberg photographs and found to be $a_0 = 15.21$, $b_0 = 7.69$, $c_0 = 9.77$ Å. and $\beta = 97.4°$. This yields a cell two-thirds the size of the orthorhombic cell, containing eight (7.99 calculated) units of $(NH_3)_3CrO_4$. Systematically absent reflections of type $h0l$ with $l \neq 2n$ and $0k0$ with $k \neq 2n$ indicated assignment to space group C^5_{2h}–$P2_1/c$.

Interpretation of the Photographs.—In this investigation the molecular configuration was of greater interest than the possible crystal forms, and therefore the advantages inherent in working with a center of symmetry, combined with the smaller unit cell, led to concentration on the data for the monoclinic crystal.

The relative intensities of the Weissenberg reflections were obtained by visual comparison with timed exposures, using

(1) From the dissertation submitted by Eugene McLaren to the Graduate Board of Washington University in partial fulfillment of the requirements for the degree of Doctor of Philosophy.

(2) Pan American Petroleum Corp. Research Center, P. O. Box 591, Tulsa, Okla.

(3) O. F. Weide, *Ber.*, **30**, 2178 (1897).

(4) O. F. Weide, *ibid.*, **32**, 378 (1899).

(5) K. A. Hofmann and H. Hiendlmaier, *ibid.*, **38**, 3059 (1905).

(6) E. H. Riesenfeld, *ibid.*, **41**, 3536 (1908).

(7) K. A. Hofmann, *ibid.*, **39**, 3181 (1906).

(8) S. S. Bhatnagar, B. Prakash and A. Hamid, *J. Chem. Soc.*, 1428 (1938).

(9) D. F. Evans, *ibid.*, 4013 (1957).

(10) D. M. Yost and H. Russell, Jr., "Systematic Inorganic Chemistry," Prentice-Hall, Inc., New York, N. Y., 1944, p. 371.

(11) E. H. Riesenfeld, W. A. Kutsch and H. Ohl, *Ber.*, **38**, 4072 (1905).

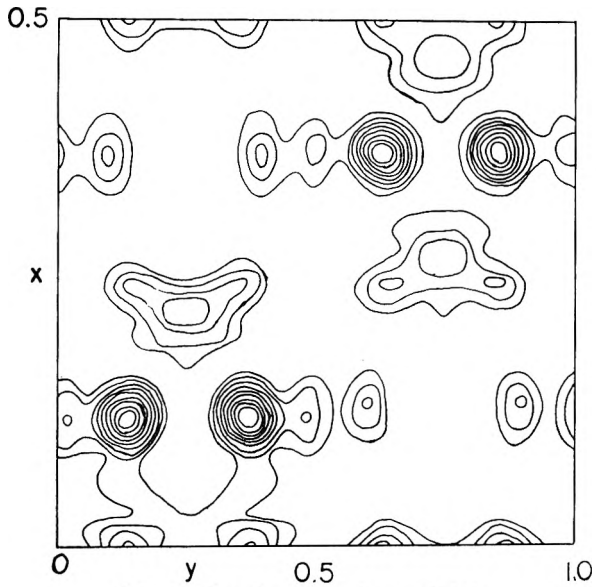

Fig. 1.—Fourier projection on (001).

multiple films to reduce by known factors the intensities of the strongest reflections. These were corrected for the Lorentz and polarization factors and, in the case of the layer reflections, for the time factor as given by Tunell.[12] Reflections obtained by oscillation around the needle axis were considerably smaller in area than those obtained by oscillation around the other two axes. Reduction to a common intensity scale was accomplished by normalization of intensities of equivalent reflections obtained from the crystal in different orientations. Average values of the extended and contracted reflections on opposite sides of the upper level photographs were used. Because of the very small size of the crystal (0.28 by 0.03 by 0.01 mm.), absorption and extinction effects were not considered.

Determination of Parameters

Derivation of *x*-*y* Parameters.—Patterson projections along all three axes were made. The projection on (001) showed immediately that two sets of fourfold general positions must be occupied, since there was no large Patterson peak equivalent to any of the special positions of $P2_1/c$. Two peaks appearing near $x = {}^1/_4$, $y = {}^1/_2$ and $x = {}^1/_2$, $y = 0$ were of magnitude comparable to that of the origin, and therefore corresponded to Cr–Cr separations. The next largest Patterson peaks were at $x = 0$, $y = {}^1/_4$; $x = {}^1/_4$, $y = {}^1/_4$; and $x = {}^1/_2$, $y = {}^1/_4$; all of these were about half as high as the first and were interpreted as representing half as many Cr–Cr vectors. Trial soon showed that these criteria placed non-equivalent chromium atoms unambiguously near $x = {}^1/_8$, $y = {}^1/_8$ and $x = {}^3/_8$, $y = {}^5/_8$.

Quantitative consideration of the size and shape of the smaller Patterson peaks indicated that there were light atoms (O or N) displaced by about $x = \pm {}^1/_8$, $y = 0$ from each Cr, with two light atoms, slightly separated in this projection, in each position. Assignment to two additional atoms of parameter values near $\pm(0, {}^1/_4)$ from each chromium atom also was suggested.

On the basis of these assignments structure factor signs were calculated for this zone. Agreement between observed and calculated intensities was good, and signs for nearly all of the stronger reflections could be assigned unambiguously. A series of two dimensional Fourier projections, with successive inclusion of weaker structure factors, led to a projection which placed the seventh light atom at about $x = {}^1/_8$, $y = 0$. This projection did not use any of the uniformly weak reflections of form $hk0$ with $h \neq 2n$. A false center of symmetry is thus introduced into the projection at $({}^1/_4, {}^1/_2)$. This converts one set of equivalent positions into the other and leads to a unit cell one-half the observed size. The false symmetry was destroyed by arbitrarily introducing the strongest reflection of this type (330) with a negative sign. Signs for the remaining structure factors could then be determined by use of further Fourier syntheses, the final one of which is shown in Fig. 1.

Derivation of *z* Parameters.—Patterson projections on (100) and (010) were very diffuse, both because of the lack of observed reflections with large l values and the large number of overlapping atoms. The absence of peaks other than at $z = 0$ and $z = {}^1/_2$ did show, considering symmetry requirements, that each of the non-equivalent chromium atoms must be located near either $z = 0$ or $z = {}^1/_4$. Also, the displacement from $z = {}^1/_2$ of a peak at $x = {}^1/_2$, $z = 0.47$ suggested a slight displacement of the Cr atoms from halves or quarters along the z-axis.

The chromium atoms shown in Fig. 1 have approximately the same environment, in which each has four near neighbors at a distance of about 2 Å.; these are at $\pm({}^1/_8, 0)$ and $\pm(0, {}^1/_4)$ from the chromium atom. These atoms must be bonded to the chromium nearest to them in the structure. If they were to be shared between chromium atoms they would give rise to a Patterson peak with a z-parameter value equal to ${}^1/_4$, in contradiction to the projections on (100) and (010). Slight movement from $z = {}^1/_4$ produces neither a satisfactory bonding and a non-bonding contact nor agreement with these projections.

The complex maxima in Fig. 1 at $x = 0$ and $x = {}^1/_4$ are due to superimposed light atoms. The same arguments used in the previous paragraph indicate that separation of these atoms in the z-direction must be either 0 ± 0.125 or ${}^1/_2 \pm 0.125$. Either case leads to the presence of pairs of light atoms. The identification of these complex maxima with two superimposed peroxide type groups seemed reasonable in view of the known peroxide ion content of K_3CrO_8,[13] formed under somewhat similar conditions. The other light atoms would then be the nitrogen atoms of the ammino groups.

Chromium z-parameters equal to zero led to unacceptable atomic separations; therefore the choice of z equal to about ${}^1/_4$ was made. The two oxygens and two nitrogens farthest from each Cr (but in the group associated with it) in the projection on (001) were assumed to have nearly the same z parameter as the Cr, while the other two oxygens of the group were displaced far enough in the z-direction to bring them to a distance of about 1.5 Å. from the first oxygen atoms, a reasonable peroxide ion distance.[14] The third nitrogen was displaced in the z-direction sufficiently to give it a Cr to N distance about equal to the other two, near 1.9 Å. The problem of the di-

(12) G. Tunell, *Amer. Min.*, **24**, 448 (1939).

(13) I. A. Wilson, *Arkiv Kemi, Min., Geol.*, **B15**, No. 5, 7 (1941).

(14) S. C. Abrahams and J. Kalnajs, *Acta Cryst.*, **7**, 838 (1954).

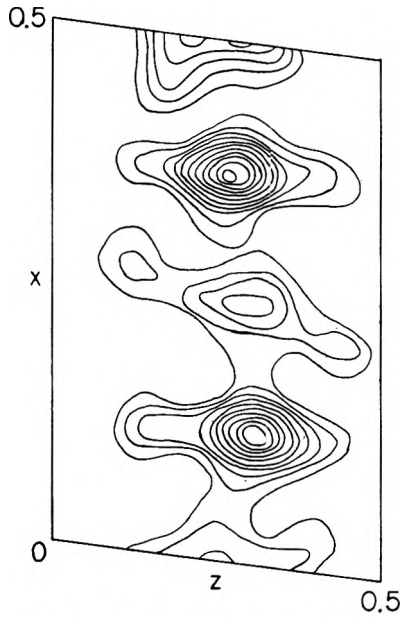

Fig. 2.—Fourier projection on (010).

rection in which these displacements should be made was solved by trial and error; for this the orders of intensities of several pairs of $h0l$ and $h0\bar{l}$ were especially useful criteria. The orientation of the peroxide type groups is indicated clearly in the Fourier projection on (010), Fig. 2. The third nitrogen was placed in each case on the side of the chromium opposite that of these oxygen atoms.

Calculation of the structure factors of type $h0l$ and $0kl$, using parameters based on the above reasoning, gave results which left no doubt as to the general correctness of this model, when compared with observed values. The final of several successive Fourier projections used for parameter refinement on (010) and (100) are shown in Figs. 2 and 3.

During this refinement process, a significant shortening of the O–O bonds, to about 1.4 Å., became apparent. Although the electron density maps were too diffuse to determine the oxygen positions precisely, they did indicate that still shorter O–O distances were required to obtain better agreement between the observed and calculated structure factors.

Final Parameter Refinement.—It was observed that for $(NH_3)_3CrO_4$ an anisotropic temperature factor was necessary, as indicated by the exceptionally rapid falling off of intensities for those planes whose normals have a large z component. Therefore a factor of the form

$$T_f = e^{-\beta(\sin^2\theta/\lambda^2)}\, e^{-\beta(B-1)(l_i/c)^2}$$

was introduced, where l_i is the Miller index, along the z-axis of length c, of the plane giving rise to the reflection. Plots of the appropriate functions of the observed and calculated structure factors yielded a value of 2.2 Å.^{2} for β and 1.3 for B. The final step in the parameter refinement was the making of Fourier syntheses on (010) and (100) using temperature corrected $(F_{obsd} - F_{calcd})$ values as coefficients. In the case of the projection along the z-axis only small and apparently random movements were indicated. For the projection on (010), however, a shortening of

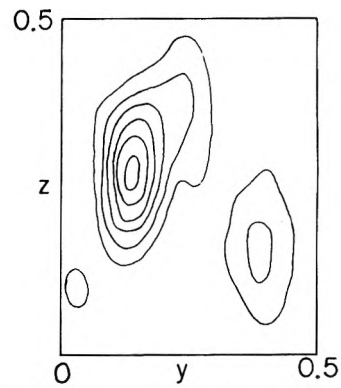

Fig. 3.—Fourier projection on (100).

the O–O distances was consistently indicated. This was done, with a resultant improvement in the agreement between observed and calculated structure factors. Final parameter values derived are listed in Table I. The atoms are numbered in such a manner that oxygens 1-4 and nitrogens 1-3 are in the molecule associated with Cr_I, while oxygens 5-8 and nitrogen atoms 4-6 are in the molecule of Cr_{II}.

TABLE I

ATOMIC PARAMETERS

Atom	x	y	z
Cr_I	0.125	0.135	0.225
Cr_{II}	.375	.633	.189
O_1	.998	.142	.209
O_2	.037	.223	.321
O_3	.259	.145	.254
O_4	.230	.220	.360
O_5	.252	.648	.164
O_6	.283	.727	.062
O_7	.498	.604	.236
O_8	.492	.690	.123
N_1	.130	.869	.307
N_2	.118	.349	.118
N_3	.120	.002	.051
N_4	.369	.396	.112
N_5	.381	.886	.248
N_6	.380	.515	.367

Observed and calculated structure factors are listed in Table II.[15] The over-all reliability index, $\Sigma||F_o| - |F_c||/\Sigma|F_o|$, is 0.20; it is 0.17 for those reflections not containing an l component, and 0.22 for those which do.

In Table III is listed a compilation of interatomic

TABLE III

INTERATOMIC DISTANCES

Atoms	Separation, Å.	Atoms	Separation, Å.	Atoms	Separation, Å.
Cr_I–O_1	1.93	Cr_I–N_3	1.98	Cr_{II}–N_5	2.03
Cr_I–O_2	1.86	Cr_{II}–O_5	1.87	Cr_{II}–N_6	1.96
Cr_I–O_3	2.02	Cr_{II}–O_6	1.89	O_1–O_2	1.33
Cr_I–O_4	2.04	Cr_{II}–O_7	1.88	O_3–O_4	1.31
Cr_I–N_1	2.20	Cr_{II}–O_8	2.02	O_5–O_6	1.31
Cr_I–N_2	1.95	Cr_{II}–N_4	1.97	O_7–O_8	1.28

(15) Table II has been deposited as Document Number 5863 with the ADI Auxiliary Publications Project, Photoduplication Service, Library of Congress, Washington 25, D. C. A copy may be had by remitting $1.25 for photoprints or for 35 mm. microfilm by check or money order payable to Chief, Photoduplication Service.

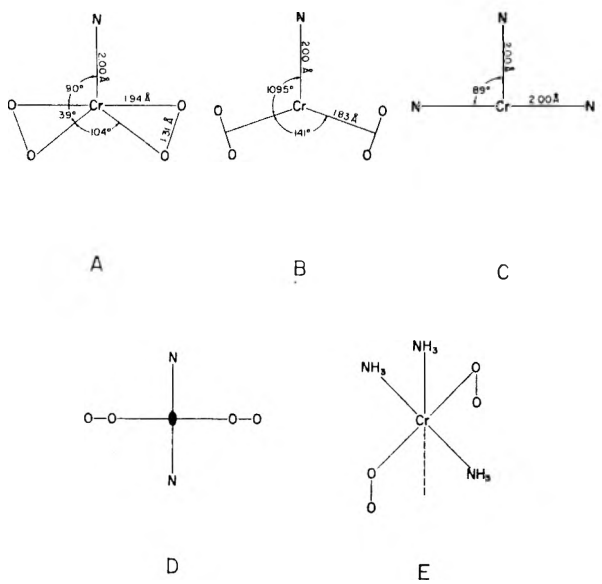

Fig. 4.—Molecular configuration of $(NH)_{33}CrO_4$: A, section in CrNOOOO mirror plane illustrating distorted pentagonal bipyramidal symmetry; B, section in CrNOOOO mirror plane illustrating quasi-trigonal bipyramidal symmetry; C, section in CrNNN mirror plane; D, plane along the twofold axis; E, perspective drawing of the molecule.

distances, and in Table IV are the results of bond angle calculations for atoms within a molecular unit.

Reliability of Results.—The estimation of limits of error to be attributed to the quantities determined in an X-ray investigation is difficult without laborious calculations. From calculations of the variation of individual parameters which lead to marked disagreement between observed and calculated intensities, however, with considerably greater weight given to the comparisons which involve little extinction or absorption, it is estimated that the Cr to light atom distances are probably reliable to ±0.05 Å., and the light atom to light atom distances reliable to ±0.08 Å. While real differences probably occur in the chromium to light atom distances in the crystal due to different environments, the discrepancies are probably not as large as some reported. The uncertainties reported are to be applied to the average distances and take into account the differences between the same pairs of atoms in different environments. The intramolecular bond angles are estimated to be reliable to ±8 degrees.

Table IV

Bond Angles in Degrees

Bonds	Angle	Bonds	Angle
O_1–Cr_I–O_2	41.0	O_5–Cr_{II}–O_6	40.6
O_3–Cr_I–O_4	37.6	O_7–Cr_{II}–O_8	38.1
N_1–Cr_I–N_3	80.0	N_4–Cr_{II}–N_6	84.2
N_2–Cr_I–N_3	89.0	N_5–Cr_{II}–N_6	101.0
N_1–Cr_I–N_2	168.7[a]	N_4–Cr_{II}–N_5	174[a]
O_2–Cr_I–O_4	99.6	O_6–Cr_{II}–O_8	108.4
N_1–Cr_I–O_1	92.0	N_4–Cr_{II}–O_5	90.2
N_1–Cr_I–O_2	98.5	N_4–Cr_{II}–O_6	96.2
N_1–Cr_I–O_3	89.8	N_4–Cr_{II}–O_7	89.6
N_1–Cr_I–O_4	94.4	N_4–Cr_{II}–O_8	94.4
N_2–Cr_I–O_1	86.6	N_5–Cr_{II}–O_5	88.8
N_2–Cr_I–O_2	88.3	N_5–Cr_{II}–O_6	79.8
N_2–Cr_I–O_3	91.6	N_5–Cr_{II}–O_7	92.4
N_2–Cr_I–O_4	93.4	N_5–Cr_{II}–O_8	82.6
N_3–Cr_I–O_1	91.7	N_6–Cr_{II}–O_5	93.2
N_3–Cr_I–O_3	94.2	N_6–Cr_{II}–O_7	76.8

[a] This angle is on the side of the chromium opposite to the third nitrogen atom.

Discussion of the Structure

Structure of the Molecule.—Average values for the bond lengths found in crystalline triamminochromium tetroxide are 1.94 Å. for Cr–O, 2.00 Å. for Cr–N (giving the 2.20 Å. value half weight) and 1.31 Å. for O–O. Average bond angles are 88.6° for N–Cr–N, 39.3° for O–Cr–O and 90.2° for N–Cr–O. Use of these averaged values furnishes a model which is probably the best appraisal of the configuration assumed by the free molecule. It gives rise to maximum symmetry for this molecule of C_{2v} −2 mm. These data and the symmetry are illustrated by sections in the mutually perpendicular mirror planes, drawn in Fig. 4A-C, by a plane along the twofold axis in Fig. 4D, and by a perspective drawing of the molecule reproduced in Fig. 4E.

One mirror plane, containing the three nitrogen atoms and the central chromium atom, separates the two pairs of oxygen atoms. The other mirror plane contains the four oxygen atoms as well as one nitrogen atom and the central chromium atom. The resulting configuration may be described as a seven-coördination complex forming a deformed pentagonal bipyramid. It is also possible to describe it in terms of a quasi-trigonal bipyramid, if each oxygen pair is considered a single ligand. This is not preferred because there is no significant experimental difference between any of the Cr–O bond lengths. Both of these descriptions are illustrated in Fig. 4. In either case the CrNOOOO mirror plane forms the pyramid base.

The two pairs of oxygen atoms, on opposite sides of the CrNNN mirror plane, are best interpreted as superoxide ions in view of the known interatomic distance of 1.32 Å. for this ion, as opposed to the 1.49 Å. for the alternative peroxide ion. If the presence of such superoxide ions is assumed, with one odd electron per ion, the chromium must be in the plus two oxidation state, with all its electrons necessarily paired in order to account properly for the paramagnetism of the molecule. The superoxide ion picture of this molecule is consistent with all of the chemical data. Specifically, the conditions of preparation are favorable for the formation of superoxide ion from hydrogen peroxide, and for the reduction of chromium to the plus two oxidation state. While the plus two oxidation state of chromium has been prepared and kept for long periods of time in oxygen-free water, it seems doubtful that the alternative plus four oxidation state would be stable in aqueous solution. The decomposition of superoxide ion into oxygen and water is typical in both acid and base. Recent measurements which have found the reducing capacity of the compound to be three equivalents per mole[9] are consistent with a chromium plus two superoxide.

The chromium to oxygen and chromium to nitrogen bond distances appear to be reasonable when compared with those found in complex compounds of other transition elements. Elements of the first transition group show covalent radii in the neigh-

borhood of 1.2 to 1.3 Å. Assumption of a radius in this range leads to agreement between radius sums and the distances found in this research, within the limits of error of the determination.

Structure of the Crystal.—The arrangement of the triamminochromium tetroxide molecules in the crystal cannot be described in terms of the usual types of atomic packing. Their distribution is rather specified by the necessity of placing the oxygen and nitrogen atoms in position for maximum hydrogen bond formation, essential to the existence of the crystal. This is accomplished by location of all of the chromium and nitrogen atoms in planes parallel to (100) at odd eighths along the x-axis, while all of the oxygen atoms are located in layers of small thickness parallel to and half-way between those containing the chromium and nitrogen atoms. Thus the oxygen atoms are in position to form hydrogen bond bridges between the layers containing the ammino groups. This is illustrated in Fig. 5, where dotted lines indicate hydrogen bonds.

Calculation of all adjacent N–O distances showed that each of the nitrogen atoms is within hydrogen bonding distance (taken as 3.25 Å. or less) of either two or three oxygens, and that each of the oxygen atoms is in position favorable for two hydrogen bonds. The average length of these bonds is 3.05 Å. It is of interest to note that there are about twice as many hydrogen bonds joining molecules in a direction parallel to (001) as there are connecting them in the z-direction. This is consistent with the fact that the intermolecular forces along the z-axis are weak, as shown by the large temperature factor in this direction.

Preliminary results obtained on the orthorhombic form of this compound, described at the beginning of this paper, indicated that the chromium atom arrangement was very closely the same as that found in the monoclinic form, in the directions parallel to (001). The molecules also appeared to have a similar configuration, although somewhat differently

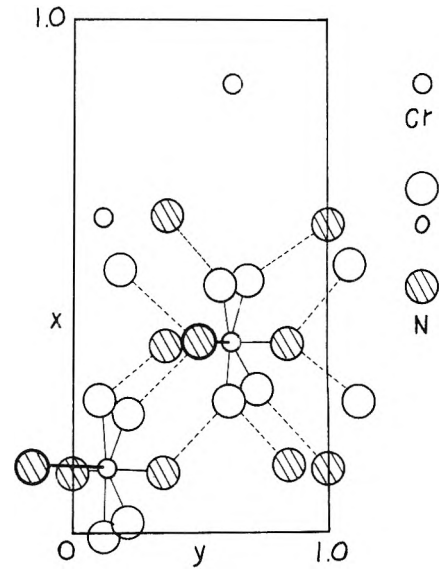

Fig. 5.—Projection of partial contents of unit cell on 001.

oriented with respect to each other. It was concluded after close examination that these were distinct forms involving different hydrogen bond arrangements with a resultant difference in molecular orientation.

It is under just such conditions of hydrogen bonding that polymorphism seems to be particularly common.[16] The lack of elongation in any direction of the $(NH_3)_3CrO_4$ molecule, together with its multiplicity of atoms capable of forming hydrogen bonds, makes it exceptionally suitable for the exhibition of such polymorphism. Many possibilities exist for hydrogen bond rearrangement with only small resultant changes in the total lattice energy. The observed commonness of intergrown and polytwinned crystals is understood in these terms.

(16) A. F. Wells, "Structural Inorganic Chemistry," 2nd Ed., Oxford Press, New York, 1950, p. 153.

THE STRUCTURE AND LUBRICITY OF ADSORBED FATTY FILMS

By Yasukatsu Tamai

Aeronautical Research Institute, University of Tokyo, Tokyo, Japan

Received January 26, 1959

A frictional study has been made on myristic acid and cetyl alcohol adsorbed on steel surfaces by retraction from their solutions and melts. The coefficient of friction was measured in reciprocating sliding at various temperatures up to 200°. It was found that the retraction film from solution was of some mixed-film nature, even when the solvent was non-polar. In the reciprocating friction the lubricity of the film depends largely on its fluidity which relates closely to the ability of repairing the broken part of the film during sliding, and the film gave high friction in solid state while on melting low friction. The premelting of cetyl alcohol also decreased friction to some extent.

Introduction

The nature of adsorbed films on metal is of great importance in the study of lubrication. Since the excellent method of Langmuir was developed, many investigations have been made on the built-up films on metal and considerable information is already given about this sort of films. Recently another method of depositing films on solid surface was introduced by Zisman, *i.e.*, retraction method. Contrary to the artificial character of the built-up method, the new method is natural in the adsorption process so that it seems of merit to work with the retraction film to investigate the nature of adsorbed films. The present work was planned to obtain further information on the structure and

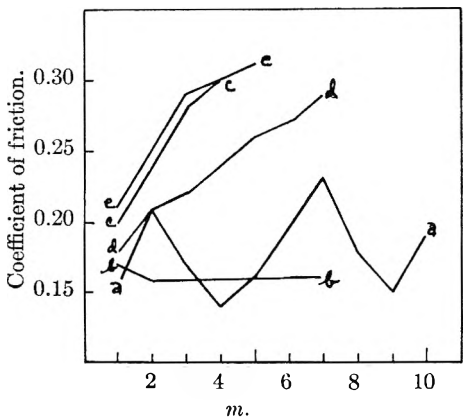

Fig. 1.—Friction at the onset of measurement.

lubricity of the retraction film, about which only a little is known.[1]

In general, friction study gives two different kinds of information; one relates to the mechanism of lubrication and the other to the nature of surface films. Most early fundamental studies were carried out on the friction of unidirectional single traverse and with the built-up film on account of their simplicities. Therefore, on the mechanism of lubrication the ability of lubricant to repair the broken part of adsorbed film during sliding was not discussed so much, which is, in repeated or reciprocating sliding, as important as the ability to protect the metallic surface. On the nature of surface film the strength was accordingly the main problem of interest, for instance, its correlation to the disorientation temperature. But in practice of lubrication, single traverse is a special condition and for this reason a study in repeated or reciprocating sliding also may be made worth while. In this paper both the mechanism of lubrication and the nature of adsorbed film were investigated under the condition of reciprocating sliding with a variety of temperatures.

Experimental

A friction pendulum was used to measure the coefficient of friction, which was reported elsewhere in detail.[2] The essential features are: the friction specimens of steel were arranged in the form of crossed cylinders, the load at each contact was about 100 g., the maximum sliding velocity was 3 mm./sec., and the period of swing was 2 c./s.

The steel specimens were degreased in a boiling mixture of alcohol and KOH (5%). Various fatty films were adsorbed on the specimen by retraction from solution or molten substance, the details of which are described in the following section together with the specified notes on the fatty materials used.

The measuring procedure was composed of inclining the pendulum at an angle of 28° and then setting it free to oscillate until it stopped. The coefficient of friction f was determined from the damping character of the pendulum. In case the damping was not linear, the average value was adopted. Usually the measurement was repeated without any change of friction arrangements. Thus a series of f's were obtained, which settled generally to a steady value with successive measurements. In this paper these steady values are described unless a special reference is given.

Measurements were made in the laboratory atmosphere and at various temperatures which were controlled by electrical heating. The change of f with temperature was not always reversible on cooling. Furthermore, it was observed with some substances that the f-curve is not reproducible but fluctuated to a certain extent in the characteristic range of temperature. In the following figures of friction–temperature curve, the reversible range alone is represented by full line and the others by dotted line. It also was found that all films changed catastrophically at their characteristic temperature of high limit with the result of marked rise of f. This change always was accompanied by a peculiar decrease of f prior to the ultimate increase. In the present paper, however, these phenomena are not discussed, because they are mainly due to a chemical change and not to a structural one. Therefore, the f-curve is terminated just before the beginning of the last decrease.

In some cases, differential thermal analysis was desired to see the correspondence of the change in friction to the phase transition of the film. In this analysis, measurements were made on heating at a relatively slow rate of $^1/_2$ or $^2/_3$° per minute.

Results

(1) **Fatty Acid.**—Five different kinds of adsorbed film of myristic acid were examined, which were made by retraction from (a) saturated solution of benzene at 30°, (b) saturated solution of cetane at 30°, (c) molten pure myristic acid at 70°, (d) molten mixture of acid and cetane (1:1 by vol.) at 70°, (e) molten mixture of acid and cetyl alcohol (1:1 by vol.) at 70°. Benzene and cetane were of highest purity. Myristic acid was refined by vacuum distillation and recrystallization. Cetyl alcohol was commercially pure.

The steel specimen was dipped for three minutes in these media and retracted. Immediately after the retraction, the specimen was rolled on clean filter paper and rubbed with grease-free cotton to wipe off any excess.

Frictional behavior at the onset of measurement was very characteristic of the nature of the film. Figure 1 shows the change of friction on the newly prepared surface with the successive measurements at room temperature, where m and f represent the number of measurement and the coefficient of friction at the transient stage. On examination of Fig. 1, it is seen readily that these f–m curves are divided into two groups. Films from the melt belong to the first group in which f increases monotonously. On the other hand, films from solution belong to the second group, in which f does not increase. However, it is not essential for this grouping whether a film is from the solution or from the melt. Film from benzene solution changed its group from the second to the first after previous heating up to about 40° or higher. It is of special interest that the extrapolation of curves for b,c,d and e suggests that at $m = 0$ f becomes 0.1 for all films. It is also interesting that the curve for acid–alcohol (melt) is quite similar to that for acid(melt) and the curve for acid–cetane(melt) is intermediate between those for acid(melt) and for acid–cetane (solution).

The variation of f with temperature is shown in Fig. 2 for the solution series and in Fig. 3 for the melt series. It is found that the friction of pure acid film is rather high, 0.4, in its solid range, decreases suddenly to the lower value of 0.17 at its melting point, 54°, and then increases gradually and monotonously up to 0.20 at 180° or so. This is in complete disagreement with the earlier findings, that is, friction is low when film is solid and becomes high on melting.

(1) R. L. Cottington, E. G. Shafrin and W. A. Zisman, THIS JOURNAL, **62**, 513 (1958).

(2) Y. Tamai, *Wear*, **1**, 377 (1957/58).

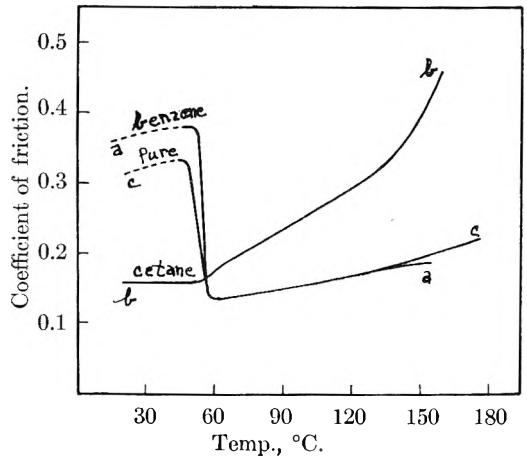

Fig. 2.—Myristic acid (solution series).

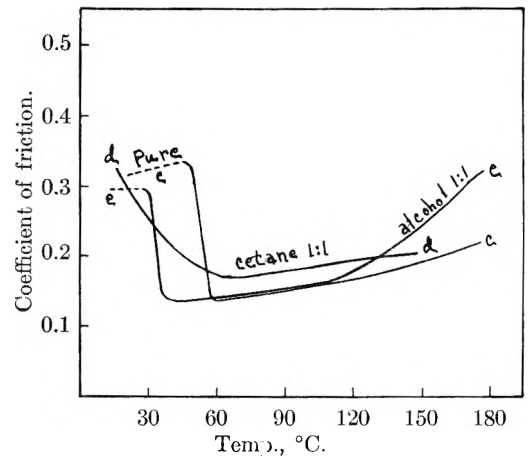

Fig. 3.—Myristic acid (melt series).

The friction of film from benzene solution agrees perfectly with the acid film after preheating. Film from the molten acid–alcohol mixture also behaves quite similarly to that of the acid in the 60 to 120° range, but differs in that the sudden decrease occurs at lower temperature of *ca.* 35°, and the increase above 120° is at a higher rate. But films from medium containing cetane showed, unlike the pure acid film, a lower friction even below the melting point of acid, and above the point, on the contrary, a higher friction than the other films. It might be meaningful that the film from cetane solution, having the lowest friction in the solid range of acid, shows the poorest lubricity at the higher temperatures.

Some consideration has been given to explain the observed phenomena and the following hypothesis was proposed on the mechanism of lubrication. There exist two factors against the breakdown of adsorbed film in reciprocating sliding. One is the film strength, as is already pointed out, and the other is the fluidity of the film which is responsible for repairing the broken part during sliding. Lack of any one factor of the two results in an increase of friction.

Thus the solid film, being unable to repair the disruption, exhibits a larger friction. Curves for c, d and e in Fig. 1 demonstrate the breakdown process. Sharp drop of *f* in curves of a, c and e in Figs. 2 and 3 indicates the appearance of fluidity in films. In fact it occurs at the melting point of acid for curves of a and c.

The film strength is influenced by temperature and by the adhesive and cohesive tendencies of film molecules. After melting, film is agitated thermally which is the primary cause of increase in friction with temperature, as shown with all curves, although the decrease of surface viscosity of film may play some role.

At this stage of the argument it is necessary to discuss the structure of the adsorbed film. From the results obtained it is evident that the film is not always composed of pure myristic acid, and, when deposited from solution, is affected by the other component. Acid–cetane films possess some fluidity, at least in the sense of high mobility on the surface enough to repair the broken part, even in the solid range of acid. This fluid-like property is observed more markedly with the film b than with film d, which suggests that the film may contain a certain amount of cetane, being larger as the cetane-to-acid ratio in medium is larger. These explanations are not contradictory to the fact that after melting the film b shows the highest friction. This probably is due to the large amount of cetane in the film which has no adhering ability.[3]

The film from the acid–alcohol (melt) may also contain a considerable amount of cetyl alcohol, as is properly expected from the character of curve e. It might be suggested further that myristic acid adheres more tenaciously than cetyl alcohol to the steel surface.

(2) **Higher Alcohol.**—Two different kinds of cetyl alcohol were used, that is, (f) alcohol of commercial purity and (g) alcohol of special purity. These alcohols were deposited on the specimen from their melt in the same way as the acid.

The experimental results are shown in Fig. 4,

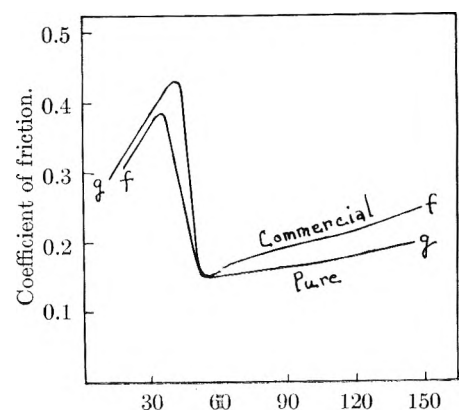

Fig. 4.—Cetyl alcohol.

where both curves of f and g have a distinct maximum and a minimum. The minimum point appears at *ca.* 50° in common, which can be explained as the appearance of fluidity in film (melting point of cetyl alcohol is 49.5°). The most striking feature of alcohol is the existence of the maximum of friction. It was found distinctly at 35 and 43° for commercial and special alcohols, respectively. As

(3) Y. Tamai, *J. Inst. Petrol.*, **44**, 207 (1958).

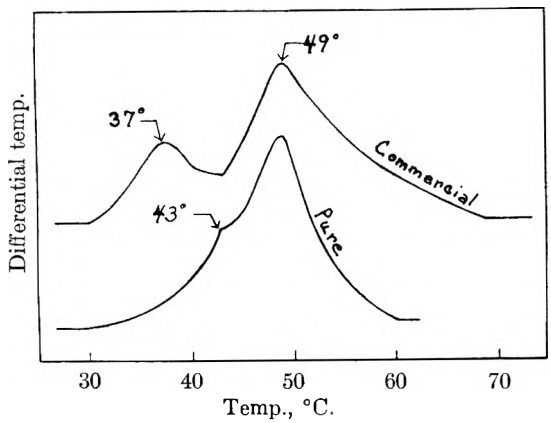

Fig. 5.—Thermogram of cetyl alcohol.

the maximum point is on the reversible range of the friction curve and in the solid range of temperature, it would be reasonable to expect that the maximum point may correspond to some phase change in the film.

To confirm this aspect, differential thermal analyses was made, the results of which are given in Fig. 5. As shown in their thermogram two peaks were observed in every case, that is, for the commercial alcohol at 37 and 49°, and for the alcohol of special purity at 43 and 49°. The peak of 49° represents, of course, melting. The other peak of 37 or 43° is known to indicate the so-called premelting.

Comparing the maximum point of friction with the premelting point, it is clear that they are in fair agreement with each other. This probably means that the adsorbed film gets some fluidity or surface-diffusing ability after premelting.

Another finding in Fig. 4 is that in the liquid range of temperature the friction of commercial alcohol becomes larger than that of the special one as the temperature rises from the melting point. This may suggest that the impurity in the commercial alcohol is of poorer lubricity than cetyl alcohol, if not of no polarity.

Discussion

The first point we must discuss is whether the retraction film is monomolecular or multimolecular. Zisman[4] has reported its monomolecular nature, but Dobry[5] noted to the contrary the multimolecular structure. From the present results it seems to be multimolecular. The rate of increase in friction of solid film with successive measurements suggests a few tens molecular film, as shown in Fig. 1, when compared with Bowden's[6] experiment. However, this cannot be concluded definitely, because in the liquid state the film changes its frictional character reversibly on heating and cooling, which means that the film structure does not vary irreversibly during the experiment and that if the film is multimolecular the adsorption should not be simply physical.

On the film structure it has been generally accepted that when adsorbed at least from non-polar solvent, fatty acid makes a perfect film of its own. But in this study the myristic acid film from the solution of cetane appeared to be a mixture with cetane. Even the film from benzene solution showed, as seen in Fig. 1, some mixed-film nature, although it was lost after slight preheating.

The results on the lubricity of acid or alcohol film are quite contradictory to those obtained by previous workers. It is considered to be due mainly to the difference in the mode of frictional sliding and partly to the relatively lighter load applied in this experiment. When compared at $m = 0$, the friction of all films examined is indeed in good agreement with the published low data. Furthermore, it was established that above the melting point the film was still effective considerably, to which little attention had been drawn in the studies of static friction with hemisphere-on-flat device.

It was observed that with solid film the steady f increased with rising temperature. One explanation of this phenomenon may be as follows. There exist valleys and hills on the metal surface, and on friction a solid pool of lubricant remains at the valley, which is able to support a considerable part of the applied load. This load-carrying ability depends on the compressibility under the local high pressure at the sliding contact, and temperature rise makes the compressibility higher with the result of increasing metallic contact and friction.

It was confirmed that some definite correlation exists between the frictional characteristics and the structure and/or phase of the adsorbed film. Therefore, it is suggested that the "frictional analysis" is available at least as a complementary method for investigating the change of the state of film substance or the adhering tendency of the adsorbed molecule.

Acknowledgments.—The author wishes to thank Asst. Prof. H. Kanbe and Mr. M. Onoue for the differential thermal analysis, and Prof. S. Makishima and Dr. Kanbe for their helpful discussion.

(4) O. Levine and W. A. Zisman, THIS JOURNAL, **61**, 1068 (1957).
(5) A. Dobry, *Lubrication Eng.*, **10**, 210 (1954).
(6) F. P. Bowden and L. Leben, *Phil. Trans. Roy. Soc.*, **A239**, 1 (1940).

THE DIFFUSION COEFFICIENT OF LACTAMIDE IN DILUTE AQUEOUS SOLUTIONS AT 25° AS MEASURED WITH THE GOUY DIFFUSIOMETER

BY RICHARD P. WENDT AND LOUIS J. GOSTING

Department of Chemistry, University of Wisconsin, Madison 6, Wisconsin

Received January 28, 1959

The diffusion coefficient D and the specific refractive index increment $\Delta n/\Delta c$ have been determined as functions of concentration for aqueous solutions of lactamide over the range 0.5 to 17.8 g./100 ml. These data are compared with corresponding data from the literature for the system α-alanine–water, and the concepts of dipole–dipole interaction and electrostriction are used to interpret the differences. Flows for four reference frames are considered, and the values of D obtained experimentally are converted to diffusion coefficients corresponding to the mass-fixed and the solvent-fixed reference frames.

Introduction

One purpose of this study was to obtain accurate data for diffusion in the system lactamide–water to compare with data reported by Gutter and Kegeles[1] for aqueous solutions of α-alanine, the functional isomer of lactamide. Such a comparison illustrates the effect of molecular polarity on the diffusion coefficient D and the specific refractive increment $\Delta n/\Delta c$. Data from the present study also provide a test of the theory of Gosting and Fujita[2] which relates measured values of $\mathfrak{D}_A$, the reduced height–area ratio, to the square of the concentration difference across the initial boundary.

The recent use[3–5] of data for isothermal diffusion in ternary systems to test the Onsager reciprocal relations has emphasized the necessity for both experimentalists and theorists to define clearly the frame of reference used when considering diffusion coefficients. To illustrate how values of D may depend on the choice of the frame of reference, the diffusion coefficients measured in this study are converted to the solvent-fixed and the mass-fixed frames of reference.

Studies of diffusion in binary systems furnish data which contribute to complete descriptions of diffusion in ternary systems. For a ternary system containing lactamide as one solute (component 1) the concentration dependence of the main diffusion coefficient[6–8] D_{11} corresponding to the flow of lactamide could be represented by a three-dimensional graph[9] of D_{11} *versus* both solute concentrations, c_1 and c_2. At $c_2 = 0$ this three-dimensional surface would intersect the D_{11}–c_1 plane in a curve describing the concentration dependence of D_{11} on c_1 only; thus, in the limit as c_2 approaches zero, the values of D_{11} become identical with the values of D reported in this study of binary diffusion.

Experimental

The lactamide was synthesized according to an ammonolysis procedure suggested by Gucker and Allen[10] in which anhydrous ammonia was passed directly into 1500 g. of Eastman White Label ethyl lactate. During the first six hours of the twelve-hour ammonolysis the heat of reaction maintained the temperature at about 100°, but it was necessary to heat the reaction mixture for the last six hours to prevent premature precipitation of the lactamide crystals. After the solution was cooled, the crystals, which formed spontaneously, were collected and dried; a 77% yield of crude lactamide was obtained. The temperature dependence of the solubility of lactamide in ethyl acetate then was utilized to recrystallize the crude material from two to five more times, using approximately one ml. of freshly distilled, boiling ethyl acetate to dissolve each gram of lactamide. After the crystals were washed with fresh cold solvent, a centrifuge was employed to spin-dry the recrystallized product. The remaining solvent then was removed by evaporation under vacuum, and the slightly hygroscopic crystals were dried over Drierite *in vacuo* to constant weight. Samples from the second, third and fifth recrystallizations melted identically (within 0.02°) over the short melting range observed. Conductance water, saturated with air, was the solvent used to prepare the solutions placed in the diffusion cell; solute concentrations c in g./100 ml. were calculated from measured weight percentages (corrected to vacuum) by using the density data of Gucker and Allen.[10]

The isothermal free-diffusion process took place in a new quartz Tiselius electrophoresis cell which had been tested with a Gauss-eyepiece telescope for both flatness and parallelism of its windows and side-walls. For this cell the distance a between windows (as measured along the optic axis) was found to be 2.5092 cm.; the optical distance b from the center of the cell to the image plane at the photographic plate was 306.67 cm. The Gouy diffusiometer which was used for this work without modification has been previously described.[11,12] Monochromatic light having a wave length λ of 5460.7 Å. in air illuminated the source slit. The temperature of the water-bath surrounding the diffusion cell was within 0.01° of 25.000° for all experiments, and temperature variations were no greater than 0.005° during any experiment.

Previous articles[2,7] have described the method of computing the reduced height–area ratio[13] $\mathfrak{D}_A$. For this study, from eight to ten Gouy fringe photographs were taken during each experiment; an apparent value, $\mathfrak{D}'_A$, of $\mathfrak{D}_A$ then was cal-

(1) F. J. Gutter and G. Kegeles, *J. Am. Chem. Soc.*, **75**, 3893 (1953).

(2) L. J. Gosting and H. Fujita, *ibid.*, **79**, 1359 (1957).

(3) D. G. Miller, THIS JOURNAL, **62**, 767 (1958).

(4) P. J. Dunlop and L. J. Gosting, *ibid.*, **63**, 86 (1959).

(5) P. J. Dunlop, *ibid.*, **63**, 612 (1959).

(6) R. L. Baldwin, P. J. Dunlop and L. J. Gosting, *J. Am. Chem. Soc.*, **77**, 5235 (1955).

(7) P. J. Dunlop and L. J. Gosting, *ibid.*, **77**, 5238 (1955).

(8) The two solute flows, J_1 and J_2, may be related to the solute concentration gradients by the equations

$$J_1 = -D_{11}\frac{\partial c_1}{\partial x} - D_{12}\frac{\partial c_2}{\partial x}$$

$$J_2 = -D_{21}\frac{\partial c_1}{\partial x} - D_{22}\frac{\partial c_2}{\partial x}$$

The quantities D_{11} and D_{22} are generally referred to as *main diffusion coefficients*, and D_{12} and D_{21} are referred to as *cross-term diffusion coefficients* (see refs. 6, 7 and 9).

(9) I. J. O'Donnell and L. J. Gosting, a paper presented in a Symposium at the 1957 meeting of the Electrochemical Society in Washington, D. C.; see chapter 11 in "The Structure of Electrolytic Solution," (W. J. Hamer, ed.), John Wiley and Sons, Inc., New York, N.Y., 1959.

(10) F. T. Gucker, Jr., and T. W. Allen, *J. Am. Chem. Soc.*, **64**, 191 (1942).

(11) L. J. Gosting, E. M. Hanson, G. Kegeles and M. S. Morris, *Rev. Sci. Instr.*, **20**, 209 (1949).

(12) P. J. Dunlop and L. J. Gosting, *J. Am. Chem. Soc.*, **75**, 5073 (1953).

(13) See equations 32 and 35, ref. 7.

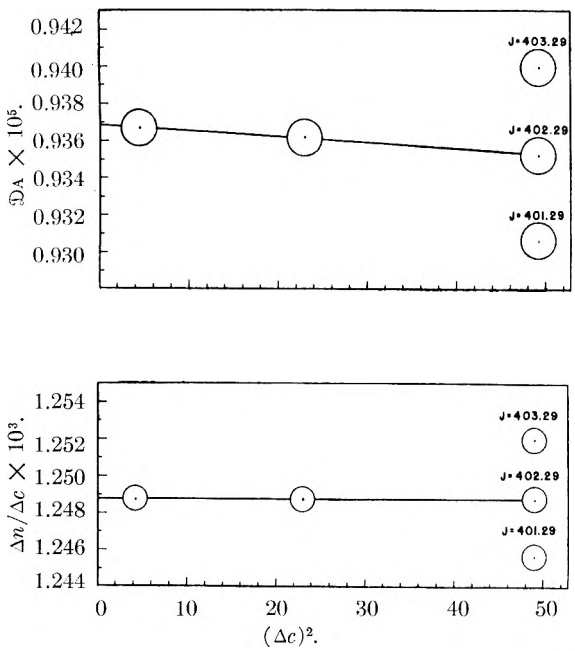

Fig. 1.—The dependence on $(\Delta c)^2$ of $\mathfrak{D}_A$ and $\Delta n/\Delta c$ at $\bar{c}$ = 3.505 g./100 ml. On each graph the two points at the smaller values of Δc correspond to expts. V and X, for which the integral part of J was determined directly. Circles represent the maximum estimated experimental error.

culated from each picture, using the observed time t' measured from the instant that boundary sharpening was stopped. Because this initial boundary, formed between the two solutions in the diffusion cell by siphoning with a single-pronged capillary, was never perfectly sharp, each $\mathfrak{D}'_A$ was corrected for the error Δt in the starting time. This was accomplished by using the method of least squares to express $\mathfrak{D}'_A$ as a linear function of $1/t'$; the corrected value $\mathfrak{D}_A$ was obtained as the limiting value of $\mathfrak{D}'_A$, at infinite time,[14,15] *i.e.*, when $1/t' = 0$. Average deviations of the experimental values of $\mathfrak{D}'_A$ from this linear expression were no greater than 0.09% for any experiment, and the largest value of Δt was 23.4 sec.

Specific refractive index increments were computed from the expression

$$\frac{\Delta n}{\Delta c} = \frac{\lambda J}{a \Delta c} \qquad (1)$$

Here $\Delta c = c_B - c_A$, where A and B denote the solutions placed in the upper and lower portions of the cell, respectively; similarly, $\Delta n = n_B - n_A$, the refractive index difference (referred to air as unity) between solutions B and A. Both a and λ have been previously defined. The number of interference fringes J in each experiment is not necessarily an integer; it has an integral and a fractional part. The fractional part was determined for all experiments by measuring the vertical displacement of ordinary Rayleigh fringes[16] photographed during the boundary sharpening process. The integral part of J was obtained by counting the number of fringes on Rayleigh (integral fringe) interferograms[17] photographed as soon as possible after the diffusion process had started and the fringes in the central part of the pattern were all resolved. This procedure was used to find J for all experiments except IX (in Table I), for which only the fractional part could be directly determined: if J exceeds about 300 the aperture stop of our Rayleigh optical system[18] is too small to resolve the central fringes on the interferogram except after long times, when the fringes near the ends of the pattern become curved. However, by using a prism-type differential refractometer the value of J for expt. IX was determined independently within about one integral fringe. Three values of both $\mathfrak{D}_A$ and $\Delta n/\Delta c$ were then computed, using values of J corresponding to the one measured fractional part of J and the three possible integral parts. Both $\mathfrak{D}_A$ and $\Delta n/\Delta c$ should be linear functions[2] of $(\Delta c)^2$ for small values of Δc; the first two points on each graph in Fig. 1, for which the values of J have been directly determined, may therefore be connected by a straight line. Extrapolation of each of these lines indicates that 402 is the correct integral part of J for expt. IX.

Because the temperature of no experiment differed more than 0.01° from 25°, the Stokes–Einstein relation in the form

$$\left(\frac{\mathfrak{D}_A \eta}{T}\right)_{25°} = \left(\frac{\mathfrak{D}_A \eta}{T}\right)_{\text{Expt}} \qquad (2)$$

was used to correct each value of $\mathfrak{D}_A$ to 25.000°. In this equation T is the absolute temperature and η is the viscosity of water.

Results

Table I summarizes the results of this study. The data from this table (excluding those for expts. IX and X with large values of Δc) are represented by

$$D \times 10^5 = 0.9911 - 0.01569c + 1.07 \times 10^{-4}c^2 \qquad (c < 18 \text{ g./100 ml.}) \qquad (3)$$

$$\frac{\Delta n}{\Delta c} \times 10^3 = 1.2439 + 1.588 \times 10^{-3}\bar{c} - 7.12 \times 10^{-5}\bar{c}^2 + 1.13 \times 10^{-6}\bar{c}^3 \qquad (\bar{c} < 18 \text{ g./100 ml.}) \qquad (4)$$

The coefficients in these equations were calculated by the method of least squares, and $\bar{c} = (c_A + c_B)/2$, the average solute concentration across the initial boundary. In equation 3, D and c are used instead of $\mathfrak{D}_A$ and $\bar{c}$ for reasons which will be discussed in the next paragraph. The average deviations of the experimental points from equations 3 and 4 are 0.03 and 0.02%, respectively. From equation 4 an expression for the dependence of the refractive index on concentration is readily obtained[19]

$$n = n_0 + 1.2439 \times 10^{-3} c + 0.794 \times 10^{-5}c^2 - 2.37 \times 10^{-8}c^3 + 2.82 \times 10^{-10}c^4 \qquad (5)$$

Here, n_0 is the refractive index of pure water at 25.00$_0$° for light of 5460.7 Å. wave length.

To confirm the identification of the reduced height–area ratio $\mathfrak{D}_A$ with D, the diffusion coefficient desired, three experiments (V, IX, and X) were performed at different values of Δc but at the same value of $\bar{c}$. In Fig. 1 the values of $\mathfrak{D}_A$ for these experiments are plotted as a function of $(\Delta c)^2$. According to equation 6 below, this graph should be a straight line with $\mathfrak{D}_A \to D$ as $(\Delta c)^2 \to 0$.

(19) Equation 5 may be calculated from the cubic expression (equation 4) for $\Delta n/\Delta c$ by first writing n as a quartic in c

$$n = n_0 + n_1 c + n_2 c^2 + n_3 c^3 + n_4 c^4$$

where n_0 is the refractive index of water and $n_1, \ldots, n_4$ are constants for the given temperature and the given wave length of light. After substituting the definitions $\bar{c} = (c_A + c_B)/2$ and $\Delta c = c_B - c_A$, it follows that

$$\frac{\Delta n}{\Delta c} = n_1 + 2n_2\bar{c} + 3n_3\bar{c}^2 + 4n_4\bar{c}^3 + \left(\frac{n_3}{4} + n_4\bar{c}\right)(\Delta c)^2 \qquad (4a)$$

For the values of Δc used in these experiments the term in $(\Delta c)^2$ is less than the error in $\Delta n/\Delta c$; therefore the term in $(\Delta c)^2$ may be neglected and equation 4a can be written as

$$\frac{\Delta n}{\Delta c} = b_0 + b_1\bar{c} + b_2\bar{c}^2 + b_3\bar{c}^3$$

where $b_0 = n_1$, $b_1 = 2n_2$, $b_2 = 3n_3$, and $b_3 = 4n_4$. The coefficients $n_1 \ldots n_4$ for equation 5 are thus readily determined from the coefficients $b_0, \ldots, b_3$ in equation 4.

(14) L. G. Longsworth, *J. Am. Chem. Soc.*, **69**, 2516 (1947).
(15) H. Fujita, *J. Phys. Soc. Japan*, **11**, 1018 (1956).
(16) Similar to the fringes illustrated in Fig. 8, ref. 11.
(17) See Fig. 1B, ref. 18.
(18) J. M. Creeth, *J. Am. Chem. Soc.*, **77**, 6428 (1955).

TABLE I

DATA FOR LACTAMIDE IN WATER AT 25°

Expt. no.[a]	Times recryst.	$\bar{c}$, g./100 ml.[b]	Δc, g./100 ml.[c]	J	$\mathcal{D}_A \times 10^5$, cm.²/sec.	$(\Delta n/\Delta c) \times 10^3$ (g./100 ml.)$^{-1}$
II	3	0.49381	0.98762	56.46	0.9830	1.2441
I	2	0.49790	0.99579	56.95	.9836	1.2446
VI	5	1.02918	2.05835	117.84	.9751	1.2459
IV	3	2.03575	1.91852	109.23	.9601	....
V	5	3.50452	2.05821	118.10	.9367	1.2488
X	2	3.50451	4.79088	274.90	.9362	1.2488
IX	5	3.50533	7.01066	402.29	.9353	1.2488
III	2	4.88414	1.90196	109.27	.9171	1.2503
VII	5	8.87146	2.05645	118.39	.8605	1.2529
VIII	2	17.81426	2.05729	118.73	.7455	1.2560

[a] Experiments are numbered chronologically. [b] $\bar{c} = (c_A + c_B)/2$, where c_A and c_B are the original solute concentrations in the upper and lower portions of the diffusion cell, respectively. [c] $\Delta c = c_B - c_A$.

The line drawn through the first two points (corresponding to experiments for which the integral part of J had been directly determined from Rayleigh interferograms) is seen to have such a small slope that the value of $\mathcal{D}_A$ corresponding to the first point is identical with D within experimental error. This slope is not expected to vary appreciably with $\bar{c}$, and $\mathcal{D}_A$ thus may be identified with D for all experiments in Table I except no. IX and X (performed with large values of Δc). Therefore, D and c are used instead of $\mathcal{D}_A$ and $\bar{c}$ in equation 3.

According to the theory of Gosting and Fujita,[2] $\mathcal{D}_A$ at a given value of $\bar{c}$ varies linearly with $(\Delta c)^2$ for moderately small values of Δc

$$\mathcal{D}_A = D[1 - K(\Delta c)^2 + \ldots] \qquad (6)$$

In this expression K is a constant, independent of Δc but dependent on $D(c)$, $dn(c)/dc$, and certain higher derivatives of these quantities, each evaluated at $c = \bar{c}$. To find the value of the theoretical slope, $-DK$, of the upper graph in Fig. 1, the appropriate data from equations 3 and 5 were used[20] to calculate K; the value of $-DK$ obtained was -0.328×10^{-9}, as compared with -0.31×10^{-9}, the value of the slope measured from the graph. Although this value of $-DK$ is much smaller than for the system butanol–water (previously used[2] to test the theory), the agreement within experimental error of this predicted slope and the slope measured from Fig. 1 provides some additional confirmation of the theory. By using a quadratic expression instead of a cubic to fit the experimental data for $\Delta n/\Delta c$ as a function of $\bar{c}$, a second value, -0.308×10^{-9}, was calculated for $-DK$. Because this value is also identical with -0.31×10^{-9} within the error of measurement, it is believed that the cubic expression in equation 4 adequately represents the data for $\Delta n/\Delta c$ for this test of the theory.

In Table I, the second column specifies the number of times the solute used for each experiment had been recrystallized. One purpose of expts. I and II was to test the relative purity of lactamide which had been recrystallized two times and three times, respectively. Because the two measured values of both $\mathcal{D}_A$ and $\Delta n/\Delta c$ were identical within experimental error, the twice recrystallized material seemed to be sufficiently pure to be used for several of the other experiments. Data from experiments in which the five-times recrystallized lactamide was used showed negligible deviations from equations 3 and 4, indicating similar purity of all of the recrystallized material. Additional evidence of solute purity was furnished by fringe-deviation graphs[21] for the experiments. There was no systematic dependence of the shape of these graphs on the number of times the solute had been recrystallized, and for no experiment did the maximum relative fringe deviation[22] differ from zero by more than 2.8×10^{-4}.

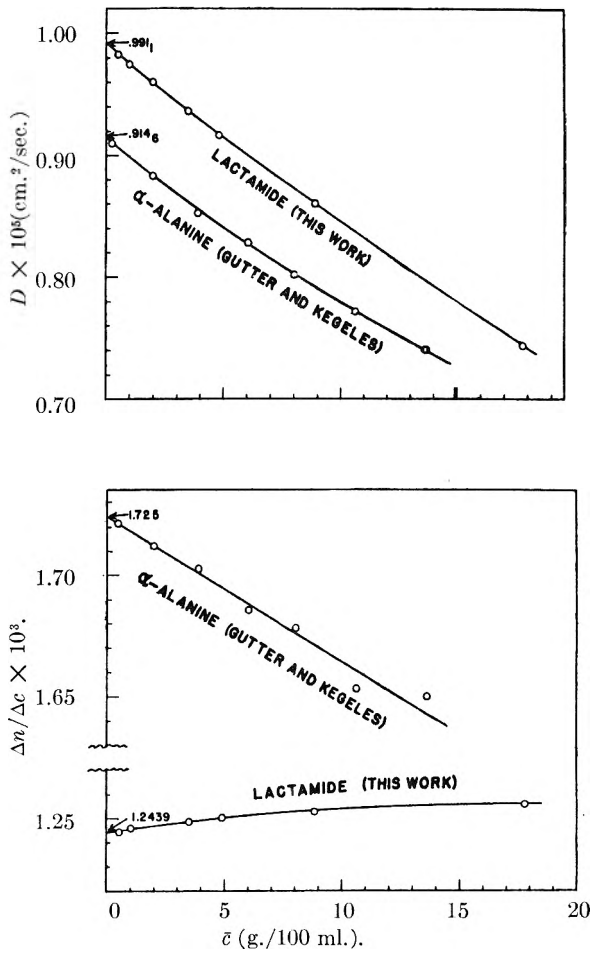

Fig. 2.—The concentration dependence of D and $\Delta n/\Delta c$ for the systems α-alanine-water and lactamide–water at 25°.

Discussion

Comparison of Data for Isomeric Compounds.—In Fig. 2 the data for lactamide obtained from this study are compared graphically with data for α-alanine.[1] At corresponding concentrations (including infinite dilution), D for lactamide is greater than D for α-alanine, supporting the concept of dipole–dipole interaction between α-alanine and water molecules; this interaction would produce an α-alanine–water aggregate which would diffuse

(20) See equation 58 or 58a, ref. 2.

(21) D. F. Akeley and L. J. Gosting, *J. Am. Chem. Soc.*, **75**, 5685 (1953).

(22) See equation 9, ref. 21.

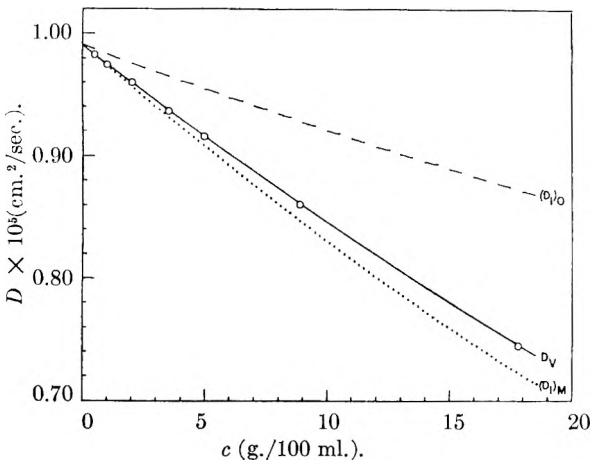

Fig. 3.—The concentration dependence of the diffusion coefficient of lactamide in water for three frames of reference: the solvent-fixed (top curve); volume-fixed (center curve); mass-fixed (bottom curve).

more slowly than the relatively non-polar lactamide molecule.[23] Electrostriction of water around the polar α-alanine molecule has been suggested by Gucker and Allen[10] to account for the small value of the partial molal volume at infinite dilution, $\bar{V}^\circ$, for that compound, as compared to the value of $\bar{V}^\circ$ for lactamide. It seems reasonable that electrostriction also accounts for the greater limiting value of $\Delta n/\Delta c$ for the more dense α-alanine solutions, as illustrated by the bottom graph in Fig. 2. The slope of the α-alanine curve is much greater than the almost zero slope of the lactamide curve, a fact which correlates well with the relative concentration dependence of $\bar{V}$ for each compound.[10]

This comparison of data for the functional isomers lactamide and α-alanine shows striking similarities to the previously reported[12] comparison of data for two homologs of those compounds, glycolamide and glycine. The value of D at infinite dilution (D°) for glycolamide was found to be 7.4% greater than D° for glycine, compared to a difference of 8.4% between the values of D° for lactamide and α-alanine; the limiting value of $\Delta n/\Delta c$ for glycine was 46.2% greater than the value of that quantity for glycolamide, compared to a difference of 38.6% between the limiting values of $\Delta n/\Delta c$ for α-alanine and lactamide.

Frames of Reference for Diffusion Coefficients.—The importance of properly defining the "frame of reference" when reporting diffusion coefficients is graphically illustrated in Fig. 3, where the diffusion coefficient of lactamide corresponding to its flow for each of three different reference frames is plotted as a function of concentration. Various aspects of the problem of frames of reference for flows have been considered by a number[24-27] of previous workers, although the approaches used were somewhat different from that presented here. Before summarizing the equations used in this paper to convert values of the measured diffusion coefficient to other reference frames, the frames considered here will first be defined, and the flows corresponding to each frame will be briefly discussed.

To specify the flow J_k of component k it is necessary to state its units and also the reference frame to which it is referred. As defined here, J_k is the number of grams of component k per second which crosses one square centimeter of a reference plane perpendicular to the direction of macroscopic motion of that component; for the one-dimensional flows studied in most experimental work, each reference plane is therefore perpendicular to the walls of the diffusion cell.

For any given "frame of reference" there is at each time t a particular set of reference planes; this set consists of an infinite number of planes, one at every position, x, in the diffusion cell. Furthermore, each member of this infinite set of reference planes has a velocity (generally non-zero) relative to the cell which is a particular function of x and of t. The specification of this velocity function for a particular reference frame also defines the flows corresponding to that reference frame.

The cell-fixed reference frame, designated by C, is important because it is basic to most experimental measurements. For the reference planes associated with this reference frame, the velocity function is zero (relative to the cell) at all x and t. It is the flow $(J_k)_C$ corresponding to this reference frame which appears in the continuity equation

$$\frac{\partial \rho_k}{\partial t} = -\frac{\partial (J_k)_C}{\partial x} \qquad (7)$$

when the space coördinate x is identified with the cell coördinate used experimentally. To derive an expression for the concentration ρ_k (in g./cc.) as a function of x and t, it is necessary to integrate equation 7. For binary systems this integration is usually accomplished by assuming that $(J_k)_C$ is proportional to $-\partial\rho_k/\partial x$ (Fick's first law). However, it is not always correct to write $(J_k)_C$ simply as a concentration gradient multiplied by a diffusion coefficient. Onsager[25] has pointed out that an additional term must be included if there exists bulk motion of the solution relative to the cell, caused, for example, by volume changes on mixing.

Nevertheless, there does exist[26,27] a class of reference frames for which the flows may always be written simply in terms of concentration gradients multiplied by diffusion coefficients, regardless of bulk motion of the solution. Each reference frame, R, in this class has the property that a linear relation[28]

(23) It should not be inferred that the most polar isomer of a set of isomeric compounds will always have the lowest diffusion coefficient. While this correlation seems to be true for a pair of isomers having large polarity differences such as α-alanine and lactamide or glycine and glycolamide, it may not be true if the difference in polarity between the isomers is relatively small. An interesting comparison of the latter kind between α-alanine and β-alanine has been made by Donoian and Kegeles (private communication) in connection with a study of diffusion in the system β-alanine–water, which is soon to be published.

(24) Pertinent references include: (a) B. W. Clack, *Proc. Phys. Soc. (London)*, **21**, 374 (1908); (b) L. G. Longsworth, *Ann. N. Y. Acad. Sci.*, **46**, 211 (1945); (c) I. Prigogine, *Bull. classe sci., Acad. roy. Belg.* [5], **34**, 930 (1948); (d) G. S. Hartley and J. Crank, *Trans. Faraday Soc.*, **45**, 801 (1949); (e) R. L. Baldwin and A. G. Ogston, *ibid.*, **50**, 749 (1954); (f) R. B. Bird, C. F. Curtiss and J. O. Hirschfelder, *Chem. Eng. Prog. Symposium Ser.*, No. 16, **51**, 69 (1955); (g) J. Crank, "The Mathematics of Diffusion," Oxford University Press, London, 1956; (h) O. Lamm, *Acta Chem. Scand.*, **11**, 362 (1957).

(25) L. Onsager, *Ann. N. Y. Acad. Sci.*, **46**, 241 (1945).

(26) G. J. Hooyman, H. Holtan, Jr., P. Mazur and S. R. deGroot, *Physica*, **19**, 1095 (1953).

(27) G. J. Hooyman, *ibid.*, **22**, 751 (1956).

(28) See equation 3, ref. 27.

exists between the flows, $(J_k)_R$, of the components in the system. Of the reference frames in this class only three will be considered here: the volume-fixed, the mass-fixed and the solvent-fixed frames, for which the flows are denoted by $(J_k)_V$, $(J_k)_M$ and $(J_k)_0$, respectively. This discussion is limited for simplicity to binary systems in which the solvent is denoted by 0 and the solute by 1. For the solvent-fixed reference frame the velocity function is defined so that there is no flow of solvent across any reference plane; *i.e.*, for all x and t

$$(J_0)_0 = 0 \qquad (8a)$$

The reference planes for the mass-fixed frame have a velocity function such that there is no net flow of mass across any reference plane; thus

$$(J_0)_M + (J_1)_M = 0 \qquad (8b)$$

Similarly, for the volume-fixed frame each reference plane moves so that there is no net flow of volume across it

$$(J_0)_V\bar{v}_0 + (J_1)_V\bar{v}_1 = 0 \qquad (8c)$$

Here, $\bar{v}_k$ is the partial specific volume of component k. For any reference frame R of this class the two flows are related to their corresponding concentration gradients by the simple relation[29]

$$(J_k)_R = -(D_k)_R \frac{\partial \rho_k}{\partial x} \quad (k = 0,1) \qquad (9)$$

even if there is a superimposed bulk flow.

Each flow $(J_k)_C$ in equation 7 (the continuity equation) can be expressed in terms of $(J_k)_R$ by

$$(J_k)_C = (J_k)_R + u_{RC}\rho_k \qquad (10)$$

where u_{RC} is the velocity function, relative to the cell, for the reference planes of frame R. By then using equation 9 to replace $(J_k)_R$, equation 7 may be integrated if a suitable expression is available for u_{RC}. For the volume-fixed reference frame, u_{VC} equals zero[30] whenever the $\bar{v}_k$ are independent of concentration (or the concentration difference between the solutions is so small that the $\bar{v}_k$ may be considered constant); the continuity equation for this case of $u_{VC} = 0$ has been integrated for various initial and boundary conditions. Because relatively small values of the concentration difference Δc were used for all experiments in the present study except no. IX and X, the diffusion coefficients D calculated in the usual manner and represented by equation 3 can be identified with $(D_1)_V$. From values of $(D_1)_V$ the diffusion coefficients corresponding to other reference frames then may be obtained without further approximation by using transformation equations such as 11a and 11b.

The values of $(D_1)_M$ and $(D_1)_0$ shown in Fig. 3 were calculated from values of $(D_1)_V = D$ by using the relations[31]

$$(D_1)_M = \frac{1 - \frac{\rho_1}{\rho}}{1 - \rho_1\bar{v}_1} D_V \qquad (11a)$$

$$(D_1)_0 = \frac{1}{1 - \rho_1\bar{v}_1} D_V \qquad (11b)$$

(29) See equation 23, ref. 27.

(30) See appendix I, ref. 26.

which are valid for any binary liquid system. Here $\rho = \rho_0 + \rho_1$ is the solution density and $(D_1)_V$ is written simply as D_V because

$$(D_0)_V = (D_1)_V \qquad (12a)$$

even for systems where $\bar{v}_k$ is dependent on concentration.[32] It is also of interest to note that for the mass-fixed reference frame the relation

$$(D_0)_M = \frac{\bar{v}_0}{\bar{v}_1}(D_1)_M \qquad (12b)$$

may be similarly obtained. For the solvent-fixed frame

$$(D_0)_0 = 0 \qquad (12c)$$

because, from equations 8a and 9, $(J_0)_0$ is zero but $\partial\rho_0/\partial x$ is in general not zero.

The coefficients $(D_k)_M$ and $(D_k)_0$ are of importance when considering flows for the corresponding frames of reference. Mass-fixed flows are important in theoretical work because they appear in derivations of expressions for the entropy production of certain irreversible processes. Flows for the solvent-fixed reference frame are of both experimental and theoretical interest. For example, if the flows $(J_k)_0$ are chosen to describe diffusion in three-component systems, the equations used to test the Onsager reciprocal relations have an especially simple form.[33] Furthermore, some experimental studies of diffusion of liquid solutes through solid "solvents" such as high polymers or wood fiber may in fact measure solvent-fixed flows rather than volume-fixed flows. In view of the appreciable differences between D_V, $(D_1)_M$ and $(D_1)_0$ in Fig. 3 it is evident that the frame of reference should be stated whenever interpreting accurate data concerning irreversible processes.

Acknowledgments.—The authors wish to acknowledge the helpful suggestions of Dr. Hiroshi Fujita, with whom several aspects of this paper were discussed. This work was supported by the National Science Foundation, by a du Pont Grant-in-Aid to the Department of Chemistry, and by the Research Committee of the Graduate School from funds supplied by the Wisconsin Alumni Research Foundation.

(31) Equation 10 may be rewritten as

$$u_{RC} = \frac{1}{\rho_k}(J_k)_C - \frac{1}{\rho_k}(J_k)_R \qquad (10a)$$

By setting k equal to 0 and then to 1 for a particular reference frame, two equations are obtained from which u_{RC} can be eliminated. The resulting equation is combined with a similar equation found for a second reference frame of class R, and the terms $(J_0)_C/\rho_0$ and $(J_1)_C/\rho_1$ simultaneously eliminated. Each solvent flow is then replaced by its equivalent from equations 8, and by using equation 9 each remaining solute flow is expressed in terms of the solute concentration gradient multiplied by the appropriate diffusion coefficient. The coefficients of $\partial\rho_1/\partial x$ are equated to find equations 11a and 11b, which are identical with the transformation equations that can be obtained from ref. 26 (after converting the concentration units) and from ref. 27 (when $n = 2$).

(32) This may be seen if, in equation 8c, the flows are replaced by $-(D_0)_V\partial\rho_0/\partial x$ and $-(D_1)_V\partial\rho_1/\partial x$, respectively, and the coefficients of $\partial\rho_1/\partial x$ are equated after replacing $\partial\rho_0/\partial x$ by $-(\bar{v}_1/\bar{v}_0)(\partial\rho_1/\partial x)$. The latter thermodynamic identity is true at constant temperature and pressure regardless of the dependence of $\bar{v}_k$ on concentration. Equation 12a is implied by equation 1 of ref. 25; for the special case of constant $\bar{v}_k$, a derivation is given in ref. d of footnote 24.

(33) See paragraph 3, ref. 27.

THE SORPTIVE PROPERTIES OF A ZEOLITE CONTAINING A PREADSORBED PHASE

BY PETER CANNON AND CECELIA P. RUTKOWSKI

General Electric Research Laboratory, Schenectady, New York

Received February 17, 1959

It is shown that when a degassed zeolitic substrate is saturated with respect to a given sorbate, not even the largest channels or pores are necessarily physically filled. By examining the adsorption of a second sorbate on a zeolite already saturated with respect to another vapor, information may be gained as to the positions of molecules in the preadsorbed layer with respect to the substrate structure. Even a non-dipolar species such as CCl_2F_2 appears to form clusters around the charge-compensating cations, comparable with the "hydration sheaths" of coördinated water suggested by others to explain the diffusion of water in zeolitic channels.

Among the more unusual forms in which aluminosilicate minerals occur are the zeolites, which possess very open network structures, interpenetrated in two or three dimensions by channels. These channels contain the compensating cations necessary to offset the charge unbalance caused by the presence of aluminum as a tetrahedrally bound species, and normally also contain large amounts of water which may be removed by gentle heating without destroying the lattice. In recent years the nature of this water has been the subject of some interest,[1] because of the secondary effect it has on the parent lattice, and because comparison of the properties of isolated groups of up to about twenty molecules with those of the bulk fluid are of fundamental significance. This easily removable, mobile[2] water, which may be replaced reversibly, is commonly known as "zeolitic" water, to distinguish it from the small amount of water which is essential to the lattice, and which when removed cannot be resorbed.[3]

Zeolitic water may be removed and replaced by other fluids,[4] once again with only secondary changes in the host lattice structure. An important phenomenon observed in systems such as these, which possess a large number of channels or pores of identical dimensions, is the "molecular sieve" effect, in which only those gases and vapors having molecules small enough to enter the pores are sorbed to any great extent. Some fluid materials, once sorbed into the dehydrated lattice, undergo chemical reaction, and others are extremely difficult to remove, and these phenomena may be due to the field of the charge-compensating cations.[5] Zeolitic water itself may have a range of energies required for its removal, and this may be due to an ordered arrangement of some of the water molecules in a hydration sheath near the cations. Such a scheme has been proposed by Pemsler[2] to explain water diffusion measurements in zeolites, by Hey and Bannister[6] to explain the dehydration of scolecite and by others[7] to explain the thermograms of various other hydrated aluminosilicates. In spite of this possibility, the removal of water from zeolites is continuous, though the rate may vary.[8]

A distinct problem in assessing the positions of the water molecules in the channels is the difficulty of obtaining direct structural evidence concerning the water molecules. In general, resort must be had to rather indirect techniques in such systems, but in systems where heavier species are occluded, straightforward X-ray diffraction is a powerful tool.[9] Another problem is that the channels or pores may not be filled completely by the sorbed species, be it water of some other fluid. Thus Barrer and Brook[10] found they could not apply Polanyi potential theory to polar molecules sorbed in chabazite, which would imply either considerable ordered structure or discontinuities in the sorbed polar fluids. The general applicability of the Langmuir equation to sorption in zeolite channels would also seem to show that the pores are not completely filled. Occasionally one encounters an unproved assumption that because the normalized liquid volumes of various sorbed phases on a given substrate are approximately the same,[11] then the pores or channels are completely filled by the sorbates. In some cases this assumption has been used corroboratively in the elucidation of the structure of a zeolite.[12] (In the case cited, this leads to a relative density greater than three for the anhydrous network, compared with an accepted value of 2.6 for quartz.)

The purpose of the present paper is to establish that zeolitic channels are not necessarily completely filled when saturated with respect to one adsorbate and indirectly to throw some light on the arrangement of the sorbed molecules in the incompletely filled channels.

Experimental

(a) **Apparatus, Chemicals and General Procedure.**—Volumetric adsorption apparatus of the general style described by Corrin[13] and by Gaines and Rutkowski[14] was used

(1) A review of methods employed and results obtained by a school active in this field may be found in Barrer, XVI. I.U.P.A.C. Congress reported in *Experientia*, Supp. **VII**, 113 (1957).

(2) P. Pemsler, Ph.D. thesis, New York Univ., 1957; see also *Diss. Abs.*, **18**, 2005 (1958).

(3) E. Rabinowitch, *Z. physik. Chem.*, **16B**, 43 (1932), appears to have been the first to have discussed this classification in a synoptic manner.

(4) Early examples include G. Friedel, *Bull. soc. franc. min.*, **19**, 14 (1896); also **19**, 96 (1896), to whom the original concept of a sponge-like structure for zeolites apparently is due.

(5) P. Cannon, THIS JOURNAL, **63**, 160 (1959).

(6) M. H. Hey and F. A. Bannister, *Min. Mag.*, **24**, 227 (1936).

(7) Cited in R. Grim, "Clay Mineralogy," McGraw-Hill Book Co., New York, N. Y., 1953, p. 242.

(8) W. Eitel, "The Physical Chemistry of the Silicates," Univ. of Chicago Press, 1954, pp. 997–1007, cites a number of examples of different degrees of binding of zeolitic water within the same system.

(9) R. M. Barrer and W. M. Meier, *J. Chem. Soc.*, 299 (1958).

(10) R. M. Barrer and D. W. Brook, *Trans. Faraday Soc.*, **49**, 940 (1953).

(11) D. W. Breck, *et al.*, *J. Am. Chem. Soc.*, **78**, 5963 (1956).

(12) T. B. Reed and D. W. Breck, *ibid.*, **78**, 5972 (1956).

(13) M. L. Corrin, THIS JOURNAL, **59**, 313 (1955).

(14) G. L. Gaines, Jr., and C. P. Rutkowski, *ibid.*, **62**, 1521 (1958).

for the measurement of argon adsorption. Water adsorption was measured on a magnetically counterpoised sorption balance of the general type described by Gregg,[15] the deflection of the beam being measured by a traveling microscope. Measurements of the adsorption of $CHClF_2$ vapor were made using an automatic sorption balance designed for operation at pressures up to 20 atmospheres.[16] This device had a sensitivity of 0.05 mg./g. sample.

Liquid nitrogen, liquid oxygen, melting ice and stirred water-baths were used to maintain the sample bulb at the experimental temperatures during the measurements. Gaines and Rutkowski[14] found that their nitrogen and oxygen baths did not vary more than $\pm 0.2°$ from the accepted values of 77.4 and 90.2°.

Pressures were measured with a calibrated thermistor gauge, a McLeod gauge and a wide bore manometer and capillary differential manometer system. Pressures above 1000 mm. were measured using a precision stainless steel Bourdon gauge (Heise Gauge Co., Newtown, Conn.), which had been calibrated against a high pressure mercury manometer: it was accurate to within 10 mm. up to 10^4 mm. pressure. Where appropriate, the transpiration corrections due to Bennett and Tompkins,[17] and the meniscus corrections due to Bashforth and Adams were employed.[18]

The argon used in the adsorption experiments and the helium used for volume calibrations were reagent grade materials obtained in sealed flasks from the Lamp Wire and Phosphors Department of the General Electric Company (Cleveland, Ohio). Chlorodifluoromethane was prepared from tank grade Freon 22 (E. I. du Pont de Nemours Co., Kinetic Chemicals Division) by repeated vacuum distillation and degassing. The product purity was 99.3+% (mole basis), the principal residual impurity being CCl_2F_2: these facts were established by gas–liquid chromatography. Dichloro difluoromethane was prepared from du Pont Freon 12 by vacuum distillation and degassing; its purity was 99.8+ % (mole basis). Distilled water was degassed thoroughly before being used as an adsorbate.

The experimental samples were small, about 200 mg. The zeolite chosen for this work was a synthetic variety, obtained from the Linde Co., Tonawanda, N. Y. (Linde Molecular Sieve 5A,[11,12,19] pelleted form). This material contains a clay component to permit extrusion of the pellets: it is present to the extent of about 20% but because of its relatively smaller surface area, does not noticeably affect the adsorption measurements at lower pressures.

The zeolite was prepared for argon adsorption by prior degassing at 350° at 10^{-5} mm. This temperature and pressure correspond with the conditions under which all but the constitutional water is removed from the zeolite: further heating results in a small (approx. $1/2$%) weight loss above 700°, when the crystal lattice collapses. The loss of water on heating to 350° is much larger, corresponding to an approximately 20% weight loss. Under these circumstances, therefore, it would appear that the water associated with the charge compensating Ca^{++} ions has been removed, and that these ions are bare, and available to other materials that might "solvate" them. The specimen of zeolite containing CCl_2F_2 was prepared by exposing a sample, degassed as above and then cooled to 25°, to CCl_2F_2 at its saturation pressure in a stainless steel flask. After one week, the solid was transferred in a CCl_2F_2 atmosphere to the experimental system, and the excess CCl_2F_2 pumped off (the bound CCl_2F_2 is not removable by simple pumping).[5] In some cases it was possible to perform this preparation in the adsorption apparatus: a check on the procedure in the high pressure balance[16] showed that the uptake of CCl_2F_2 was 0.193 g./g. After pumping on the prepared material for several days at room temperature, a "leak rate" into the system from the sample of a small fraction of a micron liter per hour was observable. The first dose of gas or vapor to be adsorbed was therefore added immediately after the sample had been isolated from the pumps; this placed the system pressure at several microns and effectively stopped the slow effusion of CCl_2F_2 from the penetrated lattice.

(15) S. J. Gregg, *J. Chem. Soc.*, 561 (1946); 1438 (1955).

(16) P. Cannon, *Rev. Sci. Instr.*, **29**, 1115 (1958).

(17) M. J. Bennett and F. C. Tompkins, *Trans. Faraday Soc.*, **53**, 185 (1957).

(18) F. Bashforth and J. C. Adams, "An Attempt to Test the Theories of Capillary Action," Cambridge Univ. Press, 1883.

(19) Sieve 5A is the calcium variety of Breck's synthetic zeolite A.[11]

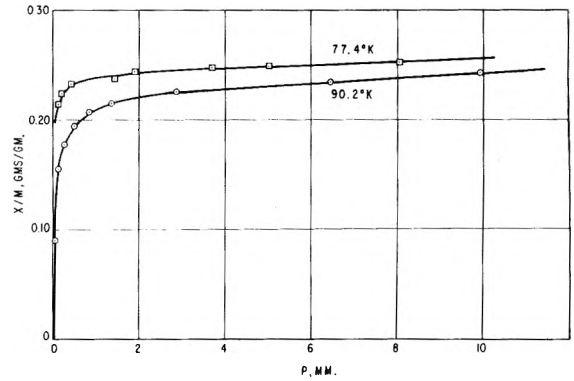

Fig. 1—Adsorption isotherms on Linde Molecular Sieve 5A

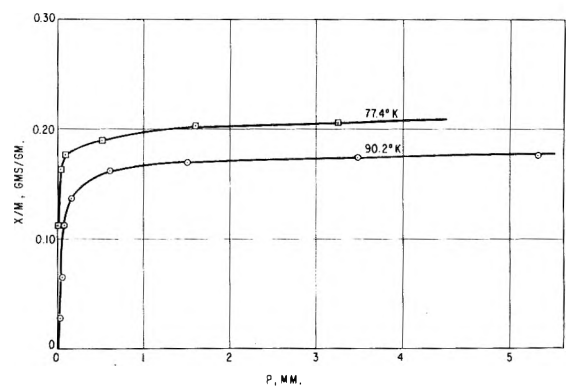

Fig. 2.—Adsorption isotherms of argon on Linde Molecular Sieve 5A containing preadsorbed CCl_2F_2 (x/m = 0.193). (The ordinate on this diagram corresponds with the uptake of argon per g. of original zeolite.)

The argon adsorption measurements were made at two different temperatures, with occasional changes from liquid nitrogen to liquid oxygen temperatures in the nitrogen temperature runs, and *vice versa*, to check the results. The experiments made at 0 and 29.6° with $CHClF_2$ were conducted similarly, the stirred water-bath being interchanged with a large ice-bath.

Isosteric heats were evaluated from the experimental isotherms on an IBM 650 computer, using least squares analysis to fit the isotherms to quartic polynomials. Residual errors involved in this analysis were so small as to be negligible.

(b) **Results. Argon Adsorption.**—The observed isotherms of the adsorption of argon on the zeolite and the modified zeolite are shown in Figs. 1 and 2, respectively. The isotherms are of the simple type I (Brunauer's classification), and the surface areas (calculated from the Langmuir plots) implied by these curves are listed in Table I.

TABLE I

SURFACE AREAS AVAILABLE TO ARGON ON MOLECULAR SIEVE 5A AND MODIFIED MOLECULAR SIEVE 5A

(areas in $m.^2/g.$)

T°K.	5A	Modified 5A
77.4	702	763
90.2	662	436

Figure 3 shows the isosteric heats of adsorption of argon in the two zeolite samples, plotted against extent of adsorption, measured in g./g. at 77.4°. This mode of plotting the heats was necessary since we had no justification for assigning any particular average value to V_m for the modified zeolite system in the temperature range covered. Consequently, a graph of heat *vs.* coverage fraction would contain a thoroughly artificial uncertainty which we wished to avoid. The vertical lines at x/m equal to 0.03 and 0.19 represent the boundaries of the field of confidence in the plotted results. Results obtained outside these bounds are subject to errors introduced by extrapolation, particularly

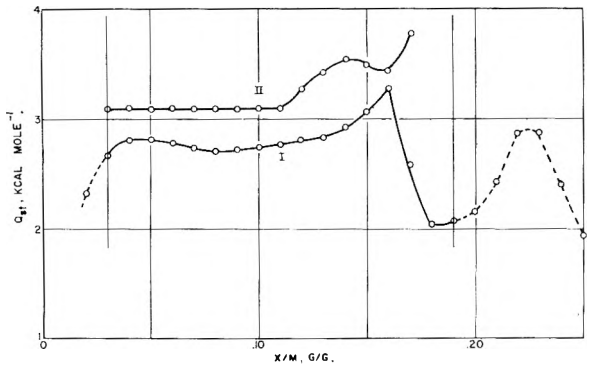

Fig. 3.—Isosteric heat plots for: 1, argon on clean zeolite; 2, argon on modified zeolite, plotted in kcal. mole^{-1} *vs.* argon uptake, x/m, in g. argon/g. original zeolite.

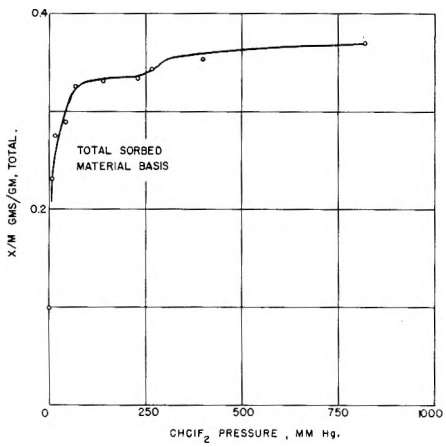

Fig. 4.—29.6° adsorption isotherm of $CHClF_2$ on Sieve 5A containing preadsorbed CCl_2F_2.

on the higher pressure side. This is due to the shape of the isotherms from which the heats have been computed.

It was found possible to remove the sorbed argon by pumping at room temperature without disturbing the CCl_2F_2.

(c) **Results. $CHClF_2$ Adsorption.**—A sample of zeolite was prepared as before so that the amount of CCl_2F_2 in the pores was 0.193 g./g. $CHClF_2$ vapor was admitted to the apparatus at 30° until the pressure was 5460 mm. Sufficient vapor was taken up that the amount of $CHClF_2$ corresponded approximately to x/m equal to 0.20, *i.e.*, a total x/m of 0.39. The system was pumped down for four hours at 150°. The weight of material adsorbed dropped to approximately x/m equal to 0.19, *i.e.*, the original value after CCl_2F_2 adsorption. It may be inferred that only the subsequently sorbed $CHClF_2$ was removed by the pumping, leaving the tightly bound CCl_2F_2 in the lattice. By further pumping at 250–300°, much more material was removed: the system was very gassy, since, at these temperatures, CCl_2F_2 begins to be removed.

Another sample of modified zeolite was prepared in which the amount of CCl_2F_2 corresponded with an x/m value of 0.11 (820 mm. CCl_2F_2 pressure at 29.6°). After evacuation, the system was dosed with $CHClF_2$ gas at 29.6° 17 times over a period of eight days. The final excess pressure of $CHClF_2$ gas was 7540 mm. The results, corrected for buoyancy effects, are shown on Figs. 4 and 5 together with the Langmuir isotherms on Fig. 6. The isotherms were unusual. The amounts adsorbed per g. of sieve were very large (x/m for $CHClF_2$ uptake alone was as much as 0.30), and are extraordinary when the amount of preadsorbed CCl_2F_2 is taken into account. The sample then was exposed to the atmosphere and pumped, after which $CHClF_2$ adsorption again was followed. The values coincided with those previously observed: exposure to the atmosphere did not affect this particular property of the modified zeolite. High pressure adsorption values then were measured at 29.6 and 0°. Finally, the $CHClF_2$ was removed from the system and compared with a reference sample by gas-liquid chromatography. There was no difference in the chromatograms: no decomposition had occurred, in strong contrast with the result on clean Sieve 5A.[20] Likewise, a controlled leak experiment conducted overnight during the sorption runs gave no indication of any chemical reaction.

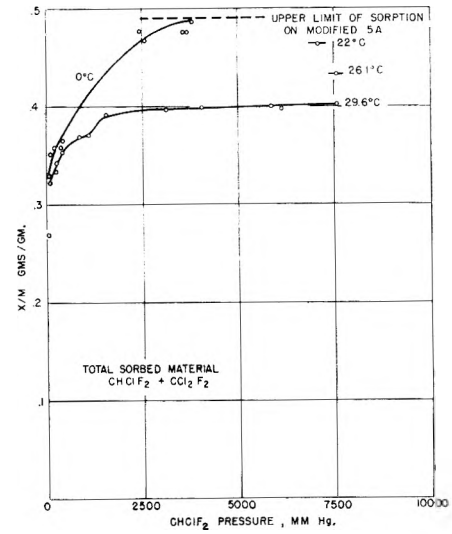

Fig. 5.—High pressure adsorption isotherms of $CHClF_2$ on Sieve 5A containing preadsorbed CCl_2F_2.

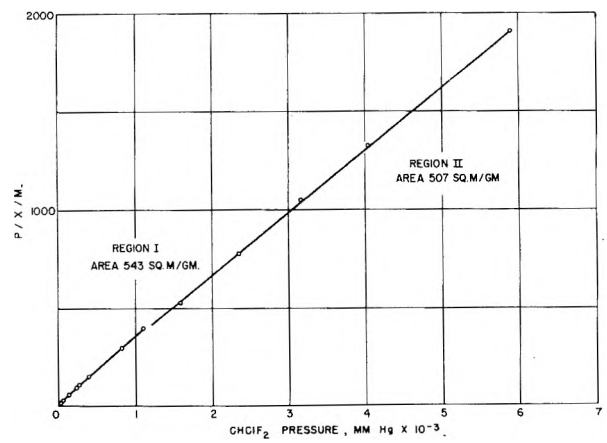

Fig. 6.—Langmuir plot for the adsorption of $CHClF_2$ on the modified sieve at 29.6°.

The adsorption of a mixture of CCl_2F_2 and $CHClF_2$ on the modified zeolite also was studied. An equal weight (58.3 mole % $CHClF_2$) mixture was used, and it was assumed that the partial pressure of each component was proportional to the molar fraction of that gas at the experimental pressures. Studies were made at total pressures of up to 500 mm. The kinetics of the system were followed; equilibrium was attained in about eight hours for each dose, compared with two hours for $CHClF_2$ alone (these time values are exact only for the geometry of this specific apparatus[16]: elsewhere they should be used only comparatively). The increases in weight with pressure in these experiments are those expected due to the partial pressure of $CHClF_2$ alone. The points were measured one a day, and the system was pumped between each dose, so that it was possible to analyze the residual gas after each point without confusing the results. The residual gas was depleted of $CHClF_2$: thus, in 5 hours at 30° and at *ca.* 120 mm. pressure, the $CHClF_2$ content of the gas fell from 58.3 to 38.3 mole %. No indication was obtained that the substrate was taking up anything other than $CHClF_2$. It was also shown possible to reverse the process merely by pumping the entire system. The pumped gas (residual and sorbed) was analyzed and was found to be of the same composition as the initial mixed gas sample.

(20) P. Cannon, *J. Am. Chem. Soc.*, **80**, 1766 (1958).

(21) Molecular Sieve Data Sheets, Linde Co., Tonawanda, N. Y.

(d) **Results. Water Adsorption.**—The adsorption of water vapor on the solid prepared in this way was followed at 25° on a glass and quartz balance. The isotherm was of Type 1, and is shown on Fig. 7 together with an isotherm[21] for water on the clean zeolite in the same pelletized form. The treated sample sorbs only slightly less water than does the clean material.

Discussion

The amounts of argon adsorbed at 77.4° at the monolayer point for synthetic zeolite A and for the modified zeolite are 161.3 cc./g. (0.2876 g./g.) and 175.4 cc./g. (0.3127 g./g.), respectively. These values are a little higher than those reported by Garden, Kington and Laing[22] for the adsorption of argon on calcium chabazite at 90.2°, even when the difference in temperature is noted. In the light of recent modifications of Wyart's[23] structure for chabazite by Dent and Smith,[24] to give a structure very like that assigned by Reed and Breck[12] to the synthetic zeolite that we used, we might have expected a more exact correspondence of the sorption data in the two cases.

Our measured isosteric heats on both zeolite specimens show the maximum at $\theta \simeq 0.7$ which was observed by Garden, Kington and Laing,[22] and analyzed by Kington[25] on the basis of a mutual interaction between argon molecules at an equilibrium distance from each other at $\theta \simeq 0.66$.

Inspection of the heat curves indicates that the differential entropies of adsorption ($S_S - S'_L$) are essentially monotonic and possess only slight minima at $\theta \sim 0.7$. The depth of the minimum in each case is of the order of 5 cal. mole^{-1} deg.$^{-1}$

The only major feature of difference between the heat plots is the approximately 400 cal. mole^{-1} difference between them, and the divergence at $x/m > 0.16$ ($\theta \sim 0.7$). This divergence is subject to considerable error introduced by extrapolation on the isotherm flat, and we shall not discuss it quantitatively. The difference of 400 cal. mole^{-1} is explicable in the following manner. Kington[25] showed by considering a random arrangement of argon atoms on sites in chabazite that the isosteric heat for this system at $\theta = 1$ should be 472 cal. mole^{-1} higher than at $\theta = 0$; he allotted three sites per cage to this material believing that no more than three argon atoms could be accommodated in each cage. Consequently, the increase in Q_{st} which he calculated corresponds with that due to the presence of clusters of three closely packed argon atoms. In the present case, the amount of preadsorbed CCl_2F (0.193 g./g.) corresponds most nearly with three molecules per cage. Using Breck and Reed's structure[12] for synthetic zeolite A and minimum and maximum diameters of 4.4 and 5.1 Å. for the CCl_2F_2 molecule (measured from projection diagrams, based on the values of atomic radii cited by Neuberger[26]), it is evident that within each cage there is available as much space as already has been occupied by the three CCl_2F_2 molecules. Consequently, on filling this residual space with a second sorbate, a total uptake of both sorbates of the observed order 0.4-0.5 g./g. may be expected. In the case of argon as a second phase, the observed weight increases correspond with the addition of between three and four atoms per cage, accounting for very nearly all the residual space.

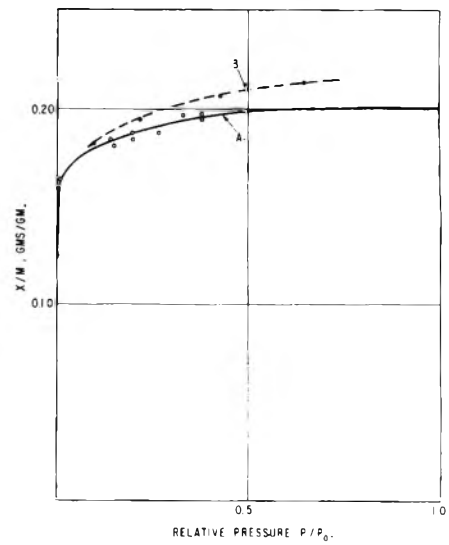

Fig. 7.—Adsorption of water vapor at 25° on: (A) Sieve 5A containing 0.193 g. CCl_2F_2/g. sieve; (B) clean Sieve 5A from reference 21, plotted as g. water/g. original sieve *vs.* reduced pressure.

If it is assumed that the preadsorbed material is present as localized clusters of about three molecules each, associated with the calcium ions in such a way as to present an essentially inert gas-like appearance to those argon molecules which are adsorbed near them, it would be expected that this preadsorbed "psuedo-argon" layer would cause the isosteric heat observed from the new argon adsorption to be 4-500 cal. mole^{-1} higher [25] than in the case of the clean zeolite, as indeed was observed. Since each one of the cluster of three CCl_2F_2 molecules would present a similar appearance to the incoming argon (Langmuir type non-interacting sites), a repetition of the sequence of events on the clean zeolite might be expected. This would include the appearance of a small maximum in the Q_{st}/θ plot at $\theta \sim 0.7$ (θ relating to argon sorbing on CCl_2F_2), since there is sufficient room for a total of 6-7 molecules in the cage. It can be argued that the maximum in Q_{st} should occur earlier, due to the generally crowded nature of the pore at this stage of occupation. An indication that this does indeed happen is to be seen in the heat plot. After this maximum has been passed, there would be room for an average of one or two more argon molecules in each cage. The filling of these residual sites would cause considerable hindrance of movement of the individual molecules in the adsorbed phase, and thus would be associated with higher energies than before. This would offer at least a qualitative interpretation of the upturn in Q_{st} at $x/m > 0.16$ in the case of argon absorption on the modified Sieve. The argon-clean zeolite system, because of the considerable residual free space in the cages at $\theta > 0.7$ gives the observed decrease in Q_{st}, if this same line of reasoning is applied there. The argon sorption results are thus consistent with a cluster model for the pre-adsorbed

(22) L. A. Garden, G. L. Kington and W. Laing, *Trans. Faraday Soc.*, **51**, 1558 (1955).
(23) J. Wyart, *Bull. soc. franc. min.*, **56**, 81 (1933).
(24) L. S. Dent and J. V. Smith, *Nature*, 1794 (1958).
(25) G. L. Kington, *Trans. Faraday Soc.*, **52**, 475 (1956).
(26) A. Neuberger, *Z. Krist.*, **93**, 1 (1936).

CCl_2F_2 molecules. Considerable further support for this idea is obtained from the results on the sorption of $CHClF_2$ into the zeolite containing preadsorbed CCl_2F_2. As described above, a salient feature of difference between the adsorption of $CHClF_2$ on the clean zeolite and that containing CCl_2F_2 is the reversibility observed with the latter substrate. Since the decomposition[5,20] which occurred on the clean substrate was due to the presence of exposed Ca^{++} ions, it appears that the preadsorbed CCl_2F_2 blocks these ions. The position of these ions is evidently around the "windows" leading into the pores, since variation in ionic type leads to variation in the effective window diameter.[11] Since the ions are blocked by CCl_2F_2 molecules, these latter must also be clustered around the windows in the structure. Corroborative support for this is obtained by our observation of the intensification of a "superlattice" X-ray diffraction pattern in the sample containing preadsorbed CCl_2F_2, corresponding with a cubic cell of twice the edge length as that described by Reed and Breck.[12] Their structure was based on a primitive cubic cell of edge 12.3 Å., but Barrer and Meier[27] observed lines corresponding with diffraction from a cell of twice this length in a specimen containing germanium in isomorphous substitution for silicon. We have seen similar lines in the original unsubstituted material, and they are intensified in the sample containing CCl_2F_2. We regard this as good presumptive evidence that the CCl_2F_2 molecules are distributed in a highly nonrandom manner throughout the channels, possibly on opposite walls of pairs of cages.

The adsorption results for water on the clean and modified zeolitic substrates show how general the described phenomena are, occurring in this case over a wide range of polarities of the second sorbate. The sorption of the second gas or vapor is thus not to be identified with some type of ion–dipole interaction, where the polarity of the sorbate would be expected to have a profound effect on the nature and extent of the phenomenon.

Conclusions

The results obtained by studying the zeolite with the preadsorbed phase all are consistent with the assumption that the CCl_2F_2 molecules are present in the channels in clusters, obscuring the charge-compensating cations from the incoming molecules of a second sorbate. It is attractive to speculate that other materials sorbing on the anhydrous, unmodified zeolite would behave similarly, and would be sorbed up to the point where the sphere of influence of the cations would be saturated. This would be as consistent with the observed constant liquid volumes of various sorbates[11] as would a model involving complete occupation of the channel space. The results of the present work indicate that the second model is not necessarily valid for a one component sorption in an open network structure such as a zeolite.

Acknowledgments.—We wish to thank Drs. G. L. Gaines and R. C. DeVries for helpful discussions.

(27) R. M. Barrer and W. M. Meier, *Trans. Faraday Soc.*, **54**, 1 (1958).

THE MOLECULAR CONFIGURATION OF ERUCIC AND *cis*-NERVONIC ACIDS IN THE CRYSTAL STRUCTURES

BY B. M. CRAVEN

The Crystallography Laboratory, The University of Pittsburgh, Pittsburgh, Pennsylvania

Received February 19, 1959

The general features of the crystal structures of erucic and *cis*-nervonic acids, two *cis*-ethylenic long chain fatty acids are deduced from the similarity of the single crystal X-ray diffraction patterns with that of *cis*-DL(11–12)-methyleneoctadecanoic acid, a typical *cis*-cyclopropyl long chain fatty acid, whose crystal structure has previously been established. It is concluded that the *cis*-ethylenic molecules are bent at the double bond so that the over-all configuration, as in the *cis*-cyclopropyl acids, is like that of a boomerang.

Introduction

The crystal structures of one *trans* and three *cis* long chain cyclopropyl fatty acids recently have been studied,[1–4] and it has been found that whereas the molecules are straight in the *trans* compound, in the *cis* they are bent at the cyclopropyl ring so that when the ring is near the center of the molecule the over-all configuration is like a boomerang. This same distinction might be expected in the configurations of the *cis*- and *trans*-ethylenic long chain fatty acids. Evidence for the bent chain configuration for two of the *cis*-ethylenic fatty acids, erucic ($C_{22}H_{42}O_2$) and *cis*-nervonic ($C_{24}H_{46}O_2$), has been derived from the similarity in the single crystal X-ray data of the two *cis*-ethylenic acids and the *cis*-cyclopropyl acids.

Erucic acid had been studied previously by Malkin and Carter,[5] who showed by X-ray powder photography that erucic and the corresponding *trans*-brassidic acid had quite different crystal structures, although brassidic acid was similar in structure to the corresponding saturated behenic acid ($C_{22}H_{44}O_2$) in which the molecules are straight chains.

Experimental

Crystals for these single crystal studies were obtained

(1) T. Brotherton and G. A. Jeffrey, *J. Am. Chem. Soc.*, **79**, 5132 (1957).

(2) T. Brotherton, B. M. Craven and G. A. Jeffrey, *Acta Cryst.*, **11**, 546 (1958).

(3) B. M. Craven and G. A. Jeffrey, *ibid.*, in press.

(4) B. M. Craven and G. A. Jeffrey, *Nature*, in press.

(5) T. Malkin and M. G. R. Carter, *J. Chem. Soc.*, 554 (1947).

with difficulty by crystallization from acetone and water mixtures. The crystals were multiply twinned so that even apparently single crystals were really slightly disoriented stacks of thin platelets, developed on the (001) face. Because of their softness, crystals frequently were also bent.

The lattice parameters were measured from oscillation, Weissenberg and precession photographs. The photographs were taken with Cu Kα X-radiation. The diffracted spots invariably were streaky and of differing sizes, so that reliable intensity measurements suitable for a complete structure analysis could not be made.

The Crystal Data.—From single crystal measurements these crystal data were obtained.

Erucic Acid $CH_3(CH_2)_7CH{=}CH(CH_2)_{11}COOH$ m.p. 33°
Triclinic

$a = 5.46 \pm 0.05$ Å. $\alpha = 102° \pm 30'$
$b = 5.17 \pm 0.05$ Å. $\beta = 96° \pm 30'$
$c = 47.8 \pm 0.1$ Å. $\gamma = 65° \pm 30'$
$U = 1191$Å.^{3} $Z = 2$ molecules/unit cell
$d_{obs} = 0.95$ g./cm.^{3} $d_x = 0.95$ g./cm.^{3}
Space group $P1$ or $P\bar{1}$

cis-Nervonic Acid $CH_3(CH_2)_7CH{=}CH(CH_2)_{13}COOH$
Triclinic M.p. 39°

$a = 5.46 \pm 0.05$ Å. $\alpha = 102° \pm 30'$
$b = 5.21 \pm 0.05$ Å. $\beta = 96° \pm 30'$
$c = 51.2 \pm 0.1$ Å. $\gamma = 65° \pm 30'$
$U = 1287$Å.^{3} $Z = 2$ molecules/unit cell
$d_{obs} = 0.95$ g./cm.^{3} $d_x = 0.95$ g./cm.^{3}
Space group $P1$ or $P\bar{1}$

The Crystal Structures.—Although a complete analysis has not been made, it is possible, by comparison with the known structure of the *cis*-cyclopropyl acids, to make some general deductions concerning the crystal structures of these two acids.

The crystal data for erucic and *cis*-nervonic acids can best be compared with those of *cis*-DL-(11–12)-methyleneoctadecanoic acid

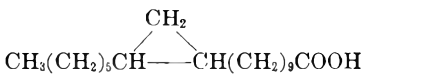

a typical *cis* long chain cyclopropyl acid, by referring the ethylenic acid to a C centered lattice (see Table I). The crystal structures are then comparable as seen in projection down the a and b crystallographic axes.

TABLE I

Crystal class Space group	Erucic acid Triclinic C1 or C$\bar{1}$	*cis*-Nervonic acid Triclinic C1 or C$\bar{1}$	*cis*-DL-(11–12)-Methylene-octadecanoic acid Monoclinic A $2/a$
a, Å.	9.88	9.87	8.93
b, Å.	5.17	5.21	5.10
c, Å.	47.8	51.2	88.6
α	102°	102°	90°
β	91	91	98
γ	87	87	90
Z	4 molecules/ cell	4 molecules/ cell	8 molecules/ cell
Density, g./cm.^{3}	0.95	0.95	1.05

(i) **The a-Projection.**—Analogous to the very intense 020 reflection of *cis*-DL-(11–12)-methyleneoctadecanoic acid (hereafter *cis* M.O. acid) there is a very intense group of reflections (020, 021 and 02$\bar{1}$) in erucic and *cis*-nervonic acids. These are all much stronger than any other $0kl$ reflection. Because of the very long c spacings, the crystallographic planes 021 and 02$\bar{1}$ do not differ greatly in orientation from 020 and so it would be expected that in the a-projection, the molecules would

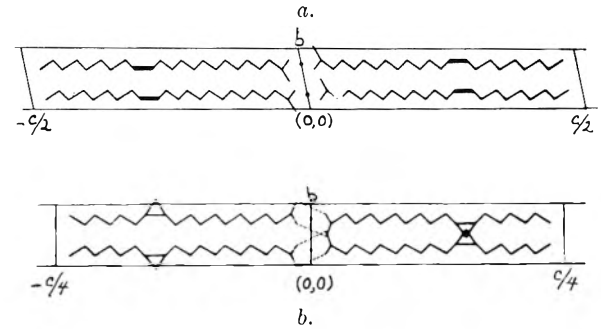

Fig. 1.—Diagrammatic projection down the a-axis of the structures: (a) erucic acid; (b) *cis*-D,L-(11–12)-methyleneoctadecanoic acid.

appear as almost straight chains approximately parallel to (010) and separated by distances of $b/2$. This has been shown to be true for *cis* M.O. acid although (see Fig. 1), in this structure, alternate molecules are D and L, related by glide planes parallel to (010), whereas there are no glide

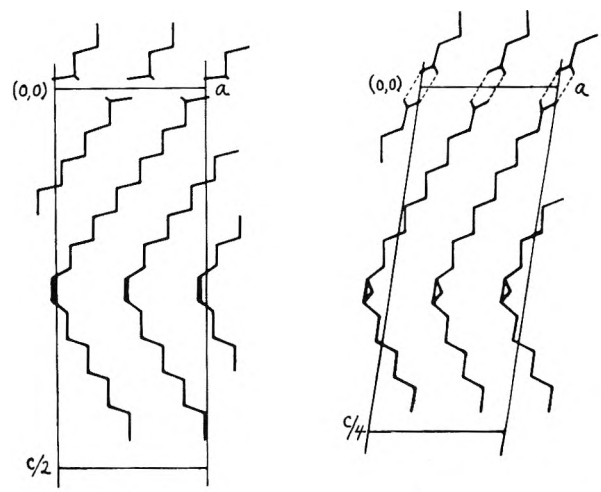

Fig. 2.—Diagrammatic projection down the b-axis of the structure: (a) erucic acid; (b) *cis*-D,L-(11–12)-methyleneoctadecanoic acid.

planes in the triclinic ethylenic acid structures. The ethylenic acid molecules are related in this projection by a simple translation of $b/2$.

In the structure proposed for erucic acid it is assumed that the space group is P$\bar{1}$ wherein molecules are also related in pairs by centers of symmetry (drawn in Fig. 1a as space group C$\bar{1}$ for comparison with Fig. 1b.)

(ii) **The b-Projection.**—The similarity among the $h0l$ Weissenberg photographs of all three acids is most striking, so that in this projection the structures should be very closely related. In each case, there is a group of very strong $20l$ and $20\bar{l}$ reflections almost symmetrically disposed with respect to the $00l$ reflections, indicating that the structures contain chains of atoms separated by translations of $a/2$, lying both acutely and obtusely

with respect to (001). If the molecules were straight chains, but overlapping in this projection to form crosses, the intensities of the groups of $20l$ and $20\bar{l}$ reflections would be about the same. This is not observed, and so it is assumed that the longer carboxyl to double bond chain is parallel to the $20l$ planes, whose reflections are stronger, while the shorter double bond to methyl group chain is parallel to the $20\bar{l}$ planes, whose reflections are weaker.

This is compatible with the bent molecule configuration for the *cis*-unsaturated acids, closely resembling that which has been established for *cis* M.O. acid (see Fig. 2).

In Table II, the strongest $20l$ and $20\bar{l}$ reflections

TABLE II

THE STRONG $20l$ AND $20\bar{l}$ REFLECTIONS

Erucic acid		*cis*-Nervonic acid		*cis*-DL-(11–12)-Methylene-octadecanoic acid		Obsd. angles of chain axes
207	53°	208	51°	208	61°	
208	49°	209	48°	2010	57°	57°
209	46°	2010	45°			
$20\bar{5}$	118°	$20\bar{5}$	116°	$20\bar{1}\bar{4}$	120°	118°
$20\bar{6}$	122°	$20\bar{6}$	121°			

are listed together with the angles which the corresponding crystallographic planes make with (001) when measured in the plane of the *b*-projection. The orientation of the chain axes can be determined approximately by averaging the angles within each group of planes. They are compared with the values observed for *cis* M.O. acid. In Table III are listed the calculated angles of bend in the boomerangs and the observed value for *cis* M.O. acid.

The *c*-axis dimensions can be calculated for each acid, subject to the assumptions

(a) The carbon chains are at maximum extension with

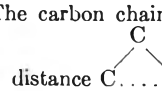

distance C....C of 2.5 Å.

(b) The distance C=C is 1.4 Å.

(c) The distance $-CH_3 \cdots\cdots CH_3-$ is 4.0 Å.

(d) The distance

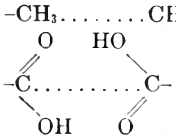

is 3.4 Å., as observed in *cis* M.O. acid.

Then, for erucic acid, $c_{calcd} = 49.0$ Å. (*cf.* $c_{obsd} = 47.8$ Å.) and for *cis*-nervonic acid, $c_{calcd} = 52.4$ Å. (*cf.* $c_{obsd} = 51.2$ Å.)

Discussion

In the structure of *cis* M.O. acid, it was found that the carbon atom chains were coplanar near the cyclopropane ring and equally inclined at about 50° in the same sense to the (010) plane, giving a non-crystallographic mirror plane perpendicular to (010) through the center of the cyclopropyl ring.

TABLE III

APPROXIMATE ANGLE OF BEND BETWEEN CHAINS, DEGREES

Erucic acid	109
cis-Nervonic acid	109
cis-DL-(11–12)-methylene-octadecanoic acid	119 (*cf.* obsd. value 119°)

The geometry is probably very similar in the unsaturated acids, although the angle between the chain axes at the double bond is about 109° in the *b*-projection, which is more acute by about 10° than in *cis* M.O. acid. This can be the case if the planes of the chains are at a steeper angle to (010) as a result of rotations of about 5° about each of the C–C single bonds adjacent to the double bond.

The difference between the observed and calculated *c*-axis dimensions is 0.6 Å. per molecule. This could be caused by the twisting of the plane of the carbon chain away from the maximum extension configuration, as a result of the chain having to conform at the carboxyl end to the stereochemical requirements of hydrogen bonding. Such twisting was observed in *cis* M.O. acid and did result in a shortening of the C_I to C_{II} chain by 0.5 Å. per molecule, as compared with a strictly planar alignment of carbon atoms.

The steric factors which give rise to the bent configuration in the crystal are likely to be important in the adsorption of these acids on surfaces and in surface films and monolayers. This is in agreement with the work of Rideal[6] who pointed out that *trans*-ethylenic acid molecules should be straight and *cis* molecules bent. He showed that oxidation of a monomolecular surface film of erucic acid could occur readily, but in the case of the *trans*-brassidic acid, only with difficulty. He argued that the reacting centers in the *trans* acid were protected by the closer packing of molecules which was possible with straight chains.

Acknowledgments.—I am grateful to Dr. K. K. Carrol, of the University of West Ontario, and Dr. T. Malkin, of The University of Bristol, for supplying samples of erucic and *cis*-nervonic acid, and also to Dr. G. A. Jeffrey for most helpful discussions.

This work was supported by a Research Grant (E-1423) from the Department of Health, Education and Welfare, The Public Health Service, The National Institutes of Health.

(6) E. K. Rideal, *Endeavour*, **4**, 83 (1945).

THE THERMODYNAMIC PROPERTIES OF THE SYSTEM: HYDROCHLORIC ACID, SODIUM CHLORIDE AND WATER FROM 0 TO 50°

BY HERBERT S. HARNED

Contribution No. 1526 from the Department of Chemistry of Yale University, New Haven, Conn.

Received February 25, 1959

The activity coefficients of hydrochloric acid in sodium chloride at 1, 2 and 3 constant total molalities from 0 to 50° have been computed. From these results, the parameters of equations which permit a simple calculation of the activity coefficient of sodium chloride in these solutions have been calculated. These numerical procedures lead to an estimate of the excess heat of mixing. Tables of osmotic coefficients of the acid and the salt solutions are appended. By their use the osmotic coefficients of the mixtures may be computed.

There are two fields for which a fundamental knowledge of the thermodynamic properties of solutions of two or more electrolytes is essential. The first of these is ion-exchange studies which require an exact knowledge of the solution medium. The second field is that of diffusion of all the components in these systems where a precise knowledge of the gradients of the chemical potentials is required.

Electromotive forces of cells of the type

$$H_2/HCl(m_1),\ NaCl(m_2)/AgCl\text{-}Ag$$

have shown that the activity coefficient, γ_1, of the acid varies according to the linear equation

$$\log \gamma_1 = \log \gamma_{1(0)} - \alpha_{12} m_2 \ldots . \qquad (1)$$

when the system is maintained at constant total molality, temperature and pressure. Here $\log \gamma_{1(0)}$ is the activity coefficient of the pure acid of concentration $m_1 = m$ and m_2 is the concentration of the sodium chloride. If equation 1 is valid, then one can apply the method of McKay[1,2] to compute the parameter α_{21} in the analogous equation

$$\log \gamma_2 = \log \gamma_{2(0)} - \alpha_{21} m_1 \qquad (2)$$

where γ_2 is the activity coefficient of the salt in the mixture and $\gamma_{2(0)}$ is its activity coefficient at a concentration $m_2 = m$. For systems containing two uni-univalent electrolytes, McKay's equation for α_{21} is

$$\alpha_{21} m_1 = [\log \gamma_{2(0)}/\log \gamma_{1(0)}]_{m=m_2}^{m=m} + m_2[\alpha_{12}]_{m=m_2}^{m=m} + \int_{m_2}^{m_1} \alpha_{12} dm \qquad (3)$$

The limiting values of α_{21} when m_1 approaches m, $\alpha_{21(m)}$, and when m_1 approaches zero, $\alpha_{21(0)}$, are

$$\alpha_{21(m)} = \log (\gamma_{2(0)}/\gamma_{1(0)})_m + \int_0^m \alpha_{12} dm \qquad (4)$$

and

$$d_{21(0)} = \frac{d \log (\gamma_{2(0)}/\gamma_{1(0)})}{dm} + m \frac{d\alpha_{12}}{dm} + \alpha_{12} \qquad (5)$$

respectively.

The Parameters α_{12} and α_{21}.—In Table I, the quantities which may be employed for the accurate calculation of the activity coefficient of hydrochloric acid, γ_1, and sodium chloride, γ_2, in the mixtures at total molalities 1. 2, and 3 are recorded. The data employed were derived from the experimental results of Harned and Ehlers,[3] Harned and Nims[4] and Harned and Mannweiler[5] as recorded by Harned and Owen.[6] The linear variation of $\log \gamma_1$ has been premised and α_{21} computed by equations 3, 4 and 5. The result of this latter

TABLE I

QUANTITIES FOR THE CALCULATION OF THE ACTIVITY COEFFICIENTS OF HYDROCHLORIC ACID, γ_1, AND SODIUM CHLORIDE, γ_2, IN SOLUTIONS OF 1, 2 AND 3 TOTAL MOLALITIES

t	$\log \gamma_{1(0)}$	$\log \gamma_{2(0)}$	$\alpha_{12(0)}$	$\alpha_{21(0)}$	β_{21}
		$m = m_1 + m_2 = 1$			
0	$\bar{1}.9253$	$\bar{1}.8045$	0.0415	−0.0735	−0.0030
10	$\bar{1}.9188$	$\bar{1}.8122$	.0375	− .0655	− .0022
20	$\bar{1}.9118$	$\bar{1}.8156$	.0335	− .0594	− .0015
25	$\bar{1}.9079$	$\bar{1}.8169$	.0315	− .0560	− .0010
30	$\bar{1}.9041$	$\bar{1}.8176$	.0299	− .0544	− .0005
40	$\bar{1}.8957$	$\bar{1}.8176$	.0258	− .0510	+ .0007
50	$\bar{1}.8863$	$\bar{1}.8169$	.0229	− .0484	+ .0015
		$m = m_1 + m_2 = 2$			
0	0.0326	$\bar{1}.8014$	0.0401	−0.0670	−0.0030
10	.0224	$\bar{1}.8142$	.0365	− .0610	− .0022
20	.0103	$\bar{1}.8228$	.0325	− .0570	− .0015
25	.0039	$\bar{1}.8261$	.0308	− .0550	− .0010
30	$\bar{1}.9969$	$\bar{1}.8287$	.0290	− .0530	− .0005
40	$\bar{1}.9824$	$\bar{1}.8312$	.0252	− .0510	+ .0007
50	$\bar{1}.9697$	$\bar{1}.8312$	.0214	− .0500	+ .0015
		$m = m_1 + m_2 = 3$			
0	0.1620	$\bar{1}.8195$	0.0396	−0.0670	−0.0015
10	.1464	$\bar{1}.8395$	.0360	− .0610	− .0012
20	.1287	$\bar{1}.8716$	.0320	− .0570	− .0008
25	.1192	$\bar{1}.8762$	.0300	− .0540	− .0006

calculation is illustrated by Fig. 1 where $(-\alpha_{21})$ has been plotted against m_1 for mixtures of constant total molality of 2 M. It is clear that $(-\alpha_{21})$ varies somewhat with m_1 and that this variation can be expressed within narrow limits by the linear equation

$$\alpha_{21} = \alpha_{21(0)} + \beta_{21} m_1 \qquad (6)$$

where $\alpha_{21(0)}$ is the value of α_{21} when m_1 equals zero. We shall now rewrite equations 1 and 2 as

$$\log \gamma_1 = \log \gamma_{1(0)} - \alpha_{12(0)} m_2 - \beta_{12} m_2^2 \qquad (7)$$

$$\log \gamma_2 = \log \gamma_{2(0)} - \alpha_{21(0)} m_1 - \beta_{21} m_1^2 \qquad (8)$$

where for the system under discussion β_{12} is zero.

(1) H. A. C. McKay, *Trans. Faraday Soc.*, **51**, 903 (1955).

(2) H. S. Harned and B. B. Owen, "The Physical Chemistry of Electrolytic Solutions," 3rd Edition, Reinhold Publ. Corp., New York, N. Y., 1958, p. 628–629.

(3) H. S. Harned and R. W. Ehlers, *J. Am. Chem. Soc.*, **55**, 2179 (1933).

(4) H. S. Harned and L. F. Nims, *ibid.*, **54**, 423 (1932).

(5) H. S. Harned and G. E. Mannweiler, *ibid.*, **57**, 1873 (1935).

(6) Ref. 2, Tables (11-4-1A), (12-1-2A) and (14-2-1A).

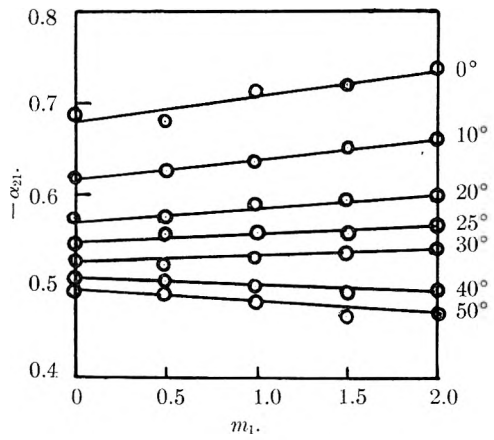

Fig. 1. — $-\alpha_{21}$ *versus* m_1.

Theoretical Considerations.—As first shown by Glueckauf, McKay and Mathieson,[7] the cross differentiation equation

$$\left.\frac{\partial \log \gamma_1}{\partial m_2}\right]_{m_1} = \left.\frac{\partial \log \gamma_2}{\partial m_1}\right]_{m_2} \quad (9)$$

will introduce certain restrictions upon the use of equations such as (7) and (8) which are used to express the variations of the activity coefficients. If we let $m_1 = mx$ and $m_2 = m(1 - x)$ and $m = m_1 + m_2$, substitution of equations 7 and 8 in equation 9 yields

$$\frac{d \log \gamma_{1(0)}}{dm} - \alpha_{12(0)} - (1 - x)m\frac{d\alpha_{12(0)}}{dm} - 2(1 - x)m\beta_{12} - (1 - x)^2m^2\frac{d\beta_{12}}{dm} = \frac{d \log \gamma_{2(0)}}{dm} - \alpha_{21(0)} - xm\frac{d\alpha_{21(0)}}{dm} - 2xm\beta_{21} - x^2m^2\frac{d\beta_{21}}{dm} \quad (10)$$

Since $\log \gamma_{1(0)}$, $\log \gamma_{2(0)}$, $\alpha_{12(0)}$, $\alpha_{21(0)}$, β_{12} and β_{21} are functions of m only, this equation is true for all values of x when

$$xm\frac{d\alpha_{12(0)}}{dm} + 2mx\beta_{12} + 2m^2x\frac{d\beta_{12}}{dm} - m^2x^2\frac{d\beta_{12}}{dm} = -xm\frac{d\alpha_{21(0)}}{dm} - 2mx\beta_{21} - m^2x^2\frac{d\beta_{21}}{dm} \quad (11)$$

Divide by mx, whence

$$\frac{d\alpha_{12(0)}}{dm} + 2\beta_{12} + 2m\frac{d\beta_{12}}{dm} - mx\frac{d\beta_{12}}{dm} = -\frac{d\alpha_{21(0)}}{dm} - 2\beta_{21} - mx\frac{d\beta_{21}}{dm} \quad (12)$$

If this is true for all values of x, then

$$\frac{d\beta_{12}}{dm} = \frac{d\beta_{21}}{dm};\ \frac{d(\beta_{12} - \beta_{21})}{dm} = 0;\ (\beta_{12} - \beta_{21}) = \text{constant} \quad (13)$$

and

$$\frac{d(\alpha_{12(0)} + \alpha_{21(0)})}{dm} + 2(\beta_{12} + \beta_{21}) + 2m\frac{d\beta_{12}}{dm} = 0 \quad (14)$$

By symmetry

$$\frac{d(\alpha_{21(0)} + \alpha_{12(0)})}{dm} + 2(\beta_{21} + \beta_{12}) + 2m\frac{d\beta_{21}}{dm} = 0 \quad (15)$$

and thus

$$\frac{d(\alpha_{12(0)} + \alpha_{21(0)})}{dm} + 2(\beta_{12} + \beta_{21}) + 2m\frac{d(\beta_{12} + \beta_{21})}{dm} = \frac{d(\alpha_{12(0)} + \alpha_{21(0)})}{dm} + 2\frac{dm(\beta_{12} + \beta_{21})}{dm} \quad (16)$$

$$= \frac{d[\alpha_{12(0)} + \alpha_{21(0)} + 2m(\beta_{12} + \beta_{21})]}{dm} = 0 \quad (17)$$

whence

$$(\alpha_{12(0)} + \alpha_{21(0)}) + 2m(\beta_{12} + \beta_{21}) = \text{constant} \quad (18)$$

The restriction imposed by this relation and the requirement of the constancy of $(\beta_{12} - \beta_{21})$ are the only restrictions on the use of the quadratic forms imposed by thermodynamics.

Critique of the Calculation by the Quadratic Forms.—Since β_{12} has been assumed to be zero in these calculations and since thermodynamics requires the constancy of $(\beta_{12} - \beta_{21})$, β_{21} must be independent of the total concentration if the quadratic equations are valid. As far as could be judged from the existing data, this condition is fulfilled at 1 and 2 total molality but not at higher concentrations. This conclusion is evidenced by the results at 3 total molality where the values of β_{21} are less than those at the lower concentrations. This discrepancy is somewhat greater at the lower temperatures. That β_{21} is less at the higher concentration is in accord with the earlier calculations which indicated that above two molal total molality, equations 7 and 8 can be used without the quadratic terms at 25°.

A very severe test illustrated by Table II is imposed by the condition expressed by equation 18.

TABLE II

COMPARISON OF $(\alpha_{12(0)} + \alpha_{21(0)}) + 2m\beta_{21}$ AT DIFFERENT TOTAL MOLALITIES, m

t	$m = 1$	$m = 2$	$m = 3$
0	−0.0380	−0.0389	−0.0454
10	− .0300	− .0343	− .0382
20	− .0274	− .0305	− .0340
25	− .0265	− .0282	− .0300
30	− .0255	− .0260	...
40	− .0237	− .0230	...
50	− .0225	− .0226	...

In this table values of $(\alpha_{12(0)} + \alpha_{21(0)}) + 2m\beta_{21}$ at total concentrations of 1, 2 and 3 total molalities are recorded. This quantity appears to vary with the concentration with the largest variation occurring at 0°.

The Excess Heat of Mixing.—Recently, values of the excess heat of mixing have been obtained for mixtures of uni-univalent electrolytes by Young, Wu and Krawetz.[8] It is a matter of considerable interest to investigate whether the present calculations of the activity coefficients are consistent with the experimental heats of mixing. To accomplish this result, we shall compute the excess free energy of mixing, $\Delta F_M{}^E$, by extending the derivation of McKay[9] and investigate the variation of this quantity with temperature.

As stated by McKay, the excess free energy of mixing is

$$\Delta F_M{}^E = 2RT\left[m_2 \ln \frac{\gamma_2}{\gamma_{2(0)}} + m_1 \ln \frac{\gamma_1}{\gamma_{1(0)}} - m_1(\phi - \phi_{1(0)}) - m_2(\phi - \phi_{2(0)})\right] \quad (19)$$

(7) E. Glueckauf, H. A. C. McKay and A. R. Mathieson, *J. Chem. Soc.*, **5**, 299 (1949); *Trans. Faraday Soc.*, **47**, 428 (1951).

(8) T. F. Young, Y. C. Wu and A. A. Krawetz, *Trans. Faraday Soc.*, 37 (1958).

(9) H. A. C. McKay, *ibid.*, 76 (1958).

where ϕ, $\phi_{1(0)}$ and $\phi_{2(0)}$ are the osmotic coefficients of the mixture, the acid in water, and the salt in water at concentration m, respectively. Upon substituting equations 7 and 8, this equation becomes

$$\Delta F_M{}^E = 2RT[2.303m_1(-\alpha_{12(0)}m_2 - \beta_{12}m_2{}^2) + 2.303m_2(-\alpha_{21(0)}m_1 - \beta_{21}m_1{}^2) - m_1(\phi - \phi_{1(0)}) - m_2(\phi - \phi_{2(0)})] \quad (20)$$

The quantities $(\phi-\phi_{1(0)})$ and $(\phi-\phi_{2(0)})$ may be computed by the Gibbs–Duhem equation and if equations 7 and 8 are employed, the result is

$$(\phi - \phi_{2(0)}) = \frac{2.303m}{2}\left[(\alpha_{12(0)} + \alpha_{21(0)})\frac{m_1{}^2}{m^2} - 2\alpha_{21(0)}\frac{m_1}{m} + 2m(\beta_{12} - \beta_{21})\frac{m_1{}^2}{m^2} - \frac{4}{3}m(\beta_{12} - \beta_{21})\frac{m_1{}^3}{m^3}\right] \quad (21)$$

A similar equation for $(\phi-\phi_{1(0)})$ is obtained by changing subscript 1 to 2 and *vice versa*.[10] Substitution of these values of $(\phi-\phi_{1(0)})$ and $(\phi-\phi_{2(0)})$ in equation 20 we obtain

$$\Delta F_M{}^E = +2.303RTm_1m_2\left[(\alpha_{12(0)} + \alpha_{21(0)}) + 2(\beta_{12}m_1 + \beta_{21}m_2) - \frac{4}{3}(\beta_{12} - \beta_{21})(m_1 - m_2)\right] \quad (22)$$

for the excess free energy of mixing. We shall restrict our calculations to the case where both electrolytes have the same concentration ($m_1 = m_2$) and β_{12} equals zero. Under these conditions equation 22 reduced to

$$\Delta F_M{}^E = -2.303RTm_1m_2[(\alpha_{12(0)} + \alpha_{21(0)}) + 2\beta_{21}m_2] \quad (23)$$

The excess heat of mixing $\Delta H_M{}^E$ is obtained from

$$\Delta H_M{}^E = T^2\frac{d\left(\frac{-\Delta F_M{}^E}{T}\right)}{dT} = 2.303RT^2m_1m_2\frac{d[(\alpha_{12(0)} + \alpha_{21(0)}) + 2\beta_{21}m_2]}{dT} \quad (24)$$

Equation 23 with the omission of the β-term was derived by McKay. It has a quadratic form as does the equation for $\Delta H_M{}^E$. This result is in close accord with results of Young, Wu and Krawetz.

It is interesting to note that the excess volume of mixing at constant temperature has a quadratic form. Thus

$$\Delta v_M{}^E = \left[\frac{d\Delta F_M{}^E}{dP}\right]_T = -2.303RTm_1m_2\frac{d[(\alpha_{12(0)} + \alpha_{21(0)}) + 2\beta_{21}m_2]}{dP} \quad (25)$$

Harned and Owen[11] have outlined the conditions under which the observed quadratic variation of the excess volume of mixing is in accord with the linear variation rule.

In Table III, both the values of $(\alpha_{12(0)} + \alpha_{21(0)})$ and $(\alpha_{12(0)} + \alpha_{21(0)}) + 2m_2\beta_{21}$ when $m_1 = m_2$ are given for 1 and 2 M total molalities. The temperature coefficient of $(\alpha_{12(0)} + \alpha_{21(0)}) + 2m_2\beta_{21}$ is positive in the neighborhood of 25° and the difference between the 20 and 30° divided by ten gives a temperature coefficient of the order of 0.00024 to 0.00025 at both total molalities. At

(10) See ref. 2, p. 616, for the derivation of equation 21.
(11) Ref. 2, p. 399–401.

TABLE III

VALUES OF $(\alpha_{12(0)} + \alpha_{21(0)})$ AND $(\alpha_{12(0)} + \alpha_{21(0)}) + 2m_2\beta_{21}$ WHEN $m_1 = m_2$ FROM 0 TO 50° AT 1 AND 2 TOTAL MOLALITIES

	$m = 1$		$m = 2$	
t	$(\alpha_{12(0)} + \alpha_{21(0)})$	$(\alpha_{12(0)} + \alpha_{21(0)}) + \beta_{21}$	$(\alpha_{12(0)} + \alpha_{21(0)})$	$(\alpha_{12(0)} + \alpha_{21(0)}) + 2\beta_{21}$
0	−0.0320	−0.0350	−0.0269	−0.0329
10	− .0280	− .0302	− .0255	− .0299
20	− .0259	− .0274	− .0245	− .0275
25	− .0251	− .0261	− .0242	− .0262
30	− .0245	− .0250	− .0240	− .0250
40	− .0252	− .0245	− .0258	− .0244
50	− .0255	− .0240	− .0286	− .0256

1 M total molality, when $m_1 = m_2 = 0.5$, $\Delta H_M{}^E$ will be approximately

$$\Delta H_M{}^E \sim 2.303 \times 2 \times (298.16)^2 \times (0.5)^2 \times 0.00024 \sim 25 \text{ cal. at } 25° \text{ per mol of solute}$$

according to equation 24. At 2 M total molality when $m_1 = m_2 = 1$, $\Delta H_M{}^E$ per mole of solute will be about 50 cal. since the temperature coefficient of $(\alpha_{12(0)} + \alpha_{21(0)}) + 2m_2\beta_{21}$ is the same as at 1 M total molality.

The result of 25 cal. at 1 M total molality compares favorably with that of Young, Wu and Krawetz who report 31 cal. for $\Delta H_M{}^E$ at 25° obtained by calorimetry. Of course, the calorimetric result is much more reliable than the one derived from the electromotive force measurements. However, the approximate agreement in sign and magnitude of the values obtained by both methods indicate our equations 7 and 8 with the parameters in Table I will yield precise values of γ_1 and γ_2.

Although high precision cannot be claimed for our estimate of $\Delta H_M{}^E$, the present calculation indicates the probable behavior of this quantity as a function of temperature. Thus, at 1 M total concentration when $m_1 = m_2 = 0.5$, $\Delta H_M{}^E$ will be approximately 35, 25 and 5 cal. at 10, 25 and 40°, respectively. There is thus every indication that as the temperature increases $\Delta H_M{}^E$ will pass through 0 and then become negative. In this respect, the acid–sodium chloride system in the neighborhood of 50° will resemble the acid–potassium chloride system at 25°. The $\Delta H_M{}^E$ of the latter system at this temperature is approximately 3 cal. negative.

Osmotic Coefficients.—The osmotic coefficient ϕ of the mixtures may be obtained by equation 21 if the osmotic coefficient of the salt in water, $\phi_{2(0)}$ at the concentration m is known or by a similar equation for $\phi - \phi_{1(0)}$ if the osmotic coefficient of the acid in water $\phi_{1(0)}$ is known. From ϕ, the activity, a_w, of the third component, water, may

TABLE IV

OSMOTIC COEFFICIENTS OF HYDROCHLORIC ACID, $\phi_{1(0)}$ AND SODIUM CHLORIDE, $\phi_{2(0)}$

m	0°	10°	20°	25°	30°	40°	50°
				$\phi_{1(0)}$			
1	1.055	1.049	1.043	1.040	1.036	1.030	1.022
2	1.216	1.206	1.197	1.189	1.183	1.170	1.156
3	1.394	1.374	1.357	1.348	...	...	...
				$\phi_{2(0)}$			
1	0.021	0.932	0.936	0.937	0.938	0.940	0.940
2	0.965	0.980	0.987	0.989	0.991	0.994	0.996
3	1.000	1.035	1.046	1.049	1.052	1.056	1.059

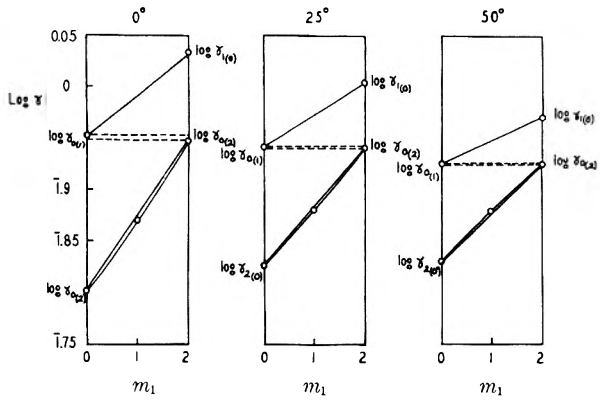

Fig. 2.—Log γ_1 and log γ_2 *versus* m_1 at 2 M total concentration at 0, 25 and 50°.

be computed readily by the equation 55.51 ln $a_w = -2m\phi$. In order to facilitate the calculation of a_w the osmotic coefficients of both the salt $\phi_{2(0)}$ and the acid $\phi_{1(0)}$ at the concentrations and temperatures at which the parameters of equation 21 are known are compiled in Table IV.

Further Considerations and Summary.—The small departure from the linear equation for variation of the activity coefficients is illustrated by Fig. 2 where log γ_1 and log γ_2 are plotted against m_1. The circles represent the values of log γ_2 at the point of maximum deviation from the straight line. At 0°, the point lies below the straight line, at 25° only the slightest departure occurs and at 50°, the point lies above the straight line. This result should prove useful to any one who applies the linear rule. It is also to be noted that at all three temperatures log $\gamma_{0(1)}$ equals $\gamma_{0(1)}$ within narrow limits. By the equations

$$\log \gamma_1 = \log \gamma_{1(0)} - \alpha_{12(0)}m_2$$
$$\log \gamma_2 = \log \gamma_{2(0)} - \alpha_{21(0)}m_1 - \beta_{21}m_{12}$$

and the data in Table I, the activity coefficient of the acid and salt may be calculated with high precision in mixtures of 1, 2 and 3 M total molalities. The restrictions imposed by the cross differention equation 9 indicate that the quadratic form of equations 7 and 8 is not sufficiently general to describe completely the behavior of these mixtures but that a form of equation which permits an approach to linearity as total concentration increases would be more satisfactory.

The calculation of excess heat of mixing lends support to the validity of the calculations. Our results indicate that this latter quantity should decrease as the temperature increases and become negative at temperatures above 40° for the 1 and 2 M mixtures. We have thus obtained a broad picture of the thermodynamic behavior of the system in anticipation of further precise results from calorimetric measurements.

This contribution was supported in part by The Atomic Energy Commission under Contract AT (30–1) 1375.

VAPOR–LIQUID EQUILIBRIUM FOR THE DIBORANE–ETHYL ETHER SYSTEM

BY GEORGE E. MACWOOD AND LEO J. PARIDON

Contribution of the McPherson Chemical Laboratory of The Ohio State University, Columbus 10, Ohio

Received March 6, 1959

The two-phase, vapor–liquid equilibrium in the diborane–ethyl ether system has been studied under three different total pressures: 25, 50 and 100 p.s.i. It is shown that the equilibrium diagram for the system can be calculated from the properties of the pure components.

Introduction

As a part of this Laboratory's program for the determination of the thermodynamic properties of boranes, the two-phase, vapor–liquid equilibrium in the diborane–ethyl ether system has been investigated under total pressures of 25, 50 and 100 p.s.i.

Experimental

Apparatus.—Essentially the same apparatus was used as has been described by Hu and MacWood.[1] The only important change was the replacement of the electromagnetic circulating pump by a Viking rotary positive displacement pump.

Procedure.—Approximately 0.5 mole of ethyl ether was introduced into the pipet. To this was added sufficient diborane to produce the desired concentration at the operating pressure of the experiment. The determination of the approximate quantity of diborane required for each pressure and composition was necessarily a trial and error procedure. The general shape of the temperature–composition curves was determined with data from one determination at each of the three operating pressures. It was a simple matter to obtain the remaining data at any desired composition simply by adding or removing diborane until the desired pressure was obtained, while maintaining the pipet at the temperature corresponding to that composition.

The pipet was immersed in a Dewar vessel containing acetone, the temperature of which was controlled to ±0.05°. The temperature was controlled by a combination of bubbling air through the coolant and periodic additions of small quantities of liquid nitrogen to a tube immersed in the cooling mixture.

The vapor was circulated through the liquid phase at a rate of approximately 200 cc./min. for 45–60 min. before sampling. The liquid- and vapor-phase samples were analyzed, utilizing identical procedures. The sample was first frozen in liquid nitrogen and allowed to warm to room temperature. All material volatile at 10^{-2} mm. was continuously removed through an 18 ft. coil of 3/8 in. copper tubing, which was immersed in a coolant at −120° (frozen *n*-propyl alcohol). The volatile material (diborane) was collected in traps immersed in liquid nitrogen. Preliminary experiments demonstrated that no ether passed through such a coil at −120°, and both diborane and ether were recovered quantitatively by this procedure. The nitrogen traps, containing the diborane portion of the sample, were allowed to warm up to room temperature, while transferring the

(1) J.-H. Hu and G. E. MacWood, THIS JOURNAL, **60**, 1483 (1956).

diborane to calibrated volumes contained in a constant temperature bath. The last traces of diborane were forced into the calibrated volumes by means of a Toepler pump. The pressure then was read, using a constant volume manometer and a Gaertner cathetometer. All readings were referred to a standard meter bar. The diborane then was removed from the measuring system. The ether portion of the sample was analyzed in the same manner.

In computing the molar quantities of ether and diborane, the equation of state

$$PV = n(RT + BP)$$

was used. The values of B used were -195 cc./mole[2] and -998 cc./mole[3] for diborane and ethyl ether, respectively, at 300°K.

The diborane and ether samples were not discarded after removal from the measuring system, but at the end of each experiment were condensed back in the system.

Accuracy.—The limiting factor in this experiment was the accuracy with which the pressures were determined. The pressures were measured with the aid of Ashcroft Laboratory Test Gages. The two lower pressures were read from a gage having a 4.5 in. dial of 0–60 p.s.i. range with 0.2 lb. subdivision. The pressure could be read to within 0.1 lb. The 100 p.s.i. pressures were read from a gage with a 6-in. dial of 0–160 p.s.i. range and 116 subdivisions. The pressure could be read to about 0.3 p.s.i.

Both gages were calibrated against a mercury manometer and a dead-weight gage.

Results.—The results of this investigation are summarized in Table I.

TABLE I

COMPOSITION OF THE DIBORANE–ETHYL ETHER SYSTEM

T, °K.	Mole fraction of diborane in Liquid x_2	Vapor y_2	Pressure, p.s.i.
195.46	0.8072	....	25.0
201.38	.6377	0.9936	25.0
213.55	.4510	.9943	25.0
230.89	.2305	.9876	25.0
236.26	.2125	....	25.0
273.51	.0718	.8270	25.0
213.57	.7694	.9936	50.0
223.11	.5412	.9935	50.0
224.50	.5417	....	50.0
237.38	.3798	.9845	50.0
246.44	.2953	.9751	50.0
291.19	....	.7754	50.0
299.75	.0552	....	50.0
291.58	.2094	.8750	100.0
256.20	.4368	.9836	100.0
236.38	.7048	.9956	100.0

Discussion

Consideration of the experimental results indicates that this system shows positive deviations from Raoult's law. However, since the vapor phase is known to be imperfect, it was assumed that the observed deviation could be accounted for if the generalized Raoult's law

$$f_i = f_i^{0''} x_i \qquad (1)$$

was used, where

f_i = fugacity of the ith component in either phase
$f_i^{0''}$ = fugacity of the ith pure liquid component under its own vapor pressure (p_i^0) at the temperature of the system
x_i = mole fraction of the ith component in the liquid phase.

(2) L. J. Paridon and G. E. MacWood, unpublished work of this Laboratory.

(3) J. D. Lambert, G. A. H. Roberts, J. S. Rowlinson and V. J. Wilkinson, *Proc. Roy. Soc.* (*London*), **A196**, 113 (1949).

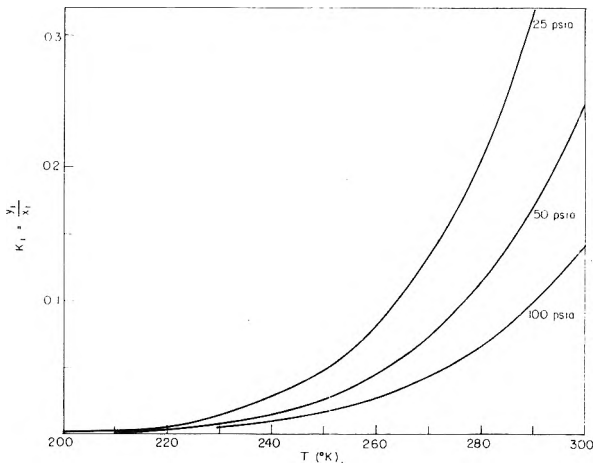

Fig. 1.—Equilibrium constant of ethyl ether.

TABLE II

EQUILIBRIUM CONSTANTS AND CALCULATED EQUILIBRIUM CONCENTRATIONS

T, °K.	p, p.s.i.	K_1	K_2	x_2	y_2
200	25	0.00192	1.515	0.660	0.994
210	25	.00375	2.215	.450	.998
	50	.00220	1.16	.863	.9996
220	25	.00547	3.09	.322	.995
	50	.00249	1.55	.644	.999
230	25	.0144	4.19	.236	.989
	50	.00829	2.17	.459	.996
	100	.00557	1.16	.861	.999
240	25	.0282	5.52	.177	.977
	50	.0160	2.84	.348	.990
	100	.00995	1.51	.660	.997
250	25	.0484	7.13	.134	.995
	50	.0271	3.66	.268	.981
	100	.0171	1.92	.516	.992
260	25	.0830	9.03	.102	.925
	50	.0460	4.62	.209	.965
	100	.0284	2.41	.407	.983
270	25	.134	11.3	.0777	.876
	50	.0736	5.75	.163	.938
	100	.0444	2.99	.324	.970
280	25	.207	13.6	.0592	.805
	50	.113	6.91	.130	.902
	100	.0666	3.41	.279	.952
290	25	.318	15.95	.0436	.696
	50	.172	8.09	.104	.846
	100	.0998	4.17	.221	.921

As described previously,[1] the fugacity of the vapor phase can be calculated from the equation

$$f_i = f_i^{0'} y_i \qquad (2)$$

where

$f_i^{0'}$ = fugacity of the ith pure vapor component at pressure p
$= p \exp(B_i p/RT)$ (3)
y_i = mole fraction of the ith component in the vapor phase
p = total pressure of the system
B_i = second virial coefficient

It has been found that the term γ^4 is negligible and has been dropped in writing eq. 3.

(4) *Vide* reference 1 for definition of γ.

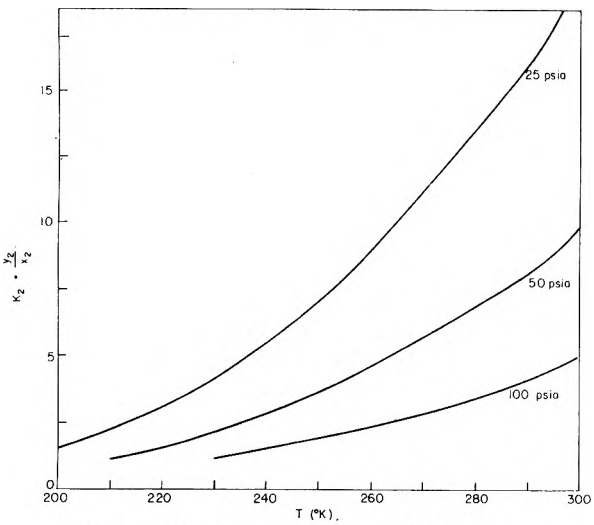

Fig. 2.—Equilibrium constant of diborane.

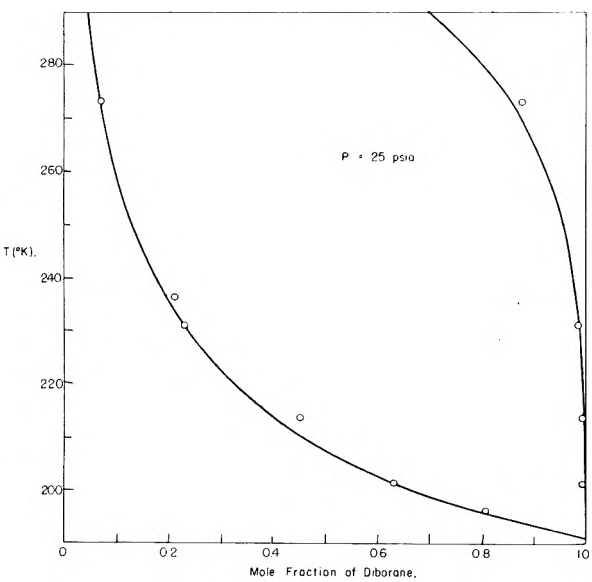

Fig. 3.

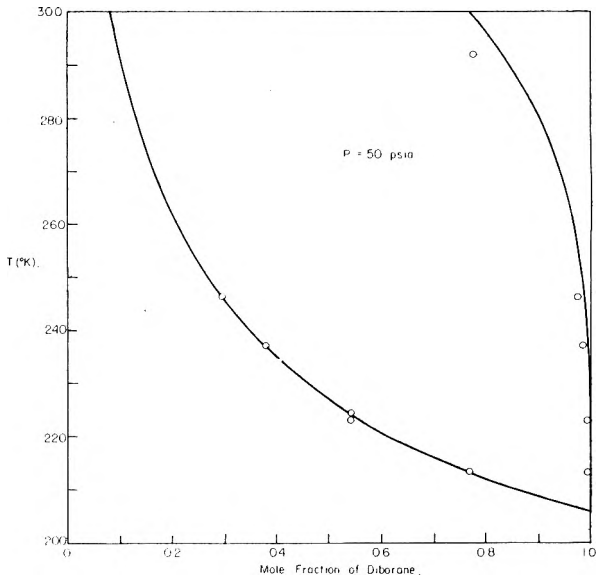

Fig. 4.

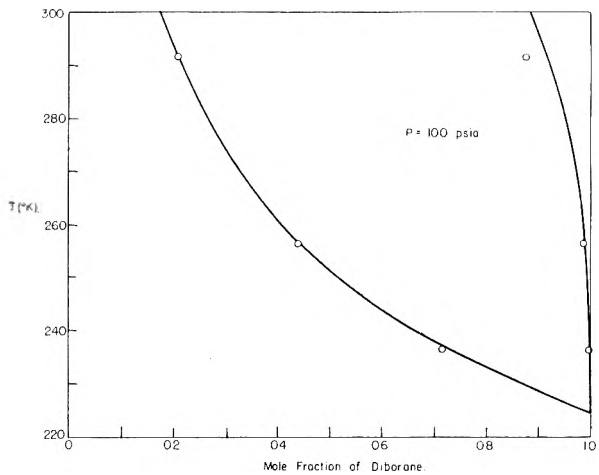

Fig. 5.

To facilitate calculations, the liquid–vapor equilibrium relationship is better expressed by

$$K_i = \frac{y_i}{x_i}$$

or

$$K_i = \frac{p_i^0}{p} \exp\left\{\frac{B_i}{RT}(p_i^0 - p)\right\} \qquad (4)$$

using eq. 1, 2 and 3. Now K_1 and K_2, the so-called "equilibrium constants" for ethyl ether and diborane, may be calculated from the properties of the pure components as a function of the total pressure and temperature. The second virial coefficients for ethyl ether were taken from the data of Lambert, *et al.*[3]; those for diborane are from unpublished work in this Laboratory. Table II and Figs. 1 and 2 give the value of K_1 and K_2, respectively, for the temperature range 200–290°K. and for three pressures 25, 50 and 100 p.s.i.

With the aid of the K-values, the equilibrium concentrations may be calculated for the various values of T and p as

$$x_2 = \frac{1 - K_1}{K_2 - K_1} \qquad (5)$$

and

$$y_2 = K_2 x_2 \qquad (6)$$

In this manner, the vapor–liquid equilibrium diagrams for the three pressures, 25, 50 and 100 p.s.i., were constructed and are shown in Figs. 3, 4 and 5. On the same figures, the experimentally determined points are shown.

Conclusions

The satisfactory agreement between the calculated and observed values indicates that the assumptions upon which the calculations were based are justified. Furthermore, the equilibrium concentrations in the vapor and liquid phases may be calculated, with the aid of the K-values, for any temperature between 200 and 290°K. and any pressure between 25 and 100 p.s.i.

THE THERMAL DECOMPOSITION OF 2-NITROPROPANE

BY TRUDY ENZER SMITH[1] AND JACK G. CALVERT

Contribution from Chemistry Division, Research Department, U. S. Naval Ordnance Test Station China Lake, California, and the McPherson Chemical Laboratory, The Ohio State University, Columbus, Ohio

Received March 9, 1959

The vapor phase pyrolysis of 2-nitropropane has been studied at temperatures ranging from 250 to 337° and has been shown to follow first-order kinetics over this range. Complete product analyses were made mass spectrometrically. The major decomposition products were propylene, nitric oxide and water. The most abundant minor ones were acetone, acetonitrile and formaldehyde. The rate of the decomposition was not affected by propylene and increased erratically when nitric oxide or additional surface was added. The addition of nitrogen dioxide at 250° did not appreciably increase the decomposition rate. In all cases, however, the product distribution was shifted from that of the homogeneous runs. From the product distribution and the rate data it could be shown that the rate of formation of propylene was not affected by additives and could be expressed by $d(C_3H_6)/dt = k'(C_3H_7NO_2)$, where $k' = 1.11 \times 10^{11} e^{-39,300/RT}$ sec.$^{-1}$. This rate law holds for all the tested conditions and for decompositions ranging from 4 to 55%. Thus, the formation of propylene proceeds by a first-order intramolecular, homogeneous process. A mechanism is proposed which, as its primary step, involves the decomposition of 2-nitropropane into propylene and nitrous acid *via* a cyclic activated complex. Subsequent short chain heterogeneous reactions between 2-nitropropane and the decomposition products of nitrous acid are proposed to account for some of the other decomposition products.

Introduction

Among the various studies of the pyrolysis of nitroparaffins, 2-nitropropane is included only in those of Fréjacques,[2] Gray, *et al.*,[3] and Wilde.[4] In these investigations complete product analyses were not carried out, and the decomposition rates were followed either by the rates of pressure rise in a closed system or by the disappearance of 2-nitropropane in a flow system. Fréjacques[2] and Gray, *et al.*,[3] favor a reaction mechanism in which the primary step is a carbon–nitrogen bond split, with subsequent chain reactions forming the products. Wilde[4] favors a unimolecular decomposition involving an activated complex similar to the aci-form observed in solutions. He postulates that minor decomposition products could be formed *via* a C–N bond split followed by radical reactions.

The present kinetic study, which was begun before the publication of Wilde's data, was undertaken in an attempt to resolve the inconsistencies in the interpretation of nitroparaffin pyrolyses. The thermal decomposition of 2-nitropropane was studied from 250 to 337°, with the amount of decomposition ranging from 4 to 55%. Complete product analysis was made in all runs. The effects of increased surface/volume ratio, and of additives such as nitric oxide, propylene and nitrogen dioxide were investigated.

Experimental

Materials.—The 2-nitropropane (Commercial Solvents Corporation) was distilled at atmospheric pressure. The middle fraction of the distillate was redistilled in a small center-rod column. The middle fraction resulting from this distillation had a refractive index of 1.3942 at 20°.

Mathieson cylinder nitric oxide was purified by passing it through a potassium hydroxide trap into a liquid nitrogen cooled container. There it was pumped repeatedly and fractionated into a storage flask. Mass spectrometric analysis indicated no nitrogen, other nitrogen oxides or other impurities.

Mathieson cylinder nitrogen dioxide was purified by repeated freezing and pumping to free it from nitric oxide and other materials until the solid nitrogen tetroxide was colorless. Mass spectrometric and infrared analyses indicated no impurities greater than 0.05%.

(1) U. S. Naval Ordnance Test Station, China Lake, California.

(2) C. Fréjacques, *Compt. rend.*, **231**, 1061 (1950).

(3) P. Gray, A. D. Yoffee and L. Roselaar, *Trans. Faraday Soc.*, **51**, 1489 (1955).

(4) K. A. Wilde, *Ind. Eng. Chem.*, **48**, 769 (1956).

Phillips' research grade propylene was used without further purification. Mass spectrometric analyses indicated that it contained less than 0.01% propane.

Apparatus.—Six sample flasks equipped with break-off seals could be filled simultaneously on a standard vacuum system equipped with a Hg manometer and the storage container for the 2-nitropropane. Nitric oxide and propylene could be introduced from their containers *via* a standard taper joint and a stopcock. A separate introduction system was used for adding nitrogen dioxide. It consisted of a 2-nitropropane storage container, a nitrogen dioxide container equipped with a break seal and a sample flask. To minimize contamination of the nitrogen dioxide, all stopcocks in this system were greased with Dow-Corning silicone high vacuum grease.

Experimental Procedure.—Samples of 2-nitropropane were prepared for pyrolysis by evacuating the sample flasks, filling them to 16 mm. with 2-nitropropane, freezing the 2-nitropropane in liquid nitrogen and sealing them off. To prepare propylene–2-nitropropane and nitric oxide–2-nitropropane mixtures a similar procedure was employed. After the 2-nitropropane was frozen into the sample flasks a known quantity of propylene or nitric oxide was added, frozen into the flasks with liquid nitrogen and the flasks were sealed off. In this manner mixtures of 2-nitropropane and propylene (1/1 and 2/3) and 2-nitropropane and nitric oxide (1/1 and 1/2) were prepared. Mixtures of 2-nitropropane and nitrogen dioxide were prepared in the special system described above. The 2-nitropropane containers on this system as well as on the regular introduction system were opened, and the vapor pressure of 2-nitropropane was read on the manometer in the reference system. The 2-nitropropane in the special system was then frozen into the sample flask. After pumping out the line the manifold was filled with nitrogen dioxide to its vapor pressure at different temperatures. A $CaCl_2$–ice-bath was used at −47.5, −45 and −43° corresponding to vapor pressures of 4.25, 5.49 and 6.49 mm. The nitrogen dioxide then was frozen into the flask containing 2-nitropropane. To prevent possible reaction these samples were stored in Dry Ice until ready for pyrolysis.

The Pyrex wool used for increasing the surface/volume ratio was baked in an annealing oven at 600° for several hours before use. The flasks then were weighed, packed with Pyrex wool and weighed again. From the weight, the density of Pyrex and the measured diameter of the Pyrex wool, the increase in surface could be calculated. A 100-fold increase in surface was obtained.

The furnace used for the pyrolyses consisted of a heated stainless steel beaker which was well insulated with Santocel. A mixture of potassium nitrite and sodium nitrite was used as the salt-bath. The bath was well stirred and the temperature easily could be maintained constant to better than 0.1°. Temperature control was effected manually by means of a Variac. A chromel-alumel thermocouple and a Leeds and Northrup type K potentiometer were used for the temperature measurements.

The following procedure was followed for the pyrolyses: the temperature was set so that the thermocouple e.m.f. was about 0.2 mv. higher than that for the desired temperature.

The sample was immersed in the furnace and a timer started. During the first 30 seconds of the pyrolysis the temperature dropped a few degrees; after that time it remained at a steady value (±0.1°) with only minor fluctuations. Readings were taken every 30 seconds and appropriate adjustments made on the Variac. At the end of the pyrolysis the samples were removed from the bath and immediately quenched in an air blast.

Product Analysis.—The mass spectrometer used in this work was a CEC Analytical Mass Spectrometer Model 21-103, equipped with a micromanometer. Preliminary experiments showed that for several introductions of the same sample the peak distribution changed with time, and that the spectra were so complex that direct identification of all components was not feasible. An equilibration procedure was devised, and the samples were fractionated from baths at −150, −80° and room temperature to simplify the spectra.

The analysis of samples containing mixtures of 2-nitropropane and nitrogen dioxide posed serious problems. Friedel and co-workers[5] have developed a method for the direct mass spectrometric analysis of nitrogen dioxide which depends on "conditioning" the mass spectrometer ion source by removing carbonaceous materials from it. The presence of large amounts of 2-nitropropane, propylene and other organic materials vitiated the adoption of this procedure.

Reasonably good analyses were obtained by fractionating the samples. The nitric oxide formed during the pyrolysis appeared primarily at −150 and −80°. Nitric oxide in the room temperature fraction was assumed to have originated in the mass spectrometer ion source as a result of the reduction of nitrogen dioxide and in the calculations was assigned to nitrogen dioxide. Similarly, carbon monoxide and carbon dioxide were assumed to have pyrolytic origins only in the −150 and −80° fractions; the appearance of these materials in the room temperature fraction was considered spurious and unrelated to the pyrolysis.

The following procedure was used for the analyses. The initial amount of 2-nitropropane used was low enough so that the complete sample could be introduced into the three liter expansion volume. Each sample was successively fractionated into the mass spectrometer from baths at −150, −80° and room temperature. For the −150 and −80° fractions, the pressure was read on the micromanometer and the scan was started. The room temperature fraction contained primarily water and 2-nitropropane. To ensure a representative analysis the valve between the expansion volume and the leak was closed and the sample was equilibrated between the expansion volume and the sample flask for 8 minutes. The pressure was then read, the valve opened and the standard analytical procedures were followed.

The spectra were reduced in the standard manner. The composition of each fraction was calculated and the sum of the computed partial pressures was compared with the pressure read on the micromanometer. Checks to better than 3% were obtained. The three fractions then were summed, and again the computed and observed pressures checked to better than 3%. Another check on the correctness of the peak assignments was the following. All decomposition products originated from 2-nitropropane, hence the carbon–hydrogen–nitrogen–oxygen ratios for all products should correspond to $C_3H_7NO_2$. Agreement with this ratio to better than 3% was found in all cases. The amount of decomposition was calculated from the total carbon or nitrogen content of the products. Thus, the amount of 2-nitropropane that had decomposed was calculated from the decomposition products, the amount of 2-nitropropane remaining was measured directly and the initial amount of 2-nitropropane was obtained by summing these two values.

Gas–liquid chromatography was used to provide an independent check on the identification of decomposition products. An apparatus[6] was used that permitted the collection of the individual components for subsequent mass spectrometer analysis. Several samples were pyrolyzed in 500-ml. flasks and analyzed on a 12-ft. coiled 1/4-inch copper tubing column packed with 1.5% squalane on Pelletex (G. L. Cabot, Boston, Mass.). Although not all of the minor components were shown on the chromatograms, all the components that were collected confirmed the previous identifications from the original mass spectra.

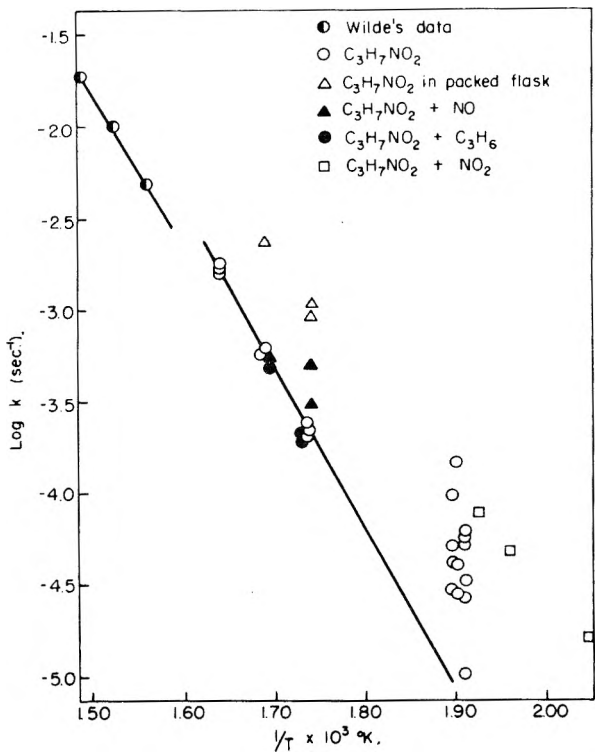

Fig. 1.—Log k *vs.* $1/T$ for the 2-nitropropane decomposition.

Results

The complete numerical results of typical mass spectral analyses are listed in Tables I and II.[7] Qualitatively, the following information could be obtained from the tables. For the homogeneous 2-nitropropane decomposition propylene, nitric oxide and water are formed in roughly equivalent amounts and comprise between 65 to 75% of the reaction products; acetone, acetonitrile and formaldehyde account for another 25 to 15%; and the remaining 10% are composed of various oxides of carbon, nitroparaffins and hydrocarbons. The relative amounts of propylene and nitric oxide show little variation as a function of per cent. decomposition and show only slight temperature dependence.

The addition of propylene did not affect the rate of pyrolysis, nor the relative concentrations of the three major reaction products.

The addition of nitric oxide resulted in an increase in rate and shift in product distribution depending in a complex manner on the amount of nitric oxide added, the reaction time and the temperature. The formation of acetonitrile and nitroparaffins was increased over the corresponding amounts in the homogeneous pyrolysis.

Packing with Pyrex wool increased the decomposition rate and shifted the product distribution so that water, acetonitrile and acetone were the

(5) R. A. Friedel, A. G. Sharkey, Jr., J. L. Shultz and C. R. Humbert, *Anal. Chem.*, **25**, 1314 (1953).

(6) C. M. Drew, J. R. McNesby, S. R. Smith and A. S. Gordon, *Anal. Chem.*, **28**, 979 (1956).

(7) Tables I, II and III referred to in this paper have been deposited as Document number 5802 with the ADI Auxiliary Publications Project, Photoduplication Service, Library of Congress, Washington 25, D. C. A copy may be secured by citing the Document number and by remitting $1.25 for 35 mm. microfilm. Make checks or money orders payable to Chief, Photoduplication Service, Library of Congress

most abundant products. As before, however, the amount of propylene formed was roughly equivalent to the amount of nitric oxide.

Calculation of Rate Constants and Activation Energies.—The data indicate that the rate of disappearance of 2-nitropropane is best represented by a first-order rate law. The rate constants k shown in Table III were calculated from

$$k = 2.303 \log \{[PrNO_2]_0/[PrNO_2]_t\}/t$$

Figure 1 is a plot of log k *vs.* $1/T$. Wilde's data have been included for comparison.

A quantity b (b = [($PrNO_2$) reacted/(C_3H_6) formed] was defined in order to test the hypothesis that intramolecular formation of propylene might be the first step in the 2-nitropropane decomposition. The rate of propylene formation was expressed by $d(C_3H_6)/dt = k'(PrNO_2)$. On integration and substitution in the rate expression for 2-nitropropane one obtains the result that $k' = k/b$. The values of k and b are also listed in Table III. Figure 2 represents an Arrhenius plot of the k's, and it can be observed that by this treatment the scatter in the data observed in Fig. 1 has been virtually eliminated. The data (with the exception of Wilde's points) have been treated by the method of least squares to give the activation energy and frequency factor for the propylene formation. Thus $k' = 1.11 \times 10^{11} e^{-39.3/RT}$ sec.$^{-1}$.

Discussion

The numerical results of this research agree we with those of Fréjacques and Wilde. The following are the expressions for the rate constants (activation energies are expressed in kcal./mole).

$k = 2.2 \times 10^{11} e^{-39.0/RT}$ sec.$^{-1}$	Fréjacques,[2] based on rate of pressure increase in a static system
$k = 1.0 \times 10^{11} e^{-39.0/RT}$ sec.$^{-1}$	Wilde (cor. by T. E. S.)[8] based on the rate of 2-nitropropane consumption in a flow system
$k' = 1.11 \times 10^{11} e^{-39.3/RT}$ sec.$^{-1}$	This research, based on propylene formation in a static system

Significant information for the consideration of a reaction mechanism has been obtained in this study. An Arrhenius plot of the rate constants based on the consumption of 2-nitropropane is shown in Fig. 1. The variations of the rate constants obtained at the same temperature but for different experimental conditions indicate that the reaction is partly heterogeneous. A large increase in the decomposition rate was noted for experiments done in packed vessels (surface/volume ratio increased 100-fold). Figure 2 shows that the scatter of points obtained for different experimental conditions is largely eliminated in an Arrhenius plot of the rate constants for propylene formation. This is good evidence for the formation of propylene by a homogeneous process.

It is then necessary, when formulating a mechanism, to consider the formation of propylene as an important primary step. The product analyses also indicate that approximately equivalent amounts of water and nitric oxide are formed in the homogeneous reaction. The rate law resulting from the proposed mechanism should indicate first order kinetics.

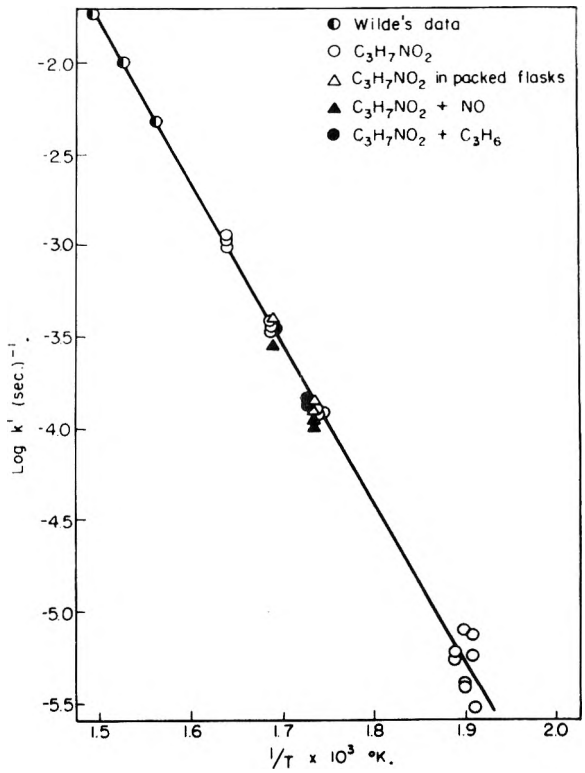

Fig. 2.—Log k^1 *vs.* $1/T$ for the homogeneous decomposition of 2-nitropropane into propylene and nitrous acid.

The following reasonable primary steps should be evaluated in formulating a mechanism.

Step A. $CH_3CHNO_2CH_3 \rightarrow CH_3CHCH_3 + NO_2$.—This primary step involving the rupture of the carbon–nitrogen bond is favored by Fréjacques and Gray. Since the observed activation energy (39 kcal.) is significantly lower than the energy of the C–N bond (estimated at 54.5 kcal.[9] and 57.6 kcal.[10]), subsequent chain processes must be important. The present work shows that the chains cannot be long since the rate of propylene formation was not affected by the addition of propylene or nitric oxide.

If step A be the primary step, additional products other than propylene would be expected from the reactions of the isopropyl radical. Propane would be expected *via* hydrogen abstraction or by disproportionation, and hexane would be expected from a recombination reaction. No hexane and only traces of propane were found among the reaction products

Mirror removal by the reaction products is insufficient proof for the occurrence of step A. The formation of radicals in secondary reactions would lead to similar observations. Again, the acceleration of the decomposition by methyl or

(8) An arithmetic error was found in Wilde's calculations of the frequency factor. In the expression log $A = E/2.303RT + \log k$, the log k term was inadvertently omitted. When included, Wilde's rate constant expression is changed from $k = 1 \times 10^{13.0} e^{-39.0/RT}$ sec.$^{-1}$ to $k = 1 \times 10^{11} e^{-39.0/RT}$ sec.$^{-1}$.

(9) D. E. Holcomb and D. L. Dorsey, Jr., *Ind. Eng. Chem.*, **41**, 2788 (1949).

(10) J. Collin, *Bull. Soc. Roy Sci. Liege*, **23**, 194 (1954).

ethyl radicals is insufficient evidence for the formation of radicals in the primary step of the unsensitized decomposition. One would expect chain reactions to be initiated by added radicals in any case, thus the supporting evidence for A is not conclusive.

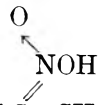

Step B. $CH_3CHNO_2CH_3 \leftrightarrows CH_3C(=NOH)-CH_3 \rightarrow C_3H_6 + HNO_2$.—This step, suggested by Wilde, appears to be unlikely for the following reasons. Spectral data do not indicate the existence of the aci-form in the vapor phase. One would not expect the rearrangement of CH_3CCH_3 into propylene to be quantitative, as would be required by the product distribution of the present study where $(C_3H_6) \cong (NO)$ corrected.

Step C. $C_3H_7NO_2 \rightarrow C_3H_7NO + O$.—The high endothermicity of this reaction ($\Delta H > 100$ kcal.[11]) makes this an unlikely primary step.

Step D. $CH_3CHNO_2CH_3 \rightarrow C_3H_6 + OH + NO$.—This step, a special case of step E, is ruled out on the basis of energy considerations.[12] The heat of reaction is estimated at about 70 kcal.

Proposed Mechanism. Step E.—The experimental evidence of this research favors primary step E, which is analogous to the one proposed by Cottrell and co-workers[13] for the nitroethane pyrolysis. Thus

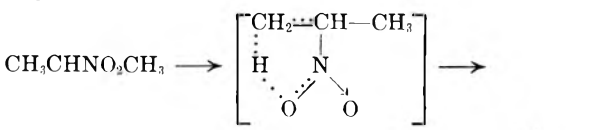

$CH_2{=}CHCH_3 + HNO_2$

This first step is energetically feasible.[14] The heat of reaction for this step is estimated at about 20 kcal., and the only requirement for the activation energy is that it equal or exceed this value. The observed value, 39.3 kcal./mole, satisfies this condition. The observed frequency factor, 1.11×10^{11} sec.$^{-1}$, suggests an entropy of activation $\Delta S = -10.8$ e.u. A cyclic activated complex would be expected to have a lower entropy than the normal configuration of the 2-nitropropane molecule, and therefore does not appear unreasonable in view of the experimental data.

The observation that neither the addition of propylene or nitric oxide, nor the increase in surface/volume ratio affected the rate of propylene formation provides further evidence for the homogeneous intramolecular formation of propylene.

It is proposed that primary step E, the intramolecular elimination of propylene and nitrous acid *via* a cyclic activated complex, is followed by a series of secondary radical processes, which are probably partly heterogeneous. Any NO_2 formed

$$HNO_2 \longrightarrow OH + NO \quad (1)$$

$$OH + CH_3CHNO_2CH_3 \begin{cases} \longrightarrow H_2O + CH_3CNO_2CH_3 & (2) \\ \longrightarrow H_2O + CH_3CHNO_2CH_2 & (2') \end{cases}$$

$$CH_3CNO_2CH_3 \longrightarrow CH_3COCH_3 + NO \quad (3)$$

$$CH_3CHNO_2CH_2 \longrightarrow CH_3CHNO + CH_2O \quad (3')$$

$$CH_3CHNO_2CH_2 \longrightarrow CH_3CH{=}CH_2 + NO_2 \text{ (minor)} \quad (3'')$$

$$CH_3CHNO \longrightarrow CH_3CNOH \quad (4)$$

$$CH_3CNOH + NO \longrightarrow CH_3CN + HNO_2 \quad (5)$$

in (3″) could abstract a hydrogen from 2-nitropropane or react with some of the other products. At low temperatures the decomposition of nitrous acid *via*

$$2HNO_2 \longrightarrow H_2O + NO + NO_2 \quad (6)$$

must be considered as a possible NO_2 contributor. Chain termination presumably occurs by the various disproportionation and recombination reactions of the 2-nitropropyl radicals.

Since the rate constants computed for propylene formation are the same for 4 and 55% decomposition, step (3″) probably is not an important one.

In considering the relative amounts of acetone and acetonitrile the probability of reactions 2 and 2′ must be considered. Reaction 2 is favored at lower temperatures because of the greater ease of abstracting a tertiary hydrogen. At higher temperatures the abstraction energy becomes less important and the sixfold greater probability of abstracting a primary hydrogen must be considered. Thus, the ratio acetonitrile/acetone should increase with increasing temperature, and this is indeed the case.

The observed mass balance indicates that approximately equivalent amounts of nitric oxide, water and propylene are formed in the decomposition. Nitric oxide is formed in (1) and (3). Nitrogen is also one of the observed reaction products. If one assumes all the nitrogen to have originated from the reduction of nitric oxide and neglects all side reactions, this relation should hold

$$(NO)_{cor} = (NO)_{obsd} + 2(N_2) - (CH_3COCH_3)$$

Water is formed largely in (2) and (2′), and thus should be somewhat larger than propylene.

This has been tested for the homogeneous py-

(11)

Species	ΔH_f	Ref.
O	59.1	National Bureau of Standards Circular No. 500. Selected Values of Chemical Thermodynamic Properties
$CH_3CHNO_2CH_3$	−33.9	Holcomb and Dorsey, ref. 9
$CH_3CHNOCH_3$	19	Estimated from data on acetaldoxime, Bichowsky and Rossini, "Thermochemistry of Chemical Substances, Reinhold Publ. Corp., New York, N. Y., 1936

(12)

Species	ΔH_f	Ref.
OH	10	P. Gray, Fifth Symposium (International) on Combustion, Reinhold Publ. Corp., New York, N. Y., 1955, p. 535
NO	21.6	Same as above
C_3H_6	4.88	National Bureau of Standards Circular 500
$CH_3CHNO_2CH_3$	−33.9	Holcomb and Dorsey, ref. 9

(14)

Species	ΔH_f	Ref.
C_3H_6	4.88	National Bureau of Standards Circular 500
$CH_3CHNO_2CH_3$	−33.9	Holcomb and Dorsey, ref. 9
HNO_2	−20	P. Gray, ref. 3

(13) T. L. Cottrell, T. E. Graham and T. I. Reid, *Trans. Faraday Soc.*, **47**, 1089 (1951).

rolyses between 302 and 337°. The results are listed in Table IV.

TABLE IV

PRODUCT MASS BALANCE

Run designation	NO_{cor}	C_3H_{6obsd}	H_2O
F-5	20.1	19.9	25.7
F-1	19.0	18.8	26.6
E-2	24.3	24.4	24.0
E-3	23.2	22.4	24.4
E-4	22.3	23.3	25.5
F-2	24.4	24.8	24.0
F-3	23.7	24.0	24.8
F-4	22.2	23.5	26.5

The agreement is satisfactory if one considers the simplifications that have been made.

The various dimers which probably are formed in the chain termination reactions would be difficult to detect mass spectrometrically because of their low vapor pressures and would not significantly affect the C–H–N–O ratio of the sum of the reaction products.

To summarize, it is proposed in this work that the thermal decomposition of 2-nitropropane proceeds *via* an intramolecular cyclic activated complex to form propylene and nitrous acid, followed by a sequence of short chains initiated by the attack of hydroxyl radicals on the parent molecule. Major products of this partly heterogeneous chain sequence are acetone, acetonitrile and formaldehyde.

Acknowledgment.—The authors wish to thank Dr. C. E. Waring (Chairman, Department of Chemistry, University of Connecticut and consultant, Naval Ordnance Test Station) and Dr. S. Ruven Smith (NOTS) for many stimulating and helpful discussions. Mr. A. V. Jensen and Mr. J. Johnson assisted with some of the mass spectrometer analyses, and Mrs. Helen R. Young with the reading of some of the spectra.

NOTES

THE DETERMINATION OF SURFACE AREAS FROM KRYPTON ADSORPTION ISOTHERMS

BY P. J. MALDEN AND J. D. F. MARSH

Fulham Laboratory, London Research Station, Gas Council, London, England

Received July 8, 1958

Since the work of Brunauer, Emmett and Teller[1] the surface areas of solids have been determined most frequently from measurements of the physical adsorption of gases at temperatures near their boiling points, preferably of nitrogen at −196°. However, if the solid has a small surface area, *e.g.*, less than 1 m.²/g., the use of a temperature below the boiling point of the adsorbate is advantageous; in this way the quantity of gas in the dead space is reduced, permitting the volume adsorbed to be obtained more accurately. Krypton at −196° is commonly used.[2]

We have determined krypton isotherms on a total of fifty low area catalysts and have found that in 80% of the cases the B.E.T. plot of $p/(V(p_0 - p)$ against p/p_0 is convex to the relative pressure axis, and does not give a straight line in the pressure region required to complete a monolayer. No complete explanation of these results has been found. The purpose of this note is to make known our experience and to describe an attempt to explain it in terms of heat of adsorption.

Curvature in the opposite direction has been discussed by Joy[3] who showed that it could be caused by a heterogeneous surface. In our cases, however, if the B.E.T. straight line is drawn as a tangent to the experimental curve at the pressure corresponding to a monolayer, the volume adsorbed at higher and lower pressures are less than those corresponding to this line. The curvature may therefore be due to a maximum in the heat of adsorption at the monolayer.

In the derivation of the B.E.T. equation it is assumed that the heat of adsorption is constant in the first layer and then falls rapidly when the monolayer is complete. Brunauer[4] has pointed out that this is often the case with nitrogen at −196° because the influence of surface heterogeneity and interactions between the adsorbed molecules counterbalance each other. However, if the surface is rather uniform and the attraction between adsorbed molecules is large, the heat of adsorption can increase to a maximum near the completion of a monolayer. To determine whether this effect is important in causing deviation from the B.E.T. equation, we have measured isosteric heats of adsorption of krypton and have also examined published data for systems giving a maximum in the heat of adsorption.

Experimental

Krypton, containing >99.5% Kr and <0.5% Xe, was obtained from British Oxygen Gases. Increments were added by a doser[5] and pressures measured by McLeod gauges. A homogeneous solid solution of 10% α-chromia in α-alumina was prepared by heating a coprecipitated mixture to 1600° for two hours. The other adsorbents were Type A activated alumina from Peter Spence and a supported nickel catalyst as used in the Onia–Gegi oil gas process for the interaction of hydrocarbons and steam. These adsorbents were evacuated for 18 hours at 480° and 10^{-4} mm. Isotherms were obtained at −196°, using liquid nitro-

(1) S. Brunauer, P. H. Emmett and E. Teller, *J. Am. Chem. Soc.*, **60**, 309 (1938).

(2) R. A. Beebe, J. B. Beckwith and J. M. Honig, *ibid.*, **67**, 1554 (1945).

(3) A. S. Joy, "Proceedings of 2nd International Congress of Surface Activity," Butterworth Scientific Publications, London, 1957.

(4) S. Brunauer "Structure and Properties of Solid Surfaces," Univ. of Chicago Press, Chicago, Ill., 1953, p. 395.

(5) D. M. Young, *Rev. Sci. Instr.*, **24**, 77 (1953).

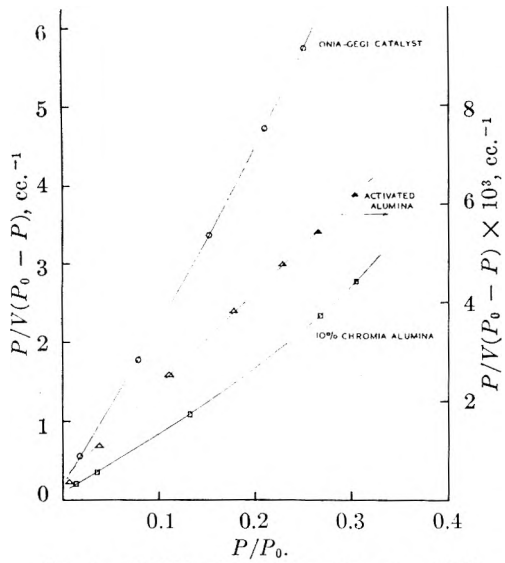

Fig. 1.—B.E.T. plots for krypton at −196°.

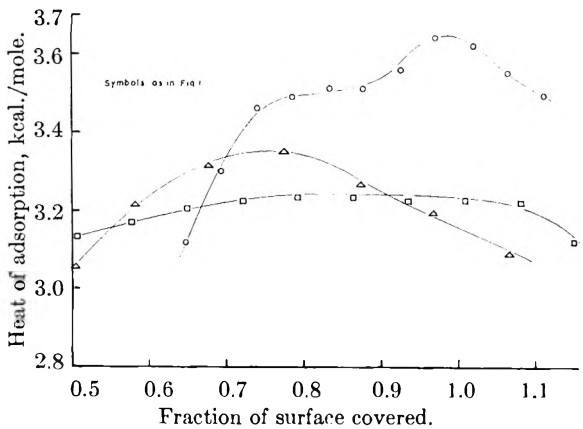

Fig. 2.—Isosteric heats of adsorption of krypton.

gen at atmospheric pressure as refrigerant, and at −189° using liquid oxygen at 38.5 cm. pressure. The pressure over the liquid oxygen varied fairly rapidly by about 0.5 cm., equivalent to 0.1°, due to the operation of the pressure controller, but the average pressure showed no drift. Isosteric heats of adsorption were calculated from the Clausius–Clapeyron equation.

Results

B.E.T. plots for krypton on Onia–Gegi catalyst, 10% Cr_2O_3/Al_2O_3 and activated alumina are shown in Fig. 1. Isosteric heats of adsorption are plotted against surface coverage for the same samples in Fig. 2. In the case of a curved B.E.T. plot it was assumed that the best value of the monolayer volume, V_m, was obtained from the tangent to the curve at the relative pressure corresponding to V_m. To obtain this value the relative pressure corresponding to a likely value of V_m was obtained from the isotherm, a tangent drawn to the B.E.T. curve at this pressure and a value of V_m obtained from this tangent. This procedure was repeated until the assumed and found values of V_m coincided.

The effect of thermal transpiration on the B.E.T. plots was negligible but the heat of adsorption curves have been corrected for it.

The p_0 value used was the extrapolated liquid vapor pressure from the formula of Meihuitzen and Cromelin.[6] This was the procedure originally proposed[2] and subsequently adopted by others.[7,8] The use of the solid vapor pressure for p_0 would increase the curvature. The curvature is reduced by increasing p_0 and, in fact, a higher value is obtained by extrapolation from the formula of Michels, *et al.*[9] However, adoption of the higher values for V_m then obtained would involve a redetermination of the cross sectional area of the krypton atom which should be used to equate krypton and nitrogen areas.

Discussion

Although there is a maximum in the heat of adsorption of krypton on Onia-Gegi catalyst and alumina and a shallow maximum in the case of chromia–alumina the B.E.T. plot is straight for alumina and curved for both Onia–Gegi catalyst and chromia–alumina. Thus there appears to be no correlation between curvature of the B.E.T. plot and a maximum in the heat of adsorption curve in the monolayer region.

Not many measurements of the heat of adsorption of krypton have been published; Zettlemoyer, *et al.*,[10] found shallow maxima on polythene, nylon and collagen, but straight B.E.T. plots. On the other hand a curved B.E.T. plot was obtained by Gulbransen and Andrew[11] for krypton on graphite.

It would seem that maxima in the heats of adsorption are observed more frequently for krypton than for nitrogen but do not necessarily lead to a curved B.E.T. plot. A maximum in the heat of adsorption of nitrogen on the 110 plane of copper was observed by Rhodin.[12] B.E.T. plots taken from his results at −189.7 and −184.0° give curves similar to those we have obtained with krypton. This effect can therefore be obtained with nitrogen, but requires a surface of quite exceptional uniformity. A maximum in the heat of adsorption of nitrogen on Graphon was observed by Joyner and Emmett[13] although the B.E.T. plot was linear in the monolayer region. The Onia–Gegi catalyst and a magnesia sample which also gave a curved B.E.T. plot with krypton both gave straight lines with nitrogen.

The accuracy of a surface area determination, and hence its value, is greatly reduced if a curved B.E.T. plot is obtained. For this reason nitrogen should be used in preference to krypton.

Acknowledgments.—We are grateful to F. A. Inkley of the British Petroleum Company Research Station and to A. S. Joy of the Fuel Research Station for determination of the nitrogen adsorption and for helpful discussions.

(6) J. J. Meihuitzen and C. A. Cromelin, *Physica*, **4**, 1 (1937).
(7) A. J. Rosenberg, *J. Am. Chem. Soc.*, **78**, 2929 (1956).
(8) R. A. W. Haul, *Ang. Chem.*, **68**, 238 (1956).
(9) A. Michels, T. Wassenaar and Th. N. Zwietering, *Physica*, **18**, 63 (1952).
(10) A. C. Zettlemoyer, A. Chand and E. Gamble, *J. Am. Chem. Soc.*, **72**, 2752 (1950).
(11) E. A. Gulbransen and K. F. Andrew, *Ind. Eng. Chem.*, **44**, 1039 (1952).
(12) T. N. Rhodin, *J. Am. Chem. Soc.*, **72**, 5691 (1950).
(13) L. G. Joyner and P. H. Emmett, *ibid.*, **70**, 2353 (1948).

POLAR EFFECTS IN THE INFRARED AND THE NEAR ULTRAVIOLET ABSORPTION SPECTRA OF ALIPHATIC KETONES

BY C. N. R. RAO,[1] G. K. GOLDMAN AND C. LURIE

Department of Chemistry, Purdue University, West Lafayette, Indiana

Received October 1, 1958

Considerable interest has been exhibited recently in correlating the spectra of a related group of organic molecules with substituent constants. The vibrational frequencies and the band intensities of benzene derivatives have been correlated with the Hammett and the electrophilic substituent constants.[2] The near ultraviolet absorption spectra of benzene derivatives have also been correlated[3] with Hammett σ constants and Taft's resonance parameters.[4] The aliphatic group frequencies[2,5] and intensities[6,7] have been correlated by the aliphatic polar substituent constants σ^* of Taft.[4] We have now investigated the substituent effects in the infrared and the near ultraviolet absorption spectra of aliphatic ketones.

Experimental

The infrared spectra were recorded in carbon tetrachloride solutions using a Perkin–Elmer spectrometer, Model 21, and the uncertainty in the frequencies is ± 5 cm.$^{-1}$. The ultraviolet absorption spectra were recorded in 95% ethanol using a Cary recording spectrophotometer. The molar extinction coefficients are not very accurate because of evaporation losses while weighing the samples.

The compounds were synthesized if they were not commercially available. In any case, they were purified by fractionation before use.

Results and Discussion

The infrared carbonyl frequencies ν and the wave lengths λ_{max} and molar extinction coefficients ϵ_{max} corresponding to the ultraviolet absorption maxima for the aliphatic ketones are summarized in Table I.

TABLE I

INFRARED AND NEAR ULTRAVIOLET ABSORPTION SPECTRA OF ALIPHATIC KETONES (R_1-CO-R_2)

Ketone		Infrared spectra	Ultraviolet spectra	
R_1	R_2	ν, cm.$^{-1}$	λ_{max}, mμ	$\epsilon_{max} \times 10^{-2}$
CH_3	CH_3	1715	270	5.8
CH_3	C_2H_5	1715	273	...
CH_3	n-C_3H_7	1710	274	5.0
CH_3	iso-C_3H_7	1715	280	...
CH_3	t-C_4H_9	1708	282	4.2
iso-C_3H_7	iso-C_3H_7	1710	285	4.3
t-C_4H_9	t-C_4H_9	1687	294	4.1
n-C_3H_7	n-C_3H_7	1710	...	...
CH_3	CF_3	1765	...	...

It is interesting to discuss the mass effects on the infrared spectra of these ketones. Halford[8] has reported that the carbonyl bond force constant is nearly constant for the unconjugated ketones of the X_2CO type. He calculates the carbonyl frequency as a function of the mass of X, (m_x), and the angle XCX. He finds that when the XCX angle is 120° (which is nearly so in most such molecules), there is relatively small frequency change for m_x larger than 12. His results, however, do not explain the low carbonyl frequency of 1687 cm.$^{-1}$ in di-t-butyl ketone. Although Halford's conclusions may hold good for unconjugated ketones where there is a narrow spread of the carbonyl frequency, they definitely do not explain the frequencies reported in the present communication, where in trifluoroacetone the carbonyl frequency is found at 1765 cm.$^{-1}$, contrary to what the mass effects would predict. Possible explanations based on hyperconjugation[8] are not valid since it is now fairly well established[9] that hyperconjugative effects are not operative in the ground state. It is therefore considered that polar effects of substituents are responsible for these marked changes in the carbonyl frequency in the aliphatic ketones.

A plot of the carbonyl frequencies in aliphatic ketones against the $\Sigma\sigma^*$ constants is found to be reasonably linear. It has been found earlier that the hydroxy group vibrational frequencies in aliphatic carboxylic acids exhibit an excellent linear relation with σ^* constants.[2,5] However, the slope for the carbonyl frequencies in aliphatic ketones is positive while it is negative for the hydroxy group frequencies in aliphatic acids. A similar observation has been made in the ν–σ or ν–σ^+ correlations in benzene derivatives.[2]

A plot of the λ_{max} of the aliphatic ketones against the $\Sigma\sigma^*$ constants is found to be excellently linear. The molar extinction coefficients seem to exhibit a trend opposite to that of the λ_{max}. The carbonyl frequencies of aliphatic ketones in the infrared region vary with the polar contributions of groups in the reverse order to that of the ultraviolet absorption bands of these derivatives. A similar observation has been made in the aromatic carbonyl derivatives.[10] The solvent effects on the ultraviolet spectra have been assumed to be similar in magnitude in all these ketones, since the resonance effects in these molecules are not appreciable. Such solvent effects may however be important in benzene derivatives.

The trends observed in the infrared and ultraviolet spectra of the ketones are markedly different from the trends in solvolysis rates of RCH(OBs)-CH_3[11] and RCC$_2$(CH$_3$)$_2$.[12] The $\rho^*\sigma^*$ correlations fail for these solvolysis reactions but are successful for the sequences observed in the spectra. This can be taken as further evidence for the proposal that σ^* values are quantitative measures of polar effects and that they are additive in nature. Further, it appears that the infrared group fre-

(1) To whom all the correspondence should be addressed, at Department of Chemistry, University of California, Berkeley, California.

(2) C. N. R. Rao and G. B. Silverman, *Curr. Sci. (India)*, **26**, 375 (1957) and the references listed there.

(3) C. N. R. Rao, *Chem. Ind.*, 666 (1956); 1239 (1957).

(4) R. W. Taft, Jr., in "Steric Effects in Organic Chemistry," edited by M. S. Newman, John Wiley and Sons, Inc., Chap. 13.

(5) L. J. Bellamy, *J. Chem. Soc.*, 4221 (1955).

(6) T. L. Brown, *Chem. Revs.*, **58**, 581 (1958).

(7) C. N. R. Rao and J. Ramachandran, *Curr. Sci. (India)*, in print.

(8) J. O. Halford, *J. Chem. Phys.*, **24**, 830 (1956).

(9) Abstracts of the Conference on Hyperconjugation, Indiana University, Bloomington, Indiana, June, 1958.

(10) W. F. Forbes and W. A. Mueller, *Canadian J. Chem.*, **35**, 498 (1957).

(11) S. Winstein, B. K. Morse, E. Grunwald, K. C. Schreiber and J. Corse, *J. Am. Chem. Soc.*, **74**, 1113 (1952); S. Winstein and H. Marshall, *ibid.*, **74**, 1120 (1952).

(12) H. C. Brown and R. S. Fletcher, *ibid.*, **71**, 1845 (1949).

quencies in aliphatic and benzene derivatives provide independent measures of the inductive effects and the over-all electronegativities of groups.

THE CUMENE CRACKING ACTIVITY OF CO-GELLED SILICA–ALUMINA CATALYSTS AS A FUNCTION OF SURFACE AREA

By Russell W. Maatman[1] and Charles D. Prater

Socony Mobil Oil Company, Inc., Research and Development Laboratory, Paulsboro, New Jersey

Received October 7, 1958

It has been reported by Dobychin and Tsellinskaya[2] that the activity per unit surface area of silica–alumina cracking catalysts for the dealkylation of cumene remains constant as the surface area of the catalyst is changed over a wide range by means of a high temperature steam treatment. This work seems to have been done on catalyst samples prepared by impregnation of silica gels with alumina-containing compounds. In this case such results might be expected. Although such an effect might not be expected with catalysts prepared by co-gelation, in this note we will present data to show that the effect is observed in such catalysts. This constancy of activity per unit surface area as the total surface area is varied implies that significant contributions to the activity are not made by structural material lying very deep within the walls of a pore. This fact can be used to eliminate some mechanisms which have been postulated to explain the cracking of cumene on silica–alumina.

The surface area per gram of the silica–alumina catalyst was changed by high temperature steam treatment. The activity per unit *area*, as a function of the surface area: 80.1 moles propylene/m.^{2}/sec. ($\times 10^9$) for 499 m.^{2}/g.; 75.8, 440; 80.4, 393; 79.8, 320. The catalyst of 499 m.^{2}/g. surface area contained 10 wt. % Al_2O_3 and it was prepared by co-gelation; the others were prepared from it. Similar results were obtained on other silica–alumina catalysts. Their initial surface areas, per cent. surface area remaining after steam treatment, and per cent. activity *per gram* remaining after steam treatment: 350 m.^{2}/g., 58%, 65%; 350 m.^{2}/g., 10%, 10%; 282 m.^{2}/g., 76%, 72%; 270 m.^{2}/g., 78%, 78%. All surface areas were obtained by the B.E.T. nitrogen adsorption method.

Catalytic activities were determined in a differential reactor described elsewhere.[3] The reaction rate was measured at 420° at atmospheric pressure, and with a flow of reactant over the catalyst sufficient to keep the conversion of reactant to products less than 1%. The catalyst was used as 100–200 mesh powder spread in a 200 μ thick layer in a tray. For these conditions the rate of diffusion of reactant into pores or into the bed does not modify the reaction rate.

Steam treatments were carried out at 550° with 100% steam at atmospheric pressure for periods up to 2.5 hours. In order to prevent a decrease in catalytic activity caused by dehydration of the catalyst during steam treatment, it is necessary to restore the condition of hydration which these catalysts had before steaming. This was accomplished by placing catalyst in a moist atmosphere (100% relative humidity) at room temperature for 18 hr., and then heating in a stream of dry air at 450° for 1 hour to remove excess water. These facts indicate that the decrease in activity which is restored by this treatment is independent of surface area. (1) The restoration of activity by the moist air treatment is not accompanied by an increase in surface area. (2) Heating the catalyst in dry air at a sufficiently high temperature leads to the same kind of reversible loss in activity without a change in surface area.

The conclusion that the available sites cannot lie very far below the surface is based upon the fact that a decrease in surface area implies an increase in the thickness of the walls. Let D be the distance from the pore wall surface beyond which no significant contribution to activity is made. Referring to Fig. 1, consider a catalyst having a wall

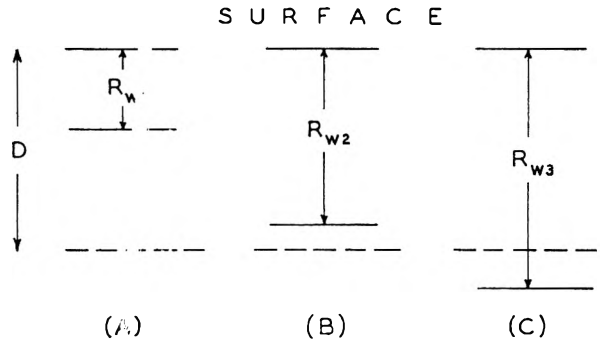

Fig. 1.—Pore walls.

half-thickness of R_{w1}. If on steam treatment the half-thickness is increased to R_{w2}, then the activity per unit surface area is increased by the effective activity of the sites between the distances R_{w1} and R_{w2} from the surface. However, if the catalyst pore walls have the thickness R_{w3}, steam treatment will not increase activity per unit area.

The constancy of activity per unit area with varying wall thickness indicates that the nature, energy and total number of sites are not changed by steam treatment. Any other conclusion would indicate that changes (during steam treatment) in the nature, energy, total number of sites and wall thickness accidentally compensate to leave the activity per unit area unchanged.

An estimate of an upper limit for the effective depth of activity can be made from an "average" wall half-thickness (radius) change on steam treatment. The "average" wall radius R for a catalyst of surface area S and pore wall volume, V_w, was calculated from the equation

$$R = \frac{2V_w}{S}$$

which is derived for a cylindrical or cubic model for the pore wall. The pore wall volume for the catalyst initially 499 m.^{2}/g. was 0.435 ml./g.; thus for this catalyst R is 17.4 Å. in the unsteamed material and 28 Å. in the sample steamed most. If one assumes that all walls have a thickness equal to the average, our results indicate that with 95% probability the increase in activity per unit area is less than 10% upon changing the average wall radius from 17.4 to 28 Å. Porosimeter measurements indicate that a large fraction of the pore walls have radii less than 17 Å. This makes the above estimate conservative. Thus, mechanisms which allow significant contributions to the activity by pore wall volume lying 17 Å. below the surface can be eliminated from consideration. How much closer to the surface one can go before observing significant activity contributions is, of course, not known.

(1) Department of Chemistry, The University of Mississippi, University, Mississippi.

(2) D. P. Dobychin and T. F. Tsellinskaya, *Doklady Akad. Nauk USSR*, **109**, 351 (1956).

(3) C. D. Prater and R. L. Lago, *Advances in Catalysis*, **8**, 293 (1956).

Tamele[4] suggests a mechanism of hydrocarbon cracking by silica–alumina catalyst according to which surface aluminum acts as a Lewis acid. Thomas[5] proposes surface protons take part in the cracking reaction. However, more general electronic interactions between the hydrocarbon and a solid catalyst are conceivable; the electron acceptors ("acid" centers) need not be surface centers. For example, four coördinated aluminums lying below the surface in the silica lattice could lead to the formation of an electron acceptor (hole). Under appropriate conditions the hole could become freed from the fixed lattice charge and become completely mobile. When this occurs acceptors in a thick boundary layer can participate in the reaction.[6] This mechanism is eliminated from consideration. This result is consistent with the results of electrical conductivity studies made by Weisz, Prater and Rittenhouse[7] which showed that no conduction by holes could be demonstrated in this catalyst.

(4) M. W. Tamele, "Heterogeneous Catalysis," Faraday Society, April, 1950, p. 270.

(5) C. L. Thomas, *Ind. Eng. Chem.*, **41**, 2564 (1949).

(6) K. Hauffe and H. J. Engell, *Z. Elektrochem.*, **56**, 366 (1952); P. Aigrand and C. Dugas, *ibid.*, **56**, 363 (1952); P. B. Weisz, *J. Chem. Phys.*, **21**, 1531 (1953).

(7) P. B. Weisz, C. D. Prater and K. D. Rittenhouse, *ibid.*, **23**, 1965 (1955).

SPECTROSCOPIC STUDIES ON RARE EARTH COMPOUNDS. III.[1] THE INTERACTION BETWEEN NEODYMIUM AND PERCHLORATE IONS

BY P. KRUMHOLZ

Contribution from the Research Laboratory of Orquima S. A., São Paulo, Brazil

Received October 15, 1958

Perchlorate ions are commonly used as a standard of non-association. Recently, however, Heidt and Berestecki[2] and Sutcliff and Weber[3] attributed the observed variations of the absorptivity of the 2960 Å. peak of cerous perchlorate solutions with the temperature and with the concentration of the perchlorate anion to the reaction

$$Ce^{+3} + ClO_4^- = CeClO_4^{+2} \qquad (1)$$

Molar absorptivities of the free cerous ion, ϵ_0, and of the complex, ϵ_1, were assumed to be independent of the temperature and of the medium and numerical values were assigned to those constants.

If those assumptions and assignments were correct, plots of absorptivities against the perchlorate concentration (or any suitable function of that concentration) should extrapolate for $(ClO_4^-) \rightarrow 0$ at all temperatures to the same value, namely, ϵ_0. Similarly, absorptivities plotted at different perchlorate concentrations against the temperature should converge at high and low temperatures toward the values assigned to ϵ_0 and ϵ_1, respectively (reaction 1 was supposed to be strongly exothermic). The experimental data presented by the authors[2,3] do not show the expected convergence.

It can be shown in still another way that the hypothesis of constant molar absorptivities is hardly justifiable. The average molar absorptivity,[2] $\bar{\epsilon}$, of a solution of cerous perchlorate, supposed to be partly associated according to equilibrium 1 can be expressed by the equation[4]

$$\bar{\epsilon} - \epsilon_0 = f(\epsilon_1 - \epsilon_0) \qquad (2)$$

where f is the degree of association of $CeClO_4^{+2}$. It follows from equation 2 that if ϵ_0 and ϵ_1 are independent of the temperature and of the medium, the ratio

$$R = \frac{\bar{\epsilon}_a - \bar{\epsilon}_b}{\bar{\epsilon}_a - \bar{\epsilon}_c} = \frac{f_a - f_b}{f_a - f_c} \qquad (3)$$

where the indices a, b and c denote any three solutions of cerous perchlorate differing in their analytical composition or/and temperature, should be independent of the wave length. Contrary to what would be expected, the data presented by Heidt and Berestecki[2] in Fig. 1 reveal a strong dependence of R on the wave length. Thus either molar absorptivities depend on the temperature or/and the medium, or a second complex is formed, or both.[4] The appearance of but one isosbestic point[2] makes the existence of a second complex improbable.

Whatever the reason for those discrepancies, not only are the numerical values of the thermodynamic constants reported[2,3] to be regarded as doubtful, but the very existence of the $CeClO_4^{+2}$ complex cannot be taken for granted.

In order to clarify further the question of a perchlorate complexing of rare earth ions we studied the influence of perchloric acid on the absorption spectrum of the neodymium ion.

Experimental

Materials.—A 0.1 *M* solution of neodymium perchlorate was prepared by dissolving neodymium oxide of 99.9% purity in slightly less than the necessary amount of 0.3 *M* perchloric acid, filtering and acidifying to 0.01 *M* $HClO_4$. The perchloric acid (Baker analyzed reagent) contained less than 0.001% of nitrate and sulfate. Five ml. of the neodymium solution was mixed with the desired amount of perchloric acid and diluted at 25° to a volume of 25 ± 0.02 ml. If necessary, the neodymium solution was evaporated within the volumetric flask to a smaller volume.

Spectrophotometric Measurements.—All measurements were made with a grating spectrophotometer previously described[1a] at a band width of 1 Å. and at an optical depth of 50 mm. Temperature was held constant during the measurements within ±0.1°. Measurements were performed by a differential method[5] comparing the absorptivities of neodymium perchlorate solutions without and with the addition of perchloric acid. Disturbances due to accidental impurities of the solutions were eliminated by comparing absorbancies at a wave length where the absorptivity of neodymium perchlorate is negligible and substracting the difference from the main result. We used as reference wave length 5430 Å. for measurements on the 5200 Å. band system and 6050 Å. for the 5750 Å. band system. No correction could be applied for the measurements on the 5200 Å. band system in 11.8 *M* perchloric acid due to the strong increase of the background absorption. Differential absorbancy measurements could be reproduced with a precision of about ±0.001. Calibration errors and drift of the amplifier introduce an additional error of about ±1% of the measured difference.

(1) Preceding communications: (a) *Spectrochim. Acta*, **10**, 269 (1957); (b) 274 (1957).

(2) L. J. Heidt and J. Berestecki, *J. Am. Chem. Soc.*, **77**, 2049 (1955).

(3) L. H. Sutcliff and J. R. Weber, *Trans. Faraday Soc.*, **53**, 1225 (1956).

(4) See T. W. Newton and F. B. Baker, THIS JOURNAL, **61**, 934 (1957).

(5) C. F. Hiskey, *Anal. Chem.*, **21**, 1440 (1949).

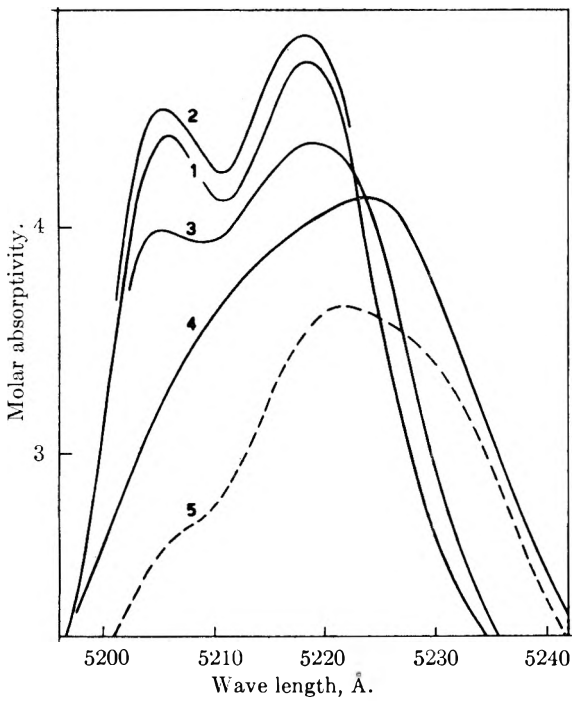

Fig. 1.—The influence of perchloric acid and of sodium nitrate on the absorption spectrum of a 0.02 *M* solution of neodymium perchlorate at 25°: curves 1, 2, 3 and 4 represent solutions 0.002, 4, 9.8 and 11.8 *M* in $HClO_4$, respectively. Curve 5 represents a solution 4 *M* in $NaNO_3$.

Results and Discussion

Absorption spectra of 0.02 *M* aqueous solutions of neodymium perchlorate were measured at 25° for a number of solutions containing perchloric acid in concentrations from 0.002 to 11.8 *M*. Typical results for the band system around 5200 and 5750 Å. are presented in Fig. 1 and in Table I.

TABLE I

THE INFLUENCE OF PERCHLORIC ACID ON THE MOLAR ABSORPTIVITIES ϵ OF A 0.02 *M* AQUEOUS SOLUTION OF NEODYMIUM PERCHLORATE AT 25°

Band system around 5750 Å.

($HClO_4$)		0.002	2	4	6	8	9.8	10.8	11.8
λ, Å.	ϵ_0				$(\epsilon - \epsilon_0) \times 10^3$				
5700	1.50	4	6	13	25	55	80	108	
5710	2.82	8	16	25	40	66	84	105	
5720	4.54	11	20	28	40	65	74	77	
5730	5.24	12	22	33	50	91	110	120	
5740	6.57	13	25	37	53	87	95	97	
5752	7.15	13	26	40	60	108	124	124	
5760	6.68	8	16	26	47	117	172	213	
5770	5.52	6	12	20	42	127	221	340	
5780	5.47	5	9	17	41	131	230	358	
5790	4.97	2	4	6	21	112	225	390	
5800	3.66	0	−1	2	21	112	235	422	
5810	3.01	−2	−3	−1	17	105	212	388	
5820	2.60	−2	−3	−1	18	104	200	345	
5830	2.20	0	−1	2	18	97	186	312	
5840	1.82	0	0	2	15	83	160	275	
5850	1.47	0	0	2	13	65	130	228	

The spectral changes produced by perchloric acid in concentrations up to about 6 *M* are similar to those produced by a decrease of temperature.[1b] Absorptivities at and around the absorption maxima increase slightly with increasing concentration of the acid, decreasing eventually at the long wave length wings of the absorption bands. Wave length shifts of the absorption maxima were not observed. Such spectral changes are of a type usually described[4] as a medium effect. Variations of the refractive index of the solutions with the concentration of perchloric acid should also contribute to the observed effect.[6] Experimental evidence is insufficient to decide which part, if any, of the observed spectral changes is due to complex formation.

Direct evidence for complex formation is however provided by the pronounced effect of perchloric acid at concentrations higher than 6 *M*. In certain spectral regions, particularly above 5760 Å. (see Table I) absorptivities are now very sensitive to variations of the concentration of perchloric acid. In the 5200 Å. region (see Fig. 1) absorptivities change now partly in opposite direction than at concentrations below 6 *M*. In 11.8 *M* perchloric acid the absorption maximum at 5218 Å. is shifted by about 6 Å.; that at 4272 Å. by 3 Å. toward longer wave lengths. As shown in Fig. 1, spectral changes produced by 11.8 *M* perchloric acid are similar to those produced by much lower concentrations of nitrates. Complex formation is rather well established in the latter case.[7] It might finally be interesting to note that the concentration dependence of the apparent molar refraction of lanthanum perchlorate seems to indicate interaction between the lanthanum and perchlorate ion at $(ClO_4^-) > 6\,M$.[8]

The spectral behavior of the Nd^{+3}–perchloric acid system is analogous to that of rare earths–chloride systems, recently reported by Jorgensen.[9] In both cases direct evidence for complex formation is obtained only under conditions of very high activities of the solutes and low activities of the solvent.

(6) See N. Q. Chako, THIS JOURNAL, **2**, 644 (1934); G. Kortum, *Z. physik. Chem.*, **B33**, 243 (1936).

(7) R. E. Connick and S. W. Meyer, *J. Am. Chem. Soc.*, **73**, 1176 (1951).

(8) J. E. Roberts and N. W. Silox, *ibid.*, **79**, 1789 (1957).

(9) Chr. K. Jorgensen, *Kgl. Danske Videnskab Selskab, Mat. fys. Medd.*, **30**, No. 22 (1956); *Acta Chem. Scand.*, **10**, 1503 (1956).

SPECTROPHOTOMETRIC STUDY OF THE IONIZATION OF HYDRAZOIC ACID IN AQUEOUS SOLUTION[1]

BY EUGENE A. BURNS AND FRANCES D. CHANG

Jet Propulsion Laboratory, California Institute of Technology, Pasadena 3, California

Received November 6, 1958

The ionization of hydrazoic acid in aqueous solution has been investigated, in the past, by several authors.[2–6] These researchers, through the use of conductivity, potentiometry and alkalinimetry, have found and reported ionization constants for hydrazoic acid in aqueous solution in the range 1.7

(1) This paper presents the results of one phase of research carried out at the Jet Propulsion Laboratory, California Institute of Technology, under Contract No. DA-04-495-Ord 18, sponsored by the Department of the Army, Ordnance Corps.

(2) C. A. West, *J. Chem. Soc.*, 705 (1900).

(3) W. S. Hughes, *ibid.*, 491 (1928).

(4) H. T. S. Britton and R. A. Robinson, *Trans. Faraday Soc.*, **28**, 531 (1932).

(5) M. Quintin, *Compt. rend.*, **210**, 625 (1940).

(6) N. Yui, *Bull. Inst. Phys. Chem. Res.*, **20**, 390 (1941).

to 2.8×10^{-5} mole/liter. Among these investigators, only Quintin[5] and Yui[6] determined the thermodynamic constant by extrapolating their data to zero ionic strength; their values are 2.8×10^{-5} and 1.91×10^{-5} mole/liter, respectively. The present study has been prompted by the observation of a significant absorption spectrum in the ultraviolet region, resulting from the presence of hydrazoic acid; the existence of this spectrum presents the opportunity to evaluate the ionization constant by an independent method.

Experimental

Materials.—Reagent grade chemicals were used at all times.

Procedure.—The concentration of the stock sodium azide solution was determined by potentiometric titration with standard hydrochloric acid, using glass and calomel electrodes in conjunction with a Beckman Model G *p*H meter. The end-point was evaluated by taking the second derivative of the titration curve. The coefficient of variation of this titration procedure was 0.16%. Stock sodium perchlorate solutions were standardized volumetrically by reduction with excess titanous chloride, using osmium tetroxide as a catalyst, followed by back-titration with ferric ammonium sulfate, with potassium thiocyanate as the indicator.[7] The experimental solutions were prepared by mixing aliquots of stock sodium azide, sodium perchlorate and perchloric acid, and then diluting to the desired volume. The solutions containing hydrazoic acid were used within 1 hr. after mixing; however, it was observed spectrophotometrically that these solutions were stable for long periods (*e.g.*, 2 wk.) if the container was well stoppered and was open for a minimum exposure time during transfer to the optical cells.

Absorbance measurements were recorded with a Beckman Model DK-2 quartz photoelectric recording spectrophotometer. Matched 0.994-cm. silica cells, equipped with ground-glass stoppers, were employed. All spectra were run against a blank solution of sodium perchlorate of the desired ionic strength. Measurements were made in an air-conditioned room whose temperature was controlled at 21.7 ± 0.6°.

Results

Data were obtained, in the region 310 to 220 mμ, on the ultraviolet absorption of 0.0100 *F* sodium azide in the presence of varying amounts of perchloric acid (0, 0.00200, 0.00400, 0.00600, 0.00900, 0.0100, 0.0110, 0.0200, 0.0500 and 0.100 *F*) maintained at a constant ionic strength.

In the absence of perchloric acid, the absorption curve rose rapidly at about 260 mμ to a value of 1.0 at about 250 mμ. As the acid concentration was increased, the absorption curve began to rise sooner (300 mμ), exhibiting a maximum at about 260 mμ and a minimum at 232 mμ, before attaining a value of 1.0 at 221 mμ. An isobestic point was observed, which is located at 254 mμ and at 0.45 absorbance units.

Perchloric acid concentrations greater than 0.0200 *F* produced no change in the spectra; hence, it was evident that the sodium azide had been completely converted to hydrazoic acid (*i.e.*, the solution contained 0.0100 *M* hydrazoic acid and 0.0100 *M* free perchloric acid). Inspection of the curves reveals that the minimum at 232 mμ is relatively sensitive to changes in acid concentration in the range 0.0090 to 0.0110 *F*, whereas the maximum at 260 mμ is not. Hence, the region 228 to 242 mμ is the optimum location for the spectrophotometric determination of the ionization constant. The data were treated in the manner indicated in the following derivation.

Let A represent the absorbance observed at a given wave length for a solution containing sodium azide, perchloric acid and sodium perchlorate

$$A = e_{N_3}(N_3^-)l + e_{HN_3}(HN_3)l \qquad (1)$$

where (N_3^-) and (HN_3) are the concentrations of azide and hydrazoic acid present in the solution, l is the path length of the optical cells, and e is the molar absorptivity of the species denoted by the subscript. Let $(H)_0$ and $(N_3)_0$ equal the analytical concentrations of hydrogen ion and azide ion, respectively. Then

$$A = e_{N_3}l(N_3)_0 + (e_{HN_3} - e_{N_3})l(HN_3) \qquad (2)$$

The degree of dissociation of azide α is thus expressed by

$$\alpha = \frac{(HN_3)}{(N_3)_0} = \frac{[A/(N_3)_0]l - e_{N_3}}{e_{HN_3} - e_{N_3}} = 1 - \frac{[A/(N_3)_0]l - e_{HN_3}}{e_{N_3} - e_{HN_3}} \qquad (3)$$

When the degree of dissociation is known, the concentration ionization constant of hydrazoic acid $k = (H)(N_3)/(HN_3)$ is calculated from the expression

$$k = \frac{[(H_0) - HN_3][(N_3)_0 - HN_3]}{(HN_3)} = \frac{(N_3)_0\left[\frac{(H)_0}{(N_3)_0} - \alpha\right][1 - \alpha]}{\alpha} \qquad (4)$$

The most accurate estimate of the ionization constant will be obtained when the analytical concentrations of azide and hydrogen ions are equal. Because of the molar absorptivities of azide ion and hydrazoic acid and the ionization constant of HN_3, the most accurate estimates of k may be obtained by fixing the analytical concentration of sodium azide at an upper level of 0.0100 *F* and observing the resulting absorbance of solutions containing 0.0090 to 0.0110 *F* perchloric acid.

Table I

Molar Absorptivities of Hydrazoic Acid and Azide Ion

Wave length, mμ	Molar absorptivity, l./mole cm. e_{N_3}	e_{HN_3}
228.0	518	33.0
230.0	483	28.2
232.0	445	26.2
234.0	411	26.4
236.0	363	27.4
238.0	327	29.1
240.0	282	31.2
242.0	232	33.5
250.0	89	41.2
260.0	18	46.9
270.0	3	39.3
280.0	..	24.7
290.0	..	12.1
300.0	..	4.1

The molar absorptivity of azide ion in the wave length region 228 to 242 mμ was determined by averaging the values obtained from four different concentrations of azide ion (*i.e.*, 0.200, 0.400, 1.00 and 2.00 m*F* NaN_3). The reproducibility of this procedure was good. The molar absorptivity of hydrazoic acid was evaluated from spectra obtained

(7) E. A. Burns and R. F. Muraca (to be published).

TABLE II

IONIZATION CONSTANT FOR HYDRAZOIC ACID AT 22° AND AT VARIOUS VALUES OF IONIC STRENGTH

Wave length, mμ	Formal perchloric acid concn. $(H)_0$	Ionization constant $k \times 10^5$				
		μ = 1.00 M	μ = 0.500 M	μ = 0.200 M	μ = 0.1000 M	μ = 0.0300 M
242.0	0.0110	4.24	3.99	4.24	3.57	3.32
	.0100	4.39	4.84	3.98	4.18	3.52
	.0090	4.26	4.73	3.98	3.73	3.37
240.0	.0110	4.17	4.24	3.97	3.84	3.00
	.0100	4.29	5.13	4.02	4.02	3.01
	.0090	3.83	4.35	3.84	4.24	3.28
238.0	.0110	4.16	4.33	4.09	3.97	3.59
	.0100	4.13	4.75	4.31	3.80	2.93
	.0090	3.88	4.31	4.50	4.11	3.28
236.0	.0110	4.01	4.58	3.85	3.71	3.14
	.0100	3.94	4.44	4.10	3.70	3.25
	.0090	4.26	4.89	4.30	3.66	3.04
234.0	.0110	3.87	4.83	4.26	3.52	3.02
	.0100	3.73	4.22	4.36	3.89	3.39
	.0090	4.31	4.67	4.47	3.95	3.38
232.0	.0110	3.99	5.28	4.70	3.95	3.51
	.0100	3.91	4.10	4.61	3.66	3.27
230.0	.0110	4.30	4.38	4.86	3.95	3.64
	.0100	4.03	4.49	4.00	3.62	3.37
228.0	.0110	4.47	4.87	4.46	4.07	3.32
	.0100	4.21	5.10	3.91	3.94	3.27
	Av.	4.11 ± 0.20[a]	4.60 ± 0.35[a]	4.23 ± 0.29[a]	3.86 ± 0.20[a]	3.28 ± 0.20[a]

[a] Standard deviation.

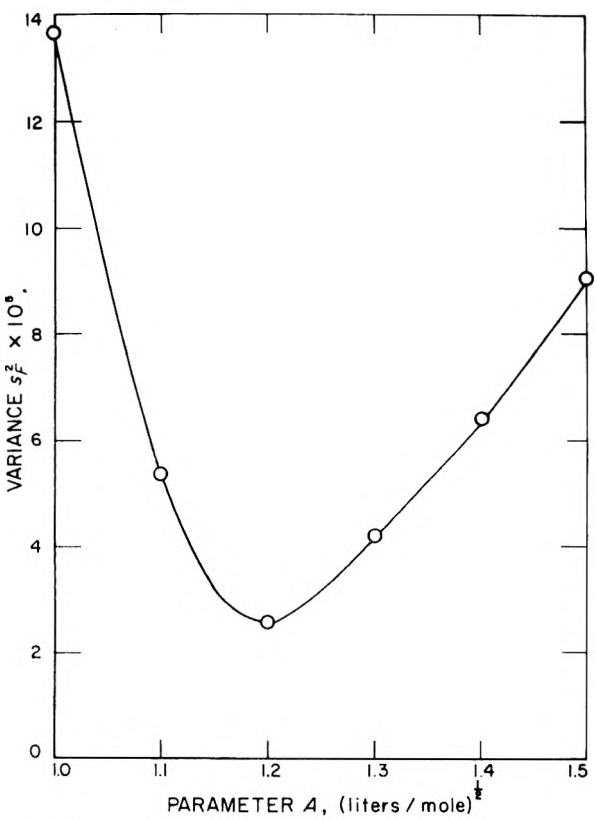

Fig. 1.—Variance s_F^2 as a function of the parameter A.

from solutions which contained 0.0100 F NaN_3, 0.100 F $HClO_4$ and which were maintained at constant ionic strengths of 0.0300, 0.100, 0.200, 0.500 and 1.000 M. Molar absorptivities of azide and hydrazoic acid in the region 250 to 300 mμ were obtained in a similar manner. Table I lists the results of the determinations of molar absorptivities.

The absorbance A of five series of solutions was recorded at 2 mμ intervals over the wave length region 228 to 242 mμ. Each series of three solutions contained 0.0100 F NaN_3, varying amounts of $HClO_4$ and sufficient $NaClO_4$ to maintain the desired constant ionic strength. The concentration constant k, which was calculated from eq. 3 and 4, is listed as a function of wave length, analytical concentration of perchloric acid and ionic strength in Table II.

Discussion

The thermodynamic ionization constant for hydrazoic acid K was estimated, using the extended form of the Debye–Hückel equation as an approximation of the activity coefficient product

$$-\log \gamma_\Delta = S_{(f)}\left(\Delta \sum_i z^2_i\right)\frac{\sqrt{\mu}}{1 + A\sqrt{\mu}} - \beta'\mu \quad (5)$$

In the case of hydrazoic acid, $\Delta\sum_i z^2_i = 2$; at 22°, $S_{(f)} = 0.5064$.[8]

Defining the function F by the expression

$$F = \log k - \frac{1.0128\sqrt{\mu}}{1 + A\sqrt{\mu}} = \log K - \beta\mu \quad (6)$$

and estimating the parameter A, the function F was plotted *vs.* μ as suggested by Guggenheim and Schindler,[9] and the best straight line was evaluated by the method of least squares.[10] The estimate of

(8) H. S. Harned and B. B. Owen, "The Physical Chemistry of Electrolytic Solutions," Reinhold Publ. Corp., New York, N. Y., 2nd ed., 1950, p. 587.

(9) E. A. Guggenheim and T. D. Schindler, THIS JOURNAL, **38**, 543 (1934).

(10) W. J. Youden, "Statistical Methods for Chemists," John Wiley and Sons, Inc., New York, N. Y., 1951, pp. 40–45.

variance s_F^2 of a single F measurement, compared with the least-squares line, was evaluated as a function of the parameter A and is plotted in Fig. 1. The minimum variance and, hence, the best fit to a straight line occurred at $A = 1.2$; accordingly, the least-squares equation of the line is $F = -4.622 - 0.221\ \mu$. It follows that the thermodynamic ionization constant is 2.39×10^{-5} mole/liter, and β in eq. 6 is 0.221 liter/mole. The error in the constant K is estimated to be $\pm 0.15 \times 10^{-5}$ mole/liter.

TABLE III

ACTIVITY COEFFICIENTS OF AZIDE ION

Ionic strength, M	$\gamma_{H^+}\gamma_{N_3^-}$	γ_{H^+}[a]	$\gamma_{N_3^-}$
0.0300	0.727	0.902[b]	0.81
.1000	.618	.86	.72
.200	.565	.83	.68
.500	.519	...	...
1.000	.581	...	...

[a] Data from ref. 11. [b] Interpolated from data of ref. 11.

Table III lists the values of the product of the activity coefficients $\gamma_{H^+}\gamma_{N_3^-}$ observed in this work at 22°. Also listed are Kielland's values for the activity coefficient of hydrogen ion and for the calculated activity coefficient of azide ion.[11] It should be pointed out that Kielland's data originated from work carried out at 25°, whereas the present study was made at 22°; these estimates do not include any correction for this discrepancy.

(11) J. Kielland, *J. Am. Chem. Soc.*, **59**, 1675 (1937).

THE RATES OF ADSORPTION OF WATER AND CARBON MONOXIDE BY ZINC OXIDE

BY MANFRED J. D. LOW AND H. AUSTIN TAYLOR

Wm. H. Nichols Laboratory, New York University, New York 53, New York

Received November 7, 1958

The chemisorption of CO on ZnO at low temperatures is generally believed to be completely reversible and non-activated.[1-3] Some rates of desorption of CO have been measured,[3] but with the exception of several experiments of Burwell and Taylor[4] no adsorption rate data appear to exist. Similarly, although the adsorption of H_2O on ZnO has been examined by Taylor and Sickman[5] and by Miyahara and Sano,[6] little information is at hand regarding the kinetics of the adsorption. Consequently details of a qualitative examination of the kinetics are presented here.

The Adsorption of CO.—The rates of adsorption of CO on 18.76 g. of ZnO *ex* oxalate[5] were measured in a system of constant volume using a dibutyl phthalate (DBP) manometer. Reproducibility of data from run to run was very poor and was probably affected by (1) incomplete degassing when this was attempted at the temperature of adsorption, so that the following run was made on a partially covered surface; (2) reduction of the surface by thorough degassing at 400°, so that the following run was made on a surface of different characteristics. At or below 100° a pressure of 10^{-6} mm. could be obtained at the end of a run by evacuating at the adsorption temperature for about 20 minutes. On then raising the temperature to 400°, however, an appreciable amount of gas was desorbed: an additional 4 hours of evacuation were required to reduce the pressure to 10^{-6} mm. At run temperatures of 147° and above, pumping for about 8 minutes at the end of a run reduced the pressure to 10^{-6} mm. On then raising the temperature to 400°, more gas was evolved for some 4 hours.

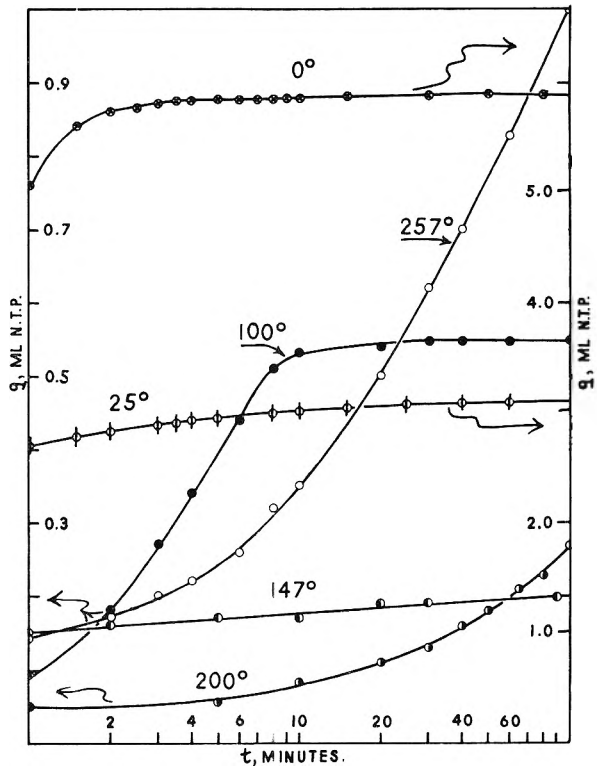

Fig. 1.—Adsorption of CO on ZnO: 0°, P_0 = 51.4 cm. DBP; 25°, P_0 = 49.8 cm. DBP; 100°, P_0 = 59.5 cm. DBP; 147°, P_0 = 42.3 cm. DBP; 200°, P_0 = 53.8 cm. DBP; 257°, P_0 = 54.2 cm. DBP.

These results thus directly contradict the statements of Garner, *et al.*, that the adsorption of CO is reversible below about 100°. Rather, it appears that the adsorption is irreversible and that more than one type of adsorption coexist over the entire temperature range covered. Such an unstable system precludes reproducibility and vitiates attempts at quantitative correlations between kinetics and temperature or pressure on the same adsorbent, because a different surface is obtained after each degassing. However, qualitative comparison of the general character of the adsorption at different temperatures is possible and useful.

Runs were made at 0, 25, 56, 100, 147, 200 and 257°, at random order of temperatures, and were numbered consecutively in order of their execution. Typical runs at initial pressures P_0 are shown in Fig. 1. Before each of the runs shown the catalyst had been degassed at 400° overnight. Since the runs were made at random order, albeit on surfaces slightly changed by rigorous degassing, comparison of these runs is permissible. In general, at temperatures below 100° the absorption was apparently complete after a few minutes. At 100°, a slow adsorption followed the rapid adsorption, while above 100° only a slow adsorption was found.

The data above 100°, and a part of the data at 100°, may be represented by the integrated Elovich equation[7]

$$q = (2.3/\alpha)\log(t + k) - (2.3/\alpha)\log(d\alpha)$$

Isothermal discontinuities[7] were found in $q - \log_{10}(t + k)$ plots at 200 and 257°, and were also found in the data of Burwell and Taylor.

The Adsorption of Water.—Rates of adsorption of water vapor could not be determined precisely in constant volume

(1) W. E. Garner, *J. Chem. Soc.*, 1239 (1947).
(2) W. E. Garner and F. J. Veal, *ibid.*, 1487 (1935).
(3) W. E. Garner and P. E. T. Kingman, *Trans. Faraday Soc.*, **27**, 322 (1931).
(4) R. L. Burwell and H. S. Taylor, *J. Am. Chem. Soc.*, **58**, 1753 (1936).
(5) H. S. Taylor and D. V. Sickman, *ibid.*, **54**, 602(1932).
(6) Y. Miyahara and I. Sano, *Kogyo Kagaku Zasshi*, **69**, 90 (1948).
(7) H. A. Taylor and N. Thon, *J. Am. Chem. Soc.*, **74**, 4169 (1952).

systems at room temperatures higher than about 25°. In order to obtain relatively high water vapor pressures the entire vacuum system was enclosed. A "room temperature" of 52 ± 0.1° was attained. It was noted that after starting a run the pressure would drop about 15% from the original pressure (on opening the stopcock to the evacuated adsorbent chamber at $t = 0$), quickly become constant, then would increase for several minutes by as much as 1 cm. DBP, and then decrease, continuing to do so in normal fashion. A series of experiments established that whenever a sudden pressure change occurred, a slow and decelerating pressure change followed, suggesting extensive ad- and desorption of water by the glass tubing of the system. Similar effects were noted with methanol and ethanol vapors. The effect was not noticed at room temperatures of 20–25°, and consequently several experiments were made with 10.0 g. of ZnO at 100 or 250°. At the end of a run a pressure of 10^{-6} mm. could be obtained by pumping for 4 hours at 410° and consequently a standard pumping-off period of 8 hours was established between runs.

A rapid, voluminous, but quickly decelerating adsorption occurred at 100°. For example, in run 40 at $P_0 = 9.1$ cm. DBP, amounts adsorbed after 1, 10 and 100 minutes were 3, 10 and 25 ml., respectively. The adsorption was diminished in magnitude and rate at 250°: in run 14 at $P_0 = 8.0$ cm. DBP, amounts adsorbed after 1, 10 and 100 minutes being 1.8, 4.25 and 4.4 ml., respectively. The Elovich equation expressed adsorption rates over major parts of the course of adsorption.

The rates and extents of water adsorption by ZnO were greatly decreased by pre-adsorbed hydrogen. At 100°, in run 38 at $P_0 = 20.3$ cm. DBP, for instance, 8, 12.5, 18, 21 and 25 ml. water adsorbed after 1, 2, 4, 6 and 10 minutes, respectively, the process continuing until 35.5 ml. had been adsorbed at 200 minutes. On pre-adsorbing 0.52 ml. H_2 (run 21P, at $P_0 = 28.6$ cm. DBP, 100°) 5.20, 5.35, 5.44, 5.45 and 5.45 ml. of water were adsorbed after 1, 2, 4, 6 and 10 minutes, respectively. Pre-adsorption of 1.5 ml. H_2 in run 24P ($P_0 = 23.7$ cm. DBP, 100°) or 3.2 ml. H_2 in run 19P ($P_0 = 21.1$ cm. DBP, 100°) decreased the amounts adsorbed after 1, 5 and 10 minutes to 3.82, 4.33 and 4.44, and to 3.35, 3.76, and 3.83 ml., respectively. Complete inhibition of hydrogen adsorption occurred of pre-adsorbing water vapor. For example, on adsorbing H_2 at $P_0 = 46$ cm. DBP at 100° on top of 23 ml. adsorbed water, no absorption but a desorption of about 0.05 ml. of gas was noted. An adsorption of about 0.05 ml. H_2 occurred on ZnO containing 7.5 ml. of pre-adsorbed water. These inhibitions are similar to those detected by Taylor and Sickman and Burwell and Taylor.

Such great inhibitions must obviously be due to effects other than simple geometric surface coverage, and reflect the great sensitivity of the ZnO surface to pre-treatment. Similar great changes in the nature of the surface due to insufficient degassing, or to thorough degassing resulting in reduction, may be inferred from the CO adsorption experiments.

REACTIONS OF MERCURY(II) WITH A CATION-EXCHANGE RESIN

BY H. F. WALTON AND J. M. MARTINEZ

University of Colorado, Boulder, Colorado

Received November 24, 1958

As part of a study of the behavior of heavy metal ions in cation exchange, we have investigated the reaction of a sulfonated polystyrene exchanger with solutions containing mercuric perchlorate and perchloric acid. Two distinct reactions occurred: the normal exchange of hydrogen ions and mercuric ions, which was complete in an hour or so under average conditions, and a reaction of the mercuric salt with the hydrocarbon matrix of the resin, which was slower and continued over several days. At 60° this secondary reaction was fast enough to interfere with the measurement of the ion-exchange equilibrium; at 25° and below, equilibrium measurements could be made satisfactorily with contact times less than 6 hours.

The resin used was Dowex 50W-X8, 50-100 mesh, a light yellow bead-type sulfonated polystyrene with 8% nominal crosslinking. It was washed, converted to the hydrogen form and air-dried before use. The exchange capacity was 5.18 meq./g. dry H-resin; the water uptake on swelling, 1.20 g./g. dry H-resin as determined by blotting the wet resin with filter paper, placing in a bottle and weighing, then drying and reweighing.[1]

(a) **The Ion-exchange Equilibrium.**—Measured weights of H-resin were stirred with known volumes of a solution of mercuric perchlorate containing perchloric acid to prevent hydrolysis. Samples of solution were withdrawn at intervals and analyzed. After 1–2 hours the mercuric ion concentration showed no further change. After 4–5 hours the solution was separated from the resin. The resin was caught on a sintered glass filter, washed with about 20 ml. of water, and its replaceable hydrogen ion content determined by transferring the resin to a beaker, adding water and 2 g. of potassium bromide, then titrating potentiometrically. The potassium ions displace H^+ and Hg^{++} from the resin, the bromide ions complex Hg^{++} and prevent its hydrolysis. The hydrogen ion content of the solution was found by potentiometric titration after adding potassium bromide or chloride. The mercuric ion content was found by titration with "Versene"[2] or, if very small, by dithizone.

The equilibrium quotient of the reaction

$$2H\ Res + Hg^{++} \rightleftharpoons Hg\ Res_2 + 2H^+$$

was computed as

$$K = \frac{(\text{meq. } Hg^{++})_r \times \text{g. resin}}{(\text{meq. } H^+)_r^2} \times \frac{(\text{meq. } H^+)_s^2}{(\text{meq. } Hg^{++})_r \times \text{ml. soln.}}$$

The subscripts r and s refer to resin and solution. Grams of resin are on the dry basis; the solution volume was corrected for the water taken into the swollen resin beads, since it was verified that electrolyte was excluded due to the Donnan equilibrium. Data for 0 and 25° are presented in Fig. 1, K being plotted against the equivalent fraction of mercury in the resin. The data at each temperature are for a constant equivalent concentration in the solution 0.137 N in every case. Since the equivalent fraction of mercury in the solution was never more than 0.27 (the maximum for the 0° series) and was usually very much less, the ionic strength was approximately constant. The hydrolysis of the mercuric ion should be less than 2% since the acid normality at equilibrium was at least 0.1.[3]

The data show that the selectivity of the resin for mercury increases with the proportion of metal ions in the resin, which seems to be characteristic of the divalent heavy metal ion–hydrogen ion exchanges so far studied in our laboratory. Similar increases of selectivity with metal ion loading have been found in certain cases by Bonner and coworkers.[4] Complete thermodynamic treatment of the data is not possible without knowledge of the activity coefficients in solution; on the assumption that these do not change with temperature, $\Delta H = 1160$ cal. for a gram-equivalent of pure H-resin reacting to form a gram-equivalent of pure Hg-

(1) O. D. Bonner, W. J. Argersinger and A. W. Davidson, *J. Am. Chem. Soc.*, **74**, 1044 (1952).

(2) G. Schwarzenbach, "Die Komplexometrische Titrationen," 1956, p. 82.

(3) S. Hietanen and L. G. Sillén, *Acta Chem. Scand.*, **6**. 747 (1952).

(4) O. D. Bonner, THIS JOURNAL, **59**, 719 (1955); O. D. Bonner and F. L. Livingston, *ibid.*, **60**, 530 (1956); O. D. Bonner and L. L. Smith, *ibid.*, **61**, 326 (1957).

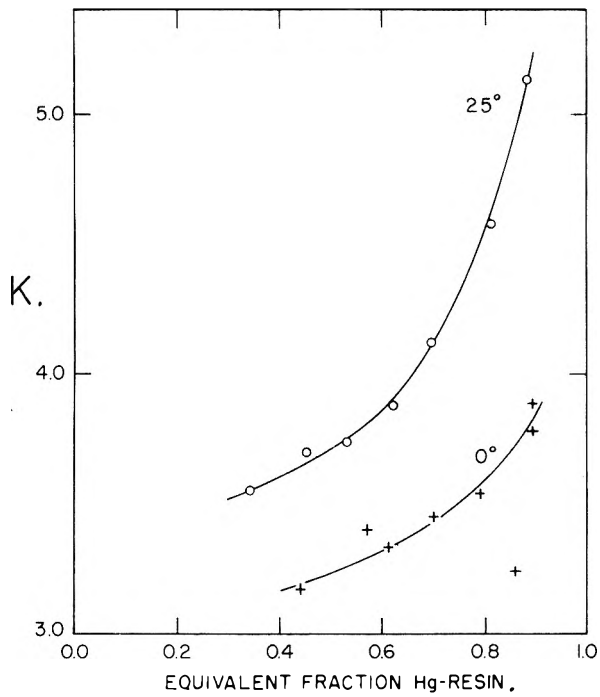

Fig. 1.

resin. This was computed using the graphical integration method of Gaines and Thomas.[5]

(b) **The Secondary Reaction.**—When resin was stirred at 60° with a solution containing enough mercuric ions to be nearly equivalent to the exchangeable hydrogen ions in the resin, the mercuric ion concentration fell continuously for several days, finally dropping below 10^{-4} molar. When the resin was separated and titrated with base after addition of potassium bromide as described above, much more replaceable hydrogen ions were found in the resin than could be explained by normal cation exchange. A typical experiment yielded the following data: H-Resin taken, 1.581 g. (air-dry) = 6.62 meq., solution taken, 50.0 ml., containing 5.87 meq. $Hg(ClO_4)_2$ and 1.10 meq. $HClO_4$. After stirring at 60° for 110 hours, the solution contained 0.0029 meq. Hg^{++} and 6.80 meq. H^+. The resin contained 3.96 meq. replaceable H^+. In this example 2.96 meq. of acid was formed during the experiment.

In other tests resin was stirred with a considerable excess of mercuric perchlorate at 80–85°. After 48 hours the mercury content of the solution was still falling, although the total normality remained unchanged. The resin had absorbed over 15 meq. of mercury per gram (dry basis), or over three times the normal exchange capacity. No replaceable hydrogen ions were found in such resins; on the contrary, a very small amount of strong base was liberated when the resin was removed and stirred with potassium bromide.

No sulfate ions were found in the solutions, suggesting that the sulfonic acid groups of the resin remained intact. No soluble mercurous salt was detected, though a very small amount of mercurous bromide was formed when the mercurated resin was stirred with aqueous potassium bromide. Mercuric ions were released slowly and very incompletely (about 0.2 meq. per gram resin) when the resin was extracted with 2 *N* sulfuric acid. Aqueous potassium iodide removed more mercury from the resin but, even so, only a fraction of the mercury could be extracted.

The heavily mercurated resin was of a darker color than the hydrogen resin and took up less water on swelling. A sample, powdered and pressed into a pellet with solid potassium bromide, showed strong infrared absorption at 8.6 μ; this band was absent in the original hydrogen resin, and was not found in a spectrum of phenyl mercuric acetate which was run for comparison.

The mode of reaction of mercuric ions with the resin is uncertain, but it seems that mercury displaced hydrogen in ionic form from the aromatic rings, perhaps in the manner

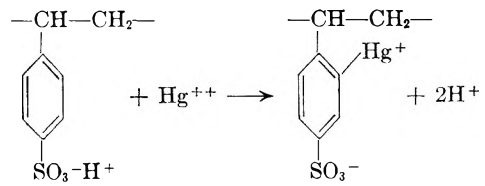

Such a reaction is like the mercuration of toluene by mercuric perchlorate reported by Klapproth and Westheimer[6] and could explain the uptake of one mercury atom per aromatic ring. Uptake of mercury proceeded beyond this stage without perchlorate ions entering the resin; this suggests that additional mercury atoms formed bridges between aromatic rings. A reaction of this type was noted by Miles, Stadtman and Kielley[7] who crosslinked a phenol–formaldehyde polymer by reaction with mercuric acetate. Such bridging would account for the reduced water uptake on swelling and may account for the infrared band at 8.6 μ.

Acknowledgments.—This work was supported by the U. S. Atomic Energy Commission, Contract No. AT(11-1)-499. Thanks are due to M. G. Suryaraman for assistance.

(5) G. L. Gaines and H. C. Thomas, *J. Chem. Phys.*, **21**, 714 (1953).

(6) W. J. Klapproth and F. H. Westheimer, *J. Am. Chem. Soc.*, **72**, 4461 (1950).

(7) H. T. Miles, E. R. Stadtman and W. W. Kielley, *ibid.*, **76**, 4041 (1954).

ALCOHOLYSIS OF BORON–BORON BONDS TO FORM HYDRIDES

BY I. SHAPIRO* AND H. G. WEISS

Research Laboratory, Olin Mathieson Chemical Corporation, Pasadena, California

Received November 29, 1958

The recently proposed mechanism for the alcoholysis of pentaborane[1] is surprisingly similar to that proposed for diborane,[2,3] yet from structural considerations a more complex mechanism related to the breaking of boron–boron bonds in the higher

* Box 24231, Los Angeles 24, California.

(1) A. F. Zhigach, E. B. Kazakova and R. A. Kigel, *Doklady Akad. Nauk SSSR*, **106**, 69 (1956).

(2) A. B. Burg and H. I. Schlesinger, *J. Am. Chem. Soc.*, **55**, 4020 (1933).

(3) H. G. Weiss and I. Shapiro, *ibid.*, **75**, 1221 (1953).

boron hydrides would be anticipated. In diborane[4] the two borons are connected by a pair of hydrogen bridges; thus the molecule can be regarded as composed of only BH_3 units, hence no B–B bonds. Such BH_3 units are capable of reacting with water[3] or alcohols[2] to yield one molecule of hydrogen per hydridic hydrogen as shown in equation 1

$$B_2H_6 + 6ROH \longrightarrow 2B(OR)_3 + 6H_2 \qquad (1)$$

In higher boron hydrides the molecules contain B–B bonds in addition to B–H bonds. For example, in the structure of tetraborane[5] (Fig. 1) two

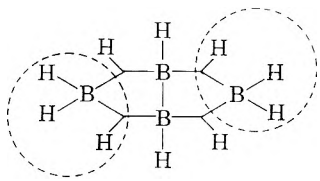

Fig. 1.—Graphic representation of molecular structure of tetraborane.

borons form a direct B–B bond while the other two borons are joined to this B–B unit through hydrogen bridges. Terminal hydrogens are attached to each boron as shown. The net effect is that two of the borons resemble BH_3 units (dotted circles, Fig. 1). In general, as the number of borons in the boron hydride increases, the greater the number of B–B bonds present.

The question now arises as to what happens when water or alcohol attacks these higher molecular weight boron hydrides. From studies on hydrolysis[6] and alcoholysis[1,7,8] the ultimate products are found to be the same as those obtained from diborane; but somewhere in the process more molecular hydrogen forms than corresponds to the number of hydridic hydrogens present in the boron hydride, as shown in the equations

$$B_4H_{10} + 12ROH \longrightarrow 4B(OR)_3 + 11H_2 \qquad (2)$$
$$B_5H_9 + 15ROH \longrightarrow 5B(OR)_3 + 12H_2 \qquad (3)$$
$$B_{10}H_{14} + 30ROH \longrightarrow 10B(OR)_3 + 22H_2 \qquad (4)$$

The number of moles of hydrogen in excess of the number of hydrogens in the boron hydride represent the number of B–B bonds that must be broken, and, as shown by the above equations, two ROH molecules ultimately are required for each of these B–B bonds. Thus, although the terminal B–H bonds are expected to react similarly to those in diborane, the presence of B–B bonds clearly introduces a new element.

Experiments using isotopically labeled reagents reveal that alcoholic protons are converted into hydridic hydrogens when B–B bonds are ruptured.

Experimental

1. **Reagents.**—**Diborane** and **deuteriodiborane** were prepared[9] by the reaction of boron trifluoride with lithium aluminum hydride or lithium aluminum deuteride (obtained from Metal Hydrides, Inc., Beverly, Mass.). **Tetraborane** and **pentaborane** were fractionated from the pyrolysis products of diborane, and identified by infrared and mass spectral analysis. **Ethanol** was purified by refluxing over and distilling from anhydrous calcium oxide. Deuterated ethanol (C_2H_5OD) was obtained from Merck and Co., Limited, Montreal, Canada.

2. **Apparatus.**—Standard high vacuum apparatus was used for preparing and handling the boron hydrides. Infrared spectra were obtained with a Perkin–Elmer Model 21 spectrophotometer equipped with sodium chloride optics. The standard 5-cm. gas cell was modified to include a mercury manometer and a side arm closed by a (self-sealing) silicone plug through which the reagents could be injected into the cell.

3. **Procedure.**—All experiments were carried out at room temperature. The appropriate isotopic species of diborane, tetraborane or pentaborane was introduced into the infrared gas cell at a measured pressure, and its spectrum was taken. Then the isotopically labeled ethanol was injected in incremental amounts through the self-sealing silicone plug by means of a 20-gage double-ended hypodermic needle whose other end was attached to the ethanol reservoir. The reservoirs also were equipped with silicone plugs and were manipulated in such a manner that only the content of the internal volume of the needle was injected at any one time. Although the reservoir, and consequently the needle, contained the reactant as a liquid, the reactant vaporized readily as it entered the cell due to the low pressure therein. An infrared spectrum was obtained immediately after each injection and again after standing for one-half hour. Negligible changes in spectra occurred on standing. The volume of the hypodermic needle was sufficiently small so that each increment of reagent consumed only a small portion of the boron hydride.

Results

The incremental addition of either isotopically normal or deuterated ethanol to isotopically normal diborane resulted in the progressive formation of diethoxyborane, $HB(OC_2H_5)_2$, which subsequently reacted with additional ethanol to form triethoxyborane. Substantially all of the diborane was converted to diethoxyborane before any triethoxyborane was detected. When deuterated diborane was treated with ethanol, the only intermediate detected was $DB(OC_2H_5)_2$. The various isotopic species of the ethoxyboranes were easily identified from their infrared spectra; the complete vibrational assignments of these compounds are being reported separately.[10]

When ethanol was added to excess tetraborane or pentaborane, $HB(OC_2H_5)_2$ was found as a product; however, when C_2H_5OD was added to these higher boron hydrides, both $HB(OC_2H_5)_2$ and $DB(OC_2H_5)_2$ were found. In the case of tetraborane the concentration of the protonated intermediate was approximately twice as great as that of the deuterated intermediate; with pentaborane the relative amounts of the two intermediate species were nearly the same. The respective ratios of the two species were maintained for each incremental addition of the ethanol-*d*. Additionally, an appreciable amount of triethoxyborane was observed even though the amount of ethanol added was comparatively small with respect to the boron hydride.

Discussion

The formation of $DB(OC_2H_5)_2$ from C_2H_5OD and tetraborane or pentaborane, and the absence of this compound in the case of diborane, show that

(4) R. P. Bell and H. C. Longuet-Higgins, *Proc. Roy. Soc.* (*London*) **A183**, 357 (1945).

(5) C. E. Nordman and W. N. Lipscomb, *J. Am. Chem. Soc.*, **75**, 4116 (1953).

(6) I. Shapiro and H. G. Weiss, *ibid.*, **76**, 6020 (1954).

(7) H. C. Beachell and T. R. Meeker, *ibid.*, **78**, 1796 (1956).

(8) H. C. Beachell and W. C. Schar, *ibid.*, **80**, 2943 (1958).

(9) I. Shapiro, H. G. Weiss, M. Schmich, S. Skolnik and G. B. L. Smith, *ibid.*, **74**, 901 (1952).

(10) W. J. Lehmann, H. G. Weiss and I. Shapiro, *J. Chem. Phys.*, in press.

a deuteride is created from the alcoholic deuterium during the breaking of the boron–boron bond. The ethoxy group apparently attaches itself to one boron atom and the deuterium goes to the other boron atom, *viz.*

$$>B—B< + C_2H_5OD \longrightarrow >B—OC_2H_5 + DB< \quad (5)$$

In general the mechanism of the rupture of the B–B bonds (I) can be regarded as analogous to that of B–H bonds (II).

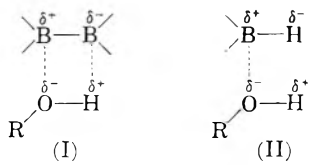

(I) (II)

The relative concentrations of the protonated and deuterated intermediate species observed for tetraborane and pentaborane are related directly to the structure of these boron hydrides. In tetraborane the two borane groups (Fig. 1) will behave similarly to those of diborane; each borane group can form one $HB(OC_2H_5)_2$, or a total of two diethoxyborane molecules per tetraborane molecule. According to equation 5 the rupture of the B–B group will lead to one $DB(OC_2H_5)_2$ in agreement with the observed over-all ratio of $2HB(OC_2H_5)_2$ per $DB(OC_2H_5)_2$. With regard to the pentaborane structure[11] two of the borons can be pictured as being extracted as "BH_3" groups[12] to yield two $HB(OC_2H_5)_2$ molecules per pentaborane molecule. The remaining three borons form a complex system made up of B–B linkages, which, upon rupture by C_2H_5OD, result in an average of two $DB(OC_2H_5)_2$ molecules, thus accounting for equimolar amounts of $HB(OC_2H_5)_2$ and $DB(OC_2H_5)_2$.

Previously, it had been considered[13] that upon hydrolysis of boron hydrides all B–H units were converted to B–OH units before the cleavage of B–B bonds began. Apparently this sequence is not correct since present experiments indicate that B–B bonds are ruptured in the presence of $HB(OR)_2$.

The observed formation of triethoxyborane in addition to the two species of diethoxyboranes under conditions of excess tetraborane or pentaborane is significant, since reactions involving diborane do not yield triethoxyborane until all of the diborane has been converted to $HB(OC_2H_5)_2$.[14] The triethoxyborane can be accounted for easily as a direct consequence of the rupture of the B–B bond as shown in equation 5, *i.e.*, the addition of one molecule of ethanol to a compound such as diboron tetraethoxide would result in formation of one molecule of triethoxyborane and one molecule of diethoxyborane.

(11) K. Hedberg, M. E. Jones and V. Schomaker, *J. Am. Chem. Soc.*, **73**, 3538 (1951); W. J. Dulmage and W. N. Lipscomb, *ibid.*, **73**, 3539 (1951).

(12) A. B. Burg, *ibid.*, **79**, 2129 (1957).

(13) N. V. Sidgwick, "The Chemical Elements and Their Compounds," Oxford University Press, London, 1950, p. 361, and references contained therein.

(14) The rate of formation of $B(OC_2H_5)_3$ from $HB(OC_2H_5)_2$ has been found to be slow at room temperature.

DISSOCIATION CONSTANT OF XANTHIC ACID AS DETERMINED BY SPECTROPHOTOMETRIC METHOD

BY I. IWASAKI AND S. R. B. COOKE

School of Mines and Metallurgy, University of Minnesota, Minneapolis, Minn.

Received December 4, 1958

The decomposition of ethyl xanthate ($C_2H_5OCSS^-$) in acid solutions has been studied spectrophotometrically and the results have been presented in a previous article.[1] It was concluded that the xanthate and xanthic acid were virtually in equilibrium and that the monomolecular decomposition of xanthic acid into carbon disulfide and alcohol was rate determining, according to the equation

$$H^+ + X^- \rightleftharpoons HX \longrightarrow ROH + CS_2 \quad (1)$$

Based on this mechanism the authors were able to calculate the dissociation constant of xanthic acid from the decomposition rate data. In the present article it will be shown that the dissociation constant also can be calculated from the initial optical density data for different acid concentrations.

If ϵ_1 and ϵ_2 represent the molar extinction coefficients of xanthic acid and xanthate ion, respectively, the optical density D of a solution containing a mixture of these two species in a cuvette of 1 cm. length is given by[2]

$$D = \epsilon_1[HX] + \epsilon_2[X^-] = \epsilon\{[HX] + [X^-]\} \quad (2)$$

$$\text{or } (\epsilon - \epsilon_1) + \frac{[X^-]}{[HX]}(\epsilon - \epsilon_2) = 0 \quad (3)$$

where the brackets denote molar concentrations and ϵ the molar extinction coefficient of a solution containing the mixture.

The dissociation constant of xanthic acid is given by

$$K = \frac{[X^-]}{[HX]} \times \frac{\gamma_{X^-}}{\gamma_{HX}} \times a_{H^+} \quad (4)$$

where γ_{X^-} and γ_{HX} are the activity coefficients of xanthate and xanthic acid, respectively, and a_{H^+} the hydrogen ion activity. Combination of equations 3 and 4 leads to another expression

$$\epsilon = \frac{(\epsilon_2 - \epsilon)}{a_{H^+}}\left(\frac{\gamma_{HX}}{\gamma_{X^-}}\right)K + \epsilon_1 \quad (5)$$

$$\epsilon = \alpha K + \epsilon_1 \quad (6)$$

Where

$$\alpha = \frac{(\epsilon_2 - \epsilon)}{a_{H^+}} \times \frac{\gamma_{HX}}{\gamma_{X^-}} \quad (7)$$

Since, in equations 6 and 7, ϵ_2, ϵ and a_{H^+} can be determined experimentally and the activity coefficients theoretically, the values of α can be calculated, and the plot of α against ϵ should be a straight line with a slope corresponding to the dissociation constant K, and the intercept to the molar extinction coefficient ϵ_1 of xanthic acid.

Experimental and Discussion

Potassium ethyl xanthate used in this experiment was prepared in the usual manner.[3] The optical density measurements were made with a Beckman DU Quartz Spectro-

(1) I. Iwasaki and S. R. B. Cooke, *J. Am. Chem. Soc.*, **80**, 285 (1958).

(2) K. P. Ang, THIS JOURNAL, **62**, 1109 (1958).

(3) L. S. Foster, *Utah Eng. Exp. St. T. P.*, 5 (1929).

photometer at the characteristic absorption peak occurring at 301 mμ.[4] A 1 cm. path length cuvette was used. The concentration of hydrochloric acid used in the experiments ranged from 0.048 to 0.963 *M*. Determinations were made at room temperature, 21°.

In the stated acid range the decomposition of xanthate is extremely rapid; hence the initial optical densities, for which both total xanthate and acid concentrations were known, have been determined by measuring the decomposition rate using a rapid mixing apparatus described previously,[1] followed by extrapolating the experimental line to zero time. Briefly, the apparatus consists of two 2-ml. syringes, with xanthate solution in one and acid in the other, which were connected through plastic tubing to a glass T-tube, where the mixing was effected. The syringes were fixed in a parallel position on a Lucite stand, and a plunger guide enabled the syringe plungers to deliver the solutions at identical rates. The mixed solution was introduced directly into the cuvette and the optical density was measured as a function of time. When the logarithm of optical density was plotted against time, a linear relationship was obtained. The theoretical basis for this relationship has been given in the previous article.[1] Three tests were made at each condition of acid and xanthate concentration. The optical density of the initial xanthate concentration was then obtained by the extrapolation of the experimental line to zero time. The results thus gathered for various concentrations of xanthate and of hydrochloric acid are presented in Table I. From the table it is evident that ϵ is strongly dependent on hydrochloric acid concentration and that the reproducibility of ϵ at a given acid concentration is satisfactory.

The value of the molar extinction coefficient of xanthate ion ϵ_2 was determined at the natural *p*H of the potassium ethyl xanthate solution. The average of eleven independent measurements was determined to be 17,398 ± 98, and this value was used for subsequent calculation of α.

As seen in Table I, the ionic strength of a mixture of xanthate and hydrochloric acid is controlled essentially by the acid concentration; hence the activity coefficient for xanthate ion was calculated using the extended Debye–Hückel equation described by Harned and Owen.[5] The activity coefficient for xanthic acid was tacitly assumed to be unity, particularly because of the conclusion reached for other neutral molecules in hydrochloric acid.[5]

TABLE I

INITIAL OPTICAL DENSITIES OF XANTHIC ACID

$[H^+]$, *M*	Total xanthate $\times 10^4$, *M*	$Dt = 0$	ϵ	$\alpha \times 10^{-5}$
0.048	2.21	1.63	7346	3.01
.048	1.58	1.15	7250	3.04
.097	3.33	1.67	4995	2.00
.097	2.21	1.11	5003	2.00
.240	2.21	0.58	2614	1.06
.240	1.58	.435	2742	1.05
.478	3.33	.475	1421	0.571
.478	6.19	.93	1496	.568
.717	6.19	.61	982	.369
.717	9.54	.94	981	.369
.963	6.19	.44	708	.245
.963	9.54	.70	731	.245

When the values of α thus calculated were plotted against ϵ a straight line was obtained, in good agreement with equation 6. From the slope of this line, *K* is determined to be 0.0239 ± 0.0002 and from the intercept $\epsilon_1 = 130 \pm 35$. It should be noted that this value of ϵ_1 is quite different from that for xanthate ion for which ϵ_2 is 17,398. The loss of symmetry in the CSS branch through the attachment of hydrogen, as indicated by this lowered molar extinction coefficient, might account for the instability of xanthic acid.

From previous decomposition rate studies the authors reported the dissociation constant of xanthic acid to be 0.020, in good agreement with the present value of 0.0239. This agreement would seem to support the validity of the two independent methods used for its determination. von Halban and Hecht[6] report a value of 0.030 from iodimetric titration data, Hantzsch and Bucirius,[7] 0.028 from conductivity measurement, King and Dublon,[8] 0.031 from vapor pressure measurements, and Cook and Nixon,[9] 0.007 from *p*H measurements. The value obtained by the present authors, although slightly smaller, is in good agreement with the first three values.

(4) I. Iwasaki and S. R. B. Cooke, *Min. Eng.*, **208**, 1267 (1957).

(5) H. S. Harned and B. B. Owen, "The Physical Chemistry of Electrolytic Solutions," Reinhold Publ. Corp., New York, N. Y., 1958, pp. 469, 532.

(6) H. von Halban and W. Hecht, *Z. Elektrochem.*, **24**, 65 (1918).

(7) A. Hantzsch and W. Bucirius, *Ber.*, **59**, 793 (1926).

(8) C. V. King and E. Dublon, *J. Am. Chem. Soc.*, **54**, 2177 (1932).

(9) M. A. Cook and J. C. Nixon, THIS JOURNAL, **54**, 445 (1950).

OBSERVATIONS ON RESIN-DEIONIZED WATER AS A SUBSTRATE FOR MONOLAYER STUDIES

BY GEORGE L. GAINES, JR.

General Electric Research Laboratory, Schenectady, New York

Received December 6, 1958

Recently, considerable interest has been shown in the details of force–area isotherms for monolayers spread at the water–air interface. Thus, both Cook and Ries[1] and LaMer and Robbins[2] have found variations in stearic acid force–area curves which seem to depend on spreading solvent effects.

In the light of the observation by Schenkel and Kitchener[3] that water deionized by passage through mixed-bed ion-exchange resin columns gave anomalous results in studies of certain surface phenomena, some observations on the behavior of stearic acid monolayers on such deionized water seem worthy of note. These results, together with our analytical data on the water, support the suggestion of Schenkel and Kitchener concerning the cause of the observed anomalies.

Experimental

The three sources of water examined included: (1) ordinary laboratory distilled water, (2) deionized water prepared by passing this distilled water through a fresh commercial mixed-bed demineralizing unit at recommended flow rates, and (3) redistilled water obtained from a two-stage fused quartz still using laboratory distilled water as feed. Trace analyses for copper were performed colorimetrically[4]; alkali metals were determined with a flame photometer; and nitrogen reactive to Nessler reagent was estimated by direct Nesslerization of 50-ml. samples[5] using reagents prepared with quartz redistilled water.

Force–area curves were measured using a commercial film balance of the Langmuir–Adam type (Cenco "Hydrophil

(1) H. D. Cook and H. E. Ries, Jr., THIS JOURNAL, **60**, 1533 (1956).

(2) V. K. LaMer and M. L. Robbins, *ibid.*, **62**, 1291 (1958).

(3) J. H. Schenkel and J. A. Kitchener, *Nature*, **182**, 131 (1958).

(4) R. E. Peterson and M. E. Bollier, *Anal. Chem.*, **27**, 1195 (1955).

(5) S. H. Yuen and A. G. Pollard, *J. Sci. Food Agric.*, **3**, 441 (1952).

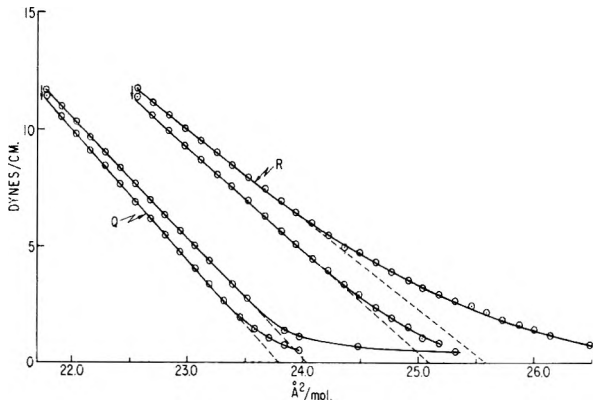

Fig. 1.—Force–area curves for stearic acid monolayers on "fresh" water surfaces: Q, quartz-redistilled water; R, resin-deionized water.

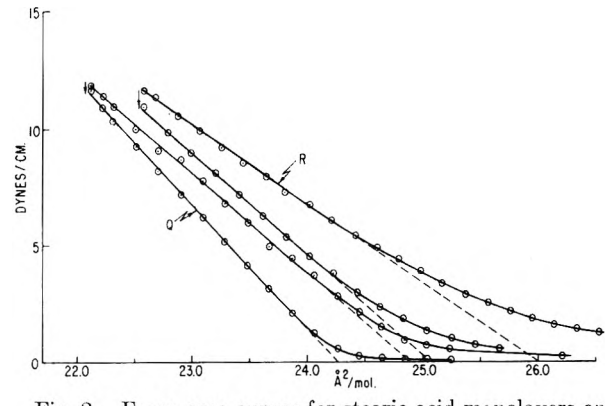

Fig. 2.—Force–area curves for stearic acid monolayers on "used" water surfaces: Q, quartz-redistilled water; R, resin-deionized water.

Balance") which had been modified by the incorporation of a 5 mil tungsten torsion wire to give a sensitivity of 0.05 dyne/cm. per degree of rotation of the torsion head. The edges of the tray, the mica float and Pt foils, and the movable barriers were coated with paraffin. Conventional precautions and procedures were observed.[6] Although no provision for temperature control was made, the air temperature immediately above the tray and the temperature of the water in the tray were measured, and in all the experiments reported the air temperature was 26.2 ± 0.5° and the water temperature was 24.5 ± 0.5°.

All experiments were performed with a spreading solution containing 0.33 mg. of stearic acid per ml. of *n*-hexane. The stearic acid was "Certified Pure" grade material supplied by Armour & Co. Research Division; the *n*-hexane was Philips 99+ mole % material which had been passed through columns containing alumina and silica gel to remove any surface active impurities. The solution was delivered to the surface of the tray with an "Agla" micrometer syringe. Volumes spread ranged from 0.20 to 0.31 ml.

In each of the measurements discussed, the stearic acid solution was applied to the water surface after sweeping and zeroing the torsion balance, the movable barrier was advanced until the pressure increased to ~0.5 dyne/cm., and the film was allowed to stand at this area for ~10 minutes. (During this time the film pressure decreased slightly, even though there was no leakage of the film. This may have been due to evaporation of solvent.) Compression was then begun by moving the barrier manually; areas and corresponding pressures were recorded. The barrier was generally advanced 1–2 mm. every 30 sec. The average rate of area change in all the experiments was 0.2–0.4 Å.²/mol. per minute. This procedure was continued until a pressure of 11.6–11.8 dynes/cm. was reached, whereupon the film was allowed to stand for 5–8 minutes at constant area. In every case, the film pressure decreased slightly during this interval. The barrier then was moved in the opposite direction at the same rate to trace the expansion curve. After the completion of the expansion curve and a delay of 2–3 minutes at constant area and a pressure of 0.2–0.5 dyne/cm. (during which the film pressure always increased slightly), a second compression curve was run. In cases when collapse was approached, this was done in this second compression. At the completion of these operations, the movable barrier was returned to the far end of the tray and the torsion head was again zeroed to verify that no significant change in the null point had occurred.

Force–area curves were obtained on "fresh" and "used" water substrates. In the case of the "used" water surfaces, several stearic acid films had been spread, compressed and expanded, allowed to stand for periods of 10–60 minutes, and swept off before the experiment illustrated was performed. For "fresh" surfaces, the water was poured into the tray, the film spread and the experiment begun immediately. Collapse curves were determined on "used" water surfaces, and in both cases represent the second compression of the film, as noted above.

(6) *Cf.* N. K. Adam, "The Physics and Chemistry of Surfaces," 3rd ed., Oxford Univ. Press, New York, N. Y., 1941, pp. 27–33.

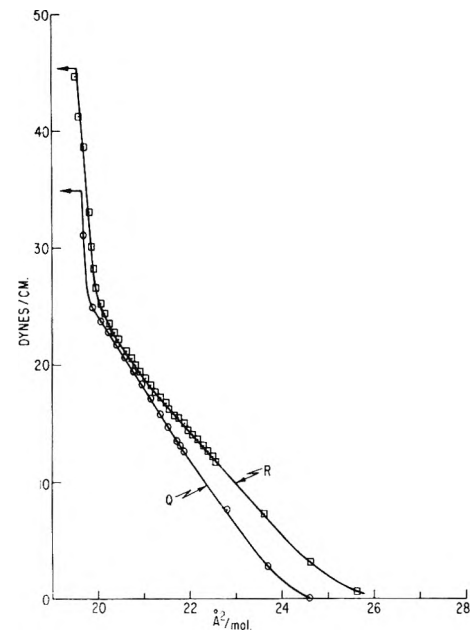

Fig. 3.—Force–area curves for stearic acid monolayers as collapse of film is approached ("used" water, second compression of each film): Q, quartz-redistilled water; R, resin-deionized water.

Results and Discussion

Analytical data are presented in Table I. Figures 1 and 2 illustrate the compression and expansion of stearic acid monolayers on the resin-deionized and quartz-redistilled water. In Table II, data derived from these curves are summarized. Figure 3 illustrates the behavior of stearic acid films on the two substrates as collapse is approached.

It is apparent that films on deionized water behave differently than those on quartz-redistilled water, exhibiting larger extrapolated areas per molecule, higher compressibility, higher collapse pressure, and slightly more curvature and hysteresis in the π–a curves. This behavior might well be interpreted in terms of the interaction of a basic polyelectrolyte with the stearic acid monolayer. These observations, together with our analytical data showing that the resin-treated water is of fair quality with respect to inorganic cationic contaminants, but contains an appreci-

TABLE I

CONTAMINANTS IN PURIFIED WATER (P.P.M.)

	Resistivity (25°), ohm. cm.	Cu	Na	K	N
(1) Distilled	$\sim 3 \times 10^5$	0.12	...	...	up to 0.07
(2) Deionized	$>1 \times 10^6$	0.07	<0.2	<0.2	0.35
(3) Redistilled in quartz	....	<0.03	...	...	<0.05

TABLE II

CHARACTERISTICS OF π-a CURVES FOR STEARIC ACID ON WATER SURFACES

	Quartz-redistilled "Fresh"	Quartz-redistilled "Used"	Resin-deionized "Fresh"	Resin-deionized "Used"
Extrap. area, $\pi = 0$, Å.²/mol.				
Compression	24.04	24.88	25.59	26.00
Expansion	23.78	24.27	25.09	25.06
$-da/d\pi$				
Compression	0.193	0.233	0.258	0.295
Expansion	.178	.188	.226	.231
$\pi_{max.}$ first compress., dynes/cm.	11.70	11.83	11.78	11.65
π at same area, second compress.	11.91	11.90	12.07	11.83

able amount of nitrogenous material reactive to Nessler reagent, lends strong support to the hypothesis advanced by Schenkel and Kitchener. They proposed that the anomalous behavior which they observed in electrokinetic studies was due to soluble polyelectrolytes derived from the resin bed, most probably from the nitrogenous anion-exchange resin. In the light of these observations, Schenkel and Kitchener's warning that "at the present time it is clearly advisable to avoid the use of (anion- or mixed-bed) resins entirely in all critical work in surface chemistry where small surface areas are concerned" should be heeded. It is possible, for example, that the presence of polyelectrolytes in the substrate might affect the nature of the island structures which Ries and Kimball[7] have found in monolayers transferred from water surfaces.

While the present data were not taken to study the properties of monolayers *per se*, and they are not sufficiently complete to justify extended discussion, certain features of the π–a curves seem worthy of note. In none of the present experiments was the nearly vertical "solid film" type of π–a curve found for stearic acid on either type of water (even though after one experiment the water was left in the tray for more than 3 days and a repeat experiment was performed after this time). This result is in accord with the explanation advanced by Myers and Harkins[8] that the behavior of films on "old" water as described by Adam[9] was due to traces of divalent ions.

A peculiar effect is the slight but significant shift of the π–a curve to larger areas which is found when the water is "used" as opposed to "fresh." The effect is more noticeable on quartz-redistilled water, but also was found in all of the experiments on deionized water. Saturation of the substrate either with stearic acid or solvent after successive runs might account for this phenomenon, but no direct evidence is available to test this possibility.

In Table II, the maximum values of film pressure in the initial compression and the values of π observed in the second compression at the same area are noted. These data afford a sensitive test for leaks; the slightly higher values on the second compression probably are due to air-borne contamination arriving in the film.

Adam[9] noted many years ago that appreciable hysteresis might occur in the liquid-compressed region of π–a curves for fatty acid films. All of the measurements reported here show such hysteresis. Further study of this behavior seems in order.

I am indebted to W. W. Welbon, H. W. Middleton and Miss C. P. Rutkowski for assistance in this work.

(7) H. E. Ries, Jr., and W. A. Kimball, "Proc. Second Internatl. Congress of Surface Activity," Vol. I, London, Butterworth Scientific Publications, 1957, p. 75.

(8) R. J. Myers and W. D. Harkins, *Nature*, **139**, 367 (1937).

(9) N. K. Adam, *Proc. Roy. Soc.* (*London*), **A101**, 466 (1922).

THE CARBONYL INTENSITIES OF SOME SIMPLE AMIDES

BY THEODORE L. BROWN, JOHN F. REGAN, ROBERT D. SCHUETZ AND JAMES C. STERNBERG

A joint contribution from Noyes Chemical Laboratory, University of Illinois, Urbana, Ill., and Kedzie Chemical Laboratory, Michigan State University, East Lansing, Michigan

Received December 8, 1958

There has been considerable interest recently in the infrared spectra of α-substituted carbonyl compounds. Of particular interest is the effect of rotational isomerism on the frequency, shape and intensity of the carbonyl band.[1-3]

The present note reports results obtained a few years ago on the carbonyl band of some simple amides of the general formula $RCONH_2$. The data are of value and interest in relating the behavior of amides to that of other carbonyl compounds.

Experimental

A Perkin–Elmer Model 21 spectrometer fitted with sodium chloride optics was employed. The calculated spectral slit width was 3.5 cm.$^{-1}$, and the cell thickness was 0.487 mm.

Reagent grade chloroform was used as solvent. Acetamide, benzamide and formamide were obtained commercially; all other compounds were synthesized by methods which are described elsewhere.[4] All the compounds were carefully purified and dried prior to use.

(1) L. J. Bellamy and R. L. Williams, *J. Chem. Soc.*, 4294 (1957).

(2) R. N. Jones and E. Spinner, *Can. J. Chem.*, **36**, 1020 (1958).

(3) T. L. Brown, *J. Am. Chem. Soc.*, **80**, 3513 (1958).

(4) J. F. Regan, Ph.D. Thesis, Michigan State University, 1957.

The procedure used in determining intensities is described elsewhere.[3] The integration interval chosen was 100 cm.$^{-1}$. Overlapping from adjacent bands was considered negligible, since the absorption fell to nearly zero at the edges of the integration interval. Solution concentrations were in the range 0.005–0.017 molar. At least three separate intensity determinations were made on each compound, and the results were averaged. Chloroform was used as solvent rather than carbon tetrachloride, because the compounds were not sufficiently soluble in the latter.

Results

Table I shows the results of the intensity studies of nine amides, $RCONH_2$; the group R is listed in the first column, the total integrated intensity A in the second, and the frequency ν_m of band maximum in the third. In some cases the band was clearly split, so that the presence of at least one other maximum could be inferred. An (S) is placed alongside the frequency in these cases. The units of intensity are 1×10^4 mole^{-1} liter cm.$^{-2}$, and the frequencies are given in cm.$^{-1}$.

The relative values of intensity are very probably correct to within 0.1 intensity unit; the frequencies are considered correct to within 2 cm.$^{-1}$.

Wing corrections[5] were not applied. For those compounds with symmetric band shapes, these half-widths, in cm.$^{-1}$, were observed: formamide, 15; trifluoroacetamide, 25; benzamide, 21; trichloroacetamide, 24.

Discussion

A number of interesting points are illustrated by the data in Table I.

TABLE I

INTEGRATED INTENSITIES AND FREQUENCIES OF THE CARBONYL BAND IN SOME AMIDES, $RCONH_2$, IN CHLOROFORM

Group R	Integrated intensity A (mole^{-1} l. cm.$^{-2}$ $\times$ 10^{-4})	ν_m (cm.$^{-1}$)
CH_3	4.21	1678, 1702
H	4.22	1709
CH_3CH_2	3.85	1687(S)
$C_2H_5OCH_2$	4.19	1691(S)
$ClCH_2$	3.95	1695
Cl_2CH	3.76	1716(S)
Cl_3C	3.37	1732
C_6H_5	4.06	1678
CF_3	4.04	1750

First, for those compounds in which the group attached to the carbonyl is symmetric, the carbonyl band is also single and symmetric about the band maximum. In all other cases, the band is clearly split or is irregular in shape, indicating the presence of rotational isomers.[1-3] Second, the intensity is considerably lower in those compounds where a bulky group is situated *cis* to the carbonyl, just as was found to be the case in esters.[3] For example, the intensity for the trichloro compound is considerably lower than that for the trifluoro, apparently as a result of the larger van der Waals radius of chlorine as compared with fluorine. Also, it is to be noted that the intensity decrease which occurs when hydrogen, as the attached group (A = 4.22), is replaced by CH_3CH_2 (A = 3.85) may be attributed to the fact that the CH_3 group can occupy a position *cis* to the carbonyl, and in this position it causes a lower carbonyl intensity. When hydrogen is replaced by the CH_3 (A = 4.21) group, there is essentially no change. Finally, the splitting caused by rotational isomerism is not as large in the amides as it is in the closely related esters. It is, in fact, too small to allow a satisfactory separation of the two peaks for the purpose of determining the area under each. It is clear, however, that the behavior of the amides is qualitatively quite similar to that of the esters: a bulky group *cis* to the carbonyl causes a lowering of the carbonyl band intensity, and the lowering increases with the size of the group.

It is surprising that the carbonyl band of acetamide is split into two well-defined maxima. Rotational isomerism of the sort which exists in, for example, the monochloro derivative cannot be the cause of this, for reasons of symmetry. The splitting has been ascribed by some investigators to intermolecular hydrogen bonds formed on association.[6,7] However the ratio of the absorbancies for the two band maxima was measured, in the present study, for acetamide in chloroform solution in the concentration range 0.005–0.014, and was found to be essentially a constant. The ratio of absorbancy of the band at 1678 cm.$^{-1}$ to that of the band at 1702 cm.$^{-1}$ is 1.80 $\pm$ 0.04, with an apparently random scatter of values. If an equilibrium between associated and non-associated molecules were responsible for the splitting, the relative sizes of the two bands should change with concentration.[8] Furthermore, the relative sizes of the two bands is not that to be expected on the basis of equilibrium constants determined from distribution coefficients.[6] It cannot be argued that the splitting is due to hydrogen bonding of chloroform to the carbonyl, producing a second carbonyl band, since the bands for formamide, benzamide, etc., are all symmetric and of reasonably narrow width.

It must be concluded that, as yet, no satisfactory explanation of the splitting of the carbonyl band in this compound has been offered.

(5) D. A. Ramsay, *J. Am. Chem. Soc.*, **74**, 72 (1952).

(6) M. Davies and H. E. Hallam, *Trans. Faraday Soc.*, **47**, 1170 (1951).

(7) C. G. Cannon, *Mikrochim. Acta*, 555 (1955).

(8) Davies and Hallam report the carbonyl absorption of acetamide in 0.04 and 0.2 molar solutions in $CHCl_3$; the relative intensities of the two bands do not appear from their figure to change by very much in this concentration interval. The relative intensities are quite different, however, in 0.002 molar carbon tetrachloride as compared with dilute chloroform.

THE HEAT OF FORMATION OF ANHYDROUS LITHIUM PERCHLORATE

BY MEYER M. MARKOWITZ, ROBERT F. HARRIS AND HARVEY STEWART, JR.

Foote Mineral Company, Research and Development Laboratories, Chemicals Division, Berwyn, Pennsylvania

Received December 8, 1958

In view of the various values reported for the heat of formation of anhydrous lithium perchlorate,[1] it was felt that a redetermination of this quantity was warranted.

(1) J. F. Suttle in "Comprehensive Inorganic Chemistry," Vol. VI, D. Van Nostrand Co., Inc., Princeton, N. J., 1957, p. 108; "Data Sheet on Anhydrous Lithium Perchlorate," American Potash and Chemical Corp., N. Y.

Using a modified Parr model 1411 calorimeter with a calorimeter thermometer capable of being read to 0.001°, the heat of reaction at 25° for LiOH (225 H_2O) + $HClO_4$ (225 H_2O) → $LiClO_4$ (451 H_2O) + H_2O was determined to be −13.54 ± 0.09 kcal./mole, which is consistent with the heat of neutralization of a strong base and a strong acid. As a result, the molar heat of formation of lithium perchlorate (451 H_2O) at 25° is calculated as −97.95 kcal./mole.[2] This latter value compares favorably with the value at infinite dilution at 18° given by Bichowsky and Rossini[3] if the more recent value of the heat of formation of perchloric acid at infinite dilution[2] is applied.

Further calorimetric determinations made in this Laboratory have yielded the values of −6.25 ± 0.03 kcal./mole and 7.91 ± 0.03 kcal./mole for the heats of solution at 25° of anhydrous lithium perchlorate (450 H_2O) and of lithium perchlorate trihydrate (450 H_2O), respectively. Consequently, the enthalpy change at 25° for the reaction $LiClO_4$(s) + H_2O(l) → $LiClO_4 \cdot 3H_2O$(s) is −14.16 ± 0.06 kcal./mole. These data are in good agreement with those reported by Smeets[4] for experiments carried out at 18°. Finally, the standard heat of formation of anhydrous lithium perchlorate is −91.70 kcal./mole, quite in contrast to existent published values.[1]

(2) Complementary heat of formation data obtained from: F. D. Rossini, D. D. Wagman, W. H. Evans, S. Levine and J. Jaffe, "Selected Values of Chemical Thermodynamic Properties," National Bureau of Standards Circular 500, U. S. Government Printing Office, Washington, D. C., 1952.

(3) T. R. Bichowsky and F. D. Rossini, "The Thermochemistry of the Chemical Substances," Reinhold Publ. Corp., New York, N. Y., 1936, p. 132.

(4) C. Smeets, *Natuurw. Tijdschrift*, **15**, 105 (1933); *C. A.*, **27**, 5267³ (1933).

ON THE DETERMINATION OF THE SEDIMENTATION EQUILIBRIUM SECOND VIRIAL COEFFICIENT IN POLYMERIC SOLUTIONS

BY HIROSHI FUJITA[1]

Department of Chemistry, University of Wisconsin, Madison, Wisconsin

Received December 8, 1958

There is some doubt whether the sedimentation equilibrium experiment may be used to study solute–solvent thermodynamic interactions in polymeric solutions.[2] With this note we seek to obtain more definite information with regard to the extent to which the experiment may be of significance with non-ideal solutions of polydisperse neutral molecules. Expressions are derived for the intercept and the limiting slope of a plot of $1/(M_w)_{app}$ *vs.* C_0 as C_0 tends to zero, and it is shown that this intercept allows evaluation of the weight-average molecular weight of the solute and the limiting slope can be correlated with the second virial coefficient obtained from light scattering measurements. Here $(M_w)_{app}$ denotes the apparent molecular weight obtained experimentally as a function of the initial concentration C_0 of the given solution.

On the assumption that the partial specific volume of each polymeric solute is independent of its molecular weight and that the compressibility of the solution is negligible, the equations for the sedimentation equilibrium of the solution consisting of a solvent 1 and $n-1$ neutral solutes 2, 3, . . . , n may be written in the form[3,4]

$$-\lambda M_i c_i = \frac{dc_i}{d\xi} + \sum_{k=2}^{n} \left(\frac{\partial \ln y_i}{\partial c_k}\right)_{T,P,c_j \neq k} c_i \frac{dc_k}{d\xi} \qquad (i = 2, 3, \ldots, n) \quad (1)$$

where

$$\lambda = \frac{(1 - \rho\bar{v})(b^2 - a^2)\omega^2}{2RT} \quad (2)$$

$$\xi = \frac{b^2 - r^2}{b^2 - a^2} \quad (3)$$

The concentration c_i of solute i is expressed in grams per volume of solution, and the activity coefficient y_i of solute i is defined in terms of the same concentration scale. The other symbols have the following significance: M_i = molecular weight of solute i, ρ = density of the solution, $\bar{v}$ = partial specific volume of each solute, ω = angular speed of the rotor, r = radial distance measured from the axis of the rotor, and a and b = positions of the meniscus and cell bottom, respectively. In deriving equation 1 it was assumed that the solution is so dilute that its density may be replaced by the density of the solvent. Because we are concerned with a system of neutral components, the logarithm of y_i may be expanded about infinite dilution to give

$$\ln y_i = M_i \sum_{k=2}^{n} B_{ik} c_k + O(c_j c_k) \quad (i = 2, 3, \ldots, n)$$

It is important to note here that the coefficients B_{ik} are independent of concentrations c_k ($k = 2,3, \ldots,n$). They must be complicated functions of molecular weights M_i and M_k but are independent of the molecular weight distribution. By substituting the above expression for $\ln y_i$ into equation 1 we obtain

$$-\lambda M_i c_i = \frac{dc_i}{d\xi} + \sum_{k=2}^{n} M_i B_{ik} c_i \frac{dc_k}{d\xi} + O(c_i c_j c_k) \quad (i = 2, 3, \ldots, n) \quad (4)$$

This is the starting equation of the present analysis.

Summation of equation 4 over all solute components, integration of the resulting equation with respect to ξ over the range $0 < \xi < 1$, and use of the relation

$$\int_0^1 c_i(\xi)\, d\xi = c_i^0 \quad (5)$$

yields

$$\lambda \sum_{i=2}^{n} c_i^0 M_i = C(0) - C(1) - \sum_{i=2}^{n} \sum_{k=2}^{n} M_i B_{ik} \int_0^1 c_i \frac{dc_k}{d\xi}\, d\xi + \text{higher terms} \quad (6)$$

Here c_i^0 is the concentration of solute i in the original solution, and $C(0)$ and $C(1)$ are the total concentration of the solution at the bottom and the meniscus

(1) On leave from the Physical Chemistry Laboratory, Department of Fisheries, University of Kyoto, Maizuru, Japan.

(2) L. Mandelkern, L. C. Williams and S. Weissberg, THIS JOURNAL, **61**, 271 (1957).

(3) R. J. Goldberg, *ibid.*, **57**, 194 (1953).

(4) J. W. Williams, K. E. Van Holde, R. L. Baldwin and H. Fujita, *Chem. Revs.*, **58**, 715 (1958).

of the cell, respectively.[5] Equation 5 readily can be derived from the conservation of mass in the sector-shaped cell. In terms of the weight-average molecular weight M_w of the system, defined as

$$M_w = \frac{\sum_{i=2}^{n} c_i^0 M_i}{\sum_{i=2}^{n} c_i^0} \tag{7}$$

equation 6 may be written

$$\lambda M_w = \frac{C(0) - C(1)}{C_0} - C_0 \frac{\sum_{i=2}^{n}\sum_{k=2}^{n} M_i B_{ik} \int_0^1 c_i (dc_k/d\xi) d\xi}{\sum_{i=2}^{n}\sum_{k=2}^{n} c_i^0 c_k^0} + \text{higher terms} \tag{8}$$

where C_0 is

$$C_0 = \sum_{i=2}^{n} c_i^0 \tag{9}$$

and represents the initial concentration of the given solution.

On the other hand, integration of equation 4 and use of condition 5 yields

$$c_i(\xi) = c_i^0 \times \frac{\exp\left\{-\lambda M_i\left[\xi + \sum_{k=2}^{n} B_{ik} c_k(\xi) + O(c_j c_k)\right]\right\}}{\int_0^1 \exp\left\{-\lambda M_i\left[\eta + \sum_{k=2}^{n} B_{ik} c_k(\eta) + O(c_j c_k)\right]\right\} d\eta} \tag{10}$$

The right-hand side of this equation may be expanded to give

$$c_i(\xi) = c_i^0 \left[\frac{\lambda M_i e^{-\lambda M_i \xi}}{1 - e^{-\lambda M_i}} + O(M_i B_{ik} C_0)\right] \tag{11}$$

where use has been made of the fact that all c_i are of the same order as C_0. Substituting equation 11 into equation 8 and performing the necessary integration leads to

$$\lambda M_w = \frac{C(0) - C(1)}{C_0} + \lambda^2 C_0 \sum_{i=2}^{n}\sum_{k=2}^{n} \frac{M_i^2 M_k^2}{M_i + M_k} B_{ik} f_i f_k \times \frac{1 - e^{-\lambda(M_i + M_k)}}{(1 - e^{-\lambda M_i})(1 - e^{-\lambda M_k})} + O(C_0^2) \tag{12}$$

where

$$f_i = c_i^0 / C_0 \tag{13}$$

is the weight fraction of solute i in the original solution. Since

$$\frac{1 - e^{-\lambda(M_i + M_k)}}{(1 - e^{-\lambda M_i})(1 - e^{-\lambda M_k})} = \frac{M_i + M_k}{\lambda M_i M_k}\left[1 + \frac{\lambda^2}{12} M_i M_k - \frac{\lambda^4 M_i^2 M_k^2}{720}(M_i^2 + M_k^2 - M_i M_k) + \ldots\right]$$

equation 12 may be put in the form

$$M_w = (M_w)_{app} + C_0 \sum_{i=2}^{n}\sum_{k=2}^{n} M_i M_k B_{ik} f_i f_k \times \left[1 + \left(\frac{\lambda^2}{12}\right) \sum_{i=2}^{n}\sum_{k=2}^{n} M_i^2 M_k^2 B_{ik} f_i f_k \Big/ \sum_{i=2}^{n}\sum_{k=2}^{n} M_i M_k B_{ik} f_i f_k + \ldots\right] + O(C_0^2) \tag{14}$$

(5) From equation 3 we see that $\xi = 0$ and 1 correspond, respectively, to the bottom and the meniscus of the cell.

Here $(M_w)_{app}$ is defined by

$$(M_w)_{app} = \frac{C(0) - C(1)}{\lambda C_0} \tag{15}$$

and may be termed the "apparent" weight-average molecular weight. This quantity can be evaluated from sedimentation equilibrium data as a function of the initial concentration C_0.

In the case when sedimentation equilibrium experiments are performed with sufficiently small values of λ, the second and higher terms in the brackets in equation 14 may be regarded as a correction. In general B_{ik} is not too strongly dependent upon M_i and M_k. Therefore we may treat it as constant for the calculation of these higher terms, provided λ is sufficiently small. Then we have

$$M_w = (M_w)_{app} + C_0[1 + (\lambda^2 M_z^2/12) + \ldots] \times \sum_{i=2}^{n}\sum_{k=2}^{n} M_i M_k B_{ik} f_i f_k + O(C_0^2) \tag{16}$$

where M_z is the z-average molecular weight of the system, *i.e.*

$$M_z = \frac{\sum_{i=2}^{n} M_i^2 f_i}{\sum_{i=2}^{n} M_i f_i} \tag{17}$$

In their theories of the sedimentation equilibrium for non-ideal polydisperse systems Schulz[6] and independently Wales, *et al.*,[7] started with the assumption that B_{ik} is independent of M_i and M_k for all combinations of i and k. The present treatment uses such an approximation only for the evaluation of the correction term which appears in the brackets of equation 14. Thus it is apparent that equation 16 represents a more rigorous formulation of the thermodynamic non-ideality of neutral polymeric systems than does the theory due to Schulz or Wales, *et al.*

If a series of sedimentation equilibrium experiments for different (sufficiently low) values of C_0 is performed with so small values of λ that terms higher than $\lambda^2 M_z^2/12$ in equation 16 may be neglected, equation 16 becomes approximately

$$M_w = (M_w)_{app} - B' C_0 + O(C_0^2) \tag{18}$$

where

$$B' = [1 + (\lambda^2 M_z^2/12)] \sum_{i=2}^{n}\sum_{k=2}^{n} M_i M_k B_{ik} f_i f_k \tag{19}$$

In the form used by Wales and others[8,9] equation 18 becomes

$$\frac{1}{(M_w)_{app}} = \frac{1}{M_w} + B'' C_0 + O(C_0^2) \tag{20}$$

where

$$B'' = [1 + (\lambda^2 M_z^2/12)] B_S \tag{21}$$

and

$$B_S = \frac{1}{(M_w)^2} \sum_{i=2}^{n}\sum_{k=2}^{n} M_i M_k B_{ik} f_i f_k \tag{22}$$

(6) G. V. Schulz, *Z. physik. Chem.*, **A193**, 168 (1944).

(7) M. Wales, M. Bender, J. W. Williams and R. H. Ewart, *J. Chem. Phys.*, **14**, 853 (1946); M. Wales, THIS JOURNAL, **52**, 235 (1948).

(8) M. Wales, *ibid.*, **55**, 282 (1951).

(9) M. Wales, F. T. Adler and K. E. Van Holde, *ibid.*, **55**, 145 (1951).

Equation 20 indicates that the values of M_w and B'' may be obtained from the *intercept* and the *initial slope* of a plot of $1/(M_w)_{app}$ *vs.* C_0. The value of λ may differ slightly for each experiment. In that case the mean value of λ for different C_0 may be substituted for λ in equation 21, because under the circumstances considered $\lambda^2 M_z^2/12$ is a correction term. Due to the same reason M_z in equation 21 may be replaced by 1.5 M_w, provided the actual value for it is not available. The factor 1.5 is based on the assumption that the weight distributions of molecular weight in polymeric systems are often well approximated by the "most probable" distribution curve. It is shown that for this distribution of molecular weight the term of order λ^4 neglected in the parentheses of equation 21 becomes $\lambda^4 M_z^4/270$. Thus it is seen that equation 21 may be correct to within 3%, provided that experiments are performed under such a condition that $\lambda M_z < 1.6$. From the values of M_w and B'' so obtained the value of B_S may be calculated.

Kirkwood and Goldberg[10,3] have shown that the virial expansion of the reduced turbidity of a solution of polydisperse non-electrolyte solutes takes the form

$$\frac{HC_0}{\tau} = \frac{1}{M_w} + B_{LS} C_0 + O(C_0^2) \qquad (23)$$

where

$$B_{LS} = \frac{1}{(M_w)^2} \sum_{i=2}^{n} \sum_{k=2}^{n} M_i M_k B_{ik} f_i f_k \qquad (24)$$

In equation 23, τ is the turbidity of the solution in excess of that of the solvent and H is the familiar constant in the theory of light scattering.

Comparison of equations 22 and 24 shows that there exists the possibility to evaluate from sedimentation equilibrium experiments the quantity which is generally called the light-scattering second virial coefficient. This implies that the sedimentation equilibrium method allows evaluation of the thermodynamic information just equivalent to that derived from the light scattering experiment, provided it is applied under the condition suggested above. It is important to note that equation 20 does not tell anything about the range of concentration over which $1/(M_w)_{app}$ changes linearly with C_0. The next term indicated by $O(C_0^2)$ in equation 20 would have to be computed to obtain any information of this kind. The conclusion from equation 20 is that if we evaluate the *intercept* and *limiting slope* at $C_0 = 0$ of an experimentally obtained plot of $1/(M_w)_{app}$ *vs.* C_0 by suitable extrapolation these two quantities can be used to evaluate the weight-average molecular weight of the solute and the light-scattering second virial coefficient of the given system.

This investigation was supported by a research grant-in-aid from the National Institutes of Health (RG-4912). The author wishes to record here his grateful acknowledgment. It is a pleasure to thank Professors J. W. Williams and L. J. Gosting for their continued interest in the course of this study.

(10) J. G. Kirkwood and R. J. Goldberg, *J. Chem. Phys.*, **18**, 54 (1950).

COMPLEXES OF BICARBONATE WITH MAGNESIUM AND CALCIUM

By Isidor Greenwald

New York University College of Medicine, New York, N. Y.

Received December 11, 1958

In their paper Halla and Van Tassel[1] made two serious errors. They overlooked the fact that my conclusion that such complexes existed was based not only upon the results of titrations but also on the determination of the solubility of $CaCO_3$ in the presence, and absence, of $NaHCO_3$. Moreover, they made no attempt to ascertain whether or not such complexes could have been detected under their conditions and by their method.

If the solubility of CO_2 is not appreciably affected by the presence of such small quantities of Mg^{++} or of Ca^{++}, [total CO_2] in their experiments may be taken as 0.0640 + 2[Mg], or 2[Ca]. The distribution between HCO_3^- and H_2CO_3 may be calculated from the equation $pH = pK'_1 + \log [HCO_3^-]/[H_2CO_3]$ and the value for pK'_1 given by Shedlovsky and MacInnes.[2]

From these values and the equation

$$([Mg] - [complex]) \times ([HCO_3^-] - [complex]) = 0.17[complex], \text{ (or } 0.15[complex] \text{ in the case of Ca),}$$

[complex] may be calculated. This may then be deducted from HCO_3^- and the pH calculated from the same Henderson–Hasselbach equation as was used for calculating $[HCO_3^-]$ and $[H_2CO_3]$ upon the assumption that there were no complexes.

The values for pH thus found in the two experiments with the highest concentrations of Mg or Ca and HCO_3^- differ from those reported by Halla and Van Tassel by only 0.02 and were, therefore, undetectable by their method.

(1) F. Halla and R. Van Tassel, This Journal, **62**, 1135 (1958).

(2) T. Shedlovsky and D. A. MacInnes, *J. Am. Chem. Soc.*, **57**, 1705 (1935).

FORMATION CONSTANTS OF METHYLBIS-(3-AMINOPROPYL)-AMINE WITH COPPER, NICKEL AND CADMIUM IONS

By David E. Goldberg and W. Conard Fernelius

Department of Chemistry, The Pennsylvania State Univ., University Park, Penna.

Received February 11, 1959

Many studies have been directed toward the determination of the influence of substitution of organic groups in the ligand on the stabilities of coordination complexes. For aliphatic diamines with N-substituted methyl groups, formation constant data are presently available for the ligands listed in Table I.[1]

In addition it is known that $(CH_3)_2NCH_2CH_2N(CH_3)_2$ forms stable complexes with Cu^{++}[2] whereas $(CH_3)_2NCH_2N(CH_3)_2$ does not.[3]

It may be seen that secondary amine groups are

(1) For a complete tabulation of formation constant data see: J. Bjerrum, G. Schwarzenbach and L. G. Sillen, "Stability Constants, Part I: Organic Ligands," Special Publication No. 6, The Chemical Society, London, 1957.

(2) B. P. Block, unpublished observations.

(3) C. R. Bertsch, W. C. Fernelius and B. P. Block, This Journal **62**, 444 (1958).

TABLE I

Ligand	Ref.	Ionic strength	Temp., °C.	pK_n $n=1$	pK_n $n=2$	log K_1 Cu^{++}	log K_1 Ni^{++}	log K_1 Co^{++}	log K_1 Cd^{++}	log K_2 Cu^{++}	log K_2 Ni^{++}	log K_2 Co^{++}	log K_2 Cd^{++}	log K_3 Ni^{++}	log K_3 Co^{++}	log K_3 Cd^{++}
$H_2NCH_2CH_2NH_2$	*a*	→ 0	30	9.81	6.79	10.36	7.27		5.34	8.93	6.11		4.38	4.20		
	b	0.5 KNO_3	30	9.87	7.23	10.55	7.52		5.47	9.05	6.28		4.55	4.26		2.07
	c	1 *M* KCl	30	10.05	7.31		7.66	5.89			6.40	4.83		4.55	3.10	
$CH_3NHCH_2CH_2NH_2$	*a*	→ 0	30	9.90	6.63	10.06	6.97			8.38	5.40			2.68		
	d	0.5 KNO_3	25	10.40	7.56	10.55	7.36			8.56	5.74			2.01		
$(CH_3)_2NCH_2CH_2NH_2$	*e*	.1 KCl	25	9.53	6.63	9.23				6.73						
$CH_3NHCH_2CH_2NHCH_3$	*e*	.1 KCl	25	10.16	7.40	9.69	6.65			6.65	3.85					
	f	5 KNO_3	25	10.29	7.47	10.47	7.11			7.63	4.73			1.5		

[a] Ref. 4. [b] G. A. Carlson, J. P. McReynolds and F. H. Verhoek, *J. Am. Chem. Soc.*, **67**, 1334 (1945). [c] J. Bjerrum, "Metal-Ammine Formation," P. Haase and Son, Copenhagen, 1941. [d] F. Basolo and R. K. Murmann, *J. Am. Chem. Soc.*, **74**, 5243 (1952). [e] H. Irving and J. M. M. Griffiths, *J. Chem. Soc.*, 213 (1954). [f] F. Basolo, R. K. Murmann, and Y. T. Chen, *J. Am. Chem. Soc.*, **75**, 1478 (1953); F. Basolo and R. K. Murmann, *ibid.*, **76**, 211 (1954).

TABLE II

VALUES FOR THE THERMODYNAMIC QUANTITIES LOG K_n, $-\Delta F_n$, $-\Delta H_n$ AND ΔS_n INVOLVED IN THE REACTION AT 10, 20, 30 AND 40° OF SEVERAL BIVALENT METAL IONS WITH METHYLBIS-(3-AMINOPROPYL)-AMINE

t, °C.	H^+	Cu^{++}	Ni^{++}	Co^{++}	Cd^{++}	H^+	Cu^{++}	Ni^{++}	Co^{++}	H^+
			log K_1				log K_2			log K_3
10	10.84 ± 0.03	13.31 ± 0.03	7.57 ± 0.02	5.95 ± 0.03	6.09 ± 0.03	9.91 ± 0.05	4.3*		3.88 ± 0.13	7.19 ± 0.09
20	10.74 ± .00	12.71 ± .03	7.39 ± .02		5.97 ± .02	9.55 ± .02	4.5*	3.8*		6.55 ± .10
30	10.33 ± .04	12.28 ± .04	7.05 ± .04		5.87 ± .02	9.19 ± .07	4.4*			6.32 ± .02
40	10.07 ± .04	12.31 ± .04	7.04 ± .04		5.75 ± .03	9.05 ± .08	4.3*	2.85*		6.47 ± .03
			$-\Delta F_1$ (kcal./mole)				$-\Delta F_2$ (kcal./mole)			$-\Delta F_3$ (kcal./mole)
10	14.04	17.24	9.80		7.89	12.83				9.31
20	14.40	17.04	9.91		8.00	12.80				8.78
30	14.32	17.03	9.77		8.14	12.74				8.76
40	14.42	17.63	10.08		8.24	12.96				9.27
			$-\Delta H_1$ (kcal./mole)				$-\Delta H_2$ (kcal./mole)			$-\Delta H_3$ (kcal./mole)
10–40	11.0	14.1	7.85		4.65	12.0				9.96
			$+\Delta S_1$ (cal./mole-deg.)				$+\Delta S_2$ (cal./mole-deg.)			$+\Delta S_3$ (cal./mole-deg.)
10	11	11	7		11	3				−2
20	12	10	7		11	3				−4
30	11	10	6		12	2				−4
40	11	11	7		12	3				−2

slightly more basic than the corresponding primary amine groups but that the formation constants for the complexes containing secondary amine groups are lower than those with only primary amine groups. The tertiary amine groups are much less basic than the other two and also are much lower in coördinating strength.

Recently formation constant data for $HN(CH_2CH_2CH_2NH_2)_2$ were published[4]: ionic strength 1 *M* KNO_3; 30°; *pK*'s 10.70, 9.70, 8.02; log *K*'s, Cu, 14.25; Ni, 9.09; Co, 6.63. These data are now augmented by similar data for $CH_3N(CH_2CH_2CH_2NH_2)_2$ (Table II). Values were obtained for only log K_1 in the cases of copper, nickel and cadmium. Log K_2 could be estimated at 10, 20, and 30° for copper and at 10 and 30° for nickel even though the values varied slightly with $\bar{n}$ (denoted by an asterik). In the cadmium system, precipitation occurred above $\bar{n} = 1$. Values were obtained for two constants for cobalt at 10° only. At the higher temperatures, precipitation occurred. No values were determinable for the system involving zinc; at the low temperatures log *K* varied with $\bar{n}$ and at the higher temperatures precipitation occurred.

Conclusions

It is evident that methyl substitution on the middle nitrogen of $HN(CH_2CH_2CH_2NH_2)_2$ causes a lowering of its base strength although direct comparison of the values cannot be made since the values for $HN(CH_2CH_2CH_2NH_2)_2$ were obtained in a strong electrolyte solution. The values of the formation constants with Cu^{++} and Ni^{++} are also lower for the methyl-substituted ligand. This result is in agreement with results for similar cases noted above for the ethylenediamines.

Experimental

Reagents.—All metal perchlorate and perchloric acid solutions were prepared from G. F. Smith Chemical Co. reagent grade materials. The concentrations of the solutions were determined by standard analytical methods.

Methylbis-(3-aminopropyl)-amine was obtained from the American Cyanamid Co. The compound was distilled at 106° (*ca.* 1 mm.). The amine was diluted with freshly boiled, distilled water. Neutral equivalents of two solutions were 49.2 and 49.4; calculated 48.4.

Procedure.—The procedures used were described by Bertsch.[5]

The calculations were done by the method of Block and McIntyre.[6]

(4) G. B. Hares, W. C. Fernelius and B. E. Douglas, *J. Am. Chem. Soc.*, **78**, 1816 (1956). The values reported for 0 and 50° are now felt to be unreliable (see G. H. McIntyre, B. P. Block and W. C. Fernelius, *ibid.*, **81**, 529 (1959)).

(5) C. R. Bertsch, W. C. Fernelius and B. P. Block, THIS JOURNAL, **62**, 444 (1958).

(6) B. P. Block and G. H. McIntyre, Jr., *J. Am. Chem. Soc.*, **75**, 5667 (1953).

THE SOLUBILITY AND HEAT OF SOLUTION OF LANTHANUM NITRATE 6-HYDRATE IN NON-AQUEOUS SOLVENTS[1]

BY DOROTHY FULMER STEWART AND WESLEY W. WENDLANDT[2]

Department of Chemistry and Chemical Engineering, Texas Technological College, Lubbock, Texas

Received December 12, 1958

Little attention has been given to the chemistry of the rare earth elements in non-aqueous solvents. Fragmentary information is available on the solubility of rare earth compounds in acetone,[3] alcohols,[4,5] dioxane,[6] ether,[6] amines,[7] tri-*n*-butyl phosphate[8] and other organic solvents.[9]

Because of the importance of non-aqueous solvents to present day separation methods, this study is concerned with the solubility and heat of solution of lanthanum nitrate 6-hydrate in alcohols, ketones, ethers, esters and other organic solvents.

Experimental

Reagents.—Lanthanum oxide of 99.99% purity was obtained from the Lindsay Chemical Co., West Chicago, Ill. The purity was that claimed by the supplier.

The organic solvents were stock materials obtained from Eastman Organic Chemicals, Rochester, N. Y., and Matheson, Coleman and Bell, East Rutherford, N. J. The solvents were not further purified for the solubility studies. For the thermochemical studies, the solvents were thoroughly dried and then fractionated.

All other chemicals were of C.P. quality.

Preparation of Lanthanum Nitrate 6-Hydrate.—The metal oxide was dissolved in a minimum amount of concentrated HNO_3, diluted with water and evaporated to a viscous liquid that formed a solid mass on cooling. The solid mass was redissolved in water and evaporated to the point of crystallization. After cooling, the resulting crystals were filtered off and the excess water removed by drying over concentrated H_2SO_4. Final drying of the crystals was over partially dehydrated lanthanum nitrate 6-hydrate contained in a desiccator. The resulting crystals were analyzed for metal content by ignition to La_2O_3 in a muffle furnace at 800°; found La_2O_3, 37.67, 37.72%; theor., 37.62%.

Solubility Studies.—A saturated solution was prepared by placing an excess of solid lanthanum nitrate 6-hydrate into 10 ml. of the organic solvent contained in a 25 × 160 mm. screw-cap vial. The vials were sealed with paraffin, allowed to stand for several hours at room temperature (25 to 35°) with occasional hand shaking and then placed into the water-bath.

The water-bath consisted of an insulated copper tank, 18 × 12 × 12 in. in dimension. A shaft, running the entire length of the tank, was rotated at 30 r.p.m. by an electric motor connected through a pulley and belt. The vials were placed in metal clips on the shaft and rotated end-over-end. The temperature of the bath was maintained by a mercury thermostat at 25 ± 0.2°.

Preliminary experiments showed that saturation equilibrium was attained, in most cases, in four days. However, many of the solutions were equilibrated for 7–14 days. After equilibration, the saturated solutions were centrifuged and the centrifugates placed into screwcap dropping bottles. The centrifugates were analyzed for metal content by placing a weighed amount into a 1% HNO_3 solution, precipitating as lanthanum oxalate and igniting to La_2O_3 in a muffle furnace at 850°.

Heat of Solution Studies.—The calorimeter is described elsewhere.[10] Sample sizes were adjusted so as to give a metal salt to solvent ratio of 1:400. It is estimated that the accuracy of the instrument is about ±3%, with a precision between measurements of about ±1%.

Results

The results of the solubility and heat of solution studies are given in Table I.

(1) Taken in part from the M.S. thesis of Dorothy F. Stewart, Texas Technological College, August, 1958.

(2) To whom correspondence should be addressed.

(3) O. L. Barnebey, *J. Am. Chem. Soc.*, **34**, 1174 (1912).

(4) B. S. Hopkins and L. L. Quill, *Proc. Nat. Acad. Sci.*, **19**, 64 (1933).

(5) R. C. Vickery, "Chemistry of the Lanthanons," Academic Press, New York, N. Y., 1953, pp. 150–2.

(6) R. C. Wells, *J. Wash. Acad. Sci.*, **20**, 146 (1930).

(7) T. Moeller and P. A. Zimmerman, *J. Am. Chem. Soc.*, **75**, 3940 (1953).

(8) W. W. Wendlandt and J. M. Bryant, THIS JOURNAL, **60**, 1145 (1956).

(9) C. C. Templeton, M.S. Thesis, Univ. of Wisconsin, 1947.

(10) J. H. Van Tassel and W. W. Wendlandt, *J. Am. Chem. Soc.*, **81**, 813 (1959).

TABLE I

THE SOLUBILITY AND HEAT OF SOLUTION OF LANTHANUM NITRATE 6-HYDRATE IN ORGANIC SOLVENTS AT 25°

Solvent	Solubility, g. $La(NO_3)_3 \cdot 6H_2O$/100 g. soln.	ΔH, kcal./mole
Methyl alcohol	87.45	−3.75
	87.47	−3.58
Ethyl alcohol, 95%	72.86	2.58
	73.28	2.58
Ethyl alcohol, 100%	71.89	1.57
	71.69	1.64
n-Propyl alcohol	45.15	6.30
	45.23	6.47
Isopropyl alcohol	42.06	12.0
	42.53	12.5
n-Butyl alcohol	28.74	8.46
	28.75	8.34
Isobutyl alcohol	14.98	
	15.15	
sec-Butyl alcohol	13.84	
	13.65	
t-Butyl alcohol	21.23	
	21.63	
n-Amyl alcohol	13.52	
	13.53	
Isoamyl alcohol	11.62	
	11.89	
t-Amyl alcohol	8.98	
	9.22	
3-Pentanol	5.68	
	5.78	
n-Hexyl alcohol	16.01	10.4[a]
	15.88	9.24[a]
Cyclohexanol	17.00	
	16.97	
Benzyl alcohol	10.96	
	11.01	
Allyl alcohol	47.01	9.85
	46.89	9.79
2-Chloroethanol	40.32	14.2
	40.40	14.4
2,2′-Oxydiethanol	75.09	
	74.69	
2-Methoxyethanol	77.93	−3.74
	78.06	−3.58
Glycerol	81.66	
	81.45	
2-Ethoxyethanol	70.00	−1.78
	70.07	−1.76
Ethylene glycol	84.06	
	84.07	
Ethyl acetate	1.73	
	1.89	
Methyl acetate	62.88	6.03
	62.85	5.93
Ethyl formate	50.04	12.9[a]
	50.01	12.0[a]
Acetone	76.64	5.00
	76.43	4.89
Cyclohexanone	42.84	12.4[a]
	43.24	16.4[a]
Dioxane	73.97	1.66
	74.13	1.56
Acetonitrile	72.45	
	72.37	
o-Toluidine	16.20	
	16.20	
Aniline	15.90	
	16.05	

[a] Dissolution of solute was slow.

The organic solvents containing the hydroxyl group were the best solvents for the salt. As was expected, the solubility decreased as the length of alcohol carbon chain increased. The branching of the alcohol carbon chain had a pronounced effect on the solvent ability; the solubility decreased in the order: *normal* > *iso* > *secondary* > *tertiary*. Polyhydroxyl alcohols were good solvents for the salt since the solubility in glycerol and ethylene glycol was about equal to that of methyl alcohol.

Of the non-hydroxy solvents, the ketones and cyclic ethers possessed a high solvent utility for the salt. The low molecular weight esters were better solvents than those of higher molecular weight.

The heat of solution could not be measured in a number of the solvents because of the slowness of the dissolution process. The values reported in Table I are those in which dissolution was rapid with the exception of *n*-hexyl alcohol, cyclohexanone and ethyl formate.

The presence of water in ethyl alcohol was readily detected by the ΔH values. The heat of solution became more endothermic, indicating that the ΔH for the salt may be endothermic in water. With the solubility studies, the presence of 5% of water had little effect on the values obtained.

CALCULATED VIBRATIONAL FREQUENCIES FOR H_2O^{18} AND D_2O^{18}

BY GILLIAN GOMPERTZ[1a] AND W. J. ORVILLE-THOMAS[1b]

The Weizmann Institute, Rehovoth, Israel

Received December 12, 1958

The frequency–force constant relations for non-linear XY_2 molecules using an incomplete potential function are given in the standard texts.[2,3] Although used implicitly by previous workers (*e.g.*, see ref. 4) the corresponding relations for a complete quadratic potential function do not appear to have been presented.

The general quadratic potential function is

$$2V = f_1(\Delta r_1^2 + \Delta r_2^2) + f_\alpha(r^2\,\Delta\alpha^2) + 2f_{1\alpha}(r\Delta\alpha)(\Delta r_1 + \Delta r_2) + 2f_{12}(\Delta r_1 \Delta r_2) \quad (1)$$

The Wilson FG-matrix method[5] leads to these frequency–force constant relations for the class A, vibrations ω_1 and ω_2.

(1) (a) Dept. of Physics, The University, Birmingham, England. (b) The Edward Davies Chemical Laboratories, University College of Wales, Aberystwyth, Wales.

(2) G. Herzberg, "Infra-red and Raman Spectra," D. Van Nostrand Co., Inc., London, 1945.

(3) T. Y. Wu, "Vibrational Spectra and Structure of Polyatomic Edwards, Molecules," Brothers, Ann Arbor, Michigan, 1946.

(4) S. Smith and J. W. Linnett, *Trans. Faraday Soc.*, **52**, 891 (1956).

(5) E. B. Wilson, J. C. Decius and P. C. Cross, "Molecular Vibrations," McGraw–Hill Book Co., Inc., New York, N.Y., 1955.

$$\lambda_1 + \lambda_2 = (f_1 + f_{12})(\mu_1 + 2\mu_2 \cos^2\beta) + 2f_\alpha(\mu_1 + 2\mu_2 \sin^2\beta) - 8f_{1\alpha}\mu_2 \sin\beta\cos\beta$$

$$\lambda_1\lambda_2 = 2[f_\alpha(f_1 + f_{12}) - f_{1\alpha}^2][\mu_1^2 + 2\mu_1\mu_2] \quad (2a)$$

and to the following relation for the Class B_1 vibration, ω_3

$$\lambda_3 = (f_1 - f_{12})(\mu_1 + 2\mu_2 \sin^2\beta) \quad (2b)$$

where $\lambda_i = 4\pi^2c^2\omega_i^2$, ω_i being a fundamental frequency, $\mu_1 = 1/m_Y$ and $\mu_2 = 1/m_X$, $\beta = {}^1/_2(\angle YXY)$ and the force constants are defined in eq. 1.

The Fundamental Frequencies of D_2O^{18} and H_2O^{18}.—As an example of the use of relations 2 frequency values have been calculated for the D_2O^{18} and H_2O^{18} isotopic modifications of water.

The infrared spectra of H_2O^{16} and D_2O^{16} have been studied many times and high-resolution studies have yielded values for the zero-order frequencies and for the anharmonicity constants.[6,7] Smith and Linnett[4] have used these data to determine values for the four force constants occurring in eq. 1. These constants used in conjunction with a value of 104°31′ for the interbond angle and the appropriate mass factors lead to the values given in Table I for the zero-order frequencies, ω, of the D_2O^{18} and H_2O^{18} molecules on substitution in eq. 2.

It seems reasonable to suppose that the anharmonicity constants will not differ greatly in the pairs of molecules H_2O^{16} and H_2O^{18} and D_2O^{16} and D_2O^{18}.

The correction for anharmonicity for a fixed force field depends in an inverse fashion on the masses of the molecules as we go from H_2O^{16} to D_2O^{16}. On a simple basis then extrapolated values can be calculated for this correction, for the H_2O^{18} and D_2O^{18} species, from the change in mass and the experimentally determined anharmonicity coefficients[6,7] for the H_2O^{16} and D_2O^{16} molecules. The frequency values calculated for the observed fundamentals, ν, are given in Table I.

We wish to thank Professor J. H. Jaffé for his support throughout this work.

TABLE I

VIBRATIONAL FREQUENCIES OF THE WATER MOLECULE (IN CM.$^{-1}$)

	Exptl.		Theor.	
Molecule	H_2O^{16}	D_2O^{16}	H_2O^{18}	D_2O^{18}
ν_1	3651.7	2666	3647	2656
ω_1	3825.3	2758.1	3804.8	2740
ν_2	1595.0	1178.7	1586	1166
ω_2	1653.9	1210.3	1635.9	1191.3
ν_3	3755.8	2789	3744	2762
ω_3	3935.6	2883.8	3905.8	2851.3
Ref.	2	2	This paper	

(6) W. S. Benedict, N. Gailar and E. K. Plyler, *J. Chem. Phys.*, **24**, 1139 (1956).

(7) B. T. Darling and D. M. Dennison, *Phys. Rev.*, **57**, 128 (1940).

THE HYDROLYSIS OF NEPTUNIUM(IV)[1]

BY J. C. SULLIVAN AND J. C. HINDMAN

Argonne National Laboratory, Lemont, Illinois

Received December 13, 1958

In a number of kinetic studies on the oxidation of neptunium(IV) in aqueous systems we have observed a term in the rate law inversely proportional to the second power of the hydrogen ion concentration.[2] These observations prompted the present investigation designed to determine: (a) whether a species such as may be implied by this type of rate law is formed in detectable quantities in a hydrolytic pre-equilibrium, and (b), the effect on such an equilibrium when deuterium is substituted for hydrogen. The latter information was desired as an aid in the interpretation of the kinetic isotope effects. For comparative purposes the effect of deuterium on the uranium(IV) hydrolysis also has been measured.

Experimental

The preparation of the neptunium(IV), sodium perchlorate and deuteroperchloric stock solutions have been previously described.[3] Uranyl perchlorate was prepared by dissolution of UO_3 in $HClO_4$ or $DClO_4$. Uranium(IV) stock solutions were prepared by electrolytic reduction of the uranyl perchlorate solutions.

Aliquots of the metal ion solutions were added to the appropriate $NaClO_4$–$HClO_4$ (or $DClO_4$) mixtures, in which a constant ionic strength of 2.0 was maintained, and then analyzed spectrophotometrically using a Cary Model 14 recording spectrophotometer. The 6000–7000 Å. region was used for the study of the uranium(IV) hydrolysis.[4] The 9400–10,000 Å. region was used for the neptunium(IV) measurements. In this region Np^{+4} (aq.) has a sharp absorption band at 9590 Å. which obeys Beer's law if the Cary spectrophotometer is employed. At this wave length the absorption of the hydrolyzed forms of neptunium(IV) is only 0.14 that of the unhydrolyzed species. The region scanned permitted monitoring of the solutions to ensure the absence of neptunium(V). The acidity of the solutions were measured with a calomel–glass electrode system using a vibrating reed electrometer assembly standardized with solutions of known acidity. The measurement and calculation technique were essentially the same as those described by Kraus and Nelson.[4]

Results and Discussion

The Hydrolysis of Neptunium(IV).—There is no change in the neptunium(IV) spectrum until the acidity is decreased to approximately 0.1 molar. The existence of Np^{+4} (aq.) as the predominant neptunium(IV) species at acidities above 0.1 molar has been established previously.[5] With further decrease in acid concentration the height of the 9590 Å. band decreases. Analysis of the data shows that the simple hydrolytic reaction

$$Np^{+4}(aq.) + H_2O = NpOH^{+3}(aq.) + H_3O^+ \quad (1)$$

holds for a limited region of acidity in both H_2O and D_2O solutions. At low acidities polymerization reactions become important as can be inferred from two types of evidence. If the only reaction of importance was that of reaction 1, a plot of $1/H^+$ or $1/D^+$ *versus* total $Np(IV)/Np^{+4}$ should be linear with a slope of K and no dependence on the total metal ion concentration. Figure 1 is such a plot for the D_2O solutions and quite clearly delineates the region of acidity at which complex reactions become important. The second type of observation that confirms this interpretation is that the hydrogen ion concentration exhibited a slow change with time in those regions where one

(1) Work performed under the auspices of the United States Atomic Energy Commission.

(2) J. C. Hindman, J. C. Sullivan and D. Cohen, *J. Am. Chem. Soc.*, **76**, 3728 (1954).

(3) J. C. Sullivan, D. Cohen and J. C. Hindman, *ibid.*, **79**, 3672 (1957).

(4) K. A. Kraus and F. Nelson, *ibid.*, **72**, 3901 (1950).

(5) J. C. Sullivan and J. C. Hindman, *ibid.*, **76**, 5931 (1954).

TABLE I
HYDROLYSIS OF Np(IV) AND U(IV) AT 25°, μ = 2.0

	K_H[a]	K_D	No. of obsn.	$[H^+]$[b] Lower Limit	K_H/K_D
Np(IV)	$5.0 \pm 0.3 \times 10^{-3}$		11	0.02	
		$3.2 \pm 0.5 \times 10^{-3}$	12	.014	1.6 ± 0.3
U(IV)	$2.1 \pm 0.1 \times 10^{-2}$		7	.05	
		$1.8 \pm 0.1 \times 10^{-2}$	20	.02	1.2 ± 0.1

[a] All uncertainties are standard deviations. [b] Experiments with H^+ less than this value were not used in the calculation of the appropriate equilibrium constants.

would infer polymerization reactions predominate. We have restricted our interpretation to the acid range where equation 1 adequately represents the data. Table I summarizes the results of the pertinent observations.

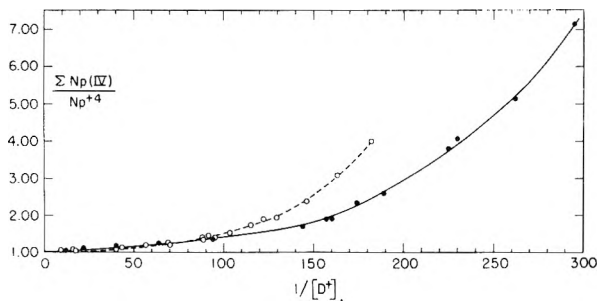

Fig. 1.—$\Sigma Np(IV)/[Np^{+4}]$ *vs.* $1/[D^+]$ at 25°, μ = 2.0: O, $\Sigma Np(IV) = 2.66_3 \times 10^{-3}$ *M*; ●, $\Sigma Np(IV) = 1.38_5 \times 10^{-3}$ *M*.

In passing it is of interest to note that the neptunium(IV) spectrum is significantly affected by change in medium as illustrated by the change in molar extinction coefficient of the 9590 Å. band from 219 in 2 *M* $HClO_4$ to 238 in 2 *M* $DClO_4$ (99% D).

The Hydrolysis of Uranium(IV).—The value given in Table I for the hydrolysis constant of the U^{+4}(aq.) ion from the present research is in reasonable agreement with that obtained by Kraus and Nelson[4] ($K_H = 2.36 \pm 0.09 \times 10^{-2}$ in H_2O media at $\mu = 2.004$).

It will be noted from Table I that deuterium has less effect on the uranium(IV) hydrolysis than on that of neptunium(IV). It was also found that the molar extinction coefficient of the 6480 Å. U(IV) band was unaffected by change in medium from H_2O to D_2O.

The first hydrolysis constant of plutonium(IV) has been reported to be quantitatively similar to that of uranium(IV).[4] The reason for the marked divergence in behavior of neptunium(IV) from that predicted[6] for the intermediate ion in this series of elements is not immediately apparent. We shall refrain from any *a posteriori* rationalization of the results in terms of arguments involving detailed electronic configurations of the ions and content ourselves with emphasizing the dangers of oversimplified generalizations.

In closing it should be pointed out that the deuterium isotope effect on the hydrolysis of these ions is consistent with that reported for other acids,[7] the acid strengths are less in D_2O than in H_2O and the effect of deuterium is less for the stronger acid. In view of these results a direct determination of the effect of deuterium on the hydrolysis of Pu(IV) would be of interest since kinetic evidence has been adduced for an increased hydrolysis of Pu(IV) in D_2O.[8]

(6) T. W. Newton, THIS JOURNAL, **62**, 943 (1958).

(7) R. W. Gurney, "Ionic Processes in Solution," McGraw-Hill Book Co., Inc., New York, N.Y., 1953, p. 150–154.

(8) S. W. Rabideau and R. J. Kline, THIS JOURNAL, **62**, 617 (1958).

HEATS OF IMMERSION OF PREHEATED HOMOIONIC CLAYS

BY W. H. SLABAUGH

Department of Chemistry, Oregon State College, Corvallis, Oregon

Received December 15, 1958

It is well known that the history of a clay of the montmorillonite type has a significant influence upon many of its properties such as the viscosity of suspensions of the clay, ease of dispersion, and other surface chemical properties. The present study constitutes an examination of the effects of the exchangeable cation, state of dispersion and preliminary heating upon the heats of total immersion of several homoionic bentonite clays prepared in both oven-dried and freeze-dried forms.

Earlier studies by Siefert,[1] Johnson,[2] and Ovcharenko and Bykov,[3] report considerable differences in the heats of immersion of calcium, hydrogen, sodium and potassium montmorillonites. However, apparently there have been no studies made of the heats of immersion of clays that have been subjected to various temperatures prior to observing their immersional properties.

Method and Materials.—The experimental measurements of heats of total immersion were accomplished by means of a calorimeter described previously[4] that was modified slightly by the installation of a multiple sample carrier. This modification permitted the consecutive observation of immersional heats of five samples in a single loading of the calorimeter, thereby considerably improving the precision of measurement because a single calibration of the instrument served for all five samples. Each of the five tubes was broken by means of separate rods extending through the neck of the reaction chamber and activated by an external screw.

Raw Bentonite.—A 200 mesh sample of Wyoming bentonite, supplied by the Baroid Division, National Lead Company, was used as the starting material. It was clarified by recovering the supernatant material from a 1% suspension after two weeks standing at room temperature.

Homoionic Bentonite.—Another portion of the supernatant clay suspension was passed through Amberlite IR 120 columns charged with the appropriate cation, and these homoionic clays were recovered by one of two methods. In the first method, the water was removed by evaporation at about 60°, after which the clays were hand-ground with a

(1) R. E. Grim, "Clay Mineralogy," McGraw-Hill Book Co., Inc., New York, N. Y., 1953, p. 185.

(2) R. E. Johnson, *Diss. Abs.*, **57**, 2435 (1957).

(3) F. D. Ovcharenko and S. F. Bykov, *Kolloid Zhur.*, **16**, 134 (1954).

(4) W. H. Slabaugh, THIS JOURNAL, **59**, 1022 (1955).

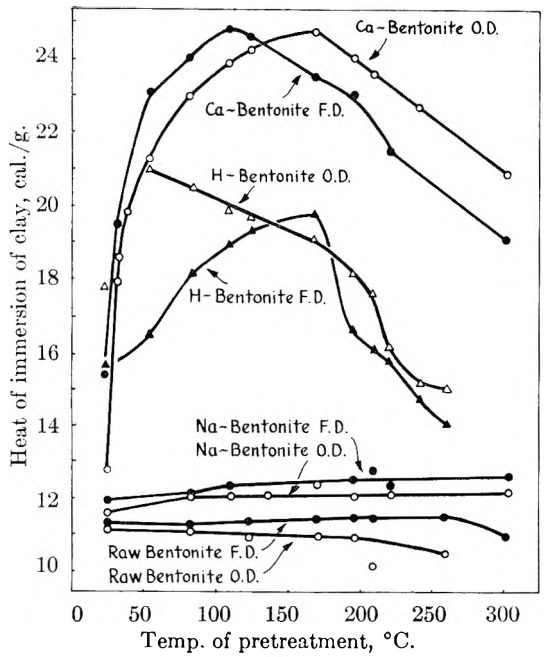

Fig. 1.—Heats of immersion of freeze-dried (F. D.) and oven-dried (O. D.) homoionic clays after various temperatures of preheating.

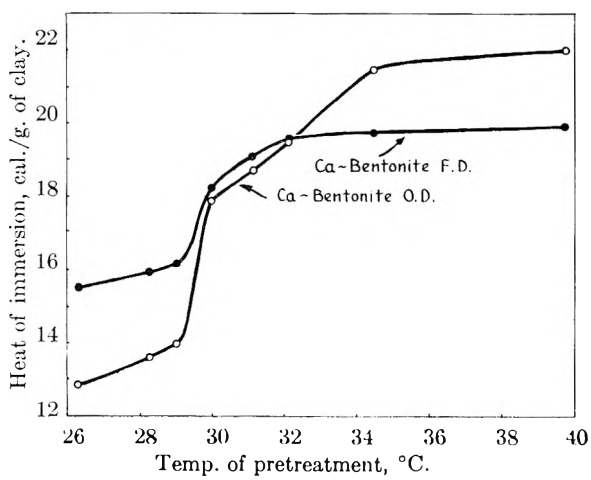

Fig. 2.—Heats of immersion of preheated calcium bentonite showing a transition at approximately 29°.

porcelain mortar and pestle to 200 mesh. In the second method, a freeze-drying technique, described by Call,[5] was employed. Both types of clays contained less than 0.1% quartz and showed cation-exchange capacities of approximately 92 meq./100 g. of clay.

Samples of clays were heated in a thermostated oven under a vacuum of 10^{-3} mm. prior to measuring the heats of immersion. All samples in a given group were placed in the oven at the same time and, after 24 hours at a given temperature, they were removed by sealing off from the vacuum system the 9 mm. glass tubes into which the samples had been weighed. The sample tubes were placed in the calorimeter, equilibrated at 27.0°, and following the breaking of the tube, the heat of immersion was measured. Corrections for the heat of breaking of the glass tube (0.20 cal.) and the energy associated with the entry of liquid into the evacuated sample tube (0.03 cal.) were applied to all observations. Maximum deviation of the calorimetric measurements was no more than 0.5%, with the average deviation of all measurements reported being 0.25%.

Results and Discussion

The heats of immersion of the raw and homoionic clays examined in this study are summarized in Fig. 1. It is noted readily that there are two radically different behaviors of these clays. The calcium and hydrogen clays, for instance, undergo rapid increases in heats of wetting as the result of higher pretreating temperatures. The maximum effect in this respect appears to be reached in the range of 100 to 150°. Higher temperatures reduce the heats of immersion of these two clays.

The raw and sodium clays, on the other hand, are affected only slightly by preheating, although the sodium clay appears to increase slightly in its heat of immersion as the pretreating temperature is increased. At temperatures above 200°, the pretreatment causes a slight decrease in the heat of immersion of the raw clay, while these values for the sodium clay remain nearly constant.

Because of the sharp rise in the heat of immersion of the calcium and hydrogen clays when pretreated at temperatures near room temperature, these clays were pretreated at much smaller temperature intervals as shown in Fig. 2. Only the calcium clay showed what appears to be a transition temperature at approximately 29°, while the hydrogen clay showed only a gradual increase with no distinguishable transition temperatures. An indication of this transition in calcium montmorillonite has already been noted as the result of the radically different adsorption isotherms shown by calcium montmorillonite at temperatures above and below this transition temperature.[6] That is, below this temperature, a two-step adsorption process occurs and above this temperature, a single, Type II adsorption isotherm is produced.

In most of the observations, particularly with raw and sodium clays, and with calcium clay at lower pretreatment temperatures, oven-dried clays gave off less heat upon immersion than the freeze-dried clays. Since the two types of clays were otherwise identical, this is attributed to the higher degree of dispersion of the latter type, with the result that, upon wetting, less energy is required by the water to force its way into the interlaminar spaces of the freeze-dried clay. The oven-dried clay, consequently, should evolve less heat upon immersion because of the more compact orientation of its laminae.

Concerning the great changes to the calcium clay while the sodium clays remain practically unaffected by preheating (the hydrogen clays are probably H-Al clays and their lack of homoionic character makes it difficult to analyze their behavior) it is recalled from Ross and Hendricks' study[7] that the gradual loss of interlaminar water upon heating is accompanied by a reduction in the 001 spacing and is seriously influenced by the size and nature of the exchangeable cation. The sodium ion probably is dehydrated completely at room temperature merely by outgassing at 1 μ. Hydrates of calcium, on the other hand, decompose only at higher temperatures until at about 150° it can be presumed that the exchangeable calcium ion is completely dehydrated. In comparing the heats of solution of various hy-

(5) F. Call, *Nature*, **172**, 126 (1953).

(6) W. H. Slabaugh, THIS JOURNAL, **63**, 436 (1959).

(7) Ross and S. B. Hendricks, "U. S. Geol. Survey Profess. Paper," 250 B, 23-80 (1954).

drated and anhydrous salts,[8] it is noted that each mole of hydrated water in a salt reduces the heat of solution approximately two to three kcal. In terms of the one gram of clay being immersed in water, and assuming that the resulting clay suspension produces a solution of the exchangeable ion, there should be about 6 cal. less of heat evolved with each additional molecule of water associated with the exchangeable cation. Since calcium clay, preheated to 150°, gives off slightly over 12 cal. more than it does when pretreated at room temperature, then there should be two molecules of water associated with each calcium ion at room temperature. This ratio of calcium to water is also indicated in the isotherms study already reported.[6] At higher temperatures, with further reduction of the 001 spacing, the heat of immersion of the calcium clay falls off because of the additional energy needed to force its way into the space between the laminae.

Comparison of the present results to customary differential thermal analysis is probably not entirely valid because the samples prepared here were outgassed at very low pressure, and this treatment may remove the physically adsorbed and hydrated water that is usually removed at 150 to 200° in the DTA studies.

Attempts to measure the 001 spacings of the pretreated samples were not successful, primarily because of the difficulty of transferring the samples from the vacuum line to the X-ray spectrometer and, at the same time, preserving the character of the clay system.

When these results are compared to other published data, such as that of Johnson[2] where samples were outgassed 72 hours and presumably at room temperature, one sees the importance of the temperature of outgassing, particularly with calcium and hydrogen clays.

(8) N. A. Lange, "Handbook of Chemistry," Handbook Publishers, Inc., Sandusky, Ohio, 1952, p. 1542.

TRANSLATIONAL FRICTION OF MICROSCOPIC SPHERES IN CONCENTRATED POLYMER SOLUTIONS

By Stephen D. Morton and John D. Ferry

Department of Chemistry, University of Wisconsin, Madison, Wisconsin

Received December 15, 1958

It has been recognized from experiments on diffusion[1-3] and sedimentation[4] that the frictional resistance for translation of a tiny particle in a matrix of flexible polymer molecules is far smaller than would be calculated from the macroscopic viscosity, and that the discrepancy is related to segmental motions of the polymer chains. There have been no systematic studies, however, of a homologous series of particles in polymer solutions of different concentrations. A few rough measurements of this sort are reported here.

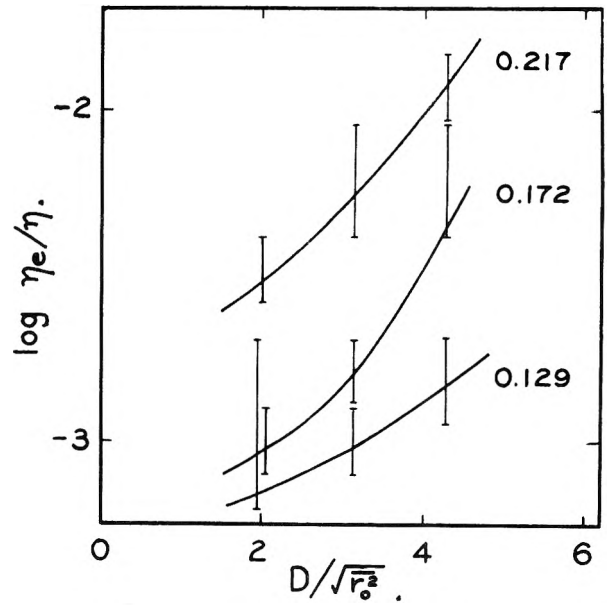

Fig. 1.—Logarithm of ratio of effective local viscosity in sedimentation to macroscopic viscosity, plotted against ratio of sphere diameter to root-mean-square end-to-end distance of polymer, for three polymer concentrations identified by their weight fractions. Vertical lines represent estimated extreme error, in several cases including duplicate determinations.

The particles were polystyrene spheres in the form of aqueous latices obtained through the generosity of the Dow Chemical Company,[5] of diameters 880, 1380 and 1880 Å. The polymer was an unfractionated polyacrylic acid, generously furnished by Rohm and Haas Company; its intrinsic viscosity in dioxane at 30° was 0.48 dl./g., its viscosity–average molecular weight calculated from the equation of Newman, *et al.*,[6] was 315,000, and the unperturbed root-mean-square end-to-end distance $(\overline{r_0^2})^{1/2}$ was 440 Å. The acid was 55% neutralized with sodium hydroxide so that both particles and polymer were negatively charged, and all solutions contained 0.2 *M* sodium chloride to minimize electrostatic effects. The polymer concentrations (made up by weight, allowing for a 9.7% moisture content in the lyophilized acid as determined by titration) were 12.9, 17.2 and 21.7%, expressed as weight fraction of unneutralized acid. The particle concentrations were of the order of 0.05%—enough to give a slight opalescence which prevented light transmission in an ultracentrifuge cell. There was no evidence of aggregation; the angular dependence of scattered light, viewed visually, was not highly asymmetric for suspensions either in the polyacrylic acid, in 0.2 *M* aqueous sodium chloride, or in distilled water.

Sedimentation coefficients of the particles were measured in the Svedberg oil turbine ultracentrifuge by following the (upward) motion of the opaque boundary. Because the supernatant solution was not perfectly clear, it was difficult to make good photographs and the displacement was measured visually on the projected image, with rather poor precision. Using Stokes' law, the effective local viscosity η_e was then calculated for each experiment. Since the density of the polystyrene[7] is 1.05 and those of the solutions ranged from 1.09 to 1.15, the Archimedes factor was also very uncertain, and the accuracy of the final values cannot be better than ±25%. This is sufficient, however, to show an enormous difference between the macroscopic viscosity and the effective local viscosity. The values of the latter ranged from 0.008 poise (essentially that of the solvent) to 2 poises.

(1) F. Grün, *Experientia*, **3**, 490 (1947).

(2) Y. Nishijima and G. Oster, *J. Polymer Sci.*, **19**, 337 (1956).

(3) S. D. Gehman, I. Auerbach, W. R. Miller and W. C. Kuryla, *ibid.*, **28**, 129 (1958).

(4) H. K. Schachman and W. F. Harrington, *J. Am. Chem. Soc.*, **74**, 3905 (1952).

(5) E. B. Bradford and J. W. Vanderhoff, *J. Appl. Phys.*, **26**, 864 (1955).

(6) S. Newman, W. R. Krigbaum, C. Laugier and P. J. Flory, *J. Polymer Sci.*, **14**, 451 (1954).

(7) T. G. Fox, Jr., and P. J. Flory, *J. Appl. Phys.*, **21**, 581 (1950).

The macroscopic viscosity, η, was measured over a range of polymer concentrations and temperatures by the conventional falling ball method[8] with glass spheres of the order of 1 mm. diameter. Values were then interpolated on a logarithmic plot for the concentrations and temperatures of the ultracentrifuge experiments (the temperatures ranged from 22 to 28°). At 25°, log η for the three polymer concentrations cited above was 0.93, 1.56 and 2.33, respectively.

Presumably an important quantity determining the ratio of η_e to η is the ratio of particle diameter (D) to some characteristic dimension of the polymer coil; clearly, as the latter ratio becomes large, η_e/η must approach unity. As a measure of coil size, we have used $(\overline{r_0^2})^{1/2}$, even though we are dealing with a charged polyelectrolyte; it probably does not deviate much from the Θ-solvent configuration in our concentrated solutions, where there is a high density of counter ions as well as added neutral salt. In Fig. 1, log η_e/η is plotted against $D/(\overline{r_0^2})^{1/2}$. The latter size ratio lies in the range from 2 to 4.3; the local effective viscosity is tremendously smaller than the steady flow viscosity, by a factor of 80 to 1400.

Log η_e/η increases with increasing $D/(\overline{r_0^2})^{1/2}$ as expected. Moreover, it increases with increasing polymer concentration. The latter dependence is probably related to the role of entanglement coupling in determining the viscosity,[9] which suggests that the average distance between entanglement points, $(\overline{r_e^2})^{1/2}$, is the important dimension rather than $(\overline{r_0^2})^{1/2}$. The average distance between entanglements certainly decreases with increasing concentration, though the functional relation is uncertain,[10] and hence the data of Fig. 1 might fall on a single composite curve if log η_e/η could be plotted against $D/(\overline{r_e^2})^{1/2}$. The accuracy of the present data is insufficient, however, for a more detailed analysis.

Data of this sort are potentially valuable in clarifying the frictional resistance encountered by polymer segments themselves in translation, as reflected in time-dependent mechanical properties.[11] This, too, is of course very much smaller than would correspond to the steady-flow viscosity, and in some diluted systems the local viscosity encountered by the polymer segments appears to be of the same order of magnitude as that of the solvent.[12]

Acknowledgments.—This work was supported in part by the Research Committee of the Graduate School of the University of Wisconsin from funds supplied by the Wisconsin Alumni Research Foundation. We are greatly indebted to Dr. J. W. Vanderhoff of Dow Chemical Company and Dr. F. J. Glavis of Rohm and Haas Company for supplying materials, and to Mr. E. M. Hanson for operating the ultracentrifuge.

(8) J. D. Ferry, L. D. Grandine, Jr., and D. C. Udy, *J. Colloid Sci.*, **8**, 529 (1953).

(9) R. F. Landel, J. W. Berge and J. D. Ferry, *ibid.*, **12**, 400 (1957).

(10) P. R. Saunders, D. M. Stern, S. F. Kurath, C. Sakoonkim and J. D. Ferry, *ibid.*, in press.

(11) J. D. Ferry and R. F. Landel, *Kolloid-Z.*, **148**, 1 (1956).

(12) J. D. Ferry, D. J. Plazek and G. E. Heckler, *J. chim. phys.*, **55**, 152 (1958).

ULTRACENTRIFUGAL STUDY OF HORSE SERUM ALBUMIN–SODIUM DODECYL SULFATE INTERACTION

BY KOICHIRO AOKI

Contribution from the Chemistry Laboratory, Nagoya City University, Mizuho-ku, Nagoya, Japan

Received December 15, 1958

It has been found by electrophoretic studies on the system horse serum albumin (HSA) and sodium dodecyl sulfate (SDS) that various complexes are formed at *p*H 6.8.[1,2a] When the weight mixing ratio of HSA to SDS (HSA/SDS) is between 100/0 and 70/30, there are three kinds of complexes, AD_1–AD_{12}, AD_n and AD_{2n} (A: HSA, D:SDS, and n = 105/2). In the mixing ratio region between 70/30 and 45/55 the complex AD_{2n} changes continuously to AD_{6n}. Measuring diffusion coefficient and intrinsic viscosity of the system HSA–SDS, Neurath and Putnam[3] found that the formation of AD_n occurs without detectable changes in molecular shape and the formation of AD_{2n} involves an increase in the molecular asymmetry of the protein. This time an ultracentrifugal study was carried out at *p*H 6.8. The results are reconciled with those by diffusion and viscosity.

Experimental

Horse serum albumin and sodium dodecyl sulfate used were the same as used previously.[1] Experiments were conducted at room temperature at 59,780 r.p.m. using a Spinco Model E ultracentrifuge. Ionic strength of the phosphate buffer was 0.10 and the sum of concentrations of HSA and SDS was 1.0%. Ultracentrifugal drive was continued for 60 minutes.

Results and Discussion

All the patterns in the weight ratio region HSA/SDS = 100/0 – 45/55 had a single boundary. One of the patterns is shown in Fig. 1.

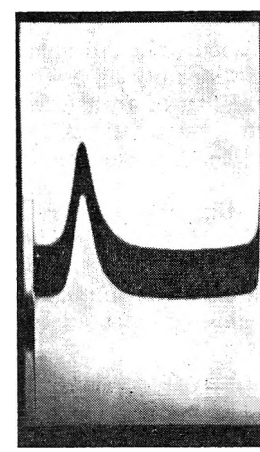

Fig. 1.—Ultracentrifugal pattern. *p*H 6.8, HSA/SDS = 90/10, and 3600 sec. after reaching full speed (59,780 r.p.m.). Sedimentation is from left to right. Bar angle 65°. Sum of concentrations of HSA and SDS was 1.0%.

Sedimentation coefficients $s_{20,w}$ calculated are shown in Fig. 2. These values are not those extrapolated to zero concentration. The $s_{20,w}$ value of 0.3% HSA solution was 4.4 *S*, agreeing with the value found in the literature.[4] Values of the partial specific volume ($\bar{v}$) were determined by simply assuming that all the SDS used was bound to HSA to form a complex and by measuring the density of the mixture at 25.00°. It was found that $\bar{v}$ was

TABLE I

WEIGHT MIXING RATIO REGION AND THE COMPOSITION OF COMPLEX FORMED

HSA/SDS	Complex formed
100/0–95/5	AD_1–AD_{12}
95/5–80/20	AD_{12} and AD_n
80/20–70/30	AD_n and AD_{2n}
70/30–45/55	AD_{2n}–AD_{6n}

(1) K. Aoki, *J. Am. Chem. Soc.*, **80**, 4904 (1958).

(2) (a) F. W. Putnam and H. Neurath, *J. Biol. Chem.*, **159**, 195 (1945); see also, (b) J. T. Yang and J. F. Foster, *J. Am. Chem. Soc.*, **75**, 5560 (1953); (c) M. J. Pallansch and D. R. Briggs, *ibid.*, **76**, 1390 (1954).

(3) H. Neurath and F. W. Putnam, *J. Biol. Chem.*, **160**, 397 (1945)

(4) P. A. Charlwood and A. Ens, *Can. J. Chem.*, **35**, 99 (1957).

(5) P. A. Charlwood, *J. Am. Chem. Soc.*, **79**, 776 (1957).

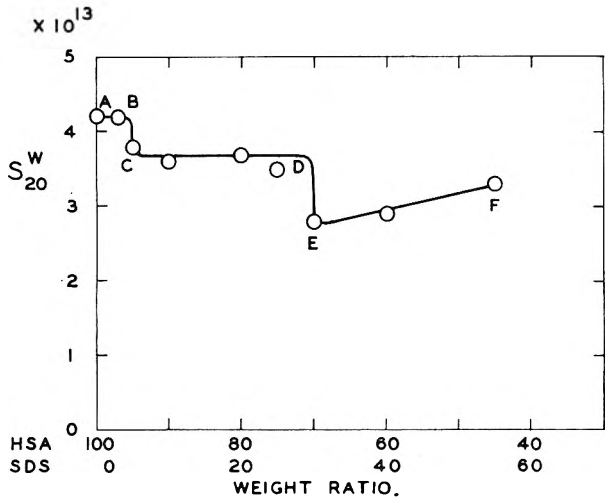

Fig. 2.—Sedimentation coefficient *vs.* weight mixing ratio HSA/SDS. (AB) HSA and complex AD_1–AD_{12}; (CD) AD_{12}, AD_n and AD_{2n}; (EF) AD_{2n+1} and complex up to AD_{6n}.

closely a linear function of the weight mixing ratio, $\bar{v}$ being 0.73_0[5] at 100/0 and 0.80_5 at 45/55.

It is seen in Fig. 2 that the $s_{20,w}$ value drops at HSA/SDS = 95/5 and at 70/30, and that then increases. Figure 2 is now interpreted referring to results by electrophoresis.[1] Table I gives the composition of the complex formed at *p*H 6.8[1]. In the weight ratio region 100/0–95/5, where complexes AD_1–AD_{12} are formed, the $s_{20,w}$ value is constant, although the electrophoretic mobility increased.

While electrophoretic patterns had two boundaries in the weight ratio region 95/5 – 70/30, ultracentrifugal patterns had a single boundary in the same weight ratio region. The sedimentation coefficient was almost constant, *ca.* 3.7S. This indicates that there is no difference in the $s_{20,w}$ value between AD_n and AD_{2n}, or that the difference is so small that it is within the resolving power by 60 minutes' ultracentrifugal drive. Unfortunately, it was not made clear whether the $s_{20,w}$ value of AD_{12} is 4.2 or 3.7 *S*.[6] At HSA/SDS = 90/10, where AD_{12} and AD_n existed almost in equal amounts in electrophoretic pattern, the sedimentation experiment was continued longer than 60 min. There was no resolution of the ultracentrifugal pattern. It seems likely, however, that slight change in shape takes place when AD_{12} changes to AD_n, since $s_{20,w}$ value in Fig. 2 changes at 95/5.

When the complex AD_n is changed to AD_{2n+1} at 70/30, there is a gross change in $s_{20,w}$ value, indicating that remarkable change in shape, probably unfolding, takes place in HSA. This is in agreement with the results by viscosity and diffusion.[3] In the region 70/30–45/55 the $s_{20,w}$ value increases, corresponding to the continuous increase in the electrophoretic mobility in the same weight ratio region.[1] This indicates that further unfolding would not occur, and that SDS anions are bound successively after AD_{2n+1} was formed until HSA is saturated by 6*n* SDS anions. In other words, the molecular shape would be the same and the weight of the complex increases resulting in the continuous increase in the sedimentation coefficient.

(6) If the difference in sedimentation coefficient of two components having *ca* 3 *S*, is within 0.6 S. the two boundaries would not be separated by 60 minutes drive at 59,780 r.p.m.

THE ELECTRICAL CONDUCTIVITY OF MOLTEN SILICA

By M. B. Panish

Research and Advanced Development Division, AVCO Corp., Wilmington, Mass.

Received December 15, 1958

In connection with studies of the properties of materials at high temperatures we have determined the electrical conductivity of pure molten silica. Earlier measurements on the solid at temperatures as high as 1400° had shown that silica is an insulator. It was our purpose to determine whether or not this behavior continued into the molten state. Since the conductivity of silica is undoubtedly strongly dependent upon impurities, an attempt was made to use very pure silica with a minimum of adsorbed water.

Experimental

Materials.—The fused silica used in this work is an optical grade which was obtained from the General Electric Company in the form of cylindrical rods. Chemical analysis yielded the impurity levels

Ti	0.03 % by wt.
Zr	.01 % by wt.
Al	.001% by wt.
Fe	10 p.p.m.
Mg	5 p.p.m.
B, Na, Ca	<1 p.p.m.

The electrodes, leads and cells were constructed of tungsten.

Apparatus and Method.—The apparatus consisted of a water-jacketed silica container in which a tungsten crucible was supported on a tungsten platform. Silica rods were cut to fit the tungsten crucible and to accept the electrodes which were constructed of 0.005″ sheet tungsten. High temperatures were attained by inductive heating of the tungsten container with a 20 kw. Lepel induction heater.

After assembling and evacuating the apparatus, the cell was heated to somewhere between 1500 and 1800° in order to degas the cell and the silica. During the degassing procedure, the silica flowed into contact with the electrodes. All operations were performed with the conductance cell under reduced pressure. The pressure of non-condensable gases in the container was between 10^{-5} and 10^{-6} mm. of mercury after about 30 minutes of degassing.

Temperature measurements were made by determining the brightness temperature of the tungsten crucible and making the usual corrections for the emissivity of tungsten and absorption in the optical system. Although the optical window of the system was protected by a shutter when readings were not being made, coating of the optical window by WO_3 condensate made temperature measurements difficult and those given in Fig. 1 are not considered more accurate than ±100°.

Resistance measurements were made with a Wheatstone Bridge arrangement operating at 10,000 cycles per second. These measurements were fairly crude due to interference and calibration difficulties. We have estimated their accuracy at about ±20%. Calibration was obtained by reproducing the geometry of the cell in a system utilizing 0.02 *N* KCl as the calibrating medium.

Results and Discussion

The conductivity results obtained here are shown in Fig. 1 where they are compared with data ob-

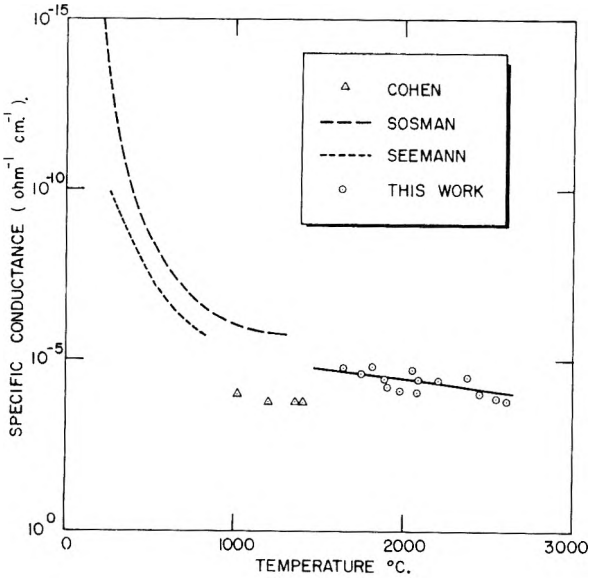

Fig. 1.

tained by previous workers.[1-3] Sosman's averaged data for several earlier workers has been plotted along with the smoothed curve from Seeman's data and several points obtained by Cohen. The higher conductivity obtained by Cohen easily could be due to the approximately 0.2% impurity in the silica used in his work.

During the degassing procedures, it was noticed that the conductivity often decreased in spite of the fact that the melt was coming into increasingly better contact with the electrodes. It thus appears that adsorbed water (as OH^-) contributes markedly to the conductivity of the solid, and it is possible that most of the water was removed by degassing before the final measurements on molten silica were made.

Inspection of the cells after cooling showed that the silica had wet the tungsten, and that once this had occurred, there was no observable reaction between tungsten and silica. The tungsten electrodes remained, in fact, mirror bright under the silica surface. It was, therefore, assumed that the contact resistance was negligible in comparison with the resistance of the silica. Above the surface of the melt, the tungsten was eroded, this obviously being due to the reaction of tungsten with oxygen deriving from the decomposition of silica to gaseous silicon monoxide and oxygen.

Acknowledgment.—The author appreciates the assistance of Mr. F. Bourgelas, Mr. R. Levy and Mr. A. Kocsi in constructing and assembling the apparatus. This work was supported by the U. S. Air Force under Contract No. AF-04(645)-30.

(1) J. Cohen, *J. Appl. Phys.*, **28**, 795 (1957).
(2) R. Sosman, "Properties of Silica," American Chemical Society Monograph, 1927, p. 528.
(3) H. E. Seeman, *Phys. Rev.*, **31**, 119 (1928).

THE ROLE OF CARBON DIOXIDE IN CATALYZED SILOXANE CLEAVAGE

By L. E. St. Pierre and A. M. Bueche
General Electric Company, Research Laboratory, Schenectady, N. Y.
Received December 16, 1958

Osthoff, Bueche and Grubb[1] have reported the

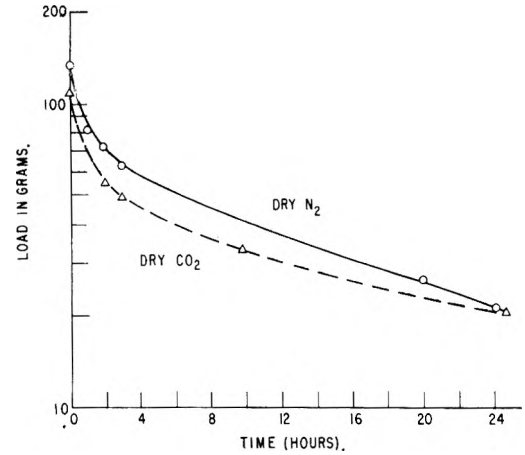

Fig. 1.—Stress relaxation of polydimethylsiloxane gum containing 0.01% potassium hydroxide and benzoyl peroxide decomposition fragments in dried carbon dioxide and nitrogen at 130°.

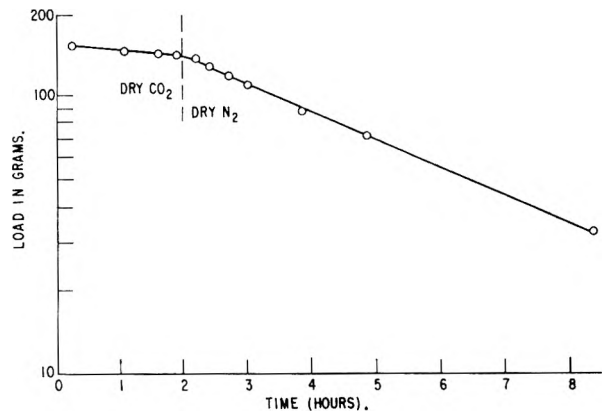

Fig. 2.—Stress relaxation of polydimethylsiloxane gum containing 0.01% potassium hydroxide (cross linked with high energy electrons) in dried carbon dioxide and nitrogen at 130°.

effects of CO_2 and water on the rate of chemical stress relaxation of polydimethylsiloxane elastomers. The effect of water is clear if it is assumed that it reacts with the catalytic agents, benzoic acid and potassium hydroxide, which are present. However, the acceleratory effect of CO_2 was inexplicable on the basis of known siloxane chemistry. It was therefore decided to reinvestigate the effect of CO_2, taking special precautions to purify it.

The apparatus used and polymer preparations are those described by Osthoff, Bueche and Grubb.[1] Dew point measurements were made by observing the temperature at which a gas stream exhibited condensation on a glass mirror.

Matheson "Bone-Dry" carbon dioxide was used and three methods of drying were tested: (i) passage through three 15 cm. tubes packed with anhydrous $MgSO_4$; (ii) passage through three 1 meter tubes packed with activated alumina; (iii) passage through two 20 cm. traps packed with brass turnings and cooled in Dry Ice–acetone baths.

The standard of comparison for the stress relaxation runs were those made in laboratory line dry nitrogen. Therefore it was desirable that the CO_2 used be of comparable dryness to offset the known effects of water. The line nitrogen had a dew point of −60°F. which indicated a water content of 0.0056 volume %. Carbon dioxide dried by means of $MgSO_4$, activated alumina and packed cooled traps contained 0.180, 0.0092 and 0.005% water, respectively.

(1) R. C. Osthoff, A. M. Bueche and W. T. Grubb, *J. Am. Chem. Soc.*, **76**, 4659 (1954).

Removal of the packing from the cooled traps destroyed their effectiveness.

Stress-relaxation runs made in the driest CO_2 (0.005 volume % water) are shown in Figs. 1 and 2.

Figure 1 shows dried CO_2 to have no more effect on the rate of stress relaxation than nitrogen of the same water content. The acceleration reported due to CO_2 previously[1] can thus be attributed to the water present in the CO_2 acting as a co-catalyst with the acid.

Figure 2 shows dried CO_2 to effect a transitory inhibition to stress relaxation in polymers containing only base. This suggests that a thermally unstable product is formed from the reaction between CO_2 and the base fragments (KOH and KOSi) catalyzing siloxane cleavage.

CONDITIONS REQUIRED FOR NON-RESONANT ABSORPTION IN ASYMMETRIC ROTOR MOLECULES

By E. Bright Wilson, Jr.

Mallinckrodt Chemical Laboratory, Harvard University Cambridge, Massachusetts

Received December 24, 1958

A number of molecules have been reported[1-3] to show non-resonant absorption in the microwave region at frequencies well below the lowest ordinary rotational transition. The corresponding dispersion of the dielectric constant has also been observed.[4] The substances studied include CH_3Cl, CH_3CN and CH_3Br, among others.

These effects have been ascribed to a pressure-broadened transition of essentially zero frequency between the states, respectively, symmetrical and antisymmetrical to molecular inversion. Such a transition, but at a rather high frequency, is well known for ammonia and should exist for any non-planar polyatomic molecule.

Certain molecules, CH_2F_2, CF_2Br_2 and CF_2Cl_2, are, however, reported[3] to show no non-resonant absorption. The purpose of this note is to offer a possible explanation of this.

The basic principle is that the transition of inversion is required by fundamental symmetry principles to be accompanied by a simultaneous change of rotational state.[5] In symmetric rotor molecules such as those in which non-resonant absorption was first observed (*e.g.*, CH_3Cl) most of the rotational energy levels are doubly degenerate, since the energy does not depend on the sign of the axial angular momentum $K(h/2\pi)$. The transition then takes place from one rotational state of one inversion level to a different rotational state of the other, but because of the rotational degeneracy there need be no contribution to the frequency from the rotation. If the inversion frequency is low enough, the over-all transition will be at essentially zero frequency and will give rise to the observed phenomena.

CH_2F_2 and CH_2Cl_2 are different because they are asymmetric rotors. Further, their point group (C_{2v}) restricts the dipole moment to lie along one principal axis of inertia, which here is known[6,7] to be the intermediate axis of inertia. This situation, which is not possible for a true symmetric rotor, leads to so-called b-type selection rules. Although many of the energy levels are for practical purposes degenerate despite the asymmetry, no transitions between members of such pairs are permitted by b-type rules. Consequently, the inversion transition is accompanied by a rotational transition of appreciable frequency and non-resonant absorption would not be expected. It is reasonable to expect that in the other C_{2v} molecules so far studied the dipole is also along the *b* axis.

The asymmetric rotors $CHFCl_2$ and $CHClF_2$ are reported[3] to display non-resonant absorption. This is to be expected since their dipole moment should have some component along the *a*-axis (least moment) which would allow transitions between the asymmetry doublet levels. Many of these levels will be nearly degenerate and therefore nearly zero inversion frequencies can occur.

Non-planar molecules with point group C_{2v} and a-type selection rules are possible, for example H_2CCCF_2. Such molecules, if heavy enough, should show non-resonant absorption.

The rotational levels with low quantum number K_{-1} (near prolate case) of asymmetric rotors may be widely split by the asymmetry so that even with a-type selection rules, they would give transitions of appreciable frequency. In very light molecules at low enough temperatures, the high K_{-1} levels which are more nearly degenerate may be very thinly populated, so that the theory predicts that non-resonant absorption would be weak, but that it should increase with increasing temperature (if a-type rules apply).

For near-oblate asymmetric rotors c-type selection rules replace a-type as a requirement for non-resonant absorption.

Although it is formally correct to consider these transitions discussed above as a combination of inversion and rotation, it is more in accord with intuitive ideas to ignore the inversion altogether[8] and consider the effects as due to pure rotational transitions of zero or nearly zero frequencies. It is known that optical isomers of structure similar to the compounds cited above would not suffer racemization for a very long period of time and it seems intuitively certain that a separated optical isomer would show non-resonant absorption without suffering racemization.

The resolution of this paradox lies in the conflicting uses of the word "inversion." In microwave spectroscopy the term "inversion transition" means a transition from a state which is antisymmetric (Ψ_A) with respect to physical inversion to a state which is symmetric (Ψ_S), or *vice versa*. In optical activity studies "inversion" means the physical change from the right-handed (Ψ_R) to the left-handed form (Ψ_L) or *vice versa*. The basic sym-

(1) G. Birnbaum, *J. Chem. Phys.*, **27**, 360 (1957).

(2) Krishnaji and G. P. Srivastava *Phys. Rev.*, **109**, 1560 (1958).

(3) J. E. Boggs and H. C. Agnew, This Journal, **63**, 1127 (1959).

(4) J. E. Boggs, J. E. Whiteford and C. M. Thompson, *ibid.*, **63**, 713 (1959).

(5) M. T. Weiss and M. W. P. Strandberg, *Phys. Rev.*, **83**, 567 (1951).

(6) D. R. Lide, Jr., *J. Am. Chem. Soc.*, **74**, 3548 (1952).

(7) R. J. Meyers and W. D. Gwinn, *J. Chem. Phys.*, **20**, 1420 (1952).

(8) The late Professor William Moffitt pointed out to me that, on intuitive grounds, it should not be necessary to invoke inversion.

metry rules forbid a transition with absorption of radiation unless the symmetry changes $\Psi_A \leftrightarrow \Psi_S$ but this is not the same as saying that $\Psi_R \rightarrow \Psi_L$. If the molecules were pure right-handed

$$\Psi_R = [1/\sqrt{2}]\,(\Psi_S + \Psi_A)$$

would be their wave function. On absorption of radiation, the molecules could go to another rotational state

$$\Psi_R' = [1/\sqrt{2}]\,(\Psi_S' + \Psi_A')$$

with a transition probability determined by

$$\int \Psi_R^* \mu \Psi_R' d\tau = {}^1/_2 \int \Psi_S^* \mu \Psi_A' \, d\tau + {}^1/_2 \int \Psi_A^* \, \mu \Psi_S' \, d\tau$$

which meets the above symmetry requirement. μ is the dipole moment.

One consequence is that planar molecules with "a" type selection rules and sufficiently populated near-degenerate states should also show typical non-resonant absorption despite the fact that they have only one form and therefore could not undergo inversion.

In any specific case it should be possible to make numerical calculations of the non-resonant absorption to be expected since tables of line strengths for asymmetric rotors are available[9] and energy levels also can be predicted.[10] The calculations would, however, be rather tedious.

NOTE ADDED IN PROOF.—My attention has been called to a paper by Krishnaji and Srivastaza, *Phys. Rev.* 106, 1186 (1957), which contains many of the principles applied above.

(9) R. H. Schwendeman and V. W. Laurie, "Tables of Line Strengths," Pergamon Press, New York, N. Y.

(10) See, for example, Townes and Schawlow, "Microwave Spectroscopy," McGraw-Hill Book Co., Inc., New York, N. Y.

MASS SPECTROMETRIC STUDIES OF THERMAL REACTIONS IN ACETYLENE–DEUTERIUM AND ACETYLENE-d_2–HYDROGEN MIXTURES[1]

BY FRED H. COATS AND ROBBIN C. ANDERSON

Contribution from the Department of Chemistry, University of Texas, Austin, Texas

Received January 5, 1959

As part of a program of study of the decomposition reactions of acetylene,[2] mass-spectrometric analyses have been made of the products of thermal reaction in mixtures of acetylene and deuterium and of acetylene-d_2 and hydrogen. These investigations were similar to those of Varnerin and Dooling on ethylene and deuterium mixtures[3] and of McNesby and Gordon[4] on cyclopropane and deuterium.

Under the conditions used, and with the apparatus available, a full statistical analysis of the products were not feasible; but the conditions for the appearance of certain characteristic peaks give useful information on the reactions occurring.

Experimental

The methane, helium and hydrogen were furnished by the Matheson Chemical Corporation. The ethylene was research grade and was obtained from Phillips Petroleum Company. Ordinary thiophene-free reagent grade benzene was used. The deuterium and deuterium oxide were of 99.5% purity or better and were obtained from the Stuart Oxygen Company of San Francisco. The purity of the deuterium was checked mass spectrometrically. Ordinary tank acetylene, which was purified as described previously,[2] was used.

The dideuteroacetylene was produced by the action of deuterium oxide on 20–30 mesh (electrolytc) calcium carbide obtained from the Fisher Scientific Company. Analysis showed the presence of 10% of the monodeuterated compound and only negligible traces of ordinary acetylene.

The gas blends to be studied were sealed in ampoules of approximately 25 ml. volume. For temperatures of 700° and below, Pyrex ampoules were prepared, attached to a gas-blending system, swept out with helium and evacuated, and then filled with the previously prepared mixture. The final total pressure was 300 mm. in each case. For temperatures above 700° Vycor ampoules were used. The blends were prepared in a 2-liter reservoir and the composition determined manometrically from the partial pressures.

The ampoules were heated in a small electric furnace which consisted of a 30-cm. length of 20-mm. Vycor tubing wound with nichrome wire. The temperature of the furnace was monitored continuously by means of a chromel–alumel thermocouple and was controlled by adjustment of a 2 KVA variable transformer. After heating for the desired length of time, the ampoules were removed from the furnace and allowed to cool before analysis.

The mass spectrometer used was a Westinghouse unit described in the previous reports.[2] All mass scans were made with an electron current of 6 microamperes at a nominal energy of 70 electron volts. Magnet currents of 55 and 35 milliamperes were used for the mass ranges of 120 to 44 and 43 to 13 mass units, respectively. The temperature of the ion chamber was 215 ± 5° and the leak line and reservoir were maintained at room temperature during the analyses.

Results

Abridged mass spectra of the reaction products of the acetylene–deuterium and dideuteroacetylene–hydrogen systems are presented in Tables I and II, respectively. The ion current intensities are given simply as relative values on an arbitrary scale since the indicated mass of the ions formed is the point of primary significance. The data were chosen so as to illustrate the results observed both for different temperatures and different heating times.

Toluene, benzene, ethylene, ethane, acetylene and methane were present in detectable amounts. In the runs at 600 and 700° a red-brown polymer condensed out on the walls on cooling; and above 700°, appreciable quantities of carbon formed as mirror-like surfaces on the walls of the ampoules.

Toluene was formed in detectable quantities only in the 600 and 700° runs. In the acetylene–deuterium system, undeuterated toluene was first observed for the 2-minute run at 600°, with the mono-deuterated compound appearing at higher temperatures and longer heating periods.

Background contamination of the mass range from 98 to 102 by doubly-ionized mercury isotopes made it impossible to observe the parent peak for the completely deuterated toluene in the dideutero-acetylene–hydrogen system but fragment peaks at mass 97 and below were observed.

Ions of mass 103 to 120 were not present in detectable quantities in the gaseous products.

At temperatures from 500 to 800°, benzene constituted the principal product. In the acetylene–deuterium system, the undeuterated compound was observed first. Similarly, hexadeuterobenzene ap-

(1) Based upon a paper presented at the 132nd National Meeting, American Chemical Society, New York, September, 1957.

(2) F. H. Coats and R. C. Anderson, *J. Am. Chem. Soc.*, **79**, 1340 (1957); J. D. Frazee and R. C. Anderson, "Sixth Symposium (International) on Combustion," Reinhold Publ. Corp., New York, N. Y., 1957, p. 247.

(3) R. E. Varnerin and J. S. Dooling, *J. Am. Chem. Soc.*, **78**, 1119 (1956).

(4) J. R. McNesby and A. S. Gordon, *J. Chem. Phys.*, **25**, 582 (1956).

TABLE I

ACETYLENE–DEUTERIUM MIXTURES
(150 mm. C_2H_2 + 150 mm. D_2)

	Ion current intensity (arbitrary)								
	500°		600°			700°		800°	900°
Mass no.	2 min.	2 min.	5 min.	10 min.	2 min.	5 min.	10 min.	2 min.	2 min.
93			0.5	0.6	1.0	1.0			
92		0.2	1.5	1.4	2.2	1.0			
91		.3	1.5	1.2	1.9	0.6			
84							0.3	0.2	0.5
83							1.4	0.9	1.7
82						0.5	2.9	2.2	2.8
81			0.1	0.2	0.4	2.5	3.9	3.5	3.1
80			0.6	1.2	1.8	8.3	3.7	3.5	2.0
79		.9	4.5	6.1	10.5	16.8	3.0	2.3	1.0
78	1.2	6.2	16.7	16.8	32.2	18.0	2.5	1.0	0.4
43		0.2	0.3	0.4	0.4	0.1			
42		.3	.7	.7	.8	.3	0.3	0.1	0.1
41	0.3	.2	.9	.8	.8	.5	0.4	.4	.4
40	0.4	.9	1.6	1.5	1.4	1.3	1.2	.6	.3
35					0.1	0.1	0.2		
34						.2	.5	0.3	
33						.5	.9	0.4	
32				0.7		1.2	2.5	1.2	0.7
31			0.3	1.2	.4	2.5	4.3	2.4	1.0
30			1.0	2.6	.9	4.3	5.3	3.5	1.5
29		.7	2.9	4.7	3.5	4.9	4.3	3.4	1.4
28	0.6	3.1	6.4	7.8	8.0	6.8	6.8	6.0	5.0
27	4.5	7.4	7.5	5.5	13.5	4.0	3.0	3.2	2.6
26	198.0	128.0	65.3	25.5	67.0	3.7	2.4	15.0	20.4
20						0.2	0.9	0.3	3.0
19					0.3	1.6	3.8	1.5	10.3
18				0.4	0.9	5.8	10.0	5.3	20.9
17		0.4	1.0	2.2	2.4	13.3	14.8	8.7	21.9
16		0.5	1.9	3.9	3.0	15.6	11.4	7.8	13.0

TABLE II

ACETYLENE-d_2–HYDROGEN MIXTURES
(150 mm. C_2D_2 + mm. H_2)

	Ion current intensity (arbitrary)							
	500°		600°		700°		800°	900°
Mass no.	2 min.	2 min.	5 min.	10 min.	2 min.	5 min.	2 min.	2 min.
97			0.4	0.9				
96			3	1.0	0.4	0.6		
95			2	0.5	0.2	.7		
94				0.2		.6		
84	0.2	2.0	12.5	16.7	11.7	7.9	1.2	0.7
83	0.1	0.9	9.2	15.0	9.7	16.7	3.2	2.0
82		.6	4.7	8.4	5.3	16.5	4.4	3.2
81		.2	1.7	3.4	1.9	10.3	3.9	3.2
80		.3	0.9	1.6	1.1	4.6	2.3	2.0
79			.4	0.7	0.3	1.8	1.0	0.9
78			.2	.3	.2	0.8	0.4	0.4
35				.2	.1	0.3	.3	
34				.5	.2	1.2	.6	
33				1.0	.4	2.3	.8	
32	0.2	.3	2.6	4.1	2.8	4.9	3.5	1.1
31		.6	4.8	7.9	5.7	9.8	6.0	1.3
30	0.1	.6	5.5	9.1	6.6	12.6	7.0	1.6
29	5.1	4.4	5.6	6.6	5.8	9.8	6.5	2.4
28	244	200	78.4	27.2	68.9	10.7	26.9	19.0
27	27.7	25.1	21.5	12.1	24.0	4.7	10.6	8.4
26	46.8	39.1	17.0	6.6	16.6	2.0	6.3	4.8
20		0.1	0.2	0.5	0.3	1.3	4.1	6.8
19		0.2	1.9	4.0	2.5	8.8	13.1	19.3
18			2.2	7.3	4.2	17.3	22.0	35.1
17			2.5	8.2	4.9	20.0	20.0	32.2
16			1.2	3.9	2.4	10.8	10.1	16.9

peared first in the dideuteroacetylene–hydrogen system.

The decrease in relative amounts of benzene and toluene at the higher temperatures is readily explainable on the basis of the tendency of these compounds, once formed, to undergo pyrolysis themselves.

Because of overlap with ions which could come from fragments in the benzene mass spectrum, the data for ion currents in the mass range of four-carbon compounds have not been included in the tables. It can be noted, however, that ion currents at masses 54, 55 and 56 were observed before the required benzene isotopes were formed in the acetylene–deuterium system.

The small ion currents at masses 43, 42, 41 and 40 in the acetylene–deuterium system indicate the formation of small amounts of propyne in pyrolysis since they cannot be attributed to the fragmentation of benzene. There were also some indications of propynes in the deuteroacetylene experiments, but the overlap with possible effects from carbon dioxide or deuterobenzene fragments in the background made it very difficult to get any quantitative data.

Trace amounts of methane were observed for both systems at 600 and at 800° methane became the predominant product. It should be noted that the appearance of methane coincides roughly with that of toluene and of propyne. At low temperatures, CH_3D and CD_3H are slightly predominant in the acetylene–deuterium and dideuterioacetylene–hydrogen systems, respectively, while at higher temperatures both systems exhibit a complex mixture of all possible isotopes such as is to be expected on the basis of isotopic mixing observed for methane–deuterium blends (Table III).

TABLE III

EXCHANGE REACTIONS IN BENZENE AND METHANE

	Ion current intensity (arbitrary)		
Mass no.	Unheated	600°, 5 min.	700°, 5 min.
20 mm. C_6H_6, 130 mm. He, 150 mm. D_2			
84		1.1	2.9
83		2.7	3.4
82		2.5	2.2
81		1.9	1.1
80		0.9	0.4
79	0.7	.4	.2
78	10.6	.2	.1
20 mm. CH_4, 130 mm. He, 150 mm. D_2			
20		0.1	0.6
19		0.8	2.7
18		3.8	7.9
17	0.2	8.7	9.9
16	19.6	14.5	7.9

To check the possibility of the deuteration of benzene and methane after their formation in the reaction, several tests were made with blends of benzene and deuterium and of methane and deuterium. The results of these are shown in Table III. At temperatures of 600° and above isotopic mixing occurs readily.

Tests were also made with helium added instead of deuterium. This resulted in a decrease in the toluene and benzene production, the difference being very marked at 700° and much less so at 900°. Methane production was not appreciably affected at 700°, but was much greater in the presence of deuterium at 900°. The rate of reaction of acetylene was apparently unaffected by the presence or absence of deuterium.

The results observed for groups involving two, four, or six carbon atoms are consistent with a pattern of reaction in which both a process involving free radicals such as C_2H and a "molecular"

process play roles in the thermal reactions. The general isotopic mixing and the variations when helium is substituted for deuterium are of the type which would be expected for a free-radical process. The relatively large peaks for mass 78 in acetylene–deuterium mixtures and for mass 84 in acetylene-d_2–hydrogen mixtures indicate some process by which C_6H_6 is formed from the original C_2H_2 or C_6D_6 from C_2D_2.

An interesting feature of the results is the early appearance of peaks for toluene and for three-carbon fragments and for methane and, in particular, the high proportion of mass 16 observed consistently in the C_2H_2–D_2 mixtures. Both the mass 16 and the high energy which would be necessary preclude the possibility of formation of methane from a single-carbon fragment obtained by splitting the triple bond in acetylene itself. The amounts of such materials as toluene, ethane, etc., are, on the other hand, not sufficient to indicate that the methane might be accounted for by their de composition. A more reasonable conclusion is that methyl radicals are present in appreciable concentrations, but the source of the CH_3 in the pyrolysis of C_2H_2 is not easy to explain.

Methane is well-known as a product in the pyrolysis of acetylene, but little has been said about how it is actually formed. In a reacting system starting with acetylene, such a relatively saturated group must result from secondary reactions such as decomposition of products of higher molecular weight; but it is not clear what condensation or rearrangements can give rise to CH_3 groups to split off. It is notable that the molecular weights observed in these experiments indicate that the hydrogen of the methyl group (or methane) comes essentially from the original acetylene present.

Acknowledgment.—This research was supported by the United States Air Force through the Air Force Office of Scientific Research of the Air Research and Development Command under contract No. AF 18(600)-430. Reproduction in whole or in part is permitted for any purpose of the United States Government.

AN INFRARED SPECTROPHOTOMETRIC STUDY OF THE PHENOL–PHENOXIDE DISSOCIATION

BY FRANK S. PARKER AND DONALD M. KIRSCHENBAUM

From the Department of Biochemistry, State University of New York, Brooklyn 3, New York

Received January 6, 1959

Many substances of biochemical importance are phenolic in nature (*e.g.*, tyrosine, pyridoxine, tyramine and serotonin). It would be interesting to examine the dissociation of the phenol group to the phenoxide ion in water in such compounds by means of infrared spectrophotometric methods. The simplest approach to this work was to use phenol itself. The dissociation of phenol to phenoxide ion can be detected in the ultraviolet region of the spectrum,[1] *i.e.*, there is a shift in the absorption band from 270 mμ for phenol to 287 mμ for the phenoxide ion. At the same time there is an enhancement of the absorbance. The authors believed that this dissociation also could be detected in the infrared region because it is similar to a carboxyl–carboxylate dissociation, which is evident in the well known shift of the absorption band in the infrared region (6 μ) in going from the carboxyl structure to the carboxylate ion structure.[2] Therefore, aqueous solutions of phenol at different *p*H values were examined in an infrared spectrophotometer.

Experimental

Mallinckrodt White Label phenol was distilled and the fraction boiling at 180° was used. All *p*H measurements were made with a Beckman Model G *p*H meter. The spectra were obtained with a Perkin–Elmer Model 21 infrared spectrophotometer (NaCl prism) on aqueous solutions in a barium fluoride cell with a thickness of 0.052 mm. A transmittance screen[3] was used in the reference beam. Instrument controls were set as follows: resolution, 984; response, 1.0; gain, 5.0; speed of recording, about 47 seconds per micron. The instrument was calibrated against water vapor and a polystyrene film.

Other details of experimental conditions appear in the legends to the figures.

Results

Examination of Fig. 1 shows that there are distinct differences in the absorption spectra of phenol and phenoxide ion. A 5% (w./v.) solution of phenol, curve 1, exhibits strong absorption bands at 6.78 μ (1475 cm.$^{-1}$) and 8.10 μ (1235 cm.$^{-1}$), a medium band at 7.28 μ (1374 cm.$^{-1}$), and weak bands at 8.56 μ (1168 cm.$^{-1}$) and 9.36 μ (1068 cm.$^{-1}$). A 5% solution of sodium phenoxide, curve 2, shows strong absorption bands at 6.78 μ (1475 cm.$^{-1}$) and 7.91 μ (1264 cm.$^{-1}$), a medium band at 8.60 μ (1163 cm.$^{-1}$), and a weak band at 9.40 μ (1064 cm.$^{-1}$). In addition, there is a band at 10.15 μ (985.2 cm.$^{-1}$), the development of which is overshadowed by the increasing absorption of water in this region. It is thus readily apparent that not only is there a distinct shift from 8.10 to 7.91 μ upon dissociation of phenol to phenoxide ion, but, in addition, the band at 7.28 μ disappears and a band at 10.15 μ appears.

Examination of Fig. 2 shows certain properties of the system phenol–phenoxide ion. Curve 2, which represents a 1:1 mixture of phenol and phenoxide ion, has characteristics also shown by the absorption curves of both phenol and phenoxide ion as seen in curve 1 and curve 2 of Fig. 1. Curve 1, Fig. 2, which represents a 3:1 mixture of phenol and phenoxide ion, shows the absorption bands for phenol and phenoxide ion in the 8 μ region, while the phenoxide band exhibits only a slight shoulder at 10.10 μ. Thus while the concentration of phenol is three times as great as phenoxide ion, the phenoxide ion, being a much stronger absorber of infrared radiation, still shows its characteristic absorption at 10.10 μ. By comparison, curve 3 of Fig. 2, where the ratio of phenol to phenoxide ion is 1 to 3, exhibits mainly the absorption characteristics of phenoxide ion, *i.e.*, a strong band at 7.93 μ, and a band at 10.10 μ. It is to be noted that the

(1) A. E. Gillam and E. S. Stern, "An Introduction to Electronic Absorption Spectroscopy in Organic Chemistry," second edition, Edward Arnold Publishers, Ltd., London, 1957, p. 140, Table 9.6.

(2) L. J. Bellamy, "The Infra-Red Spectra of Complex Molecules," second edition, Methuen and Company, Ltd., London, 1958, p. 175.

(3) W. J. Potts, Jr., and N. Wright, *Anal. Chem.*, **28**, 1255 (1956).

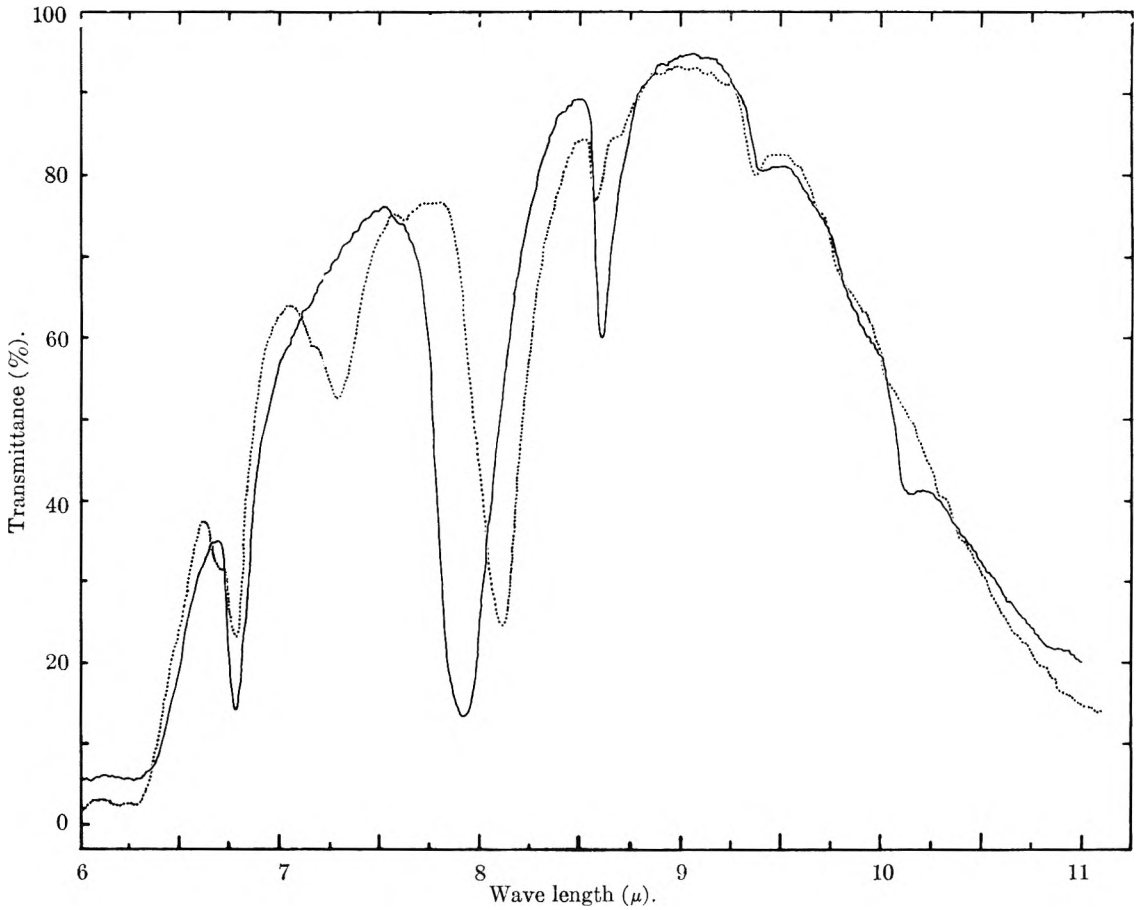

Fig. 1.—Absorption spectra of phenol and phenoxide ion: curve 1 (.....), 5% phenol in water (*p*H 5.6); curve 2 (———), 5% phenol in sodium hydroxide solution (*p*H 12.0).

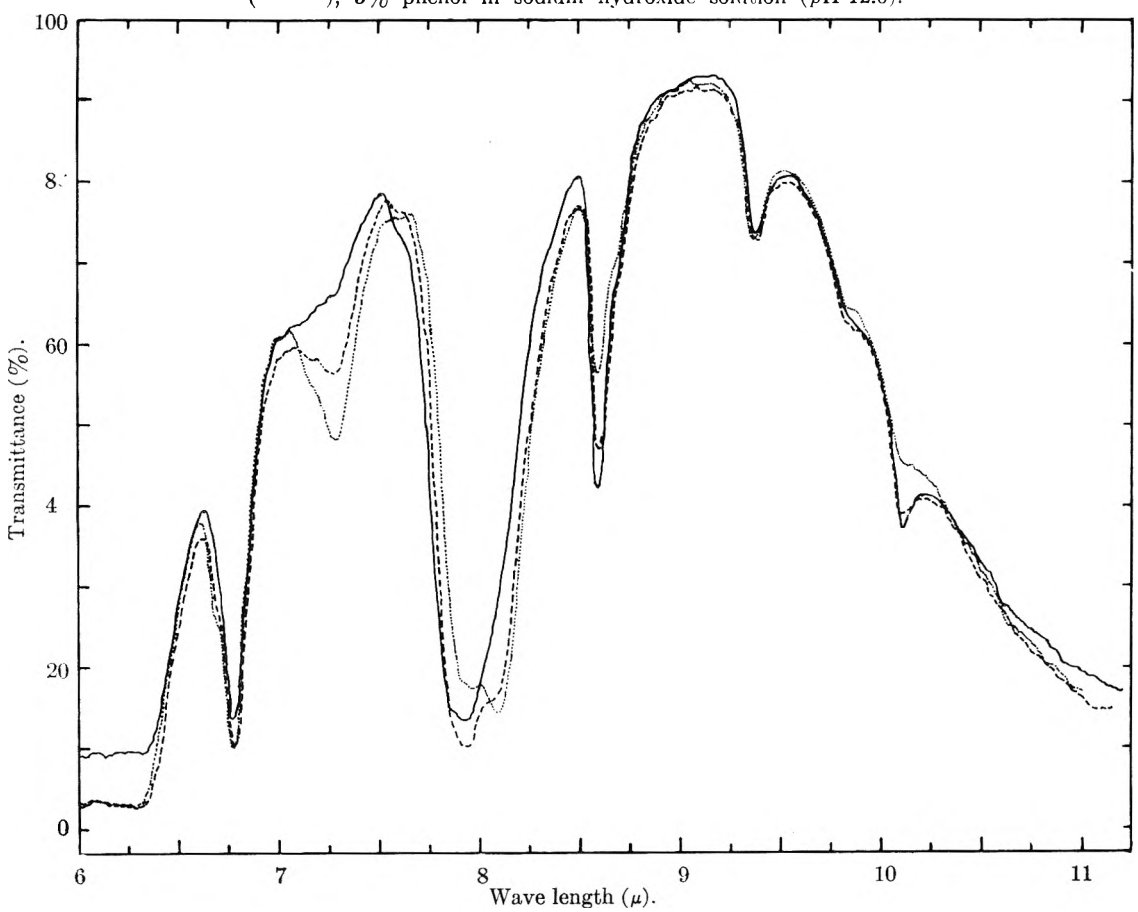

Fig. 2.—Absorption characteristics of phenol–phenoxide mixtures: curve 1 (.....), 2.60 g. of phenol plus 6.90 ml. of 1.02 *N* NaOH and diluted to 25.00 ml., *p*H 9.6. $ROH/RO^- = 3/1$; curve 2 (– – – –), 2.60 g. of phenol plus 13.70 ml. of 1.02 *N* NaOH and diluted to 25.00 ml., *p*H 10.0. $ROH/RO^- = 1/1$; curve 3 (———), 2.60 g. of phenol plus 20.60 ml. of 1.02 *N* NaOH and diluted to 25.00 ml., *p*H 10.5. $ROH/RO^- = 1/3$.

slight shoulder at 7.28 μ and the broadening of the 7.93 μ band are due to the presence of phenol.[4]

In addition to the work described above the authors also have determined that it is possible to detect phenol in aqueous solution at a concentration of 0.45% using the band at 8.15 μ, and phenoxide ion at 0.63% using the band at 7.93 μ. There are experimental indications that it is possible to detect phenoxide ion at concentrations as low as approximately 0.2% in water.[6]

(4) An approximation of the apparent dissociation constant for phenol can be obtained by plotting the decrease in intensity of the 7.28 μ band (which decreases in intensity on increasing the phenoxide ion concentration) *versus* the observed *p*H. When such a plot is made, it is seen that the mid-point of the curve is at *p*H 10, which is close to the known value for this ionization.[5] Although only three points have been used to obtain this value, the authors feel that these points are significant. An attempt will be made in the future to refine these measurements.

(5) C. M. Judson and M. Kilpatrick, *J. Am. Chem. Soc.*, **71**, 3113 (1949).

(6) The quantitative determination of phenol in water by infrared spectrophotometric methods is being explored in the authors' Laboratory.

LATTICE CONSTANTS OF AMMONIUM CHLORIDE–AMMONIUM BROMIDE SOLID SOLUTIONS

By Vincent C. Anselmo and Norman O. Smith

Department of Chemistry, Fordham University, New York, N. Y.

Received January 28, 1959

The need for a convenient means of analyzing solid solutions of ammonium chloride in ammonium bromide led to the measurement of the variation of their lattice constant with composition. The lattices of both components are of the interpenetrating simple cubic type at room temperature, and a complete series of solutions is possible between the two. Only one isolated measurement of a lattice constant of such a solid solution has ever been reported.[1]

Experimental

U.S.P. grade ammonium chloride and ammonium bromide were used without further purification. The solid solutions were made by mixing hot concentrated aqueous solutions of the components with stirring and allowing to cool. Stirring was continued for at least 48 hours to improve the homogeneity of the resulting crystals. The latter were filtered, dried overnight and stored in a desiccator. They were then analyzed potentiometrically (silver and calomel electrodes and standard silver nitrate) with the help of an adaptation of the method of McAlpine.[2] Total halide was determined, and then chloride alone, after destroying bromide with permanganate. The accuracy of the method, established by analyzing synthetic mixtures of ammonium chloride and bromide, gave mole fractions of NH_4Br within 0.01 for low bromide contents and within 0.003 for high. X-Ray powder photographs were taken at room temperature as described in an earlier study[3] and the lattice constants evaluated therefrom. The sharpness of the lines indicated that the solids were essentially homogeneous. Only the last five lines of greatest glancing angle were used for the calculation of each constant, but, for each solid, the mean deviation of these was usually less than 0.002 Å. and, at the most, 0.004 Å. (mole fraction of NH_4Br 0.23).

The lattice constants for each composition are shown in Table I, and are believed accurate to 0.005 Å., considering the inaccuracy of the wedge technique and the lack of temperature control. The values for the pure components, *viz.*, 3.875 and 4.059 Å. for the chloride and bromide, respectively, agree satisfactorily with those of the National Bureau of Standards,[4,5] 3.876 and 4.059 Å. at 26°.

Table I

Lattice Constants of NH_4Cl–NH_4Br Solid Solutions

Compn., mole fraction of NH_4Br	Lattice constant, Å.	Dev. from additivity, Å. × 10^3	Compn., mole fraction of NH_4Br	Lattice constant, Å.	Dev. from additivity, Å. × 10^3
0.00	3.875	..	0.47	3.963	+2
.04	3.875	−7	.70	4.009	+5
.08	3.882	−8	.99	4.060	+3
.11	3.883	−12	1.00	4.059	...
.23	3.907	−10			

It seems clear that the U.S.P. materials in the present work contributed no error greater than that introduced by the X-ray technique itself. Table I also gives the deviation of the lattice constants from Vegard's rule of additivity. It is seen that the solid solutions follow Vegard's rule within experimental error except for those with high ammonium chloride content, which exhibit negative deviations.

(1) R. S. Havighurst, E. Mack, Jr., and F. C. Blake, *J. Am. Chem. Soc.*, **47**, 29 (1925).

(2) R. K. McAlpine, *ibid.*, **51**, 1065 (1929).

(3) E. T. Teatum and N. O. Smith, This Journal, **61**, 697 (1957).

(4) H. E. Swanson and E. Tatge, "Standard X-Ray Diffraction Powder Patterns," Vol. I, National Bureau of Standards, 1953, p. 59.

(5) H. E. Swanson and R. K. Fuyat, ref. 4, Vol. 2, p. 49.

THE USE OF DIFFERENTIAL THERMAL ANALYSIS FOR INVESTIGATING THE EFFECTS OF HIGH ENERGY RADIATION ON CRYSTALLINE AMMONIUM PERCHLORATE

By Eli S. Freeman and David A. Anderson

Pyrotechnics Chemical Research Laboratory, Picatinny Arsenal, Dover, New Jersey

Received January 6, 1959

Differential thermal analysis (d.t.a.) involves the continuous measurement of temperature differences between a sample and thermally inert reference compound as a function of sample or reference temperature and/or time, as both the sample and reference compound are heated simultaneously at a predetermined rate. This technique has been used to characterize and to study the high temperature physico-chemical behavior of clays, minerals, inorganic and organic systems[1] as well as for investigating reaction kinetics.[2,3] In this paper we are reporting on the application of differential thermal analysis to the study of the effects of radiation on crystalline ammonium perchlorate.

A powdered sample of C.P. ammonium perchlorate was irradiated with an OEG-50 X-ray tube, in air, for 100 hours at 40 kv. and 20 ma. at a distance of 1 cm. from the tungsten target. The total dosage of radiation was approximately 10^7 roentgens. The differential thermal analysis apparatus was similar to that previously reported[4] with the exception that a two pen Leeds and

(1) C. B. Murphy, *Anal. Chem.*, **30**, 867 (1958).

(2) E. S. Freeman and B. Carroll, This Journal, **62**, 394 (1958).

(3) H. J. Borchardt and F. Daniels, *J. Am. Chem. Soc.*, **79**, 1102 (1957).

(4) S. Gordon and C. Campbell, *Anal. Chem.*, **27**, 1102 (1955).

Northrup Speedomax recorder was employed to record the differential thermal analysis curves.

The differential thermograms obtained for 250 mg. of non-irradiated and irradiated samples in air are shown in Fig. 1. At 244° an endotherm is observed with a point of inflection at 240° which corresponds to the crystalline transition of ammonium perchlorate from orthorhombic to cubic.[5] The point of inflection is not seen easily from the d.t.a. curve; however, it is obtained readily from the electronically generated derivative d.t.a. curve shown in Fig. 2 which was simultaneously recorded.[6] The crystalline transition was followed by an exothermal d.t.a. band of relatively small amplitude with a peak at 309°. During this reaction gases having chlorous and nitrous odors were detected and the sample darkened. At 430° a sharp, highly exothermal reaction occurred, which resulted in ignition leaving no residue. During this reaction the sample temperature exceeded that of the thermally inert reference compound, alumina, by more than 80°.

The behavior of the irradiated sample upon heating was significantly different from that of non-irradiated ammonium perchlorate. Unlike the non-irradiated sample, prior to the crystalline transition which occurred at the same temperature as that of non-irradiated NH_4ClO_4, two endotherms and an exotherm are observed. The peaks of these bands appear at 81, 154 and 234°, respectively. Beginning at approximately 80° a crackling sound was heard which was accompanied by splattering of the crystals. This phenomenon ceased during the crystalline transition. It was interesting to note that the tannish colored irradiated crystals turned white over this period. Small quantities of white sublimate were observed at 130° and a chlorine odor was noticed at approximately 170°.

During crystalline transition, water was liberated and the vapors condensed on the walls of the Pyrex tube containing the sample. Immediately after the crystalline transition an exothermal reaction occurred, as indicated by the band at 277°, which was accompanied by the evolution of brownish vapors due to the formation of oxides of nitrogen. This reaction was succeeded by two additional exotherms. The first occurred between 305 and 385° and the second from 385 to 455°. The latter reaction is highly exothermal and corresponded to the reactions of the non-irradiated material over the same temperature interval. However, the amplitude of the exothermal band was approximately one-eighth as large as that of the non-irradiated samples. The decrease in the extent of reaction over this temperature interval is probably due to partial decomposition of the ammonium perchlorate during and immediately following the crystalline transition.

In view of the significantly different thermal behavior of irradiated and non-irradiated ammonium perchlorate it is interesting to note that X-ray diffraction patterns and infrared analysis did not indicate any differences between the treated and untreated materials. Mass-spectrometric analysis of an irradiated sample showed the presence of small amounts of gas consisting of a relatively large fraction of H_2O and relatively small fractions of O_2, HCl and N_2O which apparently were trapped in the crystals. These products are among those reported[6] for the thermal decomposition of non-irradiated ammonium perchlorate. Upon heating, the vaporization of water and expansion of the trapped gases probably caused the rupture of the irradiated crystals.

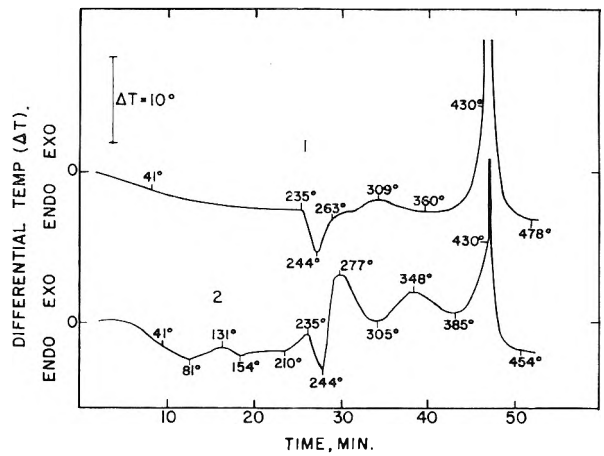

Fig. 1.—Differential thermal analysis curves for non-irradiated and irradiated ammonium perchlorate in air at atmospheric pressure; heating rate 10°/min.; sample weight 250 mg; differential temp, ΔT, °C. *vs.* time, min. 1, non-irradiated ammonium perchlorate; 2, irradiated ammonium perchlorate.

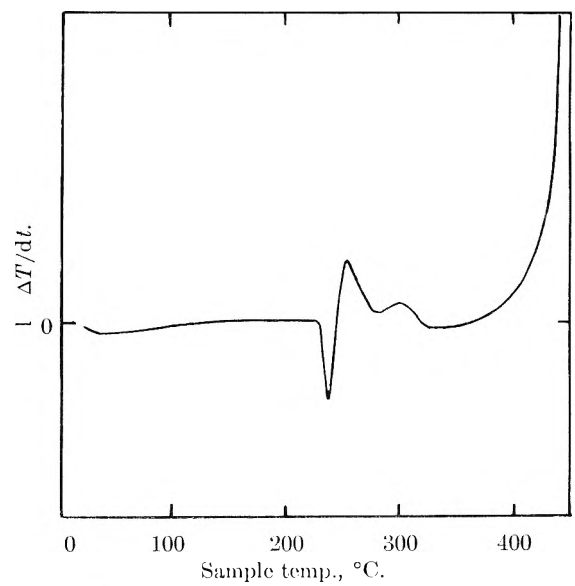

Fig. 2.—Derivative differential thermal analysis curve for non-irradiated ammonium perchlorate; $d\Delta T/dt$ *vs.* sample temperature, °C.

Acknowledgment.—The authors wish to thank Joseph J. Campisi for irradiating the samples and for carrying out the X-ray analyses; Dr. Harold J. Matsuguma, *et al.*, for the infrared analyses, and Philip Rochlin for the mass-spectrometric analysis of the gases.

(5) L. L. Bircumshaw and B. H. Newman, *Proc. Roy. Soc.* (*London*), **A227**, 115 (1954).

(6) C. Campbell, S. Gordon and C. Smith, *Anal. Chem.*, in press.

A RELATION BETWEEN THE LENGTHS OF SINGLE, DOUBLE AND TRIPLE BONDS

By Hans Feilchenfeld

Petrochemistry Laboratory of the Research Council of Israel and of the Department of Physical Chemistry, The Hebrew University, Jerusalem, Israel

Received March 2, 1959

It has been shown previously[1] that in hydrocarbons the cube of the bond length is inversely proportional to the bond energy. It will now be demonstrated that the cube of the bond length of a triple bond is $^1/_2$ that of a single bond, and the cube of the bond length of a double bond is $^2/_3$ of a single bond. In other words, if L_S, L_D and L_T designate the lengths of a single, double and triple bond, respectively, then

$$\frac{1}{L_S^3}:\ \frac{1}{L_D^3}:\ \frac{1}{L_T^3} = 2:3:4$$

This rule can be verified for CC, CN and CO bonds. In other combinations of atoms bond lengths or bond multiplicities are not known with sufficient accuracy.

Table I

Carbon–Carbon Bonds

Bond	L(Å.)	Compound	Ref.	$1/L^3$	Ratio
Single	1.543	Ethane	*a*	0.272	1.95
Double	1.337	Ethylene	*b*	.418	**3.00**
Triple	1.208	Acetylene	*c*	.567	4.07
	1.205	Acetylene	*d*	.571	4.10

[a] G. E. Hansen and M. D. Dennison, *J. Chem. Phys.*, **20**, 313 (1952). [b] H. C. Allen, Jr., and E. K. Plyler, *J. Am. Chem. Soc.*, **80**, 2673 (1958). [c] B. D. Saksena, *J. Chem. Phys.*, **20**, 95 (1952). [d] M. T. Christensen, *et al.*, *Proc. Roy. Soc.* (London), **238A**, 15 (1956).

Table II

Carbon–Nitrogen Bonds

Bond	L(Å.)	Compound	Ref.	$1/L^3$	Ratio
Single	1.474	Methylamine	*a, b, c*	0.312	1.96
Double	1.27	Dimethylglyoxime	*d*	.488	
	1.29	Acetoxime	*e*	.466	
	1.28(av.)		*f*	.477	**3.00**
Triple	1.153	Hydrogen cyanide	*g*	.652	4.10
	1.157	Acetonitrile	*h*	.646	4.06
	1.157	Propionitrile	*i*	.646	4.06

[a] D. R. Lide, Jr., *J. Chem. Phys.*, **27**, 343 (1957). [b] T. Itoh, *J. Phys. Soc. Japan*, **11**, 264 (1956). [c] T. Nishikawa, T. Itoh and K. Shimoda, *J. Chem. Phys.*, **23**, 1735 (1955). [d] L. Merrit and E. Lanterman, *Acta Cryst.*, **5**, 811 (1952). [e] T. K. Bierlein and E. C. Lingafelter, *ibid.*, 4, 450 (1951). [f] E. G. Cox and G. A. Jeffrey, *Proc. Roy. Soc.* (London) **207A**, 110 (1951). [g] A. E. Douglas and D. Sharma, *J. Chem. Phys.*, **21**, 448 (1953). [h] L. F. Thomas, E. I. Sherrard and J. Sheridan, *Trans. Faraday Soc.*, **51**, 619 (1955). [i] R. G. Lerner and B. P. Dailey, *J. Chem. Phys.*, **26**, 678 (1957).

(1) H. Feilchenfeld, This Journal, **61**, 1133 (1957).

The compounds for which bond lengths are listed in Tables I, II and III are those in which the bonds are considered pure. From a compilation recently published[2] it will be seen that those bond lengths can be considered the best estimates published so far. The C=N bond length has been measured only for diazomethane and for oximes. In diazomethane the central N atom is quadrivalent and the carbon and nitrogen are therefore not joined by a pure double bond. In the oximes the strong N . . . H–O hydrogen bond is likely to influence the adjacent C=N bond. Nevertheless the bond lengths for the oximes have been included in Table II as the best estimate. Carbon monoxide was considered an example of the C≡O triple bond.[3] In all three tables the value $1/L_S^3$ is somewhat low. The ratio $1/L_S^3:1/L_D^3:1/L_T^3$ = 1.94:3:4 appears nearer the experimental value. However, the 3% discrepancy corresponds to a discrepancy of 1% in the bond length which in many cases is within the limits of the published bond lengths.

Table III

Carbon–Oxygen Bonds

Bond	L(Å.)	Compound	Ref.	$1/L^3$	Ratio
Single	1.426	Methanol	*a*	0.345	1.93
	1.427	Methanol	*b*	.344	1.92
	1.428	Methanol	*c*	.343	1.92
Double	1.230	Formaldehyde	*d*	.537	**3.00**
Triple	1.128	Carbon monoxide	*e*	.697	3.89

[a] M. Kimura, K. Kimura and S. Shibati, *J. Chem. Phys.*, **24**, 622 (1956). [b] P. Venkateswarlu and W. Gordy, *ibid.*, **23**, 1200 (1955). [c] J. D. Swalen, *ibid.*, **23**, 1739 (1955). [d] G. Herzberg, "Infra-red and Raman Spectra of Polyatomic Molecules," D. van Nostrand Co., New York, N.Y., 1945. p. 440. [e] G. Herzberg and K. N. Rao, *J. Chem. Phys.*, N.Y., **17**, 1099 (1949).

It has been shown in the case of hydrocarbons that the values $1/L^3$ can be taken as a measure of the bond energy. If this relation is extended to other bonds as well, it follows that the increments of the bond energy of the double over the single bond and of the triple over the double bond are equal to each other and about half the energy of a single bond. The single bond energy is generally associated with the energy of a σ-bond. It then follows that the π-bond in a double bond and the two π-bonds in a triple bond each have about half the energy of a σ-bond.

(2) "Table of Interatomic Distances and Configuration in Molecules and Ions," The Chemical Society, London, 1958.

(3) C. A. Coulson, "Valence," Oxford University Press, London, 1952.

1957 EDITION

American Chemical Society DIRECTORY of GRADUATE RESEARCH

INCLUDES:

Faculties, Publications, and Doctoral Theses in Departments of Chemistry, Biochemistry, and Chemical Engineering at United States Universities

- **All institutions which offer Ph.D. in chemistry, biochemistry, or chemical engineering**
- **Instructional staff of each institution**
- **Research reported at each institution for past two years**
- **Alphabetical index of 2,878 faculty members and their affiliation; alphabetical index of 236 schools**

The ACS Directory of Graduate Research is the only U. S. Directory of its kind. The 3rd edition, prepared by the ACS Committee on Professional Training, now includes all schools and departments (with five exceptions where data were received too late for inclusion) concerned primarily with chemistry, biochemistry, or chemical engineering, known to offer the Ph.D. degree.

The Directory is an excellent indication not only of research reported during the last two years at these institutions but also of research done prior to that time. Each faculty member reports publications for 1956–57; where these have not totaled 10 papers, some articles prior to 1956 are reported. This volume fully describes the breadth of research interest of each member of the instructional staff.

Because of the indexing system, access to information is straightforward and easy—the work of a moment to find the listing you need. Invaluable to anyone interested in academic or industrial scientific research and to those responsible for counseling students about graduate research.

Paper bound.....634 pages.....$3.50

ORDER FROM

Special Issues Sales

AMERICAN CHEMICAL SOCIETY
1155–16th STREET, N.W.
WASHINGTON, D. C.